VOLUME 133 • NUMBER 3S • MARCH 2014 SUPPLEMENT www.PRSJournal.com

AMERICAN SOCIETY OF PLASTIC SURGEONS®

Supplement to

Plastic and Reconstructive Surgery®

Journal of the American Society of Plastic Surgeons
Official Organ of the American Association of Plastic Surgeons
Official Organ of the American Society of Maxillofacial Surgeons
Official Organ of the Plastic Surgery Research Council

The Plastic Surgery Research Council 59th Annual Meeting Abstract Supplement

Wolters Kluwer Health | Lippincott Williams & Wilkins

EDITORIAL BOARD

Plastic and Reconstructive Surgery

†Deceased

EDITORIAL BOARD (CONT.)

INTERNATIONAL ASSOCIATE EDITORS

Plastic and Reconstructive Surgery

Phillip Blondeel *(Gent, Belgium)*

Osvaldo Saldanha *(Santos, Brazil)*

Ricardo Baroudi *(São Paulo, Brazil)*

Dov C. Goldenberg *(São Paulo, Brazil)*

Yilin Cao *(Beijing, China)*

Jingheng Gao *(Shenyang, China)*

Wei Wang *(Shanghai, China)*

Lars Steinstraesser *(Oldenburg, Germany)*

Isao Koshima *(Tokyo, Japan)*

Fernando Molina *(Mexico City, Mexico)*

Fu-Chan Wei *(Taipei, Taiwan)*

Nazim Cerkes *(Istanbul, Turkey)*

PARTNER SOCIETY ASSOCIATE EDITORS

Rod Cooter
Australian Society of Plastic Surgeons

Mustapha Hamdi
Royal Belgian Society for Plastic Surgery, Reconstructive and Aesthetic Surgery

Claudio de Castro
Sociedade Brasileira de Cirurgia Plástica

Hiroshi Nishikawa
British Association of Plastic, Reconstructive and Aesthetic Surgeons

Katia Bustamante
Société Française de Chirurgie Plastique Reconstructrice et Esthétique

Sean M. Carroll
Irish Association of Plastic Surgeons

Riccardo Mazzola
Società Italiana di Chirugia Plastica Ricostruttiva ed Estetica

David Mendes
Israel Society of Plastic & Aesthetic Surgery

Mick Kreulen
Nederlandse Vereniging voor Plastische Chirurgie

Swee Tan
New Zealand Association of Plastic Surgeons

Vincent Yeow
Singapore Association of Plastic Surgeons

Chris Snijman
Association of Plastic and Reconstructive Surgeons of Southern Africa

Chul Park
Korean Society of Plastic and Reconstructive Surgeons

Lun-Jou Lo
Taiwan Society of Plastic Surgery

The Plastic Surgery Research Council

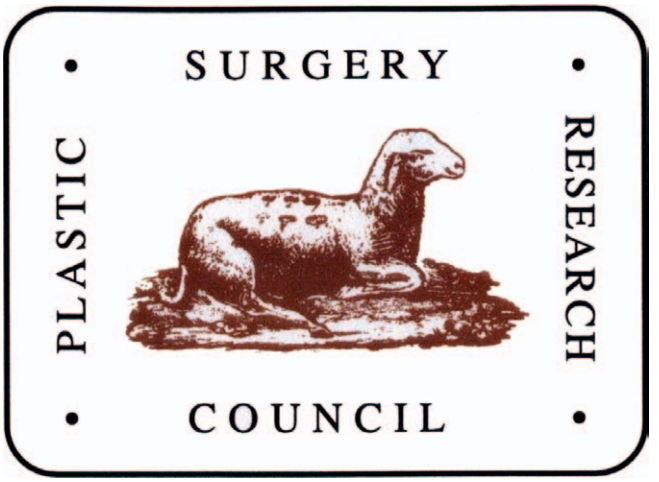

59th Annual Meeting

Hosted by Mount Sinai Medical Center
New York, New York

March 7–9, 2014

No Photography or videotaping is allowed during the scientific sessions
without prior approval by the Executive Committee.

TABLE OF CONTENTS

59TH ANNUAL MEETING OF THE PLASTIC SURGERY RESEARCH COUNCIL

OFFICERS AND EXECUTIVE COMMITTEE

Peter J. Taub, MD, FACS, FAAP
Chairman

Howard Levinson, MD
Secretary/Treasurer

David Mathes, MD
Scientific Program Chair

Timothy W. King, MD, PhD
Parliamentarian

William M. Kuzon, Jr., MD, PhD
Historian

James P. Bradley, MD
Past Chairman (2013)

Paul S. Cederna, MD
Trustee/Past Chairman (2012)

Bradon J. Wilhelmi, MD
Trustee/Past Chairman (2011)

Steven R. Buchman, MD
Endowment Chair

Kotaro Yoshimura, MD
Asian Liaison

Lars-Uwe Lahoda, MD, PhD
European Liaison

From the Office of the Chairman

I am thrilled and honored to be hosting the 59th Annual Meeting of the Plastic Surgery Research Council in my hometown of New York City. New York is described as the "Best City in the World." It is an easy destination to get to from most anywhere and has almost everything to offer. While the PSRC has been held here previously, it has not been in New York since 1995 and this will mark the first time that Mount Sinai Medical Center will serve as the host institution. I first presented at the PSRC in Galveston, Texas in 1997 as a general surgery resident and have been an active member since. I believe the PSRC is the most important society of our specialty. The work performed by our member surgeons is at the forefront of healthcare as a whole. Our members are the brightest and most creative we have to offer and to that end, I have incredible respect. This year's meeting will undoubtedly be exciting and provocative. I am fortunate to be able to plan the meeting with Dr. David Mathes who brings tremendous energy to our society. Unlike prior years, the entire program will be held at the brand new Conrad Hotel in Battery Park City, which overlooks the Hudson River, New York harbor, and the Statue of Liberty. Following the first day of presentations, there will be a Welcome Reception with attendees and exhibitors. Since the meeting coincides with the annual rite of "March Madness," we have reserved the basketball court at Stuyvesant High School for pick-up games after the reception. We may even hold the first lab tournament to be continued in the following years. Saturday night's Member's Dinner will be held at the nearby Tribeca Grill, which is co-owned by Robert De Niro, and serves a delightful New American menu. The remainder of the night was left free to explore the "City that Never Sleeps."

I welcome you to New York and look forward to hosting everyone this spring. Bring sneakers!

Peter J. Taub, MD, FACS, FAAP
2014 PSRC Chair
Mount Sinai Medical Center, New York, NY

The Plastic Surgery Research Council
500 Cummings Center, Suite 4550 – Beverly, Massachusetts – USA
t / 1-978-927-8330 f / 1-978-524-0498 e / meetings@ps-rc.org w / www.ps-rc.org

Letter from the Editor-in-Chief

The Plastic Surgery Research Council
59th Annual Meeting Abstract Supplement

Rod J. Rohrich, M.D.

In this edition of the official meeting abstracts of the Plastic Surgery Research Council (PSRC) you will be able to see the future of our field. This document represents the eighth consecutive time that these abstracts are published as a supplement to *Plastic and Reconstructive Surgery*. As Editor-in-Chief, I could not be more proud to have this perennially impressive document published in the White Journal. If the Journal represents culmination of science in our field, abstract supplements such as this one represent the birth of those scientific ideas; the abstracts presented for the 59th annual meeting of the PSRC are the raw ideas for research that will fuel clinical change and new discoveries in the years to come.

Strong ties between the Journal and American Society of Plastic Surgeons (ASPS) have existed for decades; as of this publication, the Journal has been an Official Organ of the PSRC for just over 8 years. We are grateful for the continuing support of the Council's current leaders, especially Chair Peter Taub, Chair-elect David Mathes, Timothy William Kuzon, Howard Levinson, Steven Buchman and the Council's international liaisons, Kotaro Yoshimura and Lars-Uwe Lahoda. Their efforts have lead this organization to some remarkable new discoveries that will be effecting Plastic Surgery in the years to come. In addition, we recognize the past PSRC leadership of Paul Cederna and Bradon Wilhelmi; the work of these impressive leaders work continues not only as PSRC Trustees but in myriad other areas of plastic surgery research and clinical application. We also recognize the work of James Bradley, Development Chair of the PSRC, whose efforts for the future of the organization are already manifesting in the present. We greatly appreciate the leadership of the ASPS/PSEF, especially ASPS President Robert X. Murphy, Jr., PSEF President Kevin Chung, ASPS Executive Director Michael Costelloe, ASPS Vice President of Research and Development Keith Hume, and ASPS Director of Publications Mike Stokes.

The Journal appreciates the ongoing financial support of the ASPS and PSEF to make the PSRC abstract supplement possible. As with every journal endeavor, we could not have published this special supplement without the efforts, energy and creativity of our publisher, Lippincott Williams & Wilkins, represented by Elizabeth Durzy. PSRC Executive Director Sara Neece and her dedicated staff, notably Jillian West (meeting manager) and Amy Nolfi (meeting coordinator), coordinated the receipt and review of the abstracts, supplied expertly prepared documents, and greatly facilitated the overall production of the supplement.

As with all supplements to *Plastic and Reconstructive Surgery*, all subscribers have access to all of the PSRC annual meeting abstracts. As an additional feature, I'm proud to announce that this supplement will be made available free online at PRSJournal.com for at least three months following publication; any interested party with internet access will have the ability to read this supplement. This is important because this affords us all a glimpse into what will be hitting the mainstream clinical plastic surgery advances in one to two years. By sharing this supplement free online, the PSRC is democratizing this information, giving all in our a field a chance to learn about this research.

The PSRC Meeting Abstract supplement to the Journal will share all the benefits of other PRS supplements, namely:

- Peer review of all content. Abstracts have been reviewed by the PSRC, and only those accepted after undergoing review are published here.
- Full indexing in such abstracting services as Index Medicus, Abridged Index Medicus, Current Contents/Clinical Medicine, Life Sciences, Science Citation Index, Research Alert, ISI/Bio Med, EMBASE/Excerpta Medica, and BIOSIS;
- Broad global readership through both print and web subscriptions and online databases such as OVID. Through the OVID database, the Journal and its supplements have a potential readership of over 13 million end-users worldwide.

Additionally, the contents of this supplement will be available through the PSRC website (www.psrc.org) as well as through the Journal's website (www.PRSJournal.com).

Scientific abstracts can be seen as the essence of scientific studies; the major efforts of study design, data collection, and interpretation of results have already been performed and are published in these abstracts. We encourage the authors of these abstracts to submit completed manuscripts based upon their abstracts. We look forward to these authors writing full studies based on their findings and submitting them to *Plastic and Reconstructive Surgery* or *Plastic and Reconstructive Surgery-Global Open (PRS GO)* through our online system, PRS and PRS GO's Enkwell (www.editorialmanager.com/prs).

I hope you find the Abstracts of the 59th Annual Meeting of the Plastic Surgery Research Council as fascinating, challenging and inspiring as I do.

Rod J. Rohrich, M.D.
Editor-in-Chief
University of Texas Southwestern Medical Center
5959 Harry Hines Blvd
Dallas, TX 75390–8820
rjreditor_prs@plasticsurgery.org

Historical Perspective: The Plastic Surgery Research Council

The following is compiled in part from
Peter Randall's Thirty-Five Year History of the
Plastic Surgery Research Council

Thomas S. Davis, MD
Historian Emeritus

In the early 1950's there was a "feeling" among "younger" plastic surgeons (those recently boarded or not yet boarded) of a need for an arena to discuss research in plastic surgery, including works in progress. The major plastic surgery organizations were perceived as forums for politics and jousting fields for the political giants of the day. The American College of Surgeons initiated the Surgical Forum in 1949, and later the plastic surgeon section in 1953 under the direction of Dr. Joe Murray. Still, the impression among the younger plastic surgeons was that research was "taking a back seat" in the mainstream plastic surgery organizations.

An informal meeting was held in San Diego, California in 1954. The "young bucks" enlisted the advice of trusted and more senior advisors. Drs. Lewis T. Byars (St. Louis), Brad Cannon (Boston), and Truman G. Blocker (Galveston) listened and lent encouragement. Their recommendations were to hold these meetings in a university setting and to include the local university talent in discussions in the field of research. Caution was also given regarding the possible considerable opposition to the formation of such a group. It was agreed that they would meet the following year. Sixteen individuals were picked to be invited to an "Organizational Meeting" held in Baltimore in the fall of 1955. The word "picked" implies selecting a few from the many, whereas actually this was more a search for the "any" from the "few."

At the time of the founding meeting of the Plastic Surgery Research Council in 1955 at Johns Hopkins, called by Drs. Milton Edgerton and Robin Anderson, Dr. Richard Stark submitted the drawing of Baronio's Sheep (1804) with auto and allografts in situ as a possible logo for the council.

Searching for a form other than the logo cliche of the circle, the design was made into a rectangle with rounded corners. It was accepted and has been the logo of the council since that time.

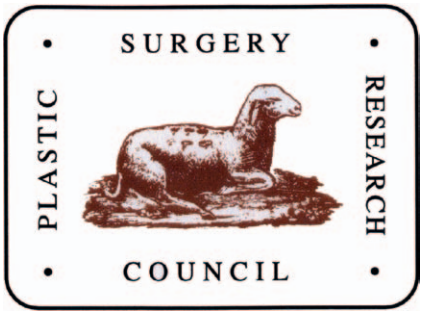

Fig. 1. PSRC BARONIO SHEEP LOGO

Following this first official meeting, Dr. Robin Anderson was asked to compose a Constitution and a set of By-Laws. A major objective of this Constitution and By-Laws was to maintain "a pure and virtuous" society "by avoiding the hierarchic pitfalls and elitist attitudes of the established societies." The members also decided not to align this meeting with any other plastic surgery organization. This two-page document was approved at the second meeting (1956) in Jackson, Mississippi, hosted by Dr. Jim Hendrix. The name of the organization was debated. One suggested the name, "Plastic University Surgeons" ("P.U.S."). However, the word "University" itself implied restriction and was ultimately discarded. The word "Council" was eventually (but not initially) chosen, and had literally been taken from the Indian usage of the word to indicate an open gathering of all those concerned.The name of the organization, "The Plastic Surgery Research Council," was officially adopted at this meeting. It has served this purpose well.

In 1981, The Peter Gingrass, MD Memorial Award was established by Dr. Ruedi Gingrass on behalf and in memory of his brother Peter. The award recognizes the medical student or non-plastic surgery resident presenting the best paper at the annual meeting of The Plastic Surgery Research Council. In 1982, The John F. Crikelair, MD

Research Award was funded by George Crikelair in memory of his son to recognize the best paper at The Plastic Surgery Research Council by a high school or college student. The Clifford C. Snyder, MD Past-Chairman Award was established in 1983 by Clifford Synder and funded in part by various past chairmen to recognize the best paper presented by a Plastic Surgery Resident or Fellow at the Plastic Surgery Research Council annual meeting. In 1997, The Best Poster Award was established by Dr. Robert Hardesty to recognize the value and contributions of Poster Presentations at the annual meeting of the Plastic Surgery Research Council. In 2000, the Shenaq International Research Award for the best paper by a foreign medical school graduate was funded by Dr. Sal Shenaq.

As time passed, the Research Council not only grew in numbers but also in respect among the "other societies and associations." The Research Council was formally asked to elect representatives to the American Association of Medical Colleges, Council of Academic Societies, Plastic Surgery Academic Advisory Council, American College of Surgeons (Plastic and Maxillofacial Council), American Association of Plastic Surgeons, the Plastic Surgery Educational Foundation Research Grants Committee, and the Council of Plastic Surgery Organizations. We are also asked to nominate candidates for the American Board of Plastic Surgery each year.

It is interesting to note that the basic tenants set down in the formative years of the Council have been maintained as guidelines for The Plastic Surgery Research Council. The original goals and concepts of an open forum with free discussion of work completed and work in progress continue, and the suggestions of "keep it young" and meet independently at research institutions continue. Specifically, at age 50 active members become senior members (with corresponding loss of voting privileges and inability to hold elected office) assuring a youthful and progressive leadership.

"Of the sixteen founding members of the Plastic Surgery Research Council, five have become Presidents of the American Society of Plastic and Reconstructive Surgeons (ASPS); four have become Presidents of the American Association of Plastic Surgery (AAPS); thirteen have been training program directors; three have been 'Clinician of the Year' of the AAPS; and two have received a Special Achievement Award of the ASPS. Eleven have become Directors of the American Board of Plastic Surgery; four have been Chairmen of the Board; and three have been Vice-Chairman of the Board"; one received the Nobel Prize in Medicine for his research on transplantation. What a magnificent heritage.

The Baronio Sheep

From time to time, members and others ask the origin of the sheep drawing that is the PSRC's official logo. The following attestation sheds a little light on this subject:

Degli innesti animali. Milan: Dalla Stamperia e Fonderia del Genio, 1804. This landmark work in the history of plastic surgery details the results of Baronio's experiments on autogenous skin grafting in animals at the close of the eighteenth century, the first such study to be carried out in scientifically organized experiments. Baronio (1759–1811), physician and naturalist, records and illustrates the first demonstration of a successful graft, removing skin from a sheep and transplanting it to a new site on the same sheep within an hour. The technique was successfully applied in humans some thirteen years later.

FRIDAY, MARCH 7, 2014

SCIENTIFIC SESSION 1
BEST PAPER PLENARY SESSION
2:30 PM – 4:00 PM

FRIDAY, MARCH 7, 2014

1
What's the Best Way to Allocate or Block Time? A Data Driven Approach to Departmental "Operations"

Jugpal Arneja, MD, MBA[1]; Jason Goto, MS[2]; Geoff Blair, MD[1]; Larry Gold, MS[2,3]; Barb Fitzsimmons, MD[1,3]; John Masterson, MD[1,3]; Erik Skarsgard, MD[1,3]

[1]University of British Columbia, Vancouver, BC, Canada, [2]Analysis Works, Vancouver, BC, Canada, [3]British Columbia Children's Hospital, Vancouver, BC, Canada

PURPOSE: In health care systems, although operating rooms (ORs) often function at high capacity, there often is a significant supply-demand mismatch resulting in waitlists for non-urgent surgery. Additionally, financial/Relative Value Unit (RVU) optimization is rarely considered when OR time is allocated. Within surgical departments, OR block allocations were traditionally based on historic apportioning and perceived priority amongst surgeons, rather than on scientific data. Since historical allocations of OR block time were simply based on conjecture, the introduction of Operating Room Allocation Methodology 'ORAM' creates an environment of transparency whereupon surgeons with the most need are recipients of the hospital's most expensive and most revenue generating fixed commodity, OR block time. Furthermore, in an effort to create value for an organization, or to incentivize departments, this methodology can be incorporated to optimize revenue in the form of allocating more OR time to services based on RVU generation. There have been no previous published reports of a similar methodology.

METHODS: A gap persists between our surgical resources and demand. ORAM reallocates the fixed pool of OR time amongst surgical divisions based on benchmarks. Over 6 months, the differences in waitlists (net arrivals) as well as completed cases were analyzed. Quantitatively, ORAM is predicated on 50% of the total calculation assigned to net arrivals and 50% given to operating on patients who were the most out-of-benchmarked-window. Reallocations occur semi-annually and a maximum 20% reallocation is possible to an individual surgeon. Qualitatively, a survey was sent to all surgical division chiefs to determine their subjective impressions of the ORAM process. An analysis was also performed to determine financial metrics associated with reallocation of block time.

RESULTS: Quantitatively, surgical waitlists reflected significant difference based on reallocations. No significant differences were found in OR costs associated with reallocation. Qualitatively, a data-driven methodology was accepted and favorably received by department members.

CONCLUSION: Although it is always a great challenge to deviate from historical comfort zones since no surgeon welcomes any loss of OR block time, feedback regarding ORAM has been positive. The method of putting science and data behind the decision making has been embraced by all services. With future iterations of ORAM we should arrive at a steady state of limited reallocations between services. ORAM provides the data needed to argue scientifically for more resources when and where needed. We are proud practitioners and teachers of evidence-based surgery, yet in the "operations" of our organizations little scientific data is employed to drive decision making. Optimization of either waitlists or RVUs can be more easily attained with the utilization of ORAM to allocate OR block time.

2
NOTCH3 Regulates Mural Cell Differentiation of HemSCs

Kyle J Glithero, MD; Naikhoba C O Munabi, BA; Ryan W England, BS; Alex Kitajewski, BS; Michelle Chang, BS; Jan K Kitajewski, PhD; Carrie J Shawber, PhD; June K Wu, MD
Columbia University Medical Center, New York, NY

PURPOSE: Infantile hemangiomas (IHs) are vascular hyperplasias with high flow and have been proposed to originate from hemangioma stem cells (HemSCs). Proper vessel maturation requires interactions between endothelial cells and their surrounding mural cells. IH pathology has been proposed to be partially due to defective mural cell function. Previous studies in our lab showed NOTCH3 inhibition in HemSC resulted in reduced blood flow in a murine IH model as detected by US Doppler. This correlated with reduced vessel diameter when compared to controls. Since Notch3 functions to regulate mural cell maturation, we determined if Notch3 has a role in mural cell differentiation of HemSCs.

METHODS: CD133+ HemSCs were isolated from resected hemangioma specimens. HemSC were transduced with lentivirus encoding a NOTCH3 shRNA (HemSC- shN3), an activated form of NOTCH3 (HemSC-N3IC) or a virus containing a scrambled sequence (HemSC-scr) serving as a control. HemSC-N3IC, HemSC-shN3 and HemSC-scr were grown in mural cell differentiation media. After two weeks, immunofluorescent staining was performed with antibodies against the mural cell markers, neuron-glial antigen 2 (NG2) and alpha smooth muscle actin (α-SMA). Fluorescence was quantified and averaged over multiple areas with ImageJ.

RESULTS: All CD133+ HemSC cell lines expressed low levels of NG2 at baseline (data not shown). When mural cell differentiation was induced, NOTCH3 knockdown upregulated NG2 compared to HemSC-scr. In contrast, NOTCH3 activation decreased NG2 expression. Expression of α-SMA was strongly upregulated in HemSC-scr and Hem-N3IC to a similar level in differentiation medium compared to cell maintained in growth medium (basal). α-SMA expression was unchanged from basal conditions in HemSC-shN3 cells.

CONCLUSIONS: In HemSCs, perturbations in NOTCH3 level differential altered the expression of mural cell proteins NG2 and α-SMA. In mural cell differentiation conditions NOTCH3 activation strongly downregulated NG2, while having no effect on the expression of α-SMA. In contrast, NOTCH3 inhibition modestly increased NG2 levels, and suppressed the upregulation of α-SMA. Thus, precise regulation of NOTCH3 signaling levels maybe necessary for proper mural cell differentiation of HemSCs.

3
Propranolol Accelerates Involution in a Murine Model of Infantile Hemangioma

Naikhoba C O Munabi, BA; Ryan W England, BS; Kyle J Glithero, MD; Michelle M Chang, BS; Alex Kitajewski, BA; Jan K Kitajewski, PhD; Carrie J Shawber, PhD; June K Wu, MD
Columbia University, New York, NY

PURPOSE: Propranolol has shown efficacy in the treatment of problematic infantile hemangiomas (IHs). Propranolol achieves this in part via an anti-vasculogenic effect on hemangioma endothelial cells. Previous studies in our laboratory suggested that propranolol induces accelerated adipogenesis of hemangioma stem cells (HemSCs) in culture. The goal of this study is to investigate the effects of propranolol treatment in a murine model of IH. We hypothesize that systemic propranolol will accelerate involution by affecting both vasculogenesis and adipogenesis.

METHODS: HemSCs isolated from human specimens and suspended in matrigel were injected subcutaneously into immunodeficient mice. Twenty-four hours after injection, mice were continuously administered oral propranolol or vehicle solution. Ultrasound (US) Doppler imaging of matrigel implants was performed weekly to assess for vascular flow. After 3 weeks, the matrigel implants were harvested and H&Es performed. Selected sections were examined for vascular density, vessel diameter, cellularity, total adipose content and number of adipocytes at 20X magnification.

RESULTS: US doppler of implants detected the presence of blood flow in mice receiving vehicle solution at 2 weeks after implantation. In contrast, there was an absence of discernable flow to the propranolol treated mice at the 3-week endpoint. Histologically, propranolol-treated IHs showed a 33% decrease in vascular density and 50% reduction in vessel caliber when compared to controls ($p < 0.0001$). Total adipose content was unchanged between vehicle and treatment groups. However adipocyte size was decreased in the propranolol-treated implant resulting in a significant increase in adipocyte number ($p < 0.05$). Despite the increase in adipocyte number, overall cellularity of the propranolol-treated implant was statistically reduced when compared to control ($p < 0.005$).

CONCLUSION: Propranolol treatment led to a loss of detectable blood flow, which correlated with decreased vessel density and caliber in a murine IH model. Propranolol treatment also resulted in increased adipocytes in the setting of decreased cellularity, which are hallmark characteristics of involuting IHs. These findings are consistent with published in vitro data and suggest that propranolol treatment accelerates involution of IH in this murine model.

4
Site Specific Targeting of PUMA Induced ROS Prevents Radiation Injury via a Smad3 Independent Mechanism

Karan Mehta, BS; Philip Lotfi, BS; Marc Soares, MD; Robert Dolitsky, BS; Piul Rabbani, PhD; April Ducksworth, MD; Nakul Rao, MD; Jessica Chang, BS; Amanda Hua, BS; Camilo Doig, BS; Camille Kim, BS; Pierre Saadeh, MD; Daniel Ceradini, MD

NYU Department of Plastic Surgery, New York, NY

PURPOSE: Although radiation therapy is an instrumental tool in the treatment of numerous cancers, it is hampered by its detrimental effects on the skin. Namely, impaired wound healing, fibrosis and scarring often requiring surgical intervention. Previously, we have demonstrated that radiation induced PUMA expression and subsequent ROS overproduction is a critical factor in the development of cutaneous fibrosis. However, it is unclear whether this effect is dependent on SMAD3 expression, a central fibrosis pathway. Here, we investigate the downstream molecular mechanism for radiation protection with PUMA knock down in cutaneous radiation injury.

METHODS: Fibroblasts treated with a single dose of radiation (15 Gy) following transfection with PUMA or nonsense siRNA were analyzed by rtPCR and Western blot for gene expression. PUMA or nonsense siRNA complexed with cationic lipid nanoparticles was applied to the skin of C57BL6 mice followed by cutaneous radiation injury. Clinical, histologic, and gene expression analysis for cutaneous fibrosis was performed. A SCAR index was calculated by staining with Sirius red and comparing the degree of pathologic dense red birefringence of collagen bundles to the yellow-green birefringence seen in uninjured tissue. Tensiometry was performed to assess the extent of fibrosis.

RESULTS: Topical silencing of PUMA using a cationic lipid nanoparticle delivery system resulted in a significant reduction in radiation induced injury in mice at 1 month. Clinically, PUMA treated mice showed markedly reduced ulceration, thickening and scarring at the site of injury as compared to nonsense siRNA treated animals. Appreciable re-growth of hair was also noted at irradiated sites in PUMA treated mice. These gross findings were supported by histology. Dermal thickness was significantly decreased in irradiated PUMA treated skin vs. nonsense treated skin (440um PUMA treated vs. 1,004um nonsense treated, $p<.001$). Vessel wall thickness was significantly improved as well (18.9um nonsense treated vs. 9.3um PUMA treated, $p<.001$). Less subcutaneous fat was lost in irradiated PUMA treated skin vs. nonsense treated skin ($1.25mm^2$ PUMA treated vs. $.63mm^2$ nonsense treated, $p<.005$). An 8.5 fold decrease in SCAR index was demonstrated in PUMA treated mice as compared to nonsense treated mice indicating a drastic reduction in fibrosis. Reduced fibrosis was supported by tensiometric measurements which indicated a 58% reduction in stiffness in PUMA silenced skin compared to irradiated nonsense control mice (0.25 N/mm nonsense control vs. 0.10 N/mm PUMA treated $p<.001$). Interestingly, PUMA silencing resulted in no change in SMAD3 expression suggesting the potential for an independent fibrotic pathway.

CONCLUSION: Through the use of PUMA silencing, we have demonstrated a powerful and effective method of limiting the destructive fibrotic and ulcerative sequelae of radiation therapy. Mechanistically, our results indicate that a pathway independent of the well established TGF-beta/SMAD3 fibrotic cascade may be at play. The use of topical inhibition of PUMA presents a clinically relevant and readily applicable approach to limiting the harmful skin effects of radiation treatment.

5
A 28-Day Prospective, Randomized, Double-Blind, Placebo Controlled Clinical Trial of Botulinum Toxin Type A for Raynaud's Phenomen

Kelli N Webb, MD; Nada N Berry, MD; Reuben A Bueno, MD; Michael W Neumeister, MD
Southern Illinois University, Springfield, IL

PURPOSE: Raynaud's phenomenon affects an estimated 28 million Americans and is a common cause of ischemic digits, severe pain, and nonhealing ulcers. Current treatment options can be ineffective, invasive, addictive, or have systemic side effects. Botulinum toxin type A (Btx-A) may be a novel therapeutic treatment option.

METHODS: A prospective, randomized, placebo-controlled clinical trial was designed to describe the efficacy of injected Btx-A in alleviating pain due to Raynaud's disease. Our secondary goal was to describe this minimally invasive therapy's effects and impact on quality-of-life by measuring subjective pain scores, pain-free intervals, ulcer healing, changes in hand function, finger survival, and subsequent treatment choices. Study participants were randomized to receive injection with either placebo (normal saline) or 100 units of Btx-A into the palm around involved digital neurovascular bundles. Data collection included subjective evaluation of pain relief, serial photography of wound healing, and objective data on tissue perfusion using a Doppler perfusion imager and Periscan image analysis software.

RESULTS: Currently, a total of 35 patients are actively participating in the study, which represents 88% of our total enrollment target (n=40). Twenty primary Raynaud's patients and fifteen secondary Raynaud's patients are enrolled. Seventeen of these subjects received placebo at the first study visit, and eighteen received the study agent, BOTOX®. At presentation, twenty-three patients reported pain as their primary complaint. At one month, one out of ten (10%) placebo patients compared with eight out of thirteen (62%) Btx-A patients reported pain relief (p=.0288). At the follow-up visit on day 28, the patients were unblinded and placebo patients were offered injection with Btx-A. We completed a follow-up retrospective survey, with average follow-up of 239 days. 22 of 35 patients (63%) report symptom relief after injection with Btx-A. Average duration of symptom relief is 127 days. 6 of 10 patients (60%) with fingertip ulceration healed after Btx-A injection.

CONCLUSION: Btx-A injection may be an effective, localized, nonsurgical treatment option without addictive properties or systemic side effects for treatment of ischemic digits. Preliminary results show a statistically significant number of Raynaud's patients injected with Btx-A report pain relief compared with placebo at 1 month follow-up and 60% of patients with fingertip ulcerations healed their wounds. The second part of this study is to follow these patients for 5 years to determine the long-term efficacy of Btx-A injection for Raynaud's Phenomenon.

6
The BREASTrial: Breast Reconstruction Evaluation of Acellular Dermal Matrix as a Sling Trial, Design and Stage I Outcomes of a Randomized Trial

Shaun D Mendenhall, MD[1]; Layla A Anderson, BA[2]; Jian Ying, PhD[3]; Kenneth M Boucher, PhD[3]; Leigh A Neumayer, MD, MS[2]; Jayant P Agarwal, MD[4]
[1]Southern Illinois University School of Medicine, Springfield, IL, [2]University of Utah School of Medicine, Department of Surgery, Salt Lake City, UT, [3]University of Utah School of Medicine, Division of Epidemiology and Biostatistics, Salt Lake City, UT, [4]University of Utah School of Medicine, Division of Plastic and Reconstructive Surgery, Salt Lake City, UT

PURPOSE: Use of acellular dermal matrix (ADM) in tissue expander (TE) breast reconstruction has become a popular alternative to the total submuscular technique. Recent meta-analyses have demonstrated increased complication rates when ADM is used in breast reconstruction, however this data is retrospective and based predominantly on one type of ADM. The BREASTrial aims to prospectively compare the incidence and severity of complications in ADM breast reconstruction between two commonly used ADMs.

METHODS: After IRB approval, a randomized trial was conducted to compare outcomes of immediate TE breast reconstruction using either AlloDerm (Lifecell) or DermaMatrix (Synthes) (clinicaltrials.gov identifier: NCT00872859). The impact of obesity, radiation, chemotherapy, mastectomy type, expander dynamics and drain time on complications and bio-integration of ADM was analyzed. The trial was divided into three different time periods/stages with the first stage results reported here. Logistic regression was utilized to determine predictors of complications.

RESULTS: 128 patients (199 breasts) were equally randomized over 2.5-years. The majority of patients were white, healthy, non-smokers. During stage I, there was no difference in overall rates of complications (33.6% vs. 38.7%, p=0.52), infections (13.9% vs. 16.3%, p=0.64), seromas (6.1% vs. 3.1%, p=0.34), hematomas (0% vs. 2%, p=na), skin necrosis (17.8% vs. 20.4%, p=0.66), or expander loss (5.0% vs. 11.2%, p=0.11) between the AlloDerm and DermaMatrix groups respectively. Complication grade was also similar (p=0.32). The AlloDerm group required less time to reach full expansion (42 vs. 70 days, p=0.001). No significant effect of obesity, radiation, or chemotherapy on incidence/severity of complications was detected. Obesity was a predictor of a longer need for drains (24% increase, p=0.02) and poor ADM bio-integration (OR 5.9, p=0.002) on multivariable logistic regression.

Longer drain time also increased odds of complication incidence, severity, skin necrosis, and poor ADM bio-integration (OR 1.04, 1.04, 1.04, 1.05 respectively, $p<0.04$). Infection, skin necrosis, and poor ADM integration were all associated with tissue expander loss ($p<0.001$).

CONCLUSION: Stage I outcomes of the BREASTrial emphasize the importance of careful patient and allograft selection in ADM-based breast reconstruction. Different types of ADM may impact outcomes such as expander dynamics and should be studied further. Multiple regression analysis indicated that obesity was a predictor of poor ADM bio-integration and a longer need for drains, both which are associated with higher complication rates. Results from this trial will assist plastic surgeons in making evidence-based decisions regarding ADM-assisted breast reconstruction.

7
Bioprosthetic versus Synthetic Mesh for Reconstruction of Oncologic Chest Wall Defects

Patrick B Garvey, MD, FACS; Mark W Clemens, MD; Johnathan P Doolittle, BS; Hong Zhang, MS; Donald P Baumann, MD, FACS; Charle E Butler, MD, FACS

The University of Texas MD Anderson Cancer Center, Houston, TX

PURPOSE: The traditional approach for reconstruction of thoracic defects following tumor extirpation has been to employ a synthetic prosthesis (i.e. polypropylene and/or methylmethacrylate). Because bioprosthetic mesh (e.g. porcine, bovine, or human acellular dermal matrix) has been demonstrated to have advantages over synthetic mesh in abdominal wall reconstruction (AWR), some surgeons are now also using bioprosthetic mesh in thoracic reconstruction, particularly in patients judged to be at increased risk for complications. However, while prior studies have demonstrated the advantages of bioprosthetic mesh in AWR, the benefits of bioprosthetic mesh over synthetic mesh for oncologic thoracic reconstruction are not well understood. We hypothesized that patients' outcomes will be superior with bioprosthetic chest wall reconstruction in comparison to synthetic mesh chest wall reconstruction.

METHODS: We retrospectively compared surgical outcomes for all consecutive patients who underwent reconstruction of complex, composite thoracic defects following oncologic tumor resection with either bioprosthetic or synthetic mesh at a single center over a ten-year period. We only included chest wall defects reconstructed with both mesh and locoregional flaps. We excluded flap only or mesh only reconstructions and patients with <6 months follow-up. The primary outcome measures for the synthetic versus bioprosthetic groups included overall complications, surgical complications, medical complications, infection, and mesh removal. Logistic regression analysis identified potential associations between patient, defect, and reconstructive characteristics and surgical outcomes.

RESULTS: 121 patients were included: 40 (33.1%) bioprosthetic versus 81 (66.9%) synthetic. Mean follow up was 36.7 months. Patient and defect characteristics were similar. Overall surgical complications were lower in the bioprosthetic (20.0%) versus the synthetic group (34.6%), although this was not statistically significant ($p=0.14$). Specific complications were also similar for the bioprosthetic versus synthetic groups, including medical complications (5.0% vs. 3.8%; $p=1.0$), infections (15.0% vs. 14.8%; $p=1.0$) and need for mesh removal (5.0% vs. 7.4%; $p=1.0$). Mulitvariate logistic regression analysis showed synthetic mesh to be an independent predictor of higher overall complications (OR=2.9; CI=1.0–8.6; $p=0.055$) in comparison to bioprosthetic mesh. Multivariate logistic regression also demonstrated preoperative radiation

therapy, ≥ 4 ribs resected, and chronic obstructive pulmonary disease to be significant independent predictors for overall complications, infection, and mesh removal. Different types of biologics generally performed similarly, although the bovine acellular dermal matrix cases did experience significantly more infections requiring mesh removal (18.7%) than did the combined human and porcine acellular dermal matrix cases (0%; p=0.0498) and the synthetic cases (0%; p=0.0038).

CONCLUSION: To our knowledge, this study is the first to directly compare outcomes for synthetic versus bioprosthetic mesh repair of composite chest wall reconstruction when combined with soft tissue flap coverage. While synthetic mesh was found to be an independent predictor of overall complications, given the findings of this study, we believe that surgeons should not routinely employ costlier bioprosthetic mesh for chest wall reconstructions that include flap coverage. Rather, surgeons should consider selectively employing a bioprosthetic mesh for chest wall reconstruction in patients with co-morbid characteristics that appear to be associated with complications such as preoperative radiation therapy, ≥ 4 ribs resected, or chronic obstructive pulmonary disease.

8
SDF-1 Regulates Adipose Niche Homeostasis and Adipose Derived Stromal Cell Function

Zeshaan N Maan, MBBS, MS, MRCS; Robert C Rennert, BA; Dominik Duscher, MD; Michael Januszyk, MD; Kevin Paik, BA; Michael T Chung, BA; Kevin Paik, BA; Toshihiro Fujiwara, MD, PhD; Melanie Rodrigues, PhD; Natalie Ho, High school; Hutton Baker, High school; Marcelina Perez, BA; Michael Hu, MD, MPH; Michael Sorkin, MD; Michael T Longaker, MD, MBA; Geoffrey C Gurtner, MD, FACS

Stanford University School of Medicine, Stanford, CA

PURPOSE: Chronic, poorly healing wounds, typically occurring in the setting of diabetes, remain a significant problem in clinical practice. Adipose derived stromal cells (ASCs) are gaining increased attention for wound healing applications. Unfortunately, diabetes affects the ASC niche environment and impairs the neovascular potential of ASCs, thereby reducing their efficacy in augmenting wound healing, limiting the therapeutic potential of autologous cell-based approaches. The factors involved in maintaining the ASC niche microenvironment are incompletely understood, though recent studies have suggested a role for endothelial cell-stromal interactions, potentially mediated by stromal-cell derived factor 1 (SDF-1). Interestingly, SDF-1 expression has been shown to be impaired in the setting of diabetes. Using a novel, Cre-lox genetic knockout, murine model, we studied the effect of global (gKO) and endothelial cell-specific SDF-1 knockout (eKO) on the ASC niche environment and ASC function.

METHODS: Inguinal fat pads were harvested from wild type (WT), diabetic, gKO and eKO mice. Whole tissue, representing the ASC niche, was processed for qRT-PCR. Primary cells were harvested from the fat for FACS analysis and cell culture. BrdU proliferation assay, human umbilical vein endothelial cell (HUVEC) co-culture tubulization assay in growth factor reduced (GFR) matrigel, adipogenic differentiation assay and survival assay were carried out on cells in passage 1.

RESULTS: ASCs from eKO and gKO mice demonstrated decreased proliferative capacity (*$p<0.001$) and survival (*$p< 0.05$) compared to WT, as well as decreased ability to induce tubulization of HUVECs (*$p<0.01$), similarly to diabetic ASCs. Adipogenic differentiation was significantly increased in eKO and gKO groups compared to WT (*$p<0.01$). eKO and gKO adipose tissue, representing the niche environment, demonstrated dramatic downregulation of FGF-2, VEGF, PDGF and their complimentary receptors, similarly to diabetic tissue (*$p<0.001$).

CONCLUSION: Endothelial cell-stromal interactions, mediated by SDF-1, play a pivotal role in maintaining ASC niche transcriptional homeostasis and preserving the functional capacity of ASCs. In the absence of SDF-1, ASCs are shunted towards adipogenesis, with reduced proliferative and pro-angiogenic capacity, impacting their physiological role within the adipose niche environment and their therapeutic potential in treating ischemia. The dysfunction of ASCs in diabetes may be related to downregulation of SDF-1 and subsequent disruption of the physiological cytokine milieu. Further investigation of the role of SDF-1 in ASC homeostasis and function, particularly in the context of diabetes, is ongoing to inform the development of autologous cell based therapies for diabetic wound healing.

9
Selectively Permeable Nanofiber Constructs to Prevent Inflammatory Scarring And Enhance Nerve Regeneration in Peripheral Nerve Injury

Karim A Sarhane, MD, MSc; Zuhaib Ibrahim, MD; Kellin Krick, PhD candidate; Russell Martin, PhD candidate; Baohan Pan, MD, PhD; Sami H Tuffaha, MD; Justin M Broyles, MD; Chris Cashman, MD/PhD candidate; Ruifa Mi, MD, PhD; Mohammed Alrakan, MD; Sepher Tehrani, MD candidate; Leah Goldberg, MD candidate; Hai-Quan Mao, PhD; WP Andrew Lee, MD; Gerald Brandacher, MD

Johns Hopkins University, Baltimore, MD

PURPOSE: Substantial advances have been made in enhancing nerve regeneration across gaps through the use of conduits and acellular nerve grafts. However, very few therapeutic approaches have been successfully studied in primary end-to-end repairs. Post-repair histologic studies commonly demonstrate scar tissue between coapted nerve stumps. In this study, we propose a novel semi-permeable nanofiber nerve wrap prepared from FDA approved biocompatible materials (polycaprolactone) to reduce inflammation at nerve coaptation site through inhibition of inflammatory cell infiltration while allowing diffusion of essential nutrients and growth factors.

METHODS: Nerve wraps were synthesized by electrospinning of randomly oriented 650-nm nanofibers, and constructs with pores smaller than 10 μm were obtained. Using Thy-1 GFP Sprague-Dawley rats, we performed sciatic nerve transection and epineural repair (control group) and with wrapping the coaptation site using the neuro-protective nanofiber construct (experimental group). Five weeks later, histologic analysis (Masson's Trichrome staining, ED1+TUJ1 immunofluorescence co-staining) was performed on nerve sections at the repair site to assess fibrosis (collagen deposition) and inflammation (macrophage invasion) *(n=5/group)*. Additionally, retrograde labeling was performed, and at the same time, the distal stump was harvested for histo-morphometric evaluation *(n=8/group)*.

RESULTS: Masson's Trichrome and double immunofluorescence staining (ED1+TUJ1) of nerve longitudinal sections 5 weeks following repair showed a significantly decreased level of intraneural scarring and inflammation in the nanofiber nerve wrap group, as determined by collagen quantification ($7.4\% \pm 1.3$ vs. $3.2\% \pm 1.3$, $p<0.05$) and macrophage counting (32.2 ± 2.4 cells/mm^2 vs. 14.6 ± 1.8 cells/mm^2, $p<0.05$) in the repair site. Collagen was trapped outside the nerve wrap in the experimental group. Nerve cross sections taken 5 mm distal to the coaptation site demonstrated a significantly increased

number of myelinated axons in the experimental group. Retrograde labeling showed a trend towards higher number of sensory dorsal root ganglion neurons that regenerated their axons in the nanofiber wrap group when compared to control.

CONCLUSION: These results provide new insights into a novel targeted anti-inflammatory approach in peripheral nerve repair. Electrospun nanofiber nerve wrap constructs protect the coaptation site from inflammation, promoting scar-free nerve repair, and enhancing axonal regeneration. This new therapeutic strategy utilizing FDA approved products holds great translational potential.

FRIDAY, MARCH 7, 2014

SCIENTIFIC SESSION 2
BEST PAPER PLENARY SESSION
4:00 PM – 5:30 PM

FRIDAY, MARCH 7, 2014

10
Global and Endothelial Cell Specific Deletion of SDF-1 Results in Delayed Wound Healing

Zeshaan N Maan, MBBS, MS, MRCS[1]; Natalie Ho, High school[1]; Robert C Rennert, BA[1]; Dominik Duscher, MD[1]; Michael Sorkin, MD[1]; Melanie Rodrigues, PhD[1]; Jerry Chen, MD[1]; Ivan N Vial, MD[2]; Michael Januszyk, MD[1]; Michael Findlay, MBBS, PhD[1]; Michael Hu, MD[1]; Graham Walmsley, BA[1]; Michael T Longaker, MD, MBA[1]; Geoffrey C Gurtner, MD, FACS[1]

[1]Stanford University School of Medicine, Stanford, CA, [2]University of Pittsburgh, Pittsburgh, PA

PURPOSE: Chronic, poorly healing wounds remain a significant problem in clinical practice, especially in the elderly and patients with diabetes mellitus. Poor neovascularization is thought to be fundamental to this problem. Stromal-derived factor-1 (SDF-1) is a chemokine involved in neovascularization and thought to play a major role in trafficking progenitor cells to ischemic tissue, under a HIF-1α dependent mechanism. Recent studies have found that diabetics and the elderly are deficient in SDF-1, suggesting a possible mechanism for poor wound healing. To better understand the role of SDF-1 in this setting, we studied the effect of global (gKO) and endothelial cell-specific SDF-1 knockout (eKO) on wound healing and cell behavior, utilizing newly developed murine models.

METHODS: A humanized excisional wound was created on the dorsum of gKO, eKO and wild type mice. Wounds were photographed and assessed at regular intervals. Tissue was harvested for histology and qRT-PCR. The excisional wound model was repeated in eKO and WT mice parabiosed to GFP+ reporter mice to assess recruitment of circulating progenitor cells.

RESULTS: The eKO and gKO groups both demonstrated slower wound healing, 15 days to closure compared with 11.75 in control mice (*p=0.006). This effect became evident by day 8, with significantly increased mean wound area relative to original size (control = 27%; gKO = 59%, *p=0.02; eKO = 55%, *p=0.03). WT mice demonstrated increased recruitment of circulating progenitor cells (GFP+, Lin-, CD64-) to wounds compared to eKO mice (*p<0.001). qRT-PCR demonstrated reduced transcription of SDF-1 (*p=0.002), epidermal growth factor (EGF) (*p=0.002), vascular endothelial growth factor (VEGF) (*p=0.03) and fibroblast growth factor-2 (FGF-2) (*p=0.02) in eKO mice v WT. Immunofluorescence studies demonstrated reduced expression of SDF-1 (*p=0.008), VEGF (*p<0.05), FGF-2 (*p=0.006) and CD31 (*p=0.02) in eKO mice.

CONCLUSION: SDF-1 plays a pivotal role in the wound healing response, particularly SDF-1 expression from endothelial cells. The importance of endothelial cell production of SDF-1 in wound healing is related to support of local cytokine expression, recruitment of circulating progenitor cells and promotion of neovascularization. Further investigation of these knockout models is ongoing to better elucidate the biology of SDF-1 within wounds.

11
The Role of Donor Antigen Persistance in Maintaining Immune Tolerance to a Vascularized Composite Allograft

Angelo A Leto Barone, MD; Zuhaib Ibrahim, MD; Saami Khalifian, BS; Karim A Sarhane, MD; Georg Furtmüller, MD; Madeline Fryer; Leah Goldberg, BS; Eric Wimmers, MD; Lehao Wu, MD; Mohammed Alrakan, MD; Jaimie Shores, MD; Steven C Bonawitz, MD; Justin M Sacks, MD; Chad R Gordon, MD; Giorgio Raimondi, PhD; Damon S Cooney, MD, PhD; WP Andrew Lee, MD; Gerald Brandacher, MD

Johns Hopkins, Baltimore, MD

PURPOSE: We have recently shown that indefinite graft survival can be achieved in a fully MHC mismatched swine hind limb transplantation model using a combined donor bone marrow infusion and co-stimulatory blockade regimen. The role of antigen persistence in the maintenance of tolerance in this setting, however, is still unknown. In this study we thus aimed to provide in vitro evidence supporting the clinical observation of tolerance and investigate whether donor-derived antigen persistence is necessary to maintain tolerance to a VCA.

METHODS: Recipients were conditioned using co-stimulatory blockade (CTLA4-Ig), BM infusion (60x107cells/kg) and a 30-day course of tacrolimus. Alloreactivity against donor and third-party antigens was assessed in vitro using Carboxyfluorescein Succinimidyl Ester-based mixed lymphocyte reaction (CFSE-MLR) assays. Graftectomy was performed in a tolerant animal on POD193 and donor-specific cellular responsiveness was assessed weekly thereafter. Upon return of responsiveness by MLR, the recipient underwent autologous, donor-matched and third party allogeneic (Yorkshire) STSGs and grafts were monitored daily to assess rejection. Serum samples were obtained weekly from POD 0 to 4 weeks following STSGs and donor-matched antibody production was assessed by flow cytometry.

RESULTS: Clinical immunosuppression free long-term survival was observed in all recipients (n=3). CFSE-MLR showed responsiveness against donor-matched peripheral blood mononuclear cells (PBMCs) before transplantation but unresponsiveness to donor while the viable graft was maintained. Response to third party allogeneic controls was maintained, confirming the ability of the conditioned animals to elicit a cellular response. Donor antigen specific tolerance was further confirmed in vivo by acceptance of donor-matched split-thickness skin grafts (STSG) and immunological competence assessed by third party allogeneic (Yorkshire) skin graft rejection. However, donor-specific responsiveness returned 5 weeks post-graftectomy. Subsequent donor-matched skin grafts were rejected by POD15 and third party Yorkshire grafts were rejected on POD7. The autologous control graft was viable at all time points. Baseline antibody levels decreased following allograft transplantation and remained low until secondary skin grafts were introduced. Following STSG, anti-donor and anti-Yorkshire antibody levels increased by week 2 (IgM) and weeks 3–4 (IgG). Antibody production was observed only following graftectomy and STSGs.

CONCLUSION: Our current conditioning regimen can induce immune tolerance in a fully MHC mismatched hind limb large animal VCA model. Such robust tolerance appears to be dependent on continuous presence of donor antigens. Furthermore, this data suggests that the return of the cellular response can trigger antibody production when a strong antigenic stimulus is present.

12
Achieving Tolerance in a Mismatched VCA Transplant While Reducing the Risk of GVHD: The Goal of Transient Chimerism

Bruce J Swearingen, MD[1]; Jeff Chang, MD[1]; David W Mathes, MD[1]; Tiffany Butts[2]; Scott Graves, PhD[2]; Rainer Storb, MD[2]

[1]University of Washington Medical Center, Seattle, WA, [2]The Fred Hutchinson Cancer Research Center Division of Transplantation Biology, Seattle, WA

BACKGROUND: Transplantation of vascularized composite allografts (VCA) to reconstruct devastating facial injuries and lost extremities offer the opportunity to truly restore both form and function. Due to the necessity of life-long immunosuppression, the clinical application of these techniques is limited. One promising method of inducing tolerance to an organ allograft is the development of mixed chimerism. We have previously demonstrated that a non-myeloablative stem cell transplant can lead to tolerance in a mismatched dog model. However, the application of this protocol has been limited by graft-versus-host disease (GVHD). We have observed several animals that, after an initial period of donor cell engraftment, lost their stem cell allograft but remained tolerant to the VCA. Conversely, animals that retained persistent donor cell chimerism inevitably developed GVHD. The hypothesis for this study was that our non-myeloablative hematopoietic stem cell transplant protocol could be used to induce tolerance to a recipient VCA without the need for persistent donor cell chimerism. To more closely mimic the clinical setting, our protocol was modified to an extended tapered cessation of immunosuppression.

METHODS: 5 Haploidentical canine recipients (median weight and age: 12.1kg and 10.9 months) received a non-myeloablative conditioning regimen of 350 cGy TBI, mobilized donor stem cells (PBMC) and VCA transplantation followed by a short course of immunosuppression (MMF for 56 days and Cyclosporine for 70 days). Peripheral blood chimerism was evaluated by PCR techniques weekly. Peripheral blood cytokine expression was evaluated by flow cytometry. VCA rejection was followed clinically and confirmed histologically after routine biopsies. 3 haploidentical canine recipients (median weight 13.3kg) were then transplanted following a modified immunosuppression protocol. Chimerism and cytokine expression were evaluated.

RESULTS: All 5 animals tolerated the conditioning regimen. One dog rejected the PBMC at 35 days post transplantation and went on to reject the VCA transplant following the cessation of immunosuppression. One dog fully engrafted and converted to 100% donor chimerism and long-term tolerance to the VCA but developed GVHD. 3 dogs demonstrated a prolonged period of transient chimerism (7 to 10 weeks post-transplant) and went on to reject their donor stem cells after the cessation of immunosuppression without acute rejection of their donor VCAs. One of these dogs was euthanized for persistent fevers at post-operative day 147 with no sign of rejection. The remaining two had long-term acceptance of their VCA (>200 days) with no evidence of acute rejection but have recently demonstrated evidence of chronic rejection. No dog developed GVHD. In the modified protocol, all 3 animals tolerated the conditioning regimen. All dogs fully engrafted and converted to 100% donor chimerism and long-term tolerance to the VCA. One dog developed GVHD upon cessation of immunosuppression.

CONCLUSIONS: We demonstrate that our non-myeloablative protocol allows for tolerance to the VCA with selective rejection of the PRBMC and reduction of GVHD risks while persistent donor chimerism can lead to GVHD.

13
Functional Analysis of Connective Tissue Growth Factor (ctgf) in Neural Crest And Craniofacial Development

Yawei Kong, PhD; Michael Grimaldi, BA; Tatiana Hoyos, MD; Eric C Liao, MD, PhD
Massachusetts General Hospital; Shriners Hospitals for Children Boston; Harvard Medical School, Boston, MA

PURPOSE: During vertebrate embryogenesis, cranial neural crest cells (CNCCs) contribute extensively to the formation of facial structures, including cartilage, bone and connective tissue. CNCCs are patterned and fated to distinct anatomical derivatives early at the onset of migration from the neural tube, target to pharyngeal segments and undergo multi-lineage differentiation. Several key pathways regulate CNCC migration and differentiation, including connective tissue growth factor (ctgf). ctgf is a member of the CCN family of secreted proteins, exhibits multiple activities in cell adhesion, migration, and differentiation. Previous studies have shown that ctgf-null mice were born with defects including cleft palate and severe chondrodysplasia, suggesting a critical role of ctgf in craniofacial development. However, the mechanistic basis of how ctgf affects CNCCs behavior and how ctgf is coordinated with other signaling pathway such as wnt signaling during development remain unclear. To this end, we took advantage of genetic approaches in zebrafish generating ctgf-mutant cleft palate model to elucidate the potential function of ctgf in CNCC migration, proliferation and/or convergence extension mechanisms.

METHODS: Gene expression profiling was analyzed by Affymetrix gene-chip. Spatiotemporal expression analysis was performed by wholemount RNA in situ hybridization (WISH). Morpholino-mediated gene knockdown was performed to assess gene function in vivo. Targeted mutagenesis of ctgf locus was achieved by the latest CRISPR/Cas genome editing method.

RESULTS: Expression profiles of two zebrafish homologues for ctgf gene, ctgfa and ctgfb, were characterized by WISH and found to be compatible with a role in craniofacial development. During embryogenesis (24–96 hpf), we observed that the spatiotemporal expression of both ctgfa and ctgfb faithfully delineate the pharyngeal arch region and the derived craniofacial skeleton. Specifically, ctgfa was expressed in the ectoderm that surrounds the palate, the oral ectoderm, as well as the chondrocytes that constitute the palate. Despite their similar expression patterns, in vivo functional analysis by Morpholino-mediated gene knockdown showed that impaired ctgfa leads to craniofacial defects, featured by loss of facial soft tissues, missing lower jaw, and truncated palate with a cleft phenotye at the anterior edge of the seam between median and lateral ethmoid plate. However, ctgfb-knockdown had subtle effects on craniofacial morphogenesis. Collectively, these results suggest an indispensible role for ctgfa in palate and lower jaw development. To gain mechanistic insight into ctgf function during craniofacial development, we have generated both ctgfa and ctgfb mutants by CRISPR/Cas, where targeted short-nucleotide deletion resulted in truncated protein translation. This ctgfa/ctgfb mutant model provides us with an important tool to access the genetic basis of cleft palate malformation.

CONCLUSION: This study underscores the important role of ctgf in CNCC development, and highlights the utility of the zebrafish model to interrogate palate and craniofacial morphogenesis using reverse genetic approaches. Our ongoing work to elucidate the molecular basis of ctgf-associated cleft palate helps to identify other risk loci and develop potentially preventive measures via pharmacologic manipulation of craniofacial development during early embryogenesis.

14
Requirement of Specc1lb in Facial Prominence Integration and Formation of the Lower Jaw

Lisa Gfrerer, MD[1]; Valeriy Shubinets, MD[1]; Christina Nguyen, MD[1]; Cynthia C Morton, PhD[2]; Richard L Maas, MD PhD[2]; Eric C Liao, MD PhD[1]

[1]MGH, Boston, MA, [2]Brigham and Women's Hospital, Boston, MA

PURPOSE: The genetic basis of the rare oblique facial cleft (ObFC) has been unknown until the identification of SPECC1L from human translocation analysis. SPECC1L is a novel scaffolding protein where its molecular function in craniofacial morphogenesis is unknown. We explore the function of SPECC1L in craniofacial development by studying its homologs in zebrafish, where specc1lb is the ortholog.

METHODS: Gene expression analysis was carried out by wholemount RNA in situ hybridization (WISH). Antisense morpholino (MO) knockdown and mRNA rescue was performed for functional analysis. Lineage tracing, cell proliferation, apoptosis assays, and molecular analysis were performed.

RESULTS: WISH revealed specc1lb expression to be in the epithelia juxtaposed to chondrocytes, suggesting expression in the ectoderm surrounding the neural crest cells. specc1lb may alter expression of other ectodermal molecules (edn,wnt9, fgf8, shh) and thereby inhibit normal chondrocyte formation. Knockdown of specc1lb showed distinct craniofacial phenotypes resulting in clefts between the median and the lateral elements of the primary palate. Lineage tracing analysis revealed that CNC cells contributing to the frontonasal prominence failed to integrate or "fuse" with the maxillary prominence CNC cells. This resembles the pathogenesis of ObFC development in humans, where failure of fusion between the lateral nasal process and maxillary prominence occurs. Cells normally contributing to the lower jaw structures were able to migrate to their destined position but failed to form the mandibular elements. This defect is also observed when wnt9a, frzb and fzd7a are targeted by morpholino. Further, the same mandibular phenotype occurs in edn1−/− morphants. In specc1lb knockdown morphants, the developing ethmoid plate failed to extend fully, a process known to be regulated by wnt9a. Furthermore, genes of the wnt receptor complex (wnt9a, frzb, fzd7a) were downregulated in specc1lb morphants. In addition, ednra2 and edn1 expressions were unchanged, but homeobox transcription factor bapx1 (a downstream target of edn1) was downregulated. Co--injection of bapx1 mRNA and specc1lb MO rescued lower jaw elements, confirming that bapx1 acts downstream of specc1lb in jaw specification.

CONCLUSION: Taken together, this analysis suggests that specc1lb is required for integration of upper jaw palatal elements and convergence of mandibular prominences, potentially acting as a scaffolding protein to integrate wnt and edn pathways. Future protein chemistry experiments are underway to elucidate the cellular function and identify interactors of specc1lb. We present the first animal model of ObFC and morphogenetic insight into the mechanisms of normal palatogenesis and cleft molecular pathogenesis.

15
Characterization of the Endothelial Progenitor Cell from Adult Tissue using Vav/Cre RFP-GFP Murine Model and Single Cell Microfluidics

Melanie Rodrigues, PhD; Robert C Rennert, BA; Sarah Bishop, MD; Michael Januszyk, MD; Zeshaan Maan, MD; Michael Sorkin, MD; Dominik Duscher, MD; Geoffrey C Gurtner, MD
Stanford University, Stanford, CA

PURPOSE: Endothelial progenitor cells (EPCs) from circulating blood have been shown to form blood vessels and are touted to aid in therapeutic neovascularization. However, EPCs are inadequately characterized and current isolation relies on intricate in vitro culture techniques rather than a defined surface-marker profile, limiting their immediate utilization.

METHODS: To characterize EPCs, our lab developed a transgenic mouse, vav-cre RFP-GFP, with cells of the hematopoietic lineage expressing GFP and non-hematopoietic cells, expressing RFP. In parallel, we established a microfluidics-based single cell transcriptional analysis technique to identify cell surface markers for these elusive cell-populations. Combining these novel techniques in a parabiotic model of neovascularization, we aimed to isolate unique EPC populations and determine their origin, hierarchy and cell surface characteristics.

RESULTS: Parabiosis of vav-cre RFP-GFP to a severe combined immunodeficiency (SCID) mouse containing an ischemic flap on its dorsal surface repeatedly drew in GFP+ but not RFP+ cells from the vav-cre mouse. GFP+ Lin- cells, considered putative progenitor cells from the vav cre were isolated on a single cell level from the flap of the SCID mouse. Single cell microfluidic PCR on these cells revealed three distinct stem cell/ progenitor sub-populations of hematopoietic origin entering the ischemic neovascularization site: a circulating hematopoietic stem cell population c-kit+, CD34-, Sca1 low, Myc+, a stem cell population of hematopoietic origin CD34+ Sca1+ Klf4+ Cxcl12+, and most importantly a putative endothelial progenitor cell population, expressing both stem cell genes Sca1, CD34, Klf4 as well as endothelial genes. These cells were traced to the bone marrow and were found to be present at the neovascularization site even after 4 weeks of injury. Cryosections of the ischemic flap on the SCID mouse confirmed the incorporation of these stem/ progentior cells at regions of neovascularization.

CONCLUSION: We have identified a circulatory endothelial precursor cell derived from the bone marrow, which incorporates into blood vessels at sites of neovascularization.

16
The Analgesic Efficacy of the Transversus Abdominis Plane (TAP) Block on the Abdominal Donor Site Following Autologous Tissue Breast Reconstruction: A Double-Blind, Placebo-Controlled Randomized Trial

Toni Zhong, MD, MHS; Marie Ojha, RN-EC; MN; Shaghayegh Bagher, Msc; Kate Butler, MHSc; Coimbatore Srinivas, MD; Stuart A McCluskey, MD; Hance Clarke, MD; Anne O'Neil, MD, PhD; Christine Novak, PhD; Stefan OP Hofer, MD, PhD
University Health Network, Toronto, ON, Canada

PURPOSE: The Transversus Abdominis Plane (TAP) block is a peripheral nerve block of the T6-L1 intercostal nerves of the abdominal wall. The analgesic efficacy of the TAP nerve block for postoperative pain control following abdominally-based breast reconstruction has never been studied in a randomized controlled trial (RCT).

METHODS: We conducted a double-blind, placebo-controlled RCT that followed a single-centre, 1:1 allocation, two-arm parallel group superiority design in patients undergoing microsurgical abdominally-based breast reconstruction. Intraoperatively, bilateral multi-orifice epidural catheter were inserted under direct vision into the transversus abdominis plane (TAP) through a 3cm incision in the Triangle of Petit. Postoperatively, patients were randomly assigned to receive intermittent boluses of a 0.2 mL/kg of 0.25% Bupivacaine (study group) or saline (placebo group) through the bilateral TAP catheters every 8 hours for the first 2 postoperative days (POD). In both groups, patients received intravenous hydromorphone through a patient-controlled analgesic (PCA) pump programmed for the demand-only mode set at 0.1mg/bolus every 5 minutes with no basal rate. Both the TAP catheters and PCA were discontinued on POD 3. The primary objective was compare the mean daily opioid consumption in the first 3 days following surgery between the control and study groups in intravenous morphine equivalent units. The secondary outcome measures included total in-hospital cumulative opioid and anti-nausea consumption, daily patient-reported pain scores, nausea and sedation scores, Quality of Recovery score, time to ambulation, and duration of hospital stay. All results were analyzed using intention-to-treat.

RESULTS: Between September 2011 and April 2013, of the 155 patients assessed for eligibility, 18 were ineligible, 44 declined participation, and 93 patients enrolled into the trial and underwent randomization and surgery. Forty-nine patients received Bupivacaine (study arm) and 44 receive isotonic saline (control arm) in their TAP catheters postoperatively. A

total of 85 patients completed the primary outcome assessments, 47/49 patients in the study group and 38/44 in the control group. Seventy-one patients had DIEP flaps and 14 patients had free muscle-sparing TRAM flaps. There were 11 postoperative complications (13%), 7 in the treatment group, 4 in the control group, and none was related to TAP catheter, and there were no flap failures. Randomization resulted in a balanced distribution of patients, and there were no differences in age, BMI, clinical or demographic characteristics between the two groups. For the primary outcome, the reduction in parenteral morphine consumption was only significantly different between the two groups on POD 1. In the Bupivacaine group, the mean parenteral morphine consumption was 20.7 (SD=20.1) mg compared to 30.0(SD=19.1) mg in the placebo group (p=0.02) on POD 1. There were no differences between the two groups in any of the secondary outcomes measures.

CONCLUSIONS: This double-blind, placebo-controlled RCT showed that the TAP block is a safe peripheral nerve block and it provides a significant reduction in parenteral morphine consumption in the early postoperative period following abdominally-based microsurgical breast reconstruction.

17
Prototype Sensory Regenerative Peripheral Nerve Interface for Artificial Limb Somatosensory Feedback

John V Larson, BS[1]; Melanie G Urbanchek, PhD[1]; Jana D Moon, BS[1]; Daniel A Hunter, PhD[2]; Piyaraj Newton, BS[2]; Philip J Johnson, PhD[2]; Matthew D Wood, PhD[2]; Theodore A Kung, MD[1]; Paul S Cederna, MD[1]; Nicholas B Langhals, PhD[1]

[1]University of Michigan, Ann Arbor, MI, [2]Washington University School of Medicine, Saint Louis, MO

PURPOSE: Major advances in both robotic and neural interface technologies have improved functional control of advanced prosthetic limbs. However, despite considerable success in improving motor function, interface technology supporting long-term somatosensory feedback remains unavailable. For this purpose, our laboratory has developed a prototype sensory regenerative peripheral nerve interface (sRPNI) to receive signals gathered from tactile sensors on an advanced prosthesis and seamlessly transfer this signal to the residual nerves of an amputated limb. As the first major investigation of sensory RPNI technology, this study examined sRPNI viability, reinnervation, and signal fidelity.

METHODS: Twelve rats underwent sRPNI fabrication. To demonstrate reinnervation, after a convalescent period of 3 - 4 months, *in vivo* sensory recordings were obtained from the sRPNI while electrically stimulating the sural nerve. sRPNI muscle, sRPNI sural nerve, and control EDL muscle and sural nerve from the contralateral limb was then harvested for mass comparisons, and evaluated through the application of both histomorphometric and immunohistochemical techniques.

RESULTS: Upon gross examination, sRPNIs appeared well vascularized, healthy, and viable. The average mass of sRPNI muscle was 75.2% that of control EDL muscle (SD 0.127). Neural-evoked responses from sRPNIs were successfully recorded, confirming sRPNI viability and signal transfer. During electrophysiological testing, the average stimulation threshold required for eliciting a compound action potential was 143.8 μA in 3-month sRPNIs and 99.6 μA in 4-month sRPNIs, indicating continued regeneration and reinnervation. Furthermore, 3-month sRPNIs demonstrated an average compound action potential peak-to-peak amplitude of 0.68 mV, compared with 2.27 mV in 4-month RPNIs. As expected, both groups exhibited similar muscle latencies. Histological analysis of sRPNI muscle revealed normal architecture with the fiber sizes and distributions comparable with control muscle. sRPNI sural nerve also demonstrated healthy nerve fiber architecture consisting of large and small myelinated fibers nearly equivalent to control sural nerve. Immunohistochemical evaluation revealed minimal cellular inflammatory response and numerous axons within sRPNI muscle tissue.

CONCLUSION: Comparisons of electrophysiological responses, muscle mass, and histology indicated that sRPNI muscle and nerve fiber recovery approached equivalence. These findings demonstrate that freely transferred muscle becomes reinnervated and viable when neurotized by a transected sensory nerve. Furthermore, electrophysiological signal is successfully transmitted between the sRPNI and residual nerve. Through electrical stimulation of this functional sRPNI, there is enormous potential for enhancing the recovery and quality of life of thousands of amputees by restoring the sense of touch.

ACKNOWLEDGEMENT: This work was sponsored by the Defense Advanced Research Projects Agency (DARPA) MTO, Pacific Grant/Contract No. N66001-11-C-4190.

18
Real-Time Proportional Control of a Neuroprosthetic Hand by a Rodent Regenerative Peripheral Nerve Interface

Christopher M Frost, BSE; Daniel Ursu, MS; Andrej Nedic, MSE; Cheryl A Hassett, BS; Jana D Moon, BS; Brent Gillespie, PhD; Nicholas Langhals, PhD; Paul S Cederna, MD; Melanie G Urbanchek, PhD
University of Michigan, Ann Arbor, MI

PURPOSE: Regenerative peripheral nerve interfaces (RPNIs) are implantable bioartifical interfaces designed to transduce signals between peripheral nerves and prosthetic limbs. RPNIs implanted into rats have shown long-term stability and viability for up to 2 years. To date, control algorithms for translating RPNI signals into real-time control of a neuroprosthetic limb have not been demonstrated. The purpose of this study was to: a) design and validate a system for translating RPNI signals into real-time control of a neuroprosthetic hand; and b) use the RPNI system to demonstrate proportional control of a neuroprosthetic hand.

METHODS: Three experimental groups were created in a rat model: 1) Control (n=2); 2) Denervated (n=1); and 3) RPNI (n=3). For the Control groups, the soleus muscle was denervated and a proximal and distal tenotomy with repair was performed. For RPNI and denervated groups, a free soleus muscle was transferred to the lateral compartment of the ipsilateral thigh. In the RPNI group the transferred muscle was reinnervated with the divided tibial nerve. In all groups, bipolar stainless steel wire electrodes were positioned on the muscle. Evaluation was performed 4–5 months after implantation. Voluntary movements were evoked in response to Von Frey monofilament stimulation on the lateral ankle. Using a peak detection algorithm in LabView, RPNI activity was scanned in 300-msec windows and integrated in real-time. Rat movements were videographed in high speed (120-fps). In total, 1040 control and 876 RPNI prosthesis activations were analyzed.

RESULTS: Voluntary rat movement activated the prosthesis in Control and RPNI groups reliably throughout the testing period of up to 15 continuous minutes with no observable instrumentation failure or biological fatigue. As expected, leg movement in the denervated group did not activate the prosthesis further validating the system and indicating minimal signal contamination from surrounding muscle groups within the RPNI. Signal to noise ratio between resting iRPNI and iRPNI after leg movement was excellent across control and RPNI groups (3.55 and 3.81, respectively). “Sensitivity” to accurately detect activation after stimulation and “specificity” to prevent unwanted activation during rest were excellent across RPNI, control, and denervated groups. Both RPNI and control groups showed a logarithmic increase in iRPNI with increasing Von Frey filament size (R^2=0.758 and R^2=0.802,

respectively). Higher iRPNI increased output voltage to the prosthesis giving graded control of hand speed.

CONCLUSION: This study demonstrates for the first time that an RPNI can be used to directly control a prosthetic arm. Signal contamination from muscles adjacent to the RPNI is minimal. Further, the RPNI can provide reliable proportional control of prosthesis hand speed.

ACKNOWLEDGEMENTS: This work was sponsored by the Defense Advance Research Projects MTO under the auspices of Dr. Jack Judy through the Space and Naval Warfare Systems Center, Pacific Grant/Contract No.N66001-11-C-4190.

SATURDAY, MARCH 8, 2014

SCIENTIFIC SESSION 3 GROUP A
ASSORTED
8:30 AM – 9:30 AM

SATURDAY, MARCH 8, 2014

19
The Effect of Whole Body Vibration on Life Expectancy, Cell Damage and Inflammation in a Murine Model

Henrik O Berdel, MD; David Moore, Medical Student; Franklin Davis, Medical Student; Jun Liu, BS; Hongyu Yin, MD; Mahmood Mozaffari, PhD, DMD; Jack C Yu, MD, DMD, ME Ed, FACS; Babak Baban, PhD
Medical College of Georgia, Augusta, SC

PURPOSE: Diabetes impairs wound healing, and increases surgical infection, leads to higher morbidity, mortality, hospital stay, and cost, thereby immensely affecting all surgical specialties. The pathogenesis of type 2 diabetes (T2D) has previously been explained by insulin resistance due to obesity and glucotoxicity in the liver and skeletal muscle. However, current models attribute these precipitating factors to immune imbalance. Chronic, low-grade inflammation has been described as preceding factor. As dietary changes and increased exercise are time consuming and strenuous, thereby often resulting in low long-term compliance, alternative strategies of treatment and prevention are under investigation. Whole body vibration (WBV) has been described as a potential preventative intervention. In this study, we tested whether WBV therapy can prolong life, reduce cell damage, and decrease the pro-inflammatory cytokine IL-17 in db/db mice.

METHODS: 4 of a total of 8 C57/BL6 db/db mice (10 week old) were subjected to high frequency (20–30 Hz), low amplitude (0.5 g) WBV therapy for 20 minutes/day, 5 days/week for 7 weeks using a fabricated vibrating platform. After 7 weeks of treatment, blood samples were subjected to flow cytometric analysis. γH2AX was measured as marker for DNA damage, and IL-17 served as index for the inflammatory response. As 3 of the 4 control mice died, the data for γH2AX and IL-17 were gathered from two separate blood drawings of the same mice. Chi-square test and student's t-test with 2 tails were used to investigate a significant difference in survival, and in γH2AX-, and IL-17 levels, respectively.

RESULTS: The survival of mice undergoing WBV therapy was significantly higher, with a P value of 0.047. DNA damage was significantly lower with an average γH2AX level of 0.47 % of total blood cells in the vibrated group, compared to 1.00 % of total blood cells in the control group (P = 0.006). The average IL-17 level of 5.29 % of total blood cells in the vibrated group was dramatically lower than the average of 8.50 % of total blood cells in the control mice (P = 0.018). Interestingly, although not quantified in this study, the vibrated group maintained their weight and lost less hair than the control mouse, which doubled its weight.

CONCLUSION: WBV therapy shows incredible promise as a preventative measure, especially in the younger population at risk for developing diabetes. In addition to improved survival, db/db mice undergoing WBV therapy show less tissue damage, and signs of a decreased systemic inflammation normally seen in diabetics. This attenuated response could prove beneficial in helping prevent and delay the progression of diabetes and its complications. Ultimately, a better understanding of WBV therapy, its potential benefits, and implementation of such therapy could be a simple yet highly effective addition to dietary changes and exercise. In contrast to the later WBV may be maintained more easily, and show higher long-term compliance.

20
Prediction of Optimal Proximal Interphalangeal Joint Fusion Angle Using Simulated Joint Arthrodesis

Yevheniy Lider, BS; Mitchell Fourman; M Phil; Karen DeChello, MS, OTR/L; Arjun Iyer, BS; Sue Sisto, PhD, PT, FACRM; Alexander Dagum, MD

Stony Brook University Medical Center, Stony Brook, NY

PURPOSE: Arthrodesis is a common surgical treatment for arthritis of the proximal interphalangeal joint (PIPJ); however, few studies have investigated the functional impact of the loss of mobility within the joint - as a result, the selection of the angle at which to fuse the PIPJ is based on the surgeon's personal experience. In this study, we comprehensively investigate the effects of index PIPJ fusion at several angles on hand performance, hand motion, and subjective perception with the goal of identifying the optimal fusion angle.

METHODS: In a randomized trial, a battery of hand function tests were administered to healthy participants whose index PIP joints have been splinted at specific angles(30°,40°,50°,60°). For each of the four splinted conditions and one unsplinted control, each participant performed the Purdue Pegboard Dexterity Test, the Jebsen-Taylor Hand Function Test, and a pulp-to-pulp pinch dynamometer while the kinematics of the upper extremity was measured using a motion capture system. The Michigan Hand Questionnaire, QuickDASH, and a custom survey were administered to measure the perceived impact of the simulated fusion. Statistical analysis was performed using the Friedman test and Wilcoxon signed-rank test. $P<0.05$ was considered significant.

RESULTS: Data were collected for 14 participants who attained the mean scores of: 16.0(SD=1.5), 14.3(SD=1.7), 14.5(SD=2.3), 14.0(SD=2.4) 13.6(SD=2.1) for the pegboard task, 10.0(SD=2.2), 8.98(SD=1.7), 9.38(SD=1.9), 9.65(SD=1.7), 9.17(SD=2.2) for the pinch strength test, and 44.7(SD=6.5), 49.0(SD=5.8), 50.6(SD=5.7), 49.2(SD=5.5), 49.1(SD=5.3) for the Jebsen-Taylor test during the unsplinted, 30°, 40°, 50°, and 60° conditions respectively. A learning trend was observed and the data were normalized using the group average for each trial prior to statistical analysis. Participants performed best while splinted at 40° during the pegboard task, 50° during the pinch strength test, and 30° during the Jebsen-Taylor task. No significant difference has been observed among the splinted conditions for the pegboard and Jebsen-Taylor tasks, but has been observed for the pinch test. Significant difference in pinch strength has been observed between the angles of 30° and 50° (t=-2.277, with df=13, P=0.048).

CONCLUSION: Preliminary performance data (N=14) suggests that optimal angle depends on the task and is trending toward an optimal angle of 40° for the pegboard task and 50° for the pinch. For the 50° condition, pinch strength did not significantly differ from unsplinted condition, indicating little loss in pinch strength at that angle. Gross functional tasks as measured by the Jebsen-Taylor assessment do not appear to be significantly affected by varying splint angles. This may be due to the relatively simple motion required for the completion of the tasks and the ability of the subject to compensate. Secondary analysis revealed that best-performing angles differed between subjects, suggesting that optimal angle may be a function of individual factors such as hand geometry.

21
Frequency and Impact of Inappropriate Emergent Transfer for Hand Surgical Consultation

Brian C Drolet, MD[1]; Yifan Guo, MD[1]; Benjamin Z Phillips, MD[1]; Vickram J Tandon, BA[2]; Scott T Schmidt, MD[1]

[1]Rhode Island Hospital, Providence, RI, [2]Alpert Medical School of Brown University, Providence, RI

PURPOSE: Approximately one in five Americans presents to an emergency department (ED) each year. With a total of 130 million visits in 2010, ED encounters made up 4% of all healthcare spending. Evaluation of hand and upper extremity diagnoses has been reported for up to 15% of ED visits. Previous studies have demonstrated that "hand surgery" evaluation is a common reason for patient transfers. We sought to identify the frequency and impact of "unnecessary" transfers for emergency evaluation by a hand surgeon.

METHODS: Our level 1 trauma center maintains an electronic database of all inter-hospital transfers and direct referrals requests for ED evaluation. We reviewed over 30,000 consecutive ED referrals in this database between April 2009 and April 2013 and identified 805 transfers related to hand and upper extremity 'emergency' evaluation. We then performed a retrospective review of these patients' charts. Three independent reviewers coded each referral as either appropriate or inappropriate based on a predetermined set of criteria. When coding discrepancies were noted, final classification was determined by consensus discussion. Other variables such as time in transfer, insurance status, and patient charges were also evaluated.

RESULTS: Most patients were transferred from a different ED (72%), and nearly all (99.7%) of these patients were transferred from a hospital with 24-hour general orthopedic coverage. The remaining patients were transferred either from urgent care (16%) or a private physician office (10%). Of all patients referred for 'emergency' hand evaluation, 194 (24%) were deemed appropriate. In fact, we found that 16% of patients received no hand surgery evaluation upon transfer, and another 22% were seen as a hand surgery consult but were discharged from the ED with no procedure or intervention. The average transit time for these inappropriately transferred patients was 71 minutes and the average ED time was 336 minutes. Average hospital charges incurred were $5381 for a total expenditure of 3.3 million dollars. Patients without insurance were more likely to be transferred inappropriately than those with insurance (OR = 1.3, $p<0.05$).

CONCLUSION: This is the first empirical study reporting appropriateness of emergency referral for hand surgery consultation. Using a classification system based on intervention, diagnosis and several other variables, we found that a minority of patients required emergent transfer (i.e., were appropriately transferred). Nearly half of patients (49%) who were transferred did not require a hand surgeon for intervention or treatment (i.e., treated and discharged by the ER or admitted to a medical service). Likewise, a portion of the transferred patients (14%) had non-emergent diagnoses and could have been treated as outpatients with a referral to a hand surgeon. Based on patient time and financial expenses for these unnecessary evaluations, significant improvements could be made in both quality and cost of care by limiting inappropriate ED referrals.

22
A Portable Handheld Facial-Grading Device for Unilateral Facial Paralysis Following Facial Reanimation Surgery: Reproducibility and Reliability

Eric M Jablonka, MD; Ilya Shnaydman, MD; Peter J Taub, MD; Elliott Rose, MD
The Mount Sinai Hospital, New York, NY

PURPOSE: The need to evaluate current facial reanimation surgical principles and techniques has lead the focus on the development of a device to objectively measure the quantitative degree of facial paralysis. We have developed the digitally based R* Facial Grading System (FGS) application for desktops and portable handheld devices (i.e., iPad) to conveniently measure smile restoration following reanimation surgery for unilateral facial paralysis. Our goal is to prove user reproducibility and reliability of our new system.

METHODS: After taking a picture of a subject at rest and in full smile, the R* FGS software walks the user through calculating a global smile score, specific scores, and smile animation scores from specifically selected facial anatomic landmarks. Six surgical residents were selected to test the intra- & inter-user reproducibility and reliability of the R* FGS system. Each user performed 5 test trials on a mock patient of the subject's face at rest and in full smile. Three users tested the R* FGS on a desktop computer while the other 3 users tested the R* FGS on an iPad.

RESULTS: The iPad users had a completion time of 52 +/- 10.4 sec at trial 5. Average intra-user reproducibility for percent smile symmetry, lip spread, degree tilt and teeth show were 0.995 (+/- 0.001), 0.972 (+/- 0.010), 0.996 (+/- 0.002) and 0.997 (+/- 0.001), respectively. The inter-user reliabilities for the same parameters were 0.999, 0.993, 0.999 and 1.000, respectively. Although the desktop users had a longer completion time of 84.2 +/- 20 sec at trail 5, Average intra-user reproducibility for percent smile symmetry, lip spread, degree tilt and teeth show were 0.997 (+/- 0.002), 0.986 (+/- 0.004), 0.999 (+/- 0.0001) and 0.998 (+/- 0.001), respectively. The inter-user reliabilities for the same parameters were 0.999, 0.993, 0.999 and 0.999, respectively.

CONCLUSION: Preliminary data suggests that the R* FGS is a reproducible and reliable reporting tool to measure the degree of smile restoration following reanimation surgery for unilateral facial paralysis. Our system allows retrospective photo-analysis from prior years by simply scanning to a desktop computer. Given that a majority of our patients reside away from our practice, our system also provides us the potential to monitor and measure patient progress through voice-over-IP software applications (i.e., Skype, FaceTime). The application is affordable, time efficient and can be conveniently used on a desktop or portable handheld device.

23
Novel Antimicrobial Coating of Non-crosslinked Acellular Porcine Dermal Matrix Provides Protection from Microbial Colonization by Common Pathogenic Microorganisms in a Rabbit Model

Thomas A Imahiyerobo, Jr, MD[1]; Jeffrey Scott, PhD[2]; Jason A Spector, MD, FACS[1]
[1]Weill Cornell Medical College, New York, NY, [2]Brown University, Providence, RI

PURPOSE: The objective of this study was to evaluate the antimicrobial efficacy of a novel antimicrobial (rifampin/minocyline)-coated non-crosslinked acellular porcine dermal matrix device (AM-coated ADM), as compared to Strattice™ Reconstructive Tissue Matrix (Strattice™) following inoculation with Methicillin-resistant Staphyloccus aureus (MRSA) or Escherichia coli (E.Coli) in a dorsal rabbit model.

METHODS: 20 male New Zealand White Rabbits were bilaterally implanted with AM-coated ADM (n=10 rabbits) and Strattice™ (n=10 rabbits) respectively. Each device location was then inoculated with clinically-isolated MRSA ($5x10^7$ CFU/ml) (n=5 devices/group) or E.Coli ($1x10^7$ CFU/ml) (n=5 devices/group) using remotely tunneled polyethylene catheters. At 14 days post-implantation, each implant site was analyzed for abscess formation, and viable MRSA/E.Coli colony forming units (CFU) on and surrounding each device.

RESULTS: Gross necropsy demonstrated significantly higher abscess scores for Strattice™ (MRSA: 3/3 score; E.Coli: 1.8/3 score), as compared to the AM-coated ADM (MRSA: 0/3 score; E.Coli: 0/3 score). Whereas Strattice™ demonstrated significant microbial colonization of the device (MRSA: $1.79 \times 10^7 \pm 4.88 \times 10^6$ CFU; E.Coli: $1.47 \times 10^5 \pm 7.70 \times 10^4$ CFU) and a greater percentage of positive pocket swabs in the medial and lateral surrounding tissues (MRSA: 10/10=100%; E.Coli: 7/10 = 70%), the AM-coated ADM and the surrounding tissues were devoid of bacterial colonization (device: MRSA: 0 ± 0 CFU; E.Coli: 0 ± 0 CFU; medial and lateral surrounding tissues: MRSA 0/10=0%; E.Coli: 0/10 = 0%).

CONCLUSIONS: AM-coated ADM completely inhibited device/surrounding tissue abscess formation and microbial colonization following inoculation with clinically-isolated MRSA and E.Coli in a dorsal rabbit model. In contrast, Strattice™ demonstrated significantly greater MRSA and E.Coli microbial colonization, and marked to moderate abscess formation respectively. These data suggest that the AM-coated ADM device, unlike Strattice™, was able to protect itself and the surrounding tissues from MRSA and E.Coli microbial colonization, which may be advantageous in the setting of complex soft tissue reconstruction of the abdominal wall.

24
Bibliometric Indices and Academic Promotion within Plastic Surgery

Katherine Gast, MD, MS; William M Kuzon, Jr, MD, PhD; Jennifer F Waljee, MD, MS, MPH
University of Michigan, Ann Arbor, MI

PURPOSE: Bibliometric indices have been proposed as a measure to quantitatively and qualitatively evaluate scholarly output within academic medicine. However, the extent to which these metrics reflect promotion in academic practice remains unclear. We sought to validate bibliometric indices as an indicator of academic productivity within plastic surgery and their association with promotion of faculty surgeons in academic practice.

METHODS: Our sample included faculty members (n=142) from ten accredited plastic surgery programs in the United States frequently represented at national research conferences. As a measure of content validity, we examined peer-reviewed publications and citations of eight past winners of the American Association of Plastic Surgeons annual research achievement award. Individual author bibliometric indices including h-index, contemporary h-index (hc-index), and g-index were calculated using Harzing Publish or Perish software. The h-index quantifies an individual's scientific research output providing a single-number metric of impact by combining number of citations with number of peer-reviewed publications. In contrast, g-indices give more weight to highly cited articles and hc-indices to recent publications. Range of bibliometric indices for all faculty was h-index of 0 to 84, g-index of 0 to 146, and hc-index of 0 to 43. Surgeons were then clustered according to academic rank and cutoff values correlated with academic promotion for associate and assistant professor were calculated using receiver-operating curves. Logistic regression was used to examine the correlation between bibliometric indices and promotion, controlling for fellowship training and advanced degrees.

RESULTS: All eight past winners of the AAPS Research Award have high bibliometric indices with mean h-index of 46.4, g-index of 83.1, and hc-index 26.6. Mean h-index, g-index, hc-index, and number of peer-reviewed publications increased with academic rank. Cutoffs for promotion between assistant to associate professor and between associate to full professor were distinguished at h-index of 9 and 13, g-index of 16 and 28, hc-index of 6 and 11, and number of peer-reviewed publications of 23 and 40. After controlling for fellowship training and advanced degrees, bibliometric indices and the number of peer-reviewed publications were associated with promotion, with h-index (OR=1.22; 95%CI: 1.12–1.34) most highly correlated with promotion to associate professor, and hc-index (OR=1.26; 95%CI: 1.16–1.39) most highly correlated with promotion to full professor.

CONCLUSIONS: Bibliometric indices predict promotion in academic surgery, and provide a useful metric for surgeons embarking on a career in academia.

SATURDAY, MARCH 8, 2014

SCIENTIFIC SESSION 3 GROUP B
ASSORTED
8:30 AM – 9:30 AM

SATURDAY, MARCH 8, 2014

25
Electrical Impedance Spectroscopy as a Tool for Analysis of In Vivo Encapsulation of Muscle Electrodes

Michelle K Leach, PhD; Stephanie A Goretski; Melanie G Urbanchek, PhD; Paul S Cederna, MD; Nicholas B Langhals, PhD
University of Michigan, Ann Arbor, MI

PURPOSE: Chronically implanted electrodes are prone to encapsulation by fibrous scar tissue which can severely decrease functionality. Electrical impedance spectroscopy (EIS) can be used to monitor the extent of this encapsulation in vivo. The majority of the literature on this subject is focused on electrodes implanted in brain. Here, we examine changes in impedance of an electrode implanted on muscle.

METHODS: Two stainless steel pad electrodes were sutured to the epimysium of the left extensor digitorum longus (EDL) muscle of the rat hind limb. The electrode wires were tunneled subcutaneously and secured to a head cap. Prior to implantation, the electrodes were characterized in a physiological saline bath in a 3-electrode configuration with a platinum counter electrode and an Ag/AgCl reference electrode using a Gamry Potentiostat. One hour following surgery, electrical impedance spectroscopy (EIS) was performed over a frequency range of 1 Hz to 100 kHz at an amplitude of 100 uV using a stainless steel needle reference electrode placed subcutaneously in the left hind limb and a counter electrode placed in the tail.

RESULTS: The shape of the Bode plot was similar at all implantation times. Impedance decreased rapidly with increasing frequency in the low frequency range and then leveled off. However, as implantation time increased, the impedance curves shifted upwards in the high-frequency range, which is indicative of an increase in encapsulation. Similarly, an arc appeared in the high-frequency portion of the Nyquist diagram as implantation time increased that can be attributed to the extracellular matrix and cellular membranes, which are well fit by a model consisting of a parallel combination of a resistance and a capacitance, respectively.

CONCLUSION: Similar changes in impedance were observed by EIS of an electrode chronically implanted in muscle as have been reported in the literature for electrodes in brain. Chronically implanted electrodes should exhibit long term stability. A thorough understanding of the foreign body response to the electrode is therefore crucial. These preliminary results indicate EIS is a sufficient tool to monitor and quantify muscle electrode encapsulation in vivo over time.

ACKNOWLEDGEMENTS: This work was sponsored by the Defense Advanced Research Projects Agency (DARPA) MTO under the auspices of Dr. Jack Judy through the Space and Naval Warfare Systems Center, Pacific Grant/Contract No. N66001-11-C-4190.

26
An Engineered Lipoproteoplex Presents Robust Delivery Mechanism For Topical Gene Therapy

Piul S Rabbani, PhD[1]; Joseph A Frezzo, MS[2]; Maria Ham, MD[1]; April Duckworth, MD[1]; Muhammad Hyder Junejo, BS[1]; Nakul Talathi,[1]; Camilo Doig-Acuna, BS[1]; Haresh More, MTech[2]; Kevin Zhang, None[2]; Jessica Chang, BS[1]; Karan Mehta, BS[1]; Amanda Hua, BS[1]; Jin K Montclare, PhD[2]; Pierre B Saadeh, MD[1]; Daniel J Ceradini, MD[1]
[1]New York University Department of Plastic Surgery, New York, NY, [2]Polytechnic Institute of New York University, New York, NY

PURPOSE: Dermal penetration, drug degradation/toxicity, and non-specific effects are challenges in implementation of topical drug delivery systems. Here, we examine a new topical siRNA delivery system using a self-assembly protein-lipid system (lipoproteoplex) comprised of cationic lipid nanoparticles (CLNs) and Cartilage Oligomeric Matrix Protein coiled coil supercharged protein (CSP) for in vivo gene silencing. CSP carries a cavity for encapsulation and release of many different therapeutic agents, as well as the ability to complex siRNA. We predict that CLN/CSP will allow efficient siRNA delivery into skin, as well as sustained presence for maximum therapeutic effect.

METHODS: Using various combinations of CSP and CLN with siRNA, we determined the optimal zeta potential of the complex in comparison to commonly used liposomal delivery systems. To analyze delivery efficiency in vivo, we complexed CSP/CLN with fluorescent siGlo Red siRNA and applied topically to wild type mouse skin. The mice were imaged in real time at 0, 3, 5, and 7 days after application with the in vivo imaging system (IVIS) and their skin sampled for histology and gene expression. In vitro, we used a Franz diffusion cell to determine release kinetics of the CSP/CLN lipoproteoplex.

RESULTS: Surface charge of CSP:CLN:siRNA measured 37.33 ± 0.67 mV compared to 25.4 ± 1.15 mV of CLN:siRNA lipoplex, indicating the lipoproteoplex is more stable and resists aggregation to have improved solubility. IVIS imaging of fluorescence from treated mouse skin revealed presence of siGlo Red beginning by day 3, and maintained at days 5 and 7 after application. Histologic examination demonstrated dermal presence of siGlo Red by day 3. We found presence of siGlo Red from epidermis to the panniculus carnosus by day 5 and the fluorescent signal was visible at 7 days after application in sections. Using several combinations of CSP and CLN, we found favorable release kinetics of the CSP:CLN:siRNA

lipoproteoplex for topical use. There was no evidence of cutaneous inflammatory reactions grossly or in histologic analysis with either delivery system.

CONCLUSION: Our results demonstrate that the lipoproteoplex offers an efficient and reliable route to deliver siRNA for topical gene silencing. The stability and non-toxic nature of lipoproteoplex gives it a unique advantage and makes it an ideal candidate for clinical cutaneous drug delivery.

27
An Evaluation of a Novel Craniofacial Skills Laboratory Curriculum: An Aid to Plastic Surgery Resident Milestone Achievement in Technical Skills and Instrument Knowledge

Nicole J Jarrett, MD[1]; Samir Shakir, BS[2]; Anand R Kumar, MD[3]

[1]Department of Plastic Surgery, University of Pittsburgh, Pittsburgh, PA, [2]Children's Hospital of Pittsburgh of UPMC, Pittsburgh, PA, [3]Department of Plastic Surgery, University of Pittsburgh, Children's Hospital of Pittsburgh of UPMC, Pittsburgh, PA

PURPOSE: Plastic Surgery Graduate Medical Education has transitioned to a model of milestones. The objective measurement of surgical skills and technical knowledge remains understudied. Surgical skills curricula have been created for microsurgery, but an educational model for training the unique technical skills for craniofacial surgery has not been defined or validated. The aims of this study are to present and validate a novel educational craniofacial skills laboratory and compare outcomes between traditional on-patient training and simulated laboratory training.

METHODS: A prospective IRB approved study was designed to evaluate 1) instrument identification, 2) time/accuracy of burr hole placement, 3) time/accuracy of craniotomy (square) resection, and 4) time/accuracy of 4 hole plating across the nasomaxillary buttress using Saw BonesTM Craniofacial Models before and after the skills laboratory. Accuracy was measured using a 1–4 scale with 4 representing best score. Minimal classroom training (30 minutes) and extensive laboratory training (7 hours 30 minutes) was provided regarding monobloc, bipartition, Lefort III, Lefort I, mandible osteotomy (BSSO) on fresh cadaver specimens but no direct training with the defined tasks was provided. The R4 group had not yet rotated on the craniofacial service, whilst the R5 group had during the previous year.

RESULTS: The R4 (n=3) group mean time in seconds pre/post-task 1, 2, 3, 4 was 117/28, 6.33/4.33, 77.3/27, and 133/98.6 respectively. Percent improvement for task 1, 2, 3, 4 was 76%, 31%, 65%, and 26% respectively. The R5 (n=6) group mean time in seconds pre/post-task 1, 2, 3, 4 was 62/44, 6/4, 32/22, and 108/82 respectively. Percent improvement for task 1, 2, 3, 4 was 29%, 33%, 30%, and 23% respectively. R4 group post-training times were not significantly different than R5 pre-training times for each of the tasks recorded (p=0.131, 0.597, 0.597, 0.790) respectively. Accuracy testing with instrument recognition demonstrated the greatest improvement from 82% to 100% (p=0.05) for the entire cohort. Accuracy changes in skills tests 2,3,4 pre/post were 2.7/3, 2.5/2.3, and 2.2/2.61(p=0.25, 0.58, 0.17) respectively.

CONCLUSIONS: A single day craniofacial skills laboratory with instruction in standard facial osteotomies measurably improved residents performance on specific tasks by indirect training. Most importantly, R4 residents after the curriculum surpassed the pre-lab R5 residents who had already performed these tasks in the traditional training environment of the operating room. Craniofacial related skills tasks may be used to assess a trainee's readiness for performing them in the operating room and may aid in proper identification of milestone attainment.

28
Effect of Glabellar Paralysis by Botulinum Toxin on Ability to Communicate Emotion

Jason T Laurita, MB[1]; Mitchell A Stotland, MD[1]; Mitchell Horn-Wyffels, MD[2]; Belinda B Ray, MA[1]

[1]Geisel School of Medicine at Dartmouth, Hanover, NH, [2]University of Minnesota, Minneapolis, MN

PURPOSE: Two important, potential behavioral effects of botulinum toxin (BTx) are debated: (1) Does paralysis of glabellar musculature alter mood or emotion through the mechanism of the facial feedback hypothesis? And, (2), does BTx significantly alter one's ability to facially express emotion? Recent neuroscientific studies have demonstrated that corrugator muscle paralysis can, in fact, alter the perception of emotional stimuli and downgrade amygdala response to anger. Regarding the second question, however, both the lay-press and prospective patients commonly disparage the presumed "expression-erasing" effects of facial BTx treatments despite a lack of any formal evidence. In this study the influence of glabellar BTx on the perceived legibility and intensity of the 6 cardinal expressions of emotion (happy, sad, afraid, surprised, angry, disgusted) is rigorously quantified for the first time.

METHODS: Phase 1: 52 "expressor" females (age 35–60) were induced to *spontaneously* express the 6 cardinal emotions both before and 1 month after glabellar injections of BTx. A hidden video camera recorded subjects as they viewed provocative movie clips previously validated to stimulate the different facial expressions of emotion. Phase II: 21 "perceivers" evaluated the video of all 52 "expressors" viewing the anger-provoking movie clips both pre-BTx treatment (perceivers blinded to treatment or study objective). Ratings for emotional intensity (1–7 scale) were tabulated. The 10 most intense "expressors" were selected out for use in Phase III. Phase III: 31 new "perceivers" viewed movie clips of the 10 most intense "expressors" pre- and post-BTx (120 clips viewed by each "perceiver", displayed in random order). Each clip was rated for *legibility* (% accuracy selecting 1 of 6 cardinal emotions) and for *intensity* (1–7 scale).

RESULTS: 1) *Legibility of facial expression:* In those expressing emotion, glabellar BTx injection does not cause a significant change in perceivers' ability to discern the 6 cardinal emotions. 2) *Intensity of facial expression:* Glabellar BTx injection results in a perceived significant reduction (3.77/7 vs 1.89/7; $p<0.0001$) in the intensity of the anger expression, but has an insignificant effect on the other 5 cardinal emotions.

CONCLUSION: BTx injections in the glabellar region significantly *reduce the intensity of anger expression* ($p<.0001$). However, perceivers *maintain an ability to discern the facial expression* of all 6 cardinal emotions.

29
Evaluation of 3D Photographic Imaging as a Method to Measure Differential Volumes in Reconstructed Breast Tissue

Priya G Lewis, BA; Gennaya L Mattison, BS; Hahns Y Kim, MD; Subhas C Gupta, MD, CM, PhD, FRCSC, FACS
Loma Linda University, Loma Linda, CA

PURPOSE: Incremental tissue expansion is commonly used for mastectomy patients in the delayed breast reconstruction process. After mastectomy, an inflatable tissue expander is placed in the subpectoral pocket and filled with saline periodically; fixed volumes, determined qualitatively by the surgeon, are added over the course of weeks until an adequate pocket is available to accommodate a permanent implant. This method relies on the physician's subjective opinions of aesthetic targets and 2D measurements. 3D photographic technology has the potential to quantitatively improve the process by measuring patients' natural breast volume thereby setting a target for fill volumes during reconstruction.

METHODS: We compared the known tissue expander fill volumes with measured breast volumes using the 3dMD® imaging system in 17 breasts. Patients were imaged before and after saline expansion at outpatient clinic appointments. Data collection for each patient was complete after permanent implant placement. The differential volumes were then measured and compared. Volume measurements were calculated with the 3dMD® software by one analyst using the same physical landmarks for each patient to standardize the process. A linear regression analysis was conducted of the measured to known volume. Also, known fill volumes were compared to the measured/filled ratio.

RESULTS: A total of 17 reconstructed breasts from 10 patients were analyzed. The ratio of measured volume to known fill volume was found to have a mean of 1.265 with a standard deviation of 1.429 and SEM of 0.215 ($p=5.07E^{-14}$) and a 95% CI of 0.843 - 1.688. The measured/fill ratio was closer to 1:1 at higher fill volumes; the fill volume correlating to exactly 1 was 91.72cc. The difference between known and measured volumes was found to have a mean of 38.336 with a standard deviation of 43.605 and SEM of 6.574 (p=0.012) and a 95% CI of 25.451 - 51.220.

CONCLUSION: 3D imaging for quantitative breast volumetry has a great deal of potential for use in reconstructive procedures. In this preliminary study, there appears to be a quantifiable relationship between the volume added and the volume achieved when measured using 3D imaging. Further data collection may elucidate a stronger relationship. 3D imaging as a clinical tool has the potential to be a powerful adjunct in the astute clinician's decision-making process for breast reconstruction.

30
The Economic Implications of Changing Trends in Breast Flap Reconstruction in the United States

Sophia Caccavale, GED; Irene Pien, BS; Michael Cheung, MD; Parag Butala, MD; Duncan Hughes, MD; Cassandra Ligh, BS; Michael R Zenn, MD; Scott T Hollenbeck, MD
Duke University Medical Center, Durham, NC

PURPOSE: Enthusiasm for the Deep Inferior Epigastric artery Perforator (DIEP) flap for breast reconstruction has grown in recent years. However, this flap is not performed at all centers or by all plastic surgeons that engage in breast reconstruction. It is unclear how widespread the DIEP flap has become in the United States and how this has affected the charges and costs associated with breast flap surgery.

METHODS: We used 3 years (2009 - 2011) of the Nationwide Inpatient Sample (NIS) to identify the population of patients undergoing Latissimus dorsi (LD), pedicle TRAM (pTRAM), free TRAM (fTRAM) and DIEP flaps as principle procedures. Patient identification was based on ICD-9 procedure codes, including LD (85.71), pTRAM (85.72), fTRAM (85.73) and DIEP (85.74). This generated 19,182 hospital discharges for review. Charges were defined by the NIS as the amount the hospital billed for services. Costs were defined by the NIS as the actual cost of production (ie. the amount the hospital received) using hospital charge-to-cost ratios. Statistical comparisons were made using linear regression, t-test and ANOVA models.

RESULTS: Between 2009 and 2011 the total number of discharges did not change significantly. In regards to number of discharges per year for each flap, there was no significant trend for LD (p=0.99) or pTRAM (p=0.29) flaps. However, the rate of fTRAM's dropped significantly (p<0.02) and the rate of DIEP's increased significantly (p<0.03). Over the 3 years evaluated, the average percentage of patients with private insurance and any of the 4 flaps increased at a rate of 4.26% per year. Overall, the group varied significantly in the rate of private insurance (ANOVA p<0.02), with DIEP flap patients having the highest overall rate of private insurance (80.3%) and LD flap patients having the lowest (67.4%). The average charge / flap was $40,704 (LD); $51,933 (pTRAM); $69,909 (fTRAM); and $82,320 (DIEP) and none of these increased significantly over the 3 years. The average costs / flap for each flap was $12,017 (LD); $15,538 (pTRAM); $20,756 (fTRAM); and $23,616 (DIEP) and only the fTRAM flap average cost increased significantly over the 3 years (p=0.03). The overall charges for all 4 flaps increased at a rate of 0.0057% while overall costs increased at a rate of 0.029%. This can be explained by the increased number of DIEP flaps performed and the decreasing charges and increasing costs per year associated with these flaps. Despite the increasing overall costs for

breast flap surgery it remains 0.27% less than the rate of inflation within the United States.

CONCLUSION: Recent trends in breast reconstruction show that the DIEP flap is being performed more frequently at both higher charge and higher costs than LD, pTRAM and fTRAM flaps. This has resulted in a non-significant increase in the overall costs for these four breast flaps. This remains less than the rate of inflation in the United States.

SATURDAY, MARCH 8, 2014

SCIENTIFIC SESSION 3 GROUP C
WOUND HEALING
8:30 AM – 9:30 AM

SATURDAY, MARCH 8, 2014

31
DNA Methylation Analysis of Radiated Skin Reveals Chonic Inflammation with a Predominance of Polymorphonuclear Granulocytes

Hui Shen, PhD; Solmaz N Leilabadi, MD; Peter W Laird, PhD; Alex K Wong, MD
Keck School of Medicine of USC, Los Angeles, CA

PURPOSE: Although radiation therapy is a useful adjunct to surgical resection in the management of a variety of solid tumors, radiation-induced injury to normal skin is an unintended consequence that can lead to chronic non-healing wounds and increased risk of complications during reconstructive surgery. Insight into the damage pathways of radiated skin may reveal opportunities to better understand radiation delayed wound healing. Radiation-induced epigenetic changes in DNA methylation has not been well characterized for human skin.

METHODS: Pairs of matched radiated and normal skin were collected at the Keck Hospital of USC using an IRB-approved protocol from patients that had adjuvant chest wall irradiation > 10 weeks prior to collection. Samples were assayed on the Infinium HumanMethylation450 Beadarray. This platform measures the DNA methylation pattern at 482,421 CpG sites which cover 99% of RefSeq genes, with an average of 17 CpG sites per gene region distributed across the promoter, 5'UTR, first exon, gene body, and 3'UTR. It covers 96% of CpG islands, with additional coverage in island shores and the regions flanking them. The R-based methylumi package was used for data preprocessing, including background correction and dye-bias normalization. The level of DNA methylation at each CpG locus is summarized as beta (β) value calculated as (M/(M+U)), ranging from 0 to 1, which represents the ratio of the methylated probe intensity to the overall intensity at each CpG locus. A p value comparing the intensity for each probe to the background level was calculated at the same time, and data points with a detection P value >0.05 were deemed not significantly different from background measurements, and therefore were masked from the analysis.

RESULTS: Unsupervised clustering of the eight samples on 1,540 most variable probes (SD>0.15) revealed intra-sample heterogeneity in terms of DNA methylation. We compared the skin samples to the DNA methylation patterns of sorted blood components on the same loci, including polymorphonuclear granulocytes (PMN), CD3+ T cells, CD19+ B cells, and CD34+CD38- cells, and saw a clear and specific PMN signature in two of the four radiated skin samples, while none of the matched normal skins showed such signature. The PMN infiltration seemed to be extensive, with estimated PMN component of 80% in one sample.

CONCLUSION: DNA methylation array of radiation damaged skin revealed significant infiltration by polymorphonuclear (PMN) granulocytes. This data supports a pathophysiologic role of PMNs in chronic inflammation related to radiation damaged skin. We hypothesize that a deregulated inflammatory process might be associated with impaired healing in radiated skin.

32
Amifostine Reduces Radiation-Induced Complications in a Murine Model of Expander-Based Breast Reconstruction

Peter A Felice, MD, MS; Noah S Nelson, BS; Erin E Page, BS; Sagar S Deshpande, BS; Alexis Donneys, MD, MS; José Rodriguez, MD; Steven R Buchman, MD

University of Michigan Medical School, Ann Arbor, MI

PURPOSE: Immediate expander-based breast reconstruction is a prevalent option for many women after mastectomy. For patients undergoing treatment regimens requiring adjuvant radiation, however, complication rates as high as 60% have been reported and often preclude the use of this reconstructive technique. Amifostine is a cytoprotectant on formulary for prophylaxis against radiation-induced mucositis and xerostomia. We hypothesize that this protective capacity of Amifostine can be extended to reduce radiation-induced soft tissue complications in the breast, thus promoting expander-based reconstructive options for women battling this devastating disease.

METHODS: 56 Sprague Dawley rats were divided into two experimental groups, Operative Expander Placement (Expander) and Operative Sham (Sham). Expander specimens underwent placement of a sub-latissimus tissue expander and subsequent expansion to a 15cc fill volume, while Sham specimens underwent identical operative intervention without expander placement. Each experimental group was further divided into three subgroups; Control specimens received no further intervention, XRT specimens received a human-equivalent dose of radiation alone, and AMF-XRT specimens received both Amifostine pre-treatment and a human-equivalent dose of radiation. Animals then underwent a 45-day recovery period, during which interval photo documentation, clinical examination, and ImageJ analysis were used to evaluate for surgical site complications.

RESULTS: In the Sham group, 0 of 10 Control specimens, 0 of 10 XRT specimens, and 0 of 10 AMF-XRT specimens showed signs of skin or soft tissue complication. For the Expander animals, AMF-XRT specimens (4 of 13, 30%) demonstrated significantly fewer substantial gross skin and soft tissue complications compared to XRT specimens (9 of 13, 69%; $p = 0.041$). ImageJ evaluation also demonstrated a significant difference for mean percentage of necrosis for XRT specimens at 12.94%, compared with 6.96% of Amifostine pre-treated animals ($p = 0.019$). The lack of complications demonstrated in Sham specimens is noteworthy in that expansion, radiation administration, and prophylactic Amifostine administration were thus isolated as the main determinants of complication and remediation. An Expander Control group was not included in this study, as it would not serve to answer our hypothesis with respect to radiation and Amifostine pre-treatment administration.

CONCLUSION: In the Expander specimens, Amifostine pre-treatment significantly reduced skin and soft-tissue complications from 69% to 30%. ImageJ analysis also demonstrated a significantly reduced rate of necrosis by almost 50% in Expander AMF-XRT specimens compared with Expander XRT specimens. Since no complications were seen in Sham specimens, we concluded that the operative procedure itself was not responsible for skin and soft tissue injury. These findings demonstrate that Amifostine prophylaxis provides substantial and significant protection against radiation-induced skin and soft tissue injury in a murine model of expander-based breast reconstruction. Our hope is to translate our findings from the bench to the bedside in an attempt to decrease the overall morbidity of breast reconstruction and increase the number of restorative treatment options available for women afflicted with breast cancer.

33
Stress Offloading through Mechanomodulation is Associated with Down-Regulation of Inflammatory Pathways in a Large Animal Model

Michael Januszyk, MD; Victor W Wong, MD; Kirit Bhatt, MD; Ivan N Vial, MD; Reinhold Dauskardt, PhD; Michael T Longaker, MD; Geoffrey C Gurtner, MD
Stanford University, Stanford, CA

PURPOSE: Cutaneous scarring represents a major source of morbidity in the United States, and understanding the mechanisms underlying this process is critical to develop effective therapies to mitigate scar formation. Although wound fibrosis and inflammation are highly linked, only recently have mechanical forces been suggested to directly modulate these pathways, both in animal and clinical studies. Our group previously developed a topical polymer device that significantly reduces post-injury scar formation via the manipulation of mechanical forces. Here we extend these studies to examine the transcriptional effects of mechanomodulation during scar formation using a validated large animal model, the red Duroc pig.

METHODS: Full-thickness incisional wounds measuring three centimeters in length were created on the pig dorsum. Polymer devices were applied immediately after closure, and separate wounds were allowed to heal under physiologic, elevated stress, and stress-shielded conditions (n = 3). Wounds were harvested for DNA microarray analysis at eight weeks post-injury. Hierarchical clustering of gene expression data for each group of wounds was performed, followed by canonical pathway calculations and network analyses.

RESULTS: Genes associated with connective tissue disorders and inflammation networks were up-regulated in elevated stress wounds and down-regulated in stress-shielded wounds. A super-network was generated, including all genes associated with either top pathway target. The central element linking these networks is extracellular-related kinase (ERK)1/2, which has previously been associated with inflammation and scarring. Further, when we artificially grew our network using a relationship database, we found that focal adhesion kinase (FAK) assumed a central position among genes associated with both pathways. These data suggest a molecular link between inflammation and fibrosis that can be mechanically regulated via FAK and ERK1/2.

CONCLUSION: We demonstrate that mechanical loading of incisional wounds up-regulates inflammatory and fibrotic pathways, and that device-mediated off-loading of these wounds can reverse these effects. These pathways appear linked by ERK1/2 and FAK, suggesting a common molecular mechanism underlying the mechanomodulation of cutaneous wound healing.

34
A Novel Immune Competent Murine Hypertrophic Scar Contracture Model: A Tool to Elucidate Disease Mechanism and Develop New Therapies

Mohamed M Ibrahim, MD[1]; Jennifer Bond, PhD[1]; Andrew Bergeron, BA[1]; Kyle J Miller, BA[1]; Tosan Ehanire, BA[1]; Carlos Quiles, MD[1]; Mark Fisher, MD[1]; Elizabeth R Lorden, BS[2]; Manuel A Medina, MD[1]; Angelica Selim, MD[3]; Bruce Klitzman, PhD[1]; Kam Leong, PhD[2]; Howard Levinson, MD[1]
[1]The Division of Plastic and Reconstructive Surgery, Department of Surgery, Duke University School of Medicine, Durham, NC, [2]The Department of Biomedical Engineering, Duke University, Durham, NC, [3]The Department of Pathology, Duke University School of Medicine, Durham, NC

PURPOSE: Hypertrophic scar contraction (HSc) following burn injury leads to contractures. Contractures are painful and disfiguring. Current HSc therapies are marginally effective. To study disease pathogenesis and develop new therapies, a murine model is needed. We have created a validated immune-competent murine HSc model.

METHODS: A third-degree burn was created on the dorsum of C57BL/6 mice. Three days post-burn, tissue was excised and wounds were grafted with ear skin. Graft contraction was analyzed by computer planimetry and tissue harvested on post-operative days 3, 7, 9, 14, 28, 70, and 168. Outcomes were compared to human condition to validate the model. To confirm graft survival, green fluorescent protein mice (GFP) were used and histologic analysis was performed to differentiate between ear and back skin. Role of panniculus carnosus (PC) in scar contraction was analyzed by tagging it with titanium clips and X-raying mice. Clip area was measured by ImageJ. Cellularity was assessed with DAPI. Collagen maturation was assessed with Picro-sirius red. Mast cells were stained with Toluidine blue. Macrophages were detected with F4/80 immune. Vascularity was assessed with CD31 immune. RNA for contractile proteins was detected by qRT-PCR. Elastic moduli of human and murine skin and scar tissue were analyzed using a microstrain analyzer. Samples were strained at a rate of 0.1mm/s until failure. Elastic modulus was stress/strain in the linear portion of the graph.

RESULTS: Grafts contracted to ~45% of their original size by day 14 and maintained their size. Grafting of GFP mouse skin onto wild type mice and vice-versa and analysis of dermal thickness and hair follicle density in grafts, confirmed graft survival. Interestingly, hair follicles disappeared after grafting and regenerated in ear skin configuration by day 30.

Radiological analysis revealed the PC does not contribute to contraction. Microscopic analyses demonstrated that grafts show increase in cellularity. Granulation tissue formed after day 3. Collagen analysis revealed increases in collagen maturation, more immature collagen fibers on day 7 and more mature collagen on day 168. CD31 stain revealed an increase in vascularity compared to normal skin. Macrophages and mast cells were increased. qRT-PCR demonstrated upregulation of TGF-β, ASMA, NMMII, and ROCK2 in HSc. Tensile testing revealed that under low extension rate, human skin and scar tissues are tougher than mouse skin and scar tissues. Both scar tissues displayed increased brittle characteristics compared to uninjured skin.

CONCLUSION: Through a methodical approach, we have created a validated immune-competent murine HSc model. We unexpectedly found that murine scar contraction occurs independent of PC. We observed that murine graft hair follicles go through a period of dissolution followed by regeneration, indicating our model may also serve to study hair growth. This model will facilitate studying the HSc pathogenesis and accelerate discoveries to prevent HSc.

35
Central Role of Early Vascularization in Burn and Trauma-Induced Heterotopic Ossification

Shailesh Agarwal, MD; Jonathan Peterson, BS; Sara De La Rosa, BS; Kavitha Ranganathan, MD; Alexis Donneys, MD; Stewart Wang, MD, PhD; Paul S Cederna, MD; Steven R Buchman, MD; Benjamin Levi, MD

University of Michigan, Ann Arbor, MI

INTRODUCTION: Heterotopic ossification (HO) is a condition in which bone forms within non-osseous tissues after severe trauma, burn and orthopedic surgery. Previous studies have demonstrated that normal bone development and repair depends on vasculogenic and angiogenic signaling. However, the roles of key mediators of angiogenesis have not been fully evaluated in the pathogenesis of burn-induced HO. We hypothesize that burn injury increases early vasculogenic signaling and vessel formation resulting in increased heterotopic bone formation.

METHODS: C57/BL6 male mice underwent Achilles tenotomy with 1) 30% total body surface area burn or 2) no burn injury (n=4/group). HO formation was evaluated weekly (1–9 weeks) using micro-CT and at 9 weeks with nano-CT. At 5 weeks postoperatively, the vascular density in the region of the HO was assessed by Microfil injection followed by micro and nano-CT. Immunohistochemistry and immunofluorescent staining with anti-CD31 and anti-HIF1A antibodies was performed to assess angiogenesis. Separately, adipose-derived mesenchymal stem cells (MSCs) were isolated after 2 hours or five days from mice with or without 30% TBSA burn injury and cultured in osteogenic differentiation medium for 3 days. The robustness of vascular signaling was evaluated using qRT-PCR to quantify Vegfa gene transcription and Western blotting to quantify protein expression (VEGFA). Furthermore, an in vivo Matrigel plug assay (1 million MSCs seeded in 20ul of matrigel and implanted subcutaneously) was used to assess the effect of burn injury on angiogenesis.

RESULTS: Mice with Achilles' tenotomy and burn injury developed HO with intertwined blood vessels as demonstrated by nano-CT at 9 weeks. Microfil quantification showed that mice with Achilles tenotomy and burn developed greater vascular density at HO sites than mice with Achilles tenotomy alone ($n=6^{*}p<0.05$). We also noted significantly more IHC staining for CD31 and HIF1A in burn mice at the site of HO. MSCs harvested from mice with a burn injury had 30% more Vegfa gene transcript and over 65% more VEGFA protein expression. Finally, in vivo tubule assays demonstrated increased angiogenic signaling in those mice with a burn injury compared to control.

CONCLUSIONS: These data suggest that early angiogenesis plays a role in HO formation. Furthermore, burn injury enhances the in vitro angiogenic capacity of MSCs and stimulates an increase in in vivo vessel formation at the Achilles tenotomy site. Increased presence of HIF-alpha and VEGF-A after a burn injury may create a permissive niche for HO to form. This is the first study demonstrating the role of angiogenesis in the formation of burn- induced HO. Localized regulation of vessel formation may serve as a viable target to treat or prevent HO in trauma and burn patients.

36
Development of a Novel Lymphatic Reporter Mouse

Gina Farias-Eisner, BA; Daniel A Cuzzone, MD; Seth Z Aschen, BS; Nicholas J Albano, BS; Swapna Ghanta, MD; Evan Weitman, MD; Babak Mehrara, MD

Memorial Sloan Kettering Cancer Setting, New York, NY

PURPOSE: The lymphovascular system is a highly specialized organ system that is responsible for interstitial fluid homeostasis and immune function. The lymphatic endothelial cell, the basic subunit of the lymphovascular system, possesses highly conserved proteins that have been targets for identifying lymphatics. These include the hyaluronan receptor lymphatic vessel endothelial receptor 1 (LYVE-1), the membrane glycoprotein podoplanin, the transcription factor Prox-1 and the VEGF-R3 tyrosine kinase. Identification of the lymphatic vessels has been instrumental in studying various congenital disease states as well as malignancy. Conventional methods for identification can be harsh and caustic. Here we describe a novel reporter mouse that displays high fidelity for lymphovascular identification.

METHODS: Transgenic lymphatic reporter mice using a tamoxifen-inducible Cre-Lox system were developed. This was achieved by crossing C57B6 transgenic mice that expressed the bacterial Cre recombinase gene driven by the mouse VEGF-R3 (FLT4) under the control of tamoxifen, with C57B6 LacZ-LoxP transgenic mice. To activate Cre-lox recombination, homozygous FLT4-Cre/LacZ-LoxP mice (FLT4-LacZ mice) were injected intraperitoneally with 200mg/kg tamoxifen for 5 days followed by sacrifice. LacZ expression was visualized by incubating tissues in Lac-Z buffer solution, followed by embedding and sectioning. To analyze the penetrance/specificity of Cre-expression, tissues were stained using antibodies directed against the LYVE-1 or Von-Willibrand factor (VWF), a marker of blood vessels.

RESULTS: Histological analysis of skin sections revealed that the expression of Flt4-Cre was tamoxifen dependent. Control mice that were not primed with tamoxifen prior to sacrifice showed no B-gal staining in LYVE-1+ lymphatic vessels. In contrast, treatment of transgenic mice with tamoxifen resulted in high-level expression of Cre-recombinase with more than 90% of LYVE-1+ vessels demonstrating B-gal staining. The expression of B-gal was limited to lymphatic vessels because we found no B-gal staining of blood vessels stained with Von Willebrand factor.

CONCLUSION: Here we describe the development of a novel reporter mouse for identifying lymphatic vessels. There is very high fidelity in the identification of lymphovascular structures. This reporter mouse has multiple applications for studies utilizing models of lymphatic manipulation.

SATURDAY, MARCH 8, 2014

SCIENTIFIC SESSION 4
BEST EPSRC PAPERS
11:00 AM – 11:40 AM

SATURDAY, MARCH 8, 2014

37
Peripheral Nerve Repair: Multimodal Comparison of The Regenerative Potential of Adipose Tissue Derived Cells in a Biodegradable Conduit

Patricia E. Engels[1], E. A. Kappos[1], M. Meyer zu Schwabedissen[1], M. Tremp[1], A. Fischmann[2], D. J. Schaefer[1], D. F. Kalbermatten[1]

[1]University Hospital Basel, Department of Plastic, Reconstructive, Aesthetic and Hand Surgery, Basel, Switzerland
[2]University Hospital Basel, Department of Radiology, Basel, Switzerland

INTRODUCTION: Tissue engineering is a popular topic in peripheral nerve repair. Combining a nerve conduit with supporting cells could offer an opportunity to improve clinical outcome. Aim of this study was to provide a broad overview over promising transplantable cells under equal experimental conditions over a long term period.

METHODS: 1 Mio. of the following cells were introduced into biodegradable fibrin conduits: rat adipose-derived stem cells (rASCs), Schwann cell (SC)-like differentiated rASC (drASC), rat SCs (rSCs), human (h-)ASCs from the superficial and deep abdominal layer as well as human stromal vascular fraction (SVF). A 10mm gap in the sciatic nerve of female Sprague Dawley rats (7 groups of 7 animals, 8 weeks old) was bridged through the conduit. As a control we re-sutured a nerve segment as an autograft.

Long-term evaluation was carried out after 16 weeks comprising walking track, morphometric and MRI analysis. The Sciatic Function Index was calculated. Cross sections of the nerve proximal, distal and in between the two sutures were analysed. Gastrocnemius muscle weights were compared and MRI analyses performed.

RESULTS: MRI proved biodegradation of the conduit. Correlating trends throughout the different evaluation techniques could be shown: Superficial hASC supported regeneration better than deep, in line with published in vitro data. SC-like drASC had the best regeneration potential compared to other adipose tissue derived cells.

CONCLUSION: Comparison of the most promising cells in a multimodal manner comprising functional and morphometric analysis revealed that particularly differentiated ASCs could be a clinically translatable route towards new methods to enhance peripheral nerve repair.

38
Tracheal Allotransplantation and Prefabrication for Long Tracheal Stenosis with Withdrawal of Immunosuppression: From Bed To Bench

Margot Den Hondt[1], P. Delaere[1], J. J. Vranckx[1]

[1]KULeuven, Plastic & Reconstructive surgery, Leuven, Belgium

INTRODUCTION: Few therapeutic options exist for repairing tracheal defects longer than 5 cm since no autologous fibrocartilagenous framework is available for reconstruction and trachea lacks an identifiable vascular pedicle that would enable direct anastomosis to recipient vessels.

MATERIALS AND METHODS: Based on our previous research, we reconstructed 6 long-segment tracheal defects using an allograft revascularized by heterotopic wrapping in radial forearm fascia. Patients received immunosuppressive therapy. After revascularization, the mucosal lining was replaced progressively using recipient buccal mucosa, creating a chimera of donor respiratory epithelium and recipient buccal mucosa. The chimera allowed for gradual withdrawal of immunosuppression. Four to ten months after implantation, the tracheal allograft was dissected with its new vascular pedicle and brought into its orthotopic location by microvascular techniques.

RESULTS: In all patients immunosuppressive therapy was withdrawn. In one patient vascularization problems of the mucosal lining occurred. Shortening the time span for the orthotopic transplantation limits quality of outcome. There is a fragile balance between the immunologic parameters and the vascularization of the internal lining.

CONCLUSION: Vascularization of the mucosal lining of the trachea determines the quality of outcome and timing of treatment. We currently analyze from bed to bench the impact of pro-angiogenic stem cell-based strategies in a rabbit model. We analyze the reduction of immunogenicity of the allogenic trachea by means of surgical and enzymatic decellularization techniques, and we investigate the replacement of inner lining by functional respiratory epithelium.

39
The Pig as an Ideal Training Model for Perforator Flap Dissection in Living Tissue

Alexandru Nistor[1], L. Jiga[1], D. Georgescu[1], G. Miclaus[2], S. Barac[1], B. Hoinoiu[1], C. Dumbuleu[1], M. Ionac[1]
[1]Victor Babes University of Medicine and Pharmacy, Division of Reconstructive Microsurgery, Timisoara, Romania
[2]Neuromed Medical Center, Timisoara, Romania

INTRODUCTION: Successful perforator flap harvesting demands precise microsurgical skills attainable only through extensive training in experimental setting. Here, we describe five new types of perforator flaps in pigs, delineate their harvesting technique and provide evidence of their role as live training models.

MATERIALS AND METHODS: Ten common-breed pigs, with an average weight of 25 kg were submitted to CT angiography (CT-angio) using a 64-detector scanner (Siemens Somatom Sensation 64). Through maximum intensity projection (MIP), three-dimensional volume rendering (VRT) and multiplanar reformatting (MPR) imaging, detailed examination of the vascular anatomy of integument was performed. Using microsurgical techniques and CT-angio perforator mapping, true perforator flap models were standardized.

RESULTS: Five perforasomes with consistent anatomy, around four anatomically distinct body areas (e.g. dorsal cervical, lateral thoracic, anterior abdominal, gluteal) were defined. On these, five different flaps were harvested based perforator vessels of either dorsal cervical artery (DCAPf), deep superior epigastric artery (DSEPf), thoracodorsal artery (TDAPf), intercostal artery (ICAPf) or superior gluteal artery (SGAPf).

CONCLUSION: The five new perforator flaps described, provide evidence that pigs can be efficiently used as live training models for perforator flap dissection.

40
Hernia Repair with Coriumflap? - Vascularized!

Barbara Iris Gruber[1], B. Todoroff[1]
[1]KH Barmherzige Schwestern Vienna, Plastic and Reconstructive Surgery, Vienna, Austria

INTRODUCTION: Over the last decades the free avascular corium patch was considered a useful solution for hernia repair. It vanished into oblivion for two reasons:

Firstly over the last years industry supplies better and better solutions with absorbable and non-absorbable meshes, up to recently disposable avascular xenogeneic dermal matrix.

Secondly the donor site (often situated on the thigh) causes mechanical and cosmetic problems.

Thus we had the idea to use a vascularised corium flap in selected cases in order to get a solid abdominal wall reconstruction for abdominal defects. This method can be used successfully if it came up to loss of fascia and muscle and yet sufficient flubby skin surplus near the defect.

METHODS: We successfully applied this method on four of our patients and submitted them to postoperative monitoring.

RESULTS: We annually operate from 150 to 200 patients with recurrent abdominal wall hernias in our hospital. Between March 2011 and September 2012 we got four possibilities to apply the before mentioned vascularised corium flap. All patients had previously undergone multiple laparotomies and mesh implants followed by mesh infections inducing the necessity of mesh explantation. Patients were aged from 35 to 82 years (mean 58 years), one female and three male. All of them resulted recurrence-free within a postoperative monitoring period of more than six months.

CONCLUSIONS: We consider the corium flap an economic solution practicable with basic surgical instruments. Anyway this method should be applied only in selected cases.

SATURDAY, MARCH 8, 2014

SCIENTIFIC SESSION 5 GROUP A
CLINICAL OUTCOMES
2:00 PM – 3:30 PM

SATURDAY, MARCH 8, 2014

41
Increased Anesthesia Duration Increases Venous Thromboembolism Risk in Plastic Surgery: A Six-Year Analysis of Over 19,000 Cases

Alexei S Mlodinow, BA[1]; Nima Khavanin, BS[1]; Jon P Ver Halen, MD[2]; Aksharananda Rambachan, BS[1]; Karol A Gutowski, MD[3]; John YS Kim, MD[1]

[1]Northwestern Feinberg School of Medicine, Chicago, IL, [2]Ingram Cancer Center, Memphis, TN, [3]Private Practice, Northbrook, IL

PURPOSE: Venous thromboembolism (VTE) is a well-documented cause of morbidity, mortality and excess healthcare cost. Various risk stratification schema such as the Caprini score and its derivatives exist in the plastic surgery literature, but do not take into account variations in procedure length. The putative risk of VTE conferred by increased length of time under anesthesia has never been rigorously explored. The goals of this study are to quantitatively assess this relationship, as well as provide a benchmark VTE rates among plastic surgery patients.

METHODS: The National Surgical Quality Improvement (ACS-NSQIP) database was queried for plastic and reconstructive surgery procedures performed under general anesthesia between 2005 and 2011. Z-scores were calculated based on procedure-specific mean surgical durations, to assess each case's length in comparison to other cases with the same primary procedure. Patients with and without post-operative VTE were compared with respect to a variety of demographics, comorbidities, and intraoperative characteristics. Potential confounders for VTE were included in a regression model, along with the Z-score for each case. This yielded an independent odds ratio for VTE, with respect to each unit increment in Z-score.

RESULTS: A total of 19,276 cases met inclusion criteria. VTE occurred in a variety of procedures, both cosmetic and reconstructive, at a total rate of 0.36% (70 incidents). There were incidents in each Z-Score interval analyzed. Increased relative surgical duration (as measured by the Z-score) was associated with increased VTE rates. Further, regression analysis showed a higher Z-score to be a statistically significant ($p<0.001$) independent risk factor for post-operative VTE, with an odds ratio of 1.772 per additional unit.

CONCLUSIONS: This validates the long-held view that increased surgical time confers risk of VTE, as well as benchmarks VTE rates in plastic surgery procedures. While this in itself does not suggest an intervention, surgical time under general anesthesia would be a useful addition to risk models in plastic surgery.

42
Risk Assessment of Concurrent Panniculectomy with Open Ventral Hernia Repair: A Propensity Score-Matched Analysis Using the 2005–2011 ACS-NSQIP

John P Fischer, MD; Charles T Tuggles, MD; Ari M Wes, BA; Stephen J Kovach, III, MD

University of Pennsylvania, Philadelphia, PA

OBJECTIVE: Develop a model of risk assessment of concurrent panniculectomy (VHR-PAN) during ventral hernia repair (VHR).

BACKGROUND: Recent studies have assessed the benefits and risks of performing concurrent PAN in the setting of hernia repair, gynecologic surgery, and oncologic resections with conflicting results. The aim of this study is to assess the added risk of VHR-PAN using the ACS-NSQIP data sets.

METHODS: The 2005–2011 ACS-NSQIP databases were queried to identify all patients undergoing VHR alone or VHR-PAN. Current Procedural Terminology (CPT) codes were used to define hernia repairs and concurrent panniculectomies. Propensity scores were used to account for potential selection bias given the non-randomized assignment of concurrent panniculectomy and the retrospective nature of this study. Multivariate logistic regression analyses were used to assess the impact of concurrent PAN on wound complications, venous thromboembolism, unplanned reoperation, and medical complications.

RESULTS: A total of 55,537 patients were identified. Propensity matching yielded two groups of patients: VHR (n=1,250) and VHR-PAN (n=1,250). Few statistically significant differences existed between matched cohorts and no significant differences in sociodemographic characteristics, clinical parameters, or comorbidities were noted. Matched analysis of obese patients showed significantly higher rates of surgical complications at BMI ranges of 30–34.9 kg/m2 (P=.001) and ≥50 kg/m2 (P=.034) in combined VHR-PAN. HR-PAN was not associated with an increased risk of surgical complications in the intermediate BMI groups (35.0–39.9kg/m2) (P=.186) and (40.0–44.9kg/m2) (P=.535). Overall, wound complications (P<.001), venous thromboembolism (P=.044), rates of reoperation (P<.001), and medical morbidity (P<.001) were significantly higher in the VHR-PAN group. In an adjusted, fixed-effects analysis, concurrent panniculectomy was associated with wound healing complications (OR=1.69, P<.001), increased rates of unplanned reoperations (OR=2.08, P=<.001), venous thromboembolism (OR=2.48, P=.043), and overall medical morbidity (OR=2.08, P<.001).

CONCLUSIONS: This analysis quantifies the added risk of performing a panniculectomy concurrent with ventral hernia repair and demonstrates a relatively unfavorable risk profile for

certain patient groups. A favorable risk-benefit was observed in the BMI range of 35.0–44.9 kg/m2. These data provide the foundation for a more comprehensive assessment of the risk-benefit of VHR-PAN and can be used to assist surgeons in informing patients and improving patient selection.

43
Prophylactic Mastectomies: Implications of Occult Histology and Lifetime Cost of Surveillance vs. Surgery

David Mattos, AB[1]; Richard G Reish, MD[2]; Curtis Cetrulo, MD[2]; Amy S Colwell, MD[2]; Jonathan M Winograd, MD[2]; Michael J Yaremchuk, MD[2]; William G Austen, Jr, MD[2]; Eric C Liao, MD, PhD[2]

[1]Harvard Medical School, Boston, MA, [2]Massachusetts General Hospital, Boston, MA

PURPOSE: During the last decade, our institution saw a 260% increase in bilateral breast reconstruction cases, consistent with national trends, and recently highlighted in the press with the bilateral elective mastectomy of a Hollywood actress.[1] We reported a drop in average age of prophylactic mastectomy from 57 to 51 years. There is limited data on the likelihood of histological abnormalities in this population. This study measures the prevalence of occult histological findings in prophylactic mastectomy patients. Given the current healthcare reform climate, we estimate the lifetime cost implications of prophylactic mastectomy with single-stage reconstruction vs. surveillance.

METHODS: A retrospective database of breast reconstructions at our institution was searched from 2004 to 2011 for prophylactic mastectomy patients. Breasts with prior biopsy-proven LCIS, DCIS, or cancer were excluded. Patient demographics, risk factors, and pathology reports were collected. Lifetime treatment costs were estimated with 2013 rates from the Center for Medicare and Medicaid Services using Current Procedural Terminology and Diagnosis Related Group codes. Costs were estimated for two groups: 45 year old patients undergoing contralateral or bilateral prophylactic mastectomies versus surveillance. Conversion rates to cancer in these patients were used to estimate the percentage patients in the surveillance group that would need surgery.

RESULTS: 436 patients were identified that had a prophylactic mastectomy on at least one breast, of which 10 patients (2.0%) had invasive cancer, 22 (5%) had DCIS, 51 (11.7%) had LCIS, and 97 (22.2%) had atypia as the highest-risk lesion, a total of 180 (41.3%) patients. The likelihood of finding LCIS, DCIS, or cancer increased with age ($P < 0.001$). LCIS, DCIS, or invasive cancer was found in 12.3% of BRCA patients and 21.9% of non-BRCA patients ($P=0.02$). The percentage of patients with LCIS, DCIS, or invasive cancer was 16.9% in the bilateral group vs. 19.4% in the contralateral group ($P=0.66$). Lifetime costs for bilateral prophylactic mastectomies were estimated to be $48,118, lower than the $55,165 necessary for bilateral surveillance. For patients with one-sided cancer, contralateral mastectomy would add $1,702 whereas surveillance would add $26,080.

CONCLUSIONS: Prophylactic mastectomy patients have a significant rate of occult histological findings, increasing with age. Unexpectedly, BRCA patients had a lower prevalence of findings, despite higher lifetime risk of breast cancer. Lifetime cost estimates suggest a cost-saving role in bilateral and contralateral prophylactic mastectomies. Ultimately, such a critical decision needs to be made individually, but should not be hindered by cost concerns. This pioneering study addresses a gap in knowledge with broad interest, contributing evidence of oncologic risk and cost to help guide decision-making in prophylactic mastectomy.

REFERENCES:

1. Fitzpatrick AM, Gao LL, Smith BL, et al. Cost and Outcome Analysis of Breast Reconstruction Paradigm Shift. Annals of plastic surgery. 2013; Epub ahead of print.

44
Components Separation for Abdominal Wall Reconstruction: The Pitt Experience, a Review of 605 Cases

Sanjay Naran, MD; Sameer Shakir, BS; Patrick Emelife, BS; Meghan Quigley, MD; James Russavage, DMD, MD; Ernest Manders, MD; J Peter Rubin, MD; Carolyn De La Cruz, MD; Michael Gimbel, MD; Vu Nguyen, MD

University of Pittsburgh, Pittsburgh, PA

PURPOSE: Components separation of the abdominal musculature is a mainstay for closing complicated midline and para-median abdominal wall defects. We set out to critically analyze our experience with this operative technique, and in doing so identify prognosticators that affect long-term clinical outcomes.

METHODS: We retrospectively reviewed all patients who underwent components separation between 2000–2010. Over 40 data points were collected for each patient and examined as to whether they affected long-term clinical outcomes. Demographics including BMI, co-morbidities, and operative details were collected. We documented major and minor complications including hernia recurrence, heamatoma, seroma, ischemia, infection, superficial wound breakdown, and DVT/PE.

RESULTS: Our cohort consists of 605 patients, 51.1% of which were female, with a mean age of 53.6±13.45 years, BMI of 32.7±7.8 kg/m2, and defect size of 202.9±228.7 cm2. The average defect width was 12±2 cm. 85% had a prior abdominal surgery, and 31.7% had a prior mesh placement. 79.1% underwent a concurrent procedure at the time of component separation, 17.7% of which involved bowel enterotomies. 2.6% required prosthetics for closure. Mean post-operative stay was 7.2±6.0 days, and average follow-up was 2.5±2.4 years. The recurrence rate was 20.0%. Post-operative complications included heamatoma (3.8%), seroma (6.4%), ischemia (3.0%), infection (13.3%), superficial wound breakdown (5.5%), and DVT/PE (3.0%). The presence of a respiratory co-morbidity ($p=0.001$) was associated with an increased risk of recurrence (OR=2.49). The prior use of a prosthetic ($p=0.001$, OR=2.01), and the use of a prosthetic at the time of separation ($p=0.048$, OR=1.73), were significant predictors of recurrence. The occurrence of any post-operative complication ($p<0.001$) significantly increased the likelihood of eventual recurrence. We found no association between recurrence and BMI. Hematoma was more likely in cases that required a blood transfusion ($p=0.003$), seroma was more likely in males, and Ischemia was more likely in patients with a higher BMI ($p=0.043$), ASA Classification >2 ($p=0.035$), and an endocrine disorder (which included diabetes) ($p=0.004$). Superficial wound dehiscence was more likely in males ($p=0.000$) and patients with respiratory ($p=0.004$), hepatorenal ($p=0.004$),

or endocrine disorders (p=0.026). DVT/PE was more likely in patients with respiratory (p=0.005) and endocrine (p=0.027) disorders. Males (p=0.005), high BMI patients (p=0.015) and large defect area patients (p=0.022) were more likely to experience any complication.

CONCLUSIONS: This study provides a comprehensive review of the largest series utilizing components separation to date. We identify various risk factors that are statistically significant in their association with particular complications. Patients with respiratory co-morbidities, prior use of a prosthetic, and use of a prosthetic at the time of separation, are significantly more likely to have a recurrence; however, in our cohort the components separation technique remains a reliable method of abdominal wall reconstruction even in the setting of co-morbidities thought to be associated with recurrence.

45
Broadening Indications for Immediate Implant-Based Breast Reconstruction

Claudia R Albornoz, MD, MSc; Gina Farias-Eisner, BA; Joseph J Disa, MD; Babak J Mehrara, MD; Colleen M McCarthy, MD, MS; Andrea L Pusic, MD, MHS; Peter G Cordeiro, MD; Evan Matros, MD, MMSc
Memorial Sloan-Kettering Cancer Center, New York, NY

BACKGROUND: Over the past 10 years there has been a 200% increase in the number of implant-based breast reconstructions performed within the US while the number of autologous reconstructions is unchanged. The rise in implant use may reflect: 1) increased patient or physician preference for implants, and/or 2) expanding indications for implants in patients previously denied breast reconstruction because of unfavorable clinical characteristics. The aim of the current study is to measure implant use over time in patients previously considered poor reconstructive candidates.

METHODS: Analysis of the prospectively collected breast disease management team database at Memorial Sloan-Kettering Cancer Center was performed. All patients who underwent a total mastectomy during the years 2001–2012, with or without reconstruction, served as the cohort. A literature review was performed to identify commonly cited relative contraindications for breast reconstruction. These included: age greater than 60 years, BMI>30, comorbidities (diabetes, cardiovascular disease, COPD), smoking, stage III or IV breast cancer, prior radiotherapy, post-mastectomy radiotherapy, and chemotherapy. Trends in use of implant reconstruction among patients with unfavorable clinical characteristics were analyzed with Poisson regression. To understand reconstructive trends within the specific group, rates for each unfavorable characteristic were adjusted by 100 total mastectomies performed for patients with that specific feature. An incidence rate ratio (IRR) greater than 1.0 with a p-value <0.05 was considered a significant rate increase

RESULTS: A total of 9,543 patients underwent total mastectomies during the study period. The immediate reconstruction rate increased from 49.9 in 2001 to 77.6 per 100 total mastectomies in 2012 (IRR 1.04, p<0.01). While autologous reconstruction rates were unchanged during this period, implant reconstruction rates increased from 43.9 to 71.8 per 100 total mastectomies (IRR 1.05, p<0.01). From 2001–2012 there was a significant increase in implant use for patients with any of the following features: age greater than 60 years, BMI>30, diabetes, cardiovascular disease, smoking, COPD, Stage III or IV breast cancer, prior radiotherapy, post-mastectomy radiotherapy, and chemotherapy. Rates of autologous tissue use were unchanged in every group except for an increase in patients with BMI>30 (IRR 1.17, p<0.01). Overall, reconstructive rates in patients with any adverse clinical characteristic

increased from 45.7 to 72.7 per 100 total mastectomies (IRR 1.04, p<0.01).

CONCLUSIONS: Broadening indications has lead to increasing immediate breast reconstruction rates in high-risk patients at a major academic medical center. The majority of patients with unfavorable clinical characteristics undergo immediate implant-based reconstruction, relative to autologous tissue, as an efficient less invasive means of recreating the breast mound. Moving forward, the long-term safety and reliability of implant use in this patient group needs to be determined.

46
The BRA Score: Creating a General Risk Calculator for Breast Reconstruction Outcomes

Nima Khavanin, BS[1]; John Y S Kim, MD[1]; Armando A Davila, MD[2]; Jon P Ver Halen, MD[3]; Alexei S Mlodinow, BA[1]; Kevin P Bethke, MD[1]; Seema A Khan, MD[1]; Jacqueline S Jeruss, MD[1]; Nora M Hansen, MD[1]; Karl Y Bilimoria, MD[1]; Albert Losken, MD[4]; Neil A Fine, MD[1]

[1]Northwestern University Feinberg School of Medicine, Chicago, IL, [2]Loma Linda University, Loma Linda, CA, [3]Baptist Cancer Center / Vanderbilt Ingram Cancer Center, Memphis, TN, [4]Emory University Hospital, Atlanta, GA

PURPOSE: With over 90,000 prosthetic and autologous reconstructions each year, there have been many studies aimed at identifying risk factors associated with a perioperative surgical site infection. None, however, are sufficiently powered to provide an objective measure of an *individual* patient's pre-operative risk for infection following the various reconstruction procedures. With data from over 300 surgical centers across the United States, the American College of Surgeon's National Surgical Quality Improvement Program (NSQIP) registry provides high powered, validated data ideal for modeling a patient's risk for perioperative complication. We aimed to develop a validated Breast Reconstruction Risk Assessment (BRA score) calculator and to assess a patient's risk for postoperative infection across the various reconstruction modalities following mastectomy with immediate reconstruction.

METHODS: Patients undergoing mastectomy with immediate prosthetic (n=12,612) or autologous (n=3,457) reconstruction between 2005 and 2011 were identified from the NSQIP database. Forward stepwise multiple logistic regression identified preoperative variables for inclusion in the model. Hosmer-Lemeshow and concordance statistics were computed to assess model calibration and discrimination. Overall model performance was evaluated with the Brier score. Bootstrap analysis was used to validate the model. Chi-squared tests were used to determine the influence of infection on 30-day readmission and reoperation. The validated model was used to develop an interactive risk calculator that accepts patient information and returns an estimated surgical site infection probability based on the logistic regression model. Predicted probabilities were calculated from the logistic function: Probability=$1/(1 + e^{-\beta})$, where β is the summation of the model constant and the relevant covariates for a given patient. The web based risk calculator is available at www.brascore.org.

RESULTS: The overall infection rate was 3.75 (603 out of 16,469 patients). The infection rate was greatest within the pedicled TRAM cohort (5.97%), followed by the free flap cohort (5.52%), prosthetic cohort (3.44%), and finally the latissimus cohort (2.80%). In addition to reconstructive modality, 5 predictors of infection were selected for inclusion within the model: BMI, age, ASA class, bleeding disorder, and history of percutaneous cardiac intervention or cardiac surgery. The model c-statistic was 0.682 and the optimism-corrected c-statistic 0.678. The model was well calibrated (HL p-value = 0.371) and the brier score was 0.036. Across all reconstructive modalities, patients with an infection experienced higher rates of reoperation (range of 38.1%-45.9% vs. 4.8%-13.5%) and readmission (50.9%-61.1% vs. 2.8%-5.3%) (all $p < 0.001$).

CONCLUSIONS: In this era of increasing emphasis on evidence-based decision making, there has been a reliance on population-based assessments of risk. Through this analysis of a large, validated multi-institutional database, we developed a modifiable risk calculator (the BRA score) to determine individual risk of outcomes following breast reconstruction. Applying the BRA score to surgical site infections, we found a gradient of risk among the common forms of reconstruction. While the precise manifestation of this BRA score can vary by database and measured outcome, it is a potentially useful educational construct to better manage physician and patient expectations.

47
Surgical Treatment of Nipple Malposition in Nipple Sparing Mastectomy Device-Based Reconstruction

Kathleen Kelly, BA; Kevin Small, MD; Alexander Swistel, MD; Briar Dent, MD; Erin Taylor, BA; Mia Talmor, MD

New York-Presbyterian Hospital/Weill Cornell Medical College, New York, NY

PURPOSE: We report our senior author's experience with nipple-areolar complex (NAC) malposition following nipple sparing mastectomy (NSM), surgical options for treatment, and an analysis of patient risk factors.

METHODS: A retrospective chart review was conducted on a prospectively-collected IRB-approved database of NSM cases with immediate implant-based reconstruction performed by a single plastic surgeon between July 2006 and October 2012. Malposition was graded as mild displacement (1cm), moderate (2cm), and severe (>3cm).

RESULTS: 319 NSMs with were reviewed. Malposition occurred in 13.79% (n=44). Significant factors associated with malposition included older age ($p < 0.0001$), comorbid diabetes mellitus ($p=0.024$), increased body mass index (BMI) ($p=0.0093$), preoperative sternal notch to nipple distance ($p=0.015$), preoperative breast base width ($p=0.0001$), periareolar mastectomy incision with lateral extension ($p<0.0001$), prior radiation therapy ($p=0.0004$), prior ipsilateral lumpectomy ($p=0.0125$), and postoperative nipple-areolar complex (NAC) ischemia ($p=0.0174$). Smoking status, breast volume resected, implant size, inframammary mastectomy incision, acellular dermal matrix, and single stage reconstruction were not significant. 19/44 (43.2%) malposition cases were satisfied and deferred surgical correction (9 mild, 7 moderate, 3 severe). 8/44 (18.2%) cases were not offered surgical correction because of an inadequate skin envelope secondary to radiation tissue fibrosis, contracture, or thinning. 8/44 (18.2%) cases were corrected with crescent mastopexy (7 mild, 1 severe), 3/44 (6.8%) with implant exchange and pocket revision (1 moderate, 2 severe), 4/44 (9.1%) with free nipple grafts (4 severe), and 2/44 (4.5%) with pedicled nipple transposition (2 severe). Of note, 2/44 (4.5%) had nipple excision and reconstruction secondary to recurrence. There were no incidences of nipple necrosis or nipple malposition after surgical correction.

CONCLUSION: NSM followed by immediate implant-based reconstruction has an identifiable risk of nipple malposition. We found several risk factors to be significantly associated with nipple malposition. Various surgical options are available to correct nipple malposition based on clinical presentation and are safe procedures in a well-selected patient population to improve overall cosmesis.

48
Identification and the Effective Repair of the Athletic Hernia

Som Kohanzadeh, MD; Morgan S. Martin; Derek Marrero, MD; Liana M Lugo, MD; Luis O Vasconez, MD
Univ of Alabama Birmingham, Birmingham, AL

PURPOSE: Athletes often suffer from specific injuries, unlike people with more sedentary lifestyles. One such entity is the athletic hernia, otherwise known as a "sports hernia"; presenting with athletic pubalgia; where the groin is affected in such individuals. Chronic inguinal pain in professional or recreational athletes without evidence of a true hernia is the presentation. There is no evidence of inguinal herniation, however, upon examination there is point tenderness at the pubic symphysis, which is accentuated by resisted hip adduction. This is secondary to rupture of the muscular attachment to the pubis. This study describes the identification and diagnosis, followed by operative outcomes using a validated survey in a consecutive series of patients following surgical repair. The repair involves repair and reinforcement of the muscular attachments at the pubic symphysis. This is accomplished through pelvic floor reinforcement with a local muscle flap and mesh.

METHODS: Over a 12 year period, from 2000 through 2012, the aforementioned sports hernia repair was performed by the senior author (L.O.V) in 51 patients. Demographic data was collected and a Pain questionnaire was used to evaluate postoperative outcomes.

RESULTS: The median age was 22 years. The patients were involved in a variety of sports, including: football (35%), soccer (20%), running (15%), basketball (10%), cycling (8%), baseball (6%), volleyball (4%), and martial arts (2%). 53% of patients were college athletes. There was a 70% survey response rate with only 8% of patients reporting no improvement; 92% with either marked or complete resolution. 78% had resolution of pain within 1 month. The remaining patients were pain free by 12 months postoperatively. 88% had no sports limitations after treatment.

CONCLUSION: Sports hernia is an often misdiagnosed problem, and thus has limited treatment and even less frequently evaluated outcomes. Imaging studies are often non-diagnostic. However, through physical exam findings, most notably point tenderness at the pubis exacerbating with forced hip adduction. Excellent outcomes were noted with the use of an internal oblique flap overlying a propylene mesh to help repair and reinforce the injury. This method served to relieve the pain and allow return to full activity in the vast majority of patients.

49
A Retrospective Review of Plastic Surgery Consultations to Evaluate the Effect of Web-Based Education on Patient Satisfaction and Consultation Time

David Boudreault, MD[1]; Chin-Shang Li, MD, PhD[2]; Michael S Wong, MD[1]
[1]UC Davis Medical Center, Sacramento, CA, [2]University of California, Davis, CA

PURPOSE: To evaluate 1) patient satisfaction and 2) consultation times in those who viewed versus those who did not view online patient education material prior to their consult. Patients expect a healthcare system that is both efficient and provides the highest quality of care. Through an independent survey published by Grote in The McKinsey Quarterly 2007, patients report the quality of education they received regarding their procedure or treatment was the most influential factor in their decision of which hospital or physician they ultimately chose. The implications of an "excellent" versus a "very good" rating had significant affects on this choice. After reviewing 176,000 surveys performed through Physician Research Consultants, a significant decrease in patients' willingness to recommend the service to family and friends was found between those rating their experience as "excellent" vs "very good" (86% vs 23%). Thus, it is important patients rate their experience as excellent. Many healthcare systems have targeted improved patient education through the use of various educational tools. Developers of the program used by our hospital report improved satisfaction and decreased consultation time by better preparing patients for consultation.

METHODS: In this retrospective review, 767 new patient consultations were seen by 4 university based plastic surgeons, between May 2012 and August 2013, and were evaluated to determine the effect of a web-based educational program covering abdominoplasty, breast augmentation, breast reduction, breast reconstruction, blepharoplasty and liposuction on patient satisfaction and consultation time. A standard 5-point Likert scale survey completed at the end of the consultation was used to assess satisfaction with their experience. A score of 1 was excellent and 5 was poor. Consult times were obtained from the electronic medical record by taking the difference between the time vital signs were entered and when an after visit summary was printed. This was compared to actual consult times recorded by one surgeon. All analyses were done with Statistical Analysis Software (SAS) version 9.2 (SAS Inc., Cary, NC). A p-value < 0.05 was considered statistically significant.

RESULTS: Those who viewed the program prior to their consultation were more satisfied with their experience compared to those who did not (satisfaction scores, mean ± SD: 1.13 ± 0.44 vs. 1.36 ± 0.74; p=0.02) and more likely to rate their experience as excellent (92% vs. 75%; p=0.02). Patients who viewed the educational program prior to consultation trended

towards longer visits compared to those who did not (mean time ± SD: 54 ± 26 vs. 50 ± 35 mins; p=0.10).

CONCLUSION: Viewing web-based educational programs significantly improved plastic surgery patients' satisfaction with their consultation, but also trended towards longer consultation times. Our surgeons report that patients who use web-based educational tools appear to have an increased understanding of their procedure and thus engage in higher-level conversations, which may contribute to additional time spent with patients.

SATURDAY, MARCH 8, 2014

SCIENTIFIC SESSION 5 GROUP B
CRANIOFACIAL/BONE
2:00 PM – 3:30 PM

SATURDAY, MARCH 8, 2014

50
Fabrication of Tissue-Engineered Human Constructs for Patient Specific Auricles

Rachel C Hooper, MD[1]; Rachel Nordberg, BA[2]; Kadria N Derrick, MD[1]; Jennifer Puetzer, BA[3]; Karina A Hernandez, DO[1]; Ope Asanbe, MD[1]; Larry Bonassar, PhD[3]; Jason A Spector, MD, FACS[1]

[1]Weill Cornell Medical College, New York, NY, [2]Cornell Univeristy, Ithaca, NY, [3]Cornell University, Ithaca, NY

PURPOSE: The reconstruction of pediatric microtia using autologous donor cartilage is limited by significant obligatory donor site, pain and scarring as well as frequent suboptimal aesthetic outcome. Tissue-engineering allows for the creation of anatomically correct auricular constructs and the minimization or even elimination of the previously mentioned complications. In previous work, we fabricated patient specific, high fidelity tissue-engineered frameworks composed of type I collagen and bovine auricular chondrocytes that not only maintained shape and size over 12 weeks, but also exhibited proteoglycan and elastin deposition, with mechanical properties indistinguishable from native auricular cartilage. As a bridge to clinical translation, we have now synthesized human auricular chondrocyte (HAC) constructs in order to determine the optimal chrondrocyte passage and seeding density for the fabrication of patient specific tissue-engineered auricles.

METHODS: Human auricular cartilage was obtained from discarded specimens following elective office otoplasty procedures; chondrocytes were extracted and expanded. Type 1 collagen (10 mg/ml) was seeded with 25million cells/mL HAC, passage 2–3 and subsequently underwent thermal gelation. After formation of a 1 mm thick sheet, 8mm diameter scaffolds were obtained using a biopsy punch. Scaffolds were stored in Dulbeco's Modified Eagle Medium (DMEM) supplemented with 10% fetal bovine serum, 100 μg/mL penicillin, 100 μg/mL streptomycin, 0.1 mM non-essential amino acids for 48 hours prior to surgical implantation. Scaffolds were implanted subcutaneously in the dorsa of 8-week-old nu/nu mice and harvested after 1 month. Following harvest, tissues were processed for imaging and histology.

RESULTS: Gross inspection of HAC scaffolds following 1 month of implantation demonstrated maintenance of scaffold size and shape. Post-harvest confocal reflectance microscopy revealed viable chondrocytes within the collagen matrix. Picrosirus red staining demonstrated the presence of lacunar chondrocytes with local deposition of cartilage whereas Verhoeff staining demonstrated elaboration of elastin fibers within the construct.

CONCLUSION: We have successfully fabricated viable human auricular chondrocyte constructs that form a cartilaginous matrix and elaborate elastin fibers in as little as 1 month after implantation. Similar techniques are currently being explored to determine the optimal passage and seeding density to allow for the generation of 250 million auricular chondrocytes necessary to seed a full-sized ear scaffold.

51
Decreased Secondary Bone Grafting but Poorer Midface Growth after Primary Alveolar Cleft Repair with Gingivoperiosteoplasty and rhBMP-2

Kristen S Yee, MD; Justine C Lee, MD, PhD; Brian T Andrews, MD; James P Bradley, MD
UCLA Division of Plastic and Reconstructive Surgery, Los Angeles, CA

PURPOSE: Studies from NYU revealed that following nasoalveolar molding/gingivoperiosteoplasty (GPP) 60% of patients did not require an alveolar bone graft. In our lab midface animal growth was not detrimentally affected after BMP-2 healing of alveolar clefts. In this study, we performed a similar procedure to NYU with alveolar molding/GPP but with BMP-2 on a resorbable matrix for primary alveolar repair in the infant. We compared long-term follow-up (10 years) for 1) No GPP, 2) GPP only or 2) GPP with BMP-2 by analyzing alveolar bone, tooth eruption, and maxillary growth.

METHODS: For the three primary unilateral cleft repair patient groups: 1) No GPP (n=15), 2) GPP only (n=15) or 2) GPP with BMP-2 (n=10) we performed follow-up studies at least 10 years after the procedure. There was one GPP patient lost to follow-up. We recorded need for secondary alveolar bone grafting, timing of tooth eruption, and clinical evidence of maxillary hypoplasia. New-Tom scans were used to analyze dentition, bone volume and bone density.

RESULTS: For dentition, there was absent cleft lateral incisor in 40% of patient (40%, 46% 50%). Cleft site secondary tooth eruption was variable but occurred at a mean of 1.8+0.4 years earlier in 2) GPP and 3) GPP/BMP-2 compared to 1) No GPP. Greater bone graft volume/density was seen at the cleft site in the 3) GPP/BMP compared to the 2) GPP only (86% vs 42% bone fill). Secondary alveolar bone grafting after expansion was necessary in 1) 'No GPP' patients (100%); 2) 'GPP only' (73%); 3) 'GPP/BMP-2' (20%). Bone volume Two patient in GPP/BMP-2 underwent Le Fort I distraction at age 13. In the other groups there were no patients, to date, who undergone Le Fort I distraction. Clinical evidence of maxillary hypoplasia was seen in 1) 'No GPP' patients (40%); 2) 'GPP only' (53%); 3) 'GPP/BMP' (60%). We are in the process of collecting and recording our lateral cephalogram data.

CONCLUSION: In a long-term follow-up, after mid-childhood but prior to skeletal maturity, GPP/BMP-2 primary alveolar cleft repairs showed similar tooth eruption, improved bone fill of the cleft site, less need for secondary alveolar grafting. However, data thus far shows poorer midface growth compared to No GPP at primary cleft repair. This study documents our group's IRB approved study primary alveolar clefts with the use of gingivoperiosteoplasty, BMP-2 and a collagen scaffold as an alternative technique to traditional care.

52
Mutating Fibroblast Growth Factor Receptor 1 (Fgfr1) in Zebrafish to Create a New Model of Craniosynostosis

Joanna P Tomaszewski, MS[1]; Michael S Gart, MD[2]; Ramy A Shoela, MD[1]; Jacek Topczewski, PhD[1]; Jolanta M Topczewska, PhD[1]; Arun K Gosain, MD[3]
[1]Ann & Robert H Lurie Children's Hospital of Chicago Research Center, Chicago, IL, [2]Northwestern University Feinberg School of Medicine, Chicago, IL, [3]Ann & Robert H Lurie Children's Hospital of Chicago, Chicago, IL

Human genomic studies and research on animal models suggest that various loci and genetic mechanisms, notably mutations in fibroblast growth factor receptor 1 (FGFR1), are involved in the development of craniosynostosis (CS), or premature suture obliteration. The goal of this project is to create a zebrafish model of CS, which would present advantages over previously established rodent models. Homologous genes and similar genetic networks are involved in morphogenesis of craniofacial skeletal elements in both zebrafish and humans (Knight and Schilling, 2006). Furthermore, the ease of complex genetic manipulations makes the zebrafish an attractive model for elucidating the etiology of CS. We aim to mimic the mutation observed in Pfeiffer syndrome by generating a stable transgenic zebrafish line that allows for inducible expression of the mutated *fgfr1*$^{(Pro252Arg)}$ gene.

METHODS: Two FGFR1 zebrafish paralogs, *fgfr1a* and *fgfr1b,* were detected in total RNA isolated from calvaria at 8-10mm standard length using RT-PCR. *fgfr1b* was cloned and mutagenized by a single base pair substitution to create the Pro252Arg mutation. Gateway Recombineering and the Tol2 system were used to create the transgenic construct, which includes an *hsp70* promoter for inducible expression of the mutated gene and an IRES-driven GFP reporter for monitoring of ectopic expression. To assess the impact of the mutation on embryonic development, single cell stage embryos were injected with mutated *fgfr1b* mRNA and tested for expression of target genes of FGF signaling using whole mount in situ hybridization. Once the final form of transgenic cassette is confirmed, it will be injected into embryos to create a stable transgenic line.

RESULTS: Preliminary results of RNA in situ hybridization revealed that the expression domain of *krox20* within the presumptive rombomeres 3rd and 5th is expanded in injected embryos, supporting the hypothesis that Pro252Arg mutation has an activating character in zebrafish. Furthermore, embryos injected with fgfr1b$^{(Pro252Arg)}$ mRNA phenotypically reveal decreased head size, consistent with fgfr1 upregulation.

CONCLUSION: An expanded krox20 expression domain at the embryonic stage of fgfr1b$^{(Pro252Arg)}$ mRNA injected embryos suggests that this mutation has activating character in zebrafish, indicating a conserved role of fgfr1 in cranial suture development among vertebrates. The effects of genetic manipulation on adult suture phenotype will be assessed through histological analysis, skeletal morphology, and cell proliferation will be studied in our transgenic fgfr1b$^{(Pro252Arg)}$ embryos. This zebrafish model of CS will advance our understanding of the role of Fgfr1b in cranial suture morphogenesis and the etiology of the disorder. In the future, it can be used for genetic and chemical screens to search for genetic modifiers and therapeutic agents that alter CS.

53
Prophylactic Amifostine Preserves the Biomechanical Properties of Irradiated Bone in the Murine Mandible

Peter A Felice, MD; Salman Ahsan, BS; Joseph E Perosky, MS; Sagar S Deshpande, BS; Noah S Nelson, BS; Alexis Donneys, MD, MS; Kenneth M Kozloff, PhD; Steven R Buchman, MD, MS

University of Michigan Medical School, Ann Arbor, MI

PURPOSE: Despite its therapeutic aims in the treatment of head and neck cancer, radiation therapy can lead to devastating consequences such as pathologic fracture. We have previously demonstrated that Amifostine prophylaxis mitigates the pernicious effects of radiation on bone in the settings of distraction osteogenesis and fracture repair; expanding on these studies, we established a translational model to analyze the biomechanical properties of native, uninjured, and unoperated mandibles exposed to both radiation and Amifostine administration. We hypothesize that radiation will significantly alter the biomechanical properties of otherwise uninjured bone. We further hypothesize that prophylactic Amifostine will preserve biomechanical properties to levels of normal bone and protect the mandible from the morbidities associated with radiation administration.

METHODS: Sprague Dawley rats were randomized into three groups; Control, radiation exposure (XRT), and Amifostine pre-treatment with radiation exposure (AMF-XRT) specimens. Irradiated animals received a fractionated dosing schedule of 7Gy/day over five days for 35Gy total human-equivalent radiation dosage to the left hemi-mandible, while Amifostine pretreated animals received 100mg/kg subcutaneous injection 45 minutes prior to radiation. Hemi-mandibles were harvested at 8 and 18 weeks and a region of interest machined for Yield Load, Ultimate Load, and Stiffness biomechanical testing metrics, as well as for micro-computed tomographic analysis.

RESULTS: The 8-week XRT specimens displayed significant elevations above Controls for all biomechanical testing metrics while 8-week AMF-XRT specimens were maintained at levels comparable to Controls. The 18-week XRT specimens displayed biomechanical properties that were degraded in comparison to Controls, while 18-week AMF-XRT specimens continued to display levels comparable to Controls. The 18-week XRT specimens demonstrated a significant decrease in Yield Load and a trending decrease in Ultimate Load when compared to AMF-XRT specimens. The most noteworthy finding for Tissue Mineral Density micro-computed tomography analysis was a significant decrease in mineralization from 8- to 18-week XRT specimens, while no such change existed for Control and AMF-XRT specimens.

CONCLUSION: Our findings demonstrate a paradoxical and transient elevation in the initial biomechanical properties of irradiated specimens that was not sustained through the later time point of our study. Amifostine pre-treatment, however, provided uninterrupted preservation of the native biomechanical properties of bone at both time points. Micro-computed tomography analysis for irradiated specimens also yielded an elevation in Tissue Mineral Density at 8 weeks, a finding reversed in Amifostine pre-treated specimens at 18 weeks. These outcomes support the contention that Amifostine is capable of providing continuous and consistent protection to bone against the untoward effects of radiation therapy. Clinical trials may now be warranted to determine whether utilizing prophylactic Amifostine is efficacious in preventing collateral damage to bone in treatment protocols for patients requiring radiation therapy.

54
TGF Beta and BMP Signaling Pathways Influence Regenerative Capacity of Calvarial Bones via Cross-Talk and Modulation of Apoptosis: The Potential Therapeutic Role of Small Molecule Inhibitors of TGF Beta Signaling

Kshemendra Senarath-Yapa, MA (Cantab) MBBChir MRCS; Nathaniel Meyer, BS; Shuli Li, MD PhD; Michael T Longaker, MD MBA; Natalina Quarto, PhD

The Hagey Laboratory for Pediatric Regenerative Medicine, Stanford University, Stanford, CA

PURPOSE: Craniofacial skeletal defects pose a significant clinical burden that is insufficiently met by current reconstructive approaches. A better understanding of calvarial osteoblast biology is essential in order to promote endogenous skeletal regeneration. Studies on transgenic mice with a Wnt1-Cre construct and a reporter R26R established that frontal bones arise from neural crest and parietal bones from paraxial mesoderm. Frontal neural crest-derived osteoblasts (FOb) possess greater osteogenic potential relative to parietal bone osteoblasts (POb) and reduced apoptotic activity. This is partly due to increased TGF-β1 signaling in parietal bones, which is known to promote apoptosis in different cell types. Determining a signaling network that modulates apoptotic activity is therefore worthwhile. We investigated the potential for enhancing calvarial regeneration by inhibiting TGF-β1 signaling with a specific small molecule inhibitor, SB431542 and the importance of apoptosis in calvarial healing with a specific caspase-3 inhibitor. Furthermore, we investigate the effect of TGF-β1 on apoptotic activity in calvarial osteoblasts and dural cells.

METHODS: Non-critical calvarial defects were made in parietal bones of CD-1 mice. A collagen sponge was used to deliver TGF-β1 (400ng) or SB431542 (26mM), a small molecule inhibitor of TGF-β1 signaling. Micro-CT evaluation of bone regeneration was done for 6 weeks and osseous healing calculated using GE Microview. The same in vivo model was use to test the effect of Ac-DEVD-CHO (1μM) a specific Caspase 3 inhibitor on calvarial healing. IHC was performed on sections through calvarial defects for Phospho-Smad 2 and 3, downstream effectors for TGFβ signaling, to assess whether SB431542 (SB) was effectively inhibiting this pathway in vivo. A Caspase-3 fluorometric protease assay was used to assess apoptotic activity in dural cells and POb during osteogenic differentiation. POb were collected at different time points of osteogenic differentiation and immunoblotting was performed for down stream effectors of the TGF-β1 pathway (P-Smad2) and BMP pathway (P-Smad5) on cell lysates during osteogenic differentiation.

RESULTS: Delivery of TGF-β1 significantly reduced the percentage healing relative to non-treated defects (*p<0.05). Inhibition of TGF-β1 signaling using SB resulted in significantly enhanced bone regeneration (*p<0.05). Direct inhibition of apoptosis with Ac-DEVD-CHO significantly improved calvarial defect healing (P<0.05). IHC for downstream effectors of TGF-β1 signaling, Phospho-Smad 2 and 3, established effective TGF-β1 inhibition in-vivo. In vitro apoptosis assays demonstrated a significant reduction in apoptotic activity in POb and dura with TGF-β1 inhibition. Immunoblotting analysis for P-Smad2 showed effective inhibition of TGF-β1 signaling by SB. Intriguingly, SB treatment also led to increased P-Smad 5, a downstream effector of BMP signaling, suggesting cross-talk between these two pathways.

CONCLUSIONS: We demonstrate that increased TGF-β1 signaling impairs calvarial healing whereas inhibition promotes regeneration. TGF-β1 inhibition using a specific small molecule inhibitor significantly reduces apoptotic activity in POb and dural cells undergoing osteogenic differentiation. We establish the presence of cross-talk between TGF-β and BMP signaling pathways during osteogenic differentiation and the importance of apoptosis during calvarial healing. The study also provides an insight into the use of small molecule inhibitors of TGF-β signaling as a novel therapeutic approach for treatment of craniofacial skeletal defects.

55
Management of Problematic Infantile Hemangioma Using Intralesional Triamcinolone: Efficacy and Safety in 87 Consecutive Infants

Javier A Couto, BA; Arin K Greene, MD, MMSc

Boston Children's Hospital, Boston, MA

PURPOSE: Several treatment options exist for a problematic proliferating hemangioma. Intralesional corticosteroid is one method used to limit the rapid growth of the tumor. The purpose of this study was to determine the efficacy and safety of corticosteroid injection for infantile hemangiomas.

METHODS: The study comprised 87 consecutive patients with a problematic infantile hemangioma managed with intralesional corticosteroid between 2007–2013. Tumors were injected with triamcinolone and followed every 4–6 weeks to determine whether additional injections were indicated. Predictive variables were patient gender, age, location of the hemangioma, tumor depth (superficial, deep, combined), and lesion size. Treatment response was defined as regression, stabilization, or no response. Rebound growth and drug morbidity were recorded.

RESULTS: Sixty-two females and 25 males were treated. Infantile hemangiomas were located on the lip (29.9%), cheek (21.8%), nose (15.0%), periorbital area (13.8%), forehead (6.9%), chin (2.3%), ear (2.3%), trunk (2.3%), upper extremity (2.3%), scalp (2.3%), and neck (1.1%). Mean tumor size was 2.3 cm2 (range 0.25–16.0cm2); 53.6% were superficial, 14.3% deep, and 32.1% were combined. Treatment was initiated at an average age of 10.8 weeks (range 3–30 weeks). The mean number of injections was 1.9 (range 1–5). The average dose of triamcinolone administered during an injection was 1.63 mg/kg (range 0.76–2.66 mg/kg). All tumors responded to the treatment: 62.1% (n=54) regressed and 37.9% (n=33) stabilized. Forty-three percent of lesions exhibited rebound growth at an average of 3.5 weeks (range 2–7 weeks) following the injection. Gender, location, lesion size, and tumor depth did not affect treatment response (p=0.7). No patient exhibited systemic side effects and 2 lesions (2.0%) had fat atrophy at the site of injection.

CONCLUSION: The administration of intralesional triamcinolone is an effective treatment for infantile hemangioma. Therapy is safe and infants are not exposed to potential side-effects associated with systemic pharmacotherapy. Corticosteroid injection is our first-line intervention for problematic infantile hemangiomas that are small and localized.

56
Differential Effects of Inflammatory Mediators TNFα, TGFβ1 on Cellular Differentiation in a Primary Murine Muscle Cell in vitro Model of Heterotopic Ossification

S Alex Rottgers, MD; Laurie B Meszaros, PhD; Anand R Kumar, MD
University of Pittsburgh, Pittsburgh, PA

INTRODUCTION: Heterotopic ossification (HO) is a pathologic condition of bone formation in extremity muscles. Systemic and local inflammatory conditions acting on muscle-derived progenitor cells (MDCs) may either support or alter myogenic differentiation and promote pathologic chondrogenic or osteogenic differentiation. The aim of this study is to evaluate the effects of inflammatory mediators (TNFα, TGFβ1) on MDC myogenic, chondrogenic, and osteogenic differentiation.

METHODS: Primary mouse muscle cells were isolated from 8-week-old C57B/6J mice. Hindlimb muscles were sterilely processed and pre-plating on collagen-coated flasks for 2 hours to minimize fibroblasts. The non-adherent mixed population of MDCs was cultured in F-10 growth medium with no greater than 3–4 passages for amplification. Four populations of cells were analyzed via FACS for surface markers. 100,000 cells per well were cultured in DMEM-based proliferation medium (PM) alone or with 1 ng/ml TNFα or with 5 ng/ml of TGFβ1 alone or in various combinations. Samples were collected after 3 days. RNA was isolated reverse transcribed to cDNA. Quantitative PCR analysis of MyoD, Sox9, and Osx, which are markers of myogenic, chondrogenic, osteogenic differentiation, was performed. Changes in target gene expression were expressed relative to untreated MDCs with expression normalized to GAPDH.

RESULTS: FACS analysis revealed a mixed population of cells, with high Sca-1 and CD34 expression and low CD31, CD 56, CD144 and CD146 expression. After 3 days, all isolations of MDCs cultured with TNFα demonstrated unaffected expression of MyoD (1.02±0.50), Sox9 (0.56±0.30) and decreased expression of Osx (0.19±0.07). TGFβ1 cultured cells demonstrated decreased expression of MyoD (0.236±0.017), Sox9 (0.151±0.023) and Osx (0.001±0.002). Cells cultured with combined with TNFα/ TGFβ1 demonstrated decreased expression of MyoD (0.158±0.036), Sox9 (0.131±0.020) and Osx (0.127±0.027).

DISCUSSION: We have demonstrated that systemic inflammatory mediators can significantly affect MDCs transcription of myogenic, chondrogenic, and osteogenic differentiation factors. TNFα may protect against pathologic differentiation as it did not significantly affect in vitro myogenic or chondrogenic differentiation but suppressed osteogenic differentiation. Cells cultured in TGFβ1 alone demonstrated decreased in vitro myogenic, chondrogenic, and osteogenic differentiation. Cells cultured with both TNFα/ TGFβ1 demonstrated similar in vitro myogenic, chondrogenic, and osteogenic suppression as cells treated with TGFβ1 alone.

57
Evaluation of Cranial Bone Transport Distraction with and without Adipose Grafting

Mikell M Yuhasz, BA; Felix P Koch, MD, DMD; Rob Travieso, MD; Kenneth Wong, BS; James Clune, MD; Zhen W Zhuang, MD; Joshua Van Houten, PhD; Derek M Steinbacher, MD, DMD
Yale School of Medicine, New Haven, CT

PURPOSE: Transport distraction osteogenesis (DO) can be used to autologously reconstitute calvarial defects. However, distraction gap biology in transport DO has not been adequately described. The purpose of this study is to histomorphologically interrogate osteogenic formation during cranial transport distraction using a novel device. We also evaluate the effect of fat grafting on the regenerate and soft-tissue stability during distraction.

METHODS: This study was approved by Yale IACUC (# 2011–11393). Ten male New Zealand white rabbits (3 months; 3.5kg) were used (8 treatment, 2 control). A 16x16mm defect was created abutted by a 10x16mm transport disc. The device was fixated anterioposteriorly. Four animals were fat-grafted using 2cc of subdermal intrascapular fat deposited along the distraction site. Latency (1d), active distraction (12-14d) (1.5 mm/day), and consolidation (4wks) followed. Calcein and xylene orange fluorochromes were injected subcutaneously during and post-distraction to mark sites of bone formation. Following sacrifice, osteogenesis was assessed using microCT, histology, and fluorescence.

RESULTS: No perioperative complications were experienced. Treatment animals demonstrated regenerate bone between distracted segments on microCT. MicroCT analysis of fat-grafted and non-fat grafted animals revealed a mean density of 2271.95 mgHA/ccm and 2254.27 mgHA/ccm (p=0.967), respectively, and defect bone versus total volume (BV/TV) of 0.0999 and 0.0766 (p=0.5979), respectively. Controls had minimal reossification. Histologically, mean densities measured 43.63% and 8.19% for non-fat and fat grafted animals, respectively.Density ratios (regenerate:native bone) were 53.96% and 23.71%, respectively. Fluorescent microscopy revealed ossification from the callus as well as bone fronts emanating from dura and periosteum.

CONCLUSION: Transport distraction is effective to reconstruct critically-sized rabbit calvarial defects. Regenerate bone arises predominantly from the callus with contribution from surrounding dura and periosteum. Adipose grafting is well tolerated but does not enhance osseous regeneration.

58
Management of Pediatric Condylar and Subcondylar Fractures: The Algorithmal Impact of Concomitant Mandibular Arch Fractures

Ali Ghasemzadeh, BS[1]; Gerhard S Mundinger, MD[2]; Alan F Utria, BA[1]; Amir H Dorafshar, MBChB[2]

[1]Johns Hopkins University School of Medicine, Baltimore, MD, [2]Johns Hopkins Hospital, Baltimore, MD

PURPOSE: The management of pediatric condylar and subcondylar fractures (CSC) is complicated by the need to preserve mandibular growth and development, as well as achieve adequate fracture reduction to prevent temporomandibular joint (TMJ) disturbance. This study examines the differences in treatment between isolated CSC fractures and CSC fractures with concomitant fractures of the mandibular arch, defined as fractures of the ramus, angle, body, parasymphysis, and/or symphysis.

METHODS: Retrospective chart review was performed for all patients between the ages of 0 and 18 presenting to the Johns Hopkins Hospital with mandibular CSC from 1990–2010. Demographic, surgical management, hospital course, and complication data was gathered. Computed tomographic (CT) imaging was reviewed for all patients to confirm mandibular fracture pattern, characteristics, and displacement. Identified mandibular fractures were codified and graded using the Strasbourg Osteosynthesis Research Group and Lindahl classification methods. For arch fractures, maximum cortical step-off (either lingual or buccal) was determined in millimeters. Statistical analysis was performed using two-tailed student's t-tests and chi square tests. Loess curve analysis was used to determine fracture displacement cutoffs. All statistical analyses were performed with STATA 12.0 software.

RESULTS: A total of 55 patients with 77 CSC fractures were identified. 43 additional mandibular arch fractures were found in this patient population (total mandibular fracture n=120). There were 25 (45.5%) patients with isolated CSC fractures and 30 (54.5%) patients with one or more CSC fracture and at least one concomitant mandibular arch fracture. Mandibular arch fracture locations included the ramus (n=2), angle (n=3), body (n=8), parasymphysis (n=20), and symphysis (n=6). Fifteen patients (60%) with isolated CSC fractures were treated with conservative therapy (range of motion exercises and soft diet), compared to only 4 patients (13%) with concomitant fractures of the mandibular arch ($p<0.001$). Seventeen of 30 patients (57%) with CSC and mandibular arch fractures received ORIF of their mandibular arch fracture(s). Eleven patients (78.5%) with CSC fractures and concomitant mandibular arch fracture with maximum cortical displacement greater than 3mm were treated with open reduction and internal fixation (ORIF) compared to 6 patients (37.5%) with less than 3mm displacement ($p<0.001$). No patients with isolated CSC fractures were treated with ORIF regardless of level of fracture displacement. Median follow up was 69 days. Differences in complication rates between patients with CSC and arch fractures receiving conservative treatment (n=2, 5.7%), maxillomandibular fixation (MMF, n=1, 2.9%), or arch fracture ORIF (n=5, 14.3%) were not statistically significant ($p=0.19$).

CONCLUSION: Pediatric CSC can be successfully managed with conservative therapy or a short course of MMF regardless of degree of fracture displacement or the presence of additional mandible fractures. Dental arch fractures with concomitant CSC fractures may require ORIF. In this setting, our data suggests that 3mm of maximum cortical arch displacement is an indication for ORIF, which can be achieved with low morbidity.

SATURDAY, MARCH 8, 2014

SCIENTIFIC SESSION 5 GROUP C
NERVE
2:00 PM – 3:30 PM

SATURDAY, MARCH 8, 2014

59
Management of Pediatric Brachial Plexus Palsy: The Role of Nerve Transfer Combined with Neurolysis or Nerve Grafting of the Upper Trunk

Wesley Sivak, MD, PhD; Brian Gander, MD; Kimberly Foster, MD; Zoe MacIsaac, MD; Stephanie Greene, MD; Anand Kumar, MD; Lorelei Grunwaldt, MD

University of Pittsburgh, Pittsburgh, PA

PURPOSE: Treatment of pediatric upper brachial plexus palsy remains controversial; the role of axon transfer from regional donor nerves is poorly defined. This study evaluates the benefit of supplemental nerve transfer (i.e. - CN XI or phrenic nerve) in combination with either neurolysis or nerve grafting of the upper trunk.

METHODS: A retrospective review of pediatric upper brachial plexus palsy patients was performed from 1997–2012. Patients treated with neurolysis or nerve grafting of the upper trunk with or without concomitant nerve transfers were identified (n=39). All patients had a minimum of 4 months observation from diagnosis to operative intervention.

RESULTS: Group 1, neurolysis alone, 12 patients (4 male/8 female, average age 9.7 months) treated January 1997-March 2012. Group 2, neurolysis with nerve transfer, 9 patients (5 male/4 female, average age 6.8 months) treated December 2001-January 2007; transfers included 1 CN XI, 4 phrenic, and 4 combined procedures. Group 3, nerve graft alone, 8 patients (5 male/3 female patients, average age 6.6 months) treated September 2000-May 2012; sural nerve grafts were used. Group 4, nerve graft with nerve transfer, 10 patients (3 male/7 female, average age 6.5 months) treated March 2000-April 2012; sural nerve grafts were used and transfers included 4 CN XI, 3 phrenic, and 3 combined procedures (age and gender distribution, $p>0.05$ all groups). Average follow-up was 55.9, 35.0, 41.0, and 55.9 months for Groups 1–4, respectively. Median preop/postop shoulder abduction, shoulder external rotation, supination, and elbow flexion Oxford scores were 2/2.5, 0/3.5, 0/2.0, 1/3 in Group 1; 2/4, 1/3, 2/4, 4/4 in Group 2; 3.5/4, 2/3.5, 2/4, 2.5/4 in Group 3; and 2/5, 2/5, 0/4, 2/5 in Group 4, respectively ($p>0.05$ all groups). Combined upper extremity functional scores demonstrated greatest improvement in Group 4 relative to all other groups ($p<0.036$). Secondary tendon transfer occurred n=9 (70%) in Group 1 at an average age 39.1 months, n=6 (67%) in Group 2 at an average age of 33.4 months, n=3 (38%) in Group 3 at an average age 30.0 months, and n=3 (30%) in Group 4 at an average age 32 months. No major complications, wound infections or early reoperations occurred in any group; no patients required tracheostomy after phrenic nerve transfer.

CONCLUSIONS: Nerve grafting with supplemental nerve transfer demonstrated the greatest functional improvement in upper extremity function among the patient cohorts. Nerve grafting demonstrated greater improvement than neurolysis with or without nerve transfer, but improvement was less robust than nerve grafting with transfer. Patients required fewer secondary tendon transfer surgeries after undergoing nerve grafting as compared to neurolysis, and fewer still when nerve transfer techniques were employed. The use of unaffected extraplexal nerves as a source of donor axons for transfer is efficacious and safe with no demonstrated increase in morbidity.

60
Signal Strength, Reliability, and Validity of Active Regenerative Peripheral Nerve Interface Device Operation during Voluntary Movement

Andrej Nedic, MSE; Daniel Ursu, MS; Jana D Moon, BS; Cheryl A Hassett, BS; Richard B Gillespie, PhD; Nicholas B Langhals, PhD; Paul S Cederna, MD; Melanie G Urbanchek, PhD
University of Michigan, Ann Arbor, MI

PURPOSE: Regenerative Peripheral Nerve Interface (RPNI) devices successfully transduce peripheral nerve action potentials to electrical signals suitable for prosthesis control. Voltage changes are the controlling mechanism and can be observed during electromyography (EMG). However, RPNI device signaling has not been characterized during voluntary movements. This study: a) characterizes active RPNI signal strength compared to background activity and b) defines the reliability and validity of RPNI signal function during purposeful movements.

METHODS: Three groups were formed in rats: Control (n=3), RPNI (n=3), 100% Denervated (n=3). Bipolar electrodes were implanted onto the soleus muscles in each group. For RPNI devices, the soleus muscle was freely grafted to the ipsilateral thigh and neurotized by the transected tibial nerve. In the 100% Denervated, the tibial nerve was transected. The Control group was left intact. While walking on a treadmill, rats were videographed and raw EMG signals were simultaneously recorded. Video and EMG recordings were synchronized to stance, swing, and sit (nonactive) gait phases. Rectified EMG was integrated (iEMG) for each gait phase. iEMG was normalized (NiEMG) to time for each phase. Data represent 16 gait cycles for each of 9 rats. Correlations were performed between iEMG and stance time to determine reliability. RPNI signaling was validated against Control group signal timing for gait phases using Chi Square analysis.

RESULTS: We compared EMG signals to background signal strength in all groups during all gait phases. Fidelity of RPNI activity (stance) to background signaling (sit) was 5.6 to 1, double the Control signal fidelity. Significant differences between stance and swing NiEMG activity were confirmed for the Control and RPNI groups. As expected, stance and swing EMG signals were not different for the Denervated group. Correlations between iEMG and stance time for the Control ($r=0.74$) and RPNI ($r=0.76$) indicate good RPNI signal reliability. EMG signals increased at the start of stance and fell to baseline at the start of swing in both Control and RPNI rat gait cycles. These data comparing gait cycle to EMG activation accuracy between Control, RPNI, and Denervated groups validated RPNI signaling as purposeful peripheral nerve activity appropriate for meaningful control of prostheses (Chi Square; $p<0.05$).

CONCLUSION: RPNI signal fidelity, reliability, and validity were examined during voluntary movement. With select filtering, signal fidelity was clear. RPNI signal reliability during the gait stance was "good." RPNI signaling was successfully validated against normal peripheral nerve signaling during walking.

ACKNOWLEDGEMENTS: This work was sponsored by the Defense Advanced Research Projects Agency (DARPA) MTO through Grant/Contract No. N66001-11-C-4190.

61
Characterization of Regenerative Peripheral Nerve Device Signaling during Evoked Maximal and Submaximal Fatiguing Conditions

Zachary P French, HS[1]; Nicklaus S Carrothers, HS[2]; Cheryl A Hassett, BS[1]; Jana D Moon, BS[1]; Nicholas B Langhals, PhD[1]; Paul S Cederna, MD[1]; Melanie G Urbanchek, PhD[1]

[1]University of Michigan, Ann Arbor, MI, [2]University of Rochester, Rochester, NY

PURPOSE: Regenerative peripheral nerve interface devices (RPNI devices) transduce signals between remaining peripheral nerves of a residual limb and motorized prostheses. RPNI devices consist of a transferred muscle neurotized by a transected peripheral nerve with electrodes secured to the muscle for RPNI signal transduction. RPNI device maximal twitch signaling has been characterized; however, device function during repetitive signaling has not been studied. Our purpose was to characterize RPNI device continuous submaximal signaling including fatigability with respect to measures of maximal signal.

METHODS: Rats were assigned to RPNI Device (n=5) or Control (n=5) groups. For the Device group, the left extensor digitorum longus (EDL) muscle was transferred to the thigh and neurotized by the transected peroneal nerve. In both groups two fine wire electrodes were secured to the EDL muscle. The EDL muscle was then wrapped with SIS, layered with fascia, and partially covered with silicone sheeting on one side, between the EDL and tibialis anterior muscle. Five months post-surgery, maximal twitch compound muscle action potential (CMAP) and maximal contractile force were measured through evoked peroneal nerve stimulation. A submaximal repeated signaling protocol was administered - 22 minutes of 360 contractions with 300 ms/s duty cycles and 360 contractions with 600 ms/s duty cycles all stimulated at 40 Hz - concluding with a final test of maximal signaling capacity with stimulation 120–180 Hz.

RESULTS: Study animals were matched for body mass and age. A tight correlation was found between maximal twitch CMAP and maximal contractile force ($r=0.82$, $p < 0.01$), in this and other RPNI device studies. We thus infer that both measurements indicate RPNI signaling. RPNI Device twitch CMAP signaling was 32% of Controls amplitude. RPNI device maximal contractile force produced 23% the signaling capacity of Controls. This decreased contractile signaling is attributed to limitations for RPNI Devices to maintain contraction signaling over longer signaling times. Contractile force signaling is held for 300 ms while twitch signaling is only 0.1 ms. During repetitive submaximal force signaling, RPNI Devices maintained 22% to 5% of their maximal force. With five minutes of rest, RPNI devices recovered maximal contractile signaling equal to 18% of the recovered Controls. The submaximal repetitive contraction protocol fatigued both RPNI Devices and Controls, with recoveries equal to 53% and 69% maximal contractile signaling respectively.

CONCLUSIONS: RPNI Devices are able to produce signals repetitively during submaximal activation with a rate of fatigue that is similar to Controls; however, RPNI Device signals during repeated activation are of lower amplitude with respect to maximal signaling than Controls. This will be studied further.

ACKNOWLEDGEMENTS: DARPA N66001-11-C-4190.

62
Development of an Optogenetic Sensory Peripheral Nerve Interface

Sahil K Kapur, MD[1]; Thomas Richner, MS[2]; Sarah Brodnick, BA[2]; Justin C Williams, PhD[2]; Samuel O Poore, MD, PhD[1]

[1]University Of Wisconsin, Madison, Madison, WI, [2]University Of Wisconsin Madison, Madison, WI

PURPOSE: Improvement in afferent sensory feedback is the necessary next step in the development of functional neuroprostheses. While electrical stimulation serves as the standard of peripheral nerve manipulation, the use of light sensitive ion channels in optogenetic models could provide a sensitive and specific alternative for afferent signal generation. In this study, we demonstrate similarities between the cortical representation of afferent neural signals that have been generated by electrical and optical stimulation of peripheral nerves. Furthermore, we demonstrate the ability to generate afferent signals that retain cortical localization following transcutaneous optical and electrical peripheral nerve stimulation.

METHODS: Flexible thin film microelectrode arrays were implanted over the sensorimotor cortex in optogenetically modified transgenic mice expressing channelrhodopsin (a blue light sensitive ion channel) in accordance with IACUC guidelines. Seven days following cortical implantation, peripheral nerve signals were generated under four different experimental conditions: electrical stimulation following surgical exposure of the sciatic and median nerves, optical stimulation following surgical exposure of the sciatic and median nerves, transcutaneous electrical stimulation of the sciatic and median nerves and transcutaneous optical stimulation of the sciatic and median nerves. Local field potentials were recorded by the implanted cortical electrode arrays during these sessions.

RESULTS: Cortical signals recorded by the multielectrode arrays were localized to regions of the hindlimb or forelimb cortex corresponding to the peripheral nerve being stimulated. Localization of the signal was preserved across both electrical and optical stimulation modalities. Furthermore, cortical signals maintained their localization during transcutaneous optical and electrical stimulation. Signal amplitudes varied proportionately with the amplitude and pulse width of peripheral nerve stimulation. Generation of consistent localized cortical signals via both electrical and optical stimulation was maintained in experiments carried out over a period of at least 5 days. Control experiments carried out on wild type mice produced similar results following electrical stimulation but no cortical signals following optical stimulation of the peripheral nerves.

CONCLUSIONS: Preserved similarity and localization of cortical signals following electrical and optical stimulation of peripheral nerves implies that ascending sensory information can be reliably transmitted to the brain via either electrical stimulation or optical pulses applied to peripheral nerves. Furthermore, the robust cortical response to transcutaneus optical and electrical stimulation permits the non-invasive manipulation of peripheral nerves. These results along with our previously demonstrated results open the possibility of developing neuroprostheses capable of generating afferent and efferent neural signals in response to optical stimulation.

63
Senescent Schwann Cells Inhibit Nerve Regeneration in a Short Conduit Model

Gwendolyn M Hoben, MD, PhD; Piyaraj Newton, BS; Dan A Hunter, RA; Sheila Stewart, PhD; Philip J Johnson, PhD; Matthew D Wood, PhD; Susan E Mackinnon, MD
Washington University, StLouis, MO

PURPOSE: Nerve injuries requiring long distances for axonal regeneration are associated with poor functional outcomes. Our laboratory has shown that increased nerve graft length (both isografts and acellular nerve allografts) results in decreased regeneration and accumulation of senescent SCs (SenSCs) both in the graft and in the nerve distal to the graft. Senescent cells activate the senescent associated secretory phenotype (SASP), which is rich in inflammatory proteins, ECM remodeling proteins, and other factors. We hypothesize that SenSCs impede axonal regeneration after injury. To test this hypothesis, we examined whether SenSCs directly limit nerve regeneration by transplanting cultured SCs induced to a senescent state into a nerve gap injury model. We measured changes to gene expression associated with nerve regeneration in these SenSCs to explore a mechanism for the limited regeneration.

METHODS: A rat sciatic nerve transection model was repaired utilizing 5mm conduits. The experimental groups were: 1) empty conduits; conduits filled with $1x10^6$ 2) normal SCs in fibrin, 3) H_2O_2 induced SenSCs in fibrin, and 4) aphidicolin induced SenSCs in fibrin. After 4 weeks, the conduits were excised and examined for nerve regeneration with histomorphometry. To confirm Schwann cell survival and examine migration following transplantation, Schwann cells transduced to express red fluorescent protein were used in groups 2, 3, and 4 and examined macroscopically after 1 wk, 2 wks, and 4 wks. Schwann cell gene expression was analyzed using qRT- PCR for markers of cell senescence (P16, IL-6, and IL-8) and nerve regeneration proteins.

RESULTS: Based on histomorphometric analysis, nerve regeneration was greatest in conduits filled with normal SCs. Rats receiving empty conduits demonstrated sporadic and poor nerve regeneration with few axons reaching the distal portion of the conduit. Although there was nerve regeneration more consistently in the conduits filled with the senescent cells, the difference was not significant compared to the empty conduits. Fluorescence microscopy confirmed the retention of both normal SCs and SenSCs for at least 2 weeks. SenSC gene expression differed from normal SCs with regard to an upregulation of cell senescence markers and differing nerve regeneration protein profiles.

CONCLUSION: It has been previously shown that seeding a conduit with normal SCs greatly enhanced nerve regeneration. Here we show that SCs induced to a senescent state reduces nerve regeneration in a conduit model. As SenSCs survived transplantation and affected gene expression of nerve regeneration proteins, SenSCs were having a direct effect on regenerating axons. This result significantly strengthens the case for senescence as a predominant cause of poor regeneration in long acellular nerve allografts. Thus, strategies to reduce SenSCs or their effects could be an important goal in future nerve regeneration studies.

64
Epineural Sheath Jacket as a New Surgical Technique for Neuroma Prevention in the Rat Sciatic Nerve Model: A Preliminary Report

Adam Bobkiewicz, MD; Halil Uygur, MD; Grzegorz Kwiecień, MD; Maria Madajka, PhD; Maria Siemionow, MD, PhD, DSc
Cleveland Clinc, Cleveland, OH

PURPOSE: Neuroma may form as a result of nerve transection or damage, causing pain and significantly impairing the quality of life. Although many techniques have been developed so far, none have been proven to be superior in prevention of neuroma formation. The aim of this study was to test the epineural sheath jacket (ESJ) as a new method for prevention of neuroma formation in the rat sciatic nerve model. Epineural sheath is a naturally occurring material, easily harvestable and expresses proneurogenic and proangiogenic markers supporting nerve regeneration.

METHODS: A total of seventy-two rats were divided into six groups (of six each). Group 1: Control- Nerve stump without any protection; Group 2: Nerve stump buried into the muscle; Group 3: ESJ covering nerve stump; Group 4: ESJ covering nerve stump and buried into the muscle; Group 5: ESJ filled with fat graft covering nerve stump; Group 6: ESJ filled with fat graft covering nerve stump and buried into the muscle. Animals were evaluated at 12 weeks and 24 weeks follow-up. Sciatic nerve was dissected and 2 cm segment of the nerve was resected. Nerve fascicles were removed using pull out technique creating an empty epineural sheath conduit. The distal part of the conduit was closed and proximal part was trimmed creating 7 mm long tube of protective ESJ. Finally, ESJ was applied over the proximal nerve stump using epineural sleeve technique (Groups 3–6). In Groups 5 and 6, before ESJ application, autologous fat was harvested from the gluteal region and following appropriate fat processing, it was injected into ESJ. Functional assessments included pin-prick (PP) test and Tinel sign were analyzed once a week. At the end of each time end point, somatosensory evoked potentials (SSEP) were recorded and nerve samples were harvested for histological and immunohistochemical analyses.

RESULTS: At 5 weeks, in Group 1 and 2, the PP test was elicited above the ankle level (grade 1) and reached plantar region (grade 2) at 9 weeks. In contrast, in Groups 3–6 grade 1 of the PP test was observed at 8 weeks. Tinel sign confirmed by squeaking and aggressive behavioral pattern was observed in all experimental groups starting at 3 weeks and was still present in Group 1 and 2, whereas it gradually disappeared in groups treated with ESJ. SSEP measurements revealed shorter N2% latency values and lower amplitude values (Amp%) in Groups 1 and 2 when compared with Groups 3–6. During nerve exploration significant adhesions were seen in Groups 1 and 2, whereas neuroma-like formation characterized by distension and disorganization of the proximal stump was observed in Group 1. In contrast, no signs of neuroma- like formation were observed morphologically in Groups 3–6. The structure and integrity of the ESJ was preserved.

CONCLUSION: This study confirmed feasibility of ESJ application as a new method for prevention of neuroma formation. The protective effect of ESJ against neuroma formation was confirmed in Groups 3–6 by clinical and functional assessments. Histological and immunohistochemical analyses are in progress.

65
Subclinical Peroneal Nerve Entrapment May be an Under-recognized Cause of Falls in Hospitalized Patients

Louis H Poppler, MD[1]; Anchal Bansal, BS[1]; Andrew Groves, BS[1]; Gina Sacks, BS[1]; Kristen Davidge, MD[2]; Susan E Mackinnon, MD[1]

[1]Washington University in St Louis School of Medicine, St Louis, MO, [2]Hospital for Sick Children, Toronto, ON, Canada

PURPOSE: Falls are a major cause of morbidity and mortality, costing the United States $30 billion in 2010. Compression of the peroneal nerve at the fibular neck is a known cause of foot drop that can lead to tripping and falling. We hypothesize that sub-clinical or early entrapment of the peroneal nerve can cause tripping, stumbling and falling. Additionally, peri- and post-operative positioning, along with other surgical factors are known causes of peripheral neuropathies. We hypothesize that lengthy surgery and ICU stays may increase the risk of peroneal neuropathy and thereby increase a patient's likelihood to fall. Early intervention could be a major opportunity to prevent falls in this population.

METHODS: *Aim 1* - A prospective cross-sectional study examined 100 randomly selected patients identified at moderate or high fall risk on four medical floors with high falls frequency. Medical co-morbidities, tripping and falls histories, and the Activities-specific Balance Confidence (ABC) Scale were collected. Medical Research Council (MRC) strength testing of ankle dorsi- and plantar-flexion, inversion and eversion, and provocative testing (Tinel's test and Scratch Collapse (SC) Test) were performed to assess for signs of peroneal neuropathy. *Aim 2* - 50 elective cardiac surgery patients were prospectively examined for peroneal neuropathy (as in Aim 1) at a pre-operative anesthesia visit and then again after discharge from the Cardiac ICU. Data on anesthesia time, ICU stay, and surgery type were collected. Weakness of dorsiflexion/eversion, provocative tests, and a history of falls were correlated using odds ratios and chi-squared test. In aim 2, frequency of weakness and positive provocative tests before and after surgery were correlated with operative time and ICU stay.

RESULTS: *Aim 1* - 100 patients, mean age 53.0 ± 13.1, 59% female were examined. 42% had at least one positive provocative sign and 38% had weakness of the peroneal nerve. A positive Tinel's, SC or both were all significantly ($p<0.05$) associated with peroneal nerve weakness (Odds ratio 4.8, 2.8 and 8.0 respectively). Patient's with a positive Tinel's were 3.8x more likely to have falls in the last year ($p=0.009$) and patients with both provocative signs were 4.4x more likely to trip or stumble frequently ($p=0.008$). *Aim 2* - 27 patients enrolled, mean age 67.2 ± 15.1, 35.7% female. 32% of pre-operative patients had a provocative sign. 63% of post op patients have a provocative sign. 48% of patients gained at least one provocative sign.

CONCLUSION: This study suggests that peroneal neuropathy is common among hospitalized patients identified as high-risk for falls. Positive provocative tests for peroneal neuropathy in this population were also significantly correlated with a recent history of falls, suggesting that peroneal neuropathy may be a contributor to outpatient falls. Furthermore, subclinical peroneal neuropathy was present in approximately 1/3 of patients undergoing elective cardiac surgery. The observed increase in the proportion of patients with clinical evidence of peroneal neuropathy postoperatively suggests that prolonged surgery and ICU stays may contribute to the development of subclinical peroneal neuropathy.

66
Single Treatment with Alpha-1-antitrypsin Enhances Nerve Regeneration After Peripheral Nerve Injury

Christine Radtke, Prof Dr; Sabina Janciauskiene, Prof Dr; Kerstin Reimers, Prof Dr; Peter M Vogt, Prof Dr
Hannover Medical School, Hannover, Germany

PURPOSE: Macrophages play a key role in axonal regeneration because they secrete IL-6 that is necessary for axonal guidance and remyelination. Pro-inflammatory cytokines stimulate macrophage migration into the lesion sites which is necessary for the removal of cell debris and Schwann cell invasion as guidance for axonal outgrowth followed by remyelination. α1-antitrypsin (AAT) is an acute phase protein and it is shown to express anti-inflammatory characteristics in neutrophil and monocyte/macrophage driven models in vitro and in vivo. We asked a question whether AAT can affect regeneration of injured peripheral nerve fibers by initial macrophage mobilization. We have established several models to study peripheral nerve injuries in small animals. In the rat sciatic nerve crush model we developed a standardized method for investigation of nerve regeneration parameters. We could demonstrate that axonal sprouting, as well as myelin sheaths and functional outcome can be improved by adjunct AAT therapy.

METHODS: In vivo sciatic nerves of adult rats were exposed and crushed for 20 sec with fine forceps to transect all axons. Immediately after nerve crush, AAT was injected proximally and distally to the lesion site in a standardized sciatic nerve crush site through a glass pipette attached to a Hamiliton syringe. During the course of the experiments the animals were tested behaviorally for functional improvement. After 21 days, the nerves were removed and histology was performed.

RESULTS: In vitro, we have demonstrated that AAT inhibits endotoxin-stimulated TNFa, IL-6, IL-1β and enhances IL-10 expression in human monocytes, neutrophils, and endothelial cells. The application of AAT into an acute axotomy model led to the significantly improved axonal regeneration and re-myelination than compared control animals. Moreover, not only histological, but also functional improvement was observed following direct injection of AAT after acute peripheral nerve lesion. Our results indicate that AAT delivered into injured peripheral nerve participate in neural repair.

CONCLUSIONS: AAT is an acute phase protein which improves peripheral nerve regeneration. Further studies are needed to delineate cellular mechanisms involved in these new biological activities of AAT.

67
The Monoclonal Antibody Herceptin Improves Regeneration after Injured Nerves are Repaired Immediately or after a Period of Chronic Denervation

Mike Hendry, MD[1]; Eva Placheta, MD[2]; Tessa Gordon, PhD[1]; Gregory Borchel, MD, MSc[1]
[1]University of Toronto, Toronto, ON, Canada, [2]University of Vienna, Vienna, Austria

PURPOSE: Chronic denervation resulting from long regeneration times and distances is a major contributor to suboptimal regenerative outcomes following nerve injuries. The molecular mechanisms regulating these harmful effects are poorly understood. The regulatory role of ErbB2, the receptor for the potent Schwann cell mitogen Neuregulin-1 (NRG-1), remains controversial. In this study we selectively inhibit ErbB2 with the high affinity monoclonal antibody, Herceptin, which is used clinically to treat breast cancer, to examine its effect on nerve regeneration in a rat model.

METHODS: The common peroneal nerves of Sprague-Dawley rats were surgically transected and repaired. Nerves were repaired either immediately at the time of injury or repair was delayed by 3 months to allow for chronic denervation. Nerves were allowed to regenerate for 1, 2 or 4 weeks following injury. Common peroneal motoneurons were retrogradely labeled 1 cm distal to the site of repair with fluorescent dye and counted in the ventral horn of the spinal cord. Histomorphometry was used to quantify total myelinated fiber number, fiber diameter and myelin thickness within the regenerating nerve. Western blot analysis of whole nerve lysate was performed to examine the impact of Herceptin on ErbB2 signaling after injury.

RESULTS: Significantly greater numbers of motoneurons regenerated in rats treated with Herceptin (169 ± 31) compared with rats receiving saline (62 ± 15) when assessed 1 week following immediate repair ($p < 0.05$). No difference was observed at 2 or 4 weeks post-repair in rats treated with Herceptin compared to saline controls. Total myelinated fiber counts were significantly increased in rats that received Herceptin (2488 ± 154) compared to rats that received saline (1896 ± 251) ($p < 0.05$). Mean regenerated fiber diameter and myelin thickness did not differ between groups following immediate repair. Similarly, after a period of chronic denervation, significantly more motoneurons regenerated in rats that received Herceptin (282 ± 31) compared to saline controls (210 ± 24) at 2 weeks post-repair. There was no difference at 4 weeks. Interestingly, Western blot analysis revealed suppression of the downstream ErbB2 signaling pathway with Herceptin administration despite immunofluorescent imaging that suggests increased Schwann cell proliferation.

CONCLUSIONS: Disrupting ErbB2 signaling with systemic, targeted molecular therapy using a commercial monoclonal antibody leads to improved nerve regeneration in the early regenerative period. This enhanced regeneration applies to the repair of either freshly repaired or chronically denervated nerves. This raises the exciting possibility of using this and similar pharmacologic therapies to improve outcomes following surgical repair of nerve injuries.

SATURDAY, MARCH 8, 2014

SCIENTIFIC SESSION 6 GROUP A
DEVELOPMENTAL BIOLOGY
4:00 PM – 5:30 PM

SATURDAY, MARCH 8, 2014

68
Identification of twist Expression Patterns and Localized Manipulation of fgfr1 Expression in Zebrafish Cranial Sutures

Michael S Gart, MD[1]; Joanna P Tomaszewski, MS[2]; Jolanta M Topczewska, PhD[2]; Arun K Gosain, MD[3]

[1]Northwestern University Feinberg School of Medicine, Division of Plastic Surgery, Chicago, IL, [2]Northwestern University Feinberg School of Medicine, Department of Surgery, Chicago, IL, [3]Ann & Robert H Lurie Children's Hospital of Chicago, Chicago, IL

PURPOSE: Mutations in TWIST and FGFR genes have been implicated in the pathogenesis of craniosynostosis in developing humans. However, these genes also play a significant role in mesenchymal cell proliferation and differentiation throughout the developing organism, making it difficult to study isolated mutations in the craniofacial skeletal tissues. The present study was undertaken to (1) determine if genes implicated in the development of human craniosynostosis could be localized in the zebrafish cranial vault; and (2) if so, determine if we can successfully manipulate expression of these genes locally, thereby avoiding the systemic implications of a germline mutation.

METHODS: Digoxigenin (DIG)-labeled RNA antisense probes were designed to bind the genes of interest for in-situ hybridization (*twist1a, twist1b, twist2, twist3)*. Wild-type fish calvaria were dissected after fixation with paraformaldehyde (PFA) solution for 24 hours. Half of the skulls underwent an additional bleaching protocol utilizing hydrogen peroxide and potassium hydroxide to remove pigmentation prior to in-situ hybridization. Fish calvaria were imaged using standard light microscopy. The transgenic zebrafish line *Tg(dnFGFR1:EGFP)* was used to develop a protocol for localized heat shock using a modified soldering iron based on previous work (Hardy, et al. 2007). Tricaine-anesthetized fish were immobilized, and heat shock was applied to the cranial sutures using a fine-tipped soldering iron at a constant energy of 28.5V for three-minute intervals. Gene expression was detected by GFP reporter expression using confocal microscopy.

RESULTS: RNA in-situ hybridization revealed that *twist1a* was not expressed in the sutures of the developing zebrafish; however, *twist1b, twist2, and twist3* all localized to different suture regions in the developing calvaria. The localized heat shock approach successfully induced expression of the dominant-negative Fgfr1 mutant protein in the coronal sutures of *Tg(dnFGFR1:EGFP)* juvenile fish, thus establishing this method for future manipulations.

CONCLUSIONS: *TWIST* genes are highly conserved across species, and encode regulatory proteins that are essential to embryonic development. Specifically, *Twist* mutations have been implicated in human craniosynostosis. Here, we characterize the differential expression patterns of the zebrafish *TWIST* gene homologs--*twist1a, twist1b, twist2,* and *twist3*--in the developing cranial sutures. Moreover, through the application of localized heat shock, we have been able to locally induce expression of an engineered transgene with downstream GFP reporters. We believe we can expand upon this model of isolated gene expression in specific tissues of interest. This technology can allow for the regulation of abnormal cranial suture development without influencing the broader activity of target genes in the developing organism.

69
Analysis of The Role of Wls in Craniofacial Development

Lucie J Rochard, PhD; Yawei Kong, PhD; Kenta C Kawasaki; Michael Grimaldi; Tatiana Hoyos, MD; Eric C Liao, MD, PhD
Massachussets General Hospital, Boston, MA

BACKGROUND: Wnt signaling is a critical pathway regulating craniofacial development, where dysregulation leads to orofacial clefts. Intracellular trafficking and secretion of wnt ligands is chaperoned by wntless (wls). In human, the WLS gene is on the short arm of the chromosome 1 (1p31.3) and several deletions of this region associated with craniofacial malformations have been reported. We hypothesize that the wls gene functions to modulate wnt signaling important in morphogenesis of the craniofacial skeleton.

MATERIAL AND METHODS: Gene expression analysis by whole mount in situ hybridization (WISH) of wls was performed in zebrafish, across embryonic timepoints, in wildtype and mutant embryos. Phenotypic analysis of the wls mutant was also carried out, by WISH to examine markers of neural crest and craniofacial development, and with Alcian blue stain to delineate the skeletal structures.

RESULTS: Gene expression analysis of wls via WISH during embryogenesis detected transcripts in the presumptive neural tissue, in the pharyngeal arches, and later in the palate. In the oropharynx, the wls expression domain corresponded to that of wnt9a. Further, the wls mutants exhibited dysmorphology of skeletal structures in the head. Each element of jaws appeared shorter and the neurocranium was also smaller in all direction, revealing a problem in extension mechanisms during craniofacial morphogenesis.

CONCLUSIONS: This study describes the requirement of wls in craniofacial development. Our group has previously defined the role of wnt9a, frzb and fzd7a in craniofacial morphogenesis, to participate in regulating convergence and extension morphogenetic mechanisms in formation of the palate, and the formation of the lower jaw. Our studies of wls take advantage of this body of work to elucidate the role of wls and wnt signaling pathway in palatogenesis. Our future experiments will focus on the studies of the secretion of wnt9a in wls mutants and regulation of wls by other signaling pathways that regulate craniofacial development.

70
Propranolol Effects on Hemangiomas are Mediated via Distinct Pathways

Ryan W England, BS; Naikhoba CO Munabi, BA; Kyle J Glithero, MD; Alex Kitajewski, BS; Jan Kitajewski, PhD; Carrie J Shawber, PhD; June K Wu, MD
Columbia University, New York, NY

PURPOSE: Propranolol has clinical efficacy in the treatment of problematic infantile hemangiomas (IHs). We have shown that propranolol caused decreased cellular proliferation and cytotoxicity on hemangioma stem cells (HemSCs) in vitro. We hypothesize that these effects are mediated by disrupting downstream signals of the beta-adrenergic receptor, although which mediators are involved are not well understood. While uncommon, infants treated with propranolol can experience symptomatic bradycardia, hypotension, hypoglycemia, and even seizures. Therefore, understanding these pharmacologic effects of propranolol will help develop targeted therapy that can minimize these adverse effects.

METHODS: CD133+ HemSCs isolated from resected IH specimens were treated over a 9-log scale with either propranolol hydrochloride or vehicle. Effects of non-selective beta-adrenergic blockade in HemSCs were assessed for cellular proliferation using a WST-8 cell counting kit, and cellular cytotoxicity using the fluorescence-based digital image microscopy system, DIMSCAN. The activation of mitrogen-activated protein kinase (MAPK) was measured by immunoblotting for phosphorylated MAPK after a 30-minute incubation with propranolol and normalized against total MAPK using ImageJ. Effects of beta-adrenergic blockade on downstream cAMP levels after isoprenaline stimulation were assessed using a LANCE Ultra cAMP kit. Student's t-test and Prism were used for statistical analysis.

RESULTS: Beta-adrenergic blockade via treatment with propranolol resulted in a significant decrease in proliferation at a low dose of 1x10-9M (1pM; $p<0.01$) and continued in a dose-dependent manner until 1x10-4M (100uM; $p<0.0001$), whereby proliferation was completely inhibited. This coincided with the decrease in cAMP activity. At concentrations above 1x10-4M, propranolol became cytotoxic to HemSCs, with an LC50 of 158uM ($R2=0.992$; $p<0.0001$). Similarly, at higher cytotoxic doses of propranolol, HemSCs also showed a significant increase in MAPK activation (LC50=55uM; $R2=0.992$), suggesting that propranolol is having an antagonistic effect at lower doses along the G-protein-cAMP pathway and an agonistic effect at the higher dosages, possibly via a G protein-independent pathway.

CONCLUSION: We have demonstrated that there are at least two distinct downstream pathways that are affected by beta-adrenergic receptor signaling. Cellular proliferation appears to be mediated via the G protein-dependent, cAMP-mediated

pathway, whereas cellular cytotoxicity is affected by a G protein-independent, MAPK-mediated pathway. By further understanding the mechanism by which propranolol causes IH involution independent of the G protein pathway, therapies can be developed that may circumvent the adverse cardiovascular effects of beta-adrenergic antagonist treatments.

71
Obesity-Induced Lymphedema: Presentation, Diagnosis, and Management

Reid A Maclellan, MD, MMSc; Arin K Greene, MD, MMSc
Boston Children's Hospital / Harvard Medical School, Boston, MA

BACKGROUND: Lymphedema results from inadequate transport of lymphatic fluid, and typically affects the extremities. The condition may be caused by maldevelopment of lymphatics (primary) or by injury to lymph nodes or vessels (secondary). Recently, obesity has been recognized as a novel cause of lower extremity lymphedema. The purpose of this study was to characterize patients with obesity-induced lymphedema.

METHODS: Patients referred to our Lymphedema Program between 2009 and 2013 with possible lower extremity lymphedema were reviewed. Individuals with a body mass index (BMI) >30 who underwent lymphoscintigraphy to assess lymphatic function were studied. Patients with a history of primary lymphedema, lymphadenectomy, or nodal radiation were excluded. Gender, age, maximum BMI history, BMI at the time of lymphoscintigraphy, and location of lymphedema were recorded.

RESULTS: Forty patients met inclusion criteria; mean age was 54.6 years (range 14–85 years). Lymphoscintigraphy showed that 27 patients had normal lymphatic function and 13 patients (7 females, 6 males) had lymphatic dysfunction consistent with obesity-induced lymphedema. Individuals with lower extremity lymphedema had a BMI at the time of the lymphoscintigram of 64.1 (range 43.9–83.0), and a maximum BMI history of 76.1 (range 60.5–105.6). Obese patients with normal lymphoscintigraphy findings had a BMI at the time of their study of 38.5 (range 30.3–56.8), and a maximum BMI history of 44.4 (range 30.3–85.4). The patient with the highest BMI history of 105.6 also had bilateral upper extremity lymphedema confirmed by lymphoscintigraphy. One patient with obesity-induced lymphedema (BMI 80.1) had improved lymphatic function by lymphoscintigraphy after reducing her BMI to 70.9.

CONCLUSIONS: Massive obesity can cause extremity lymphatic dysfunction. A BMI threshold appears to exist at which point lower extremity lymphedema occurs, followed by upper extremity disease. Patients with obesity-induced lymphedema are referred to a bariatric center because weight loss appears to improve lymphatic function, but may not reverse the condition. Obesity-induced lower extremity lymphedema; a BMI threshold appears to exist between 53–59 when lymphatic dysfunction occurs. (*Left*) Adult female with a BMI of 53.3. Lymphoscintigraphy illustrates normal transit to inguinal nodes 20 minutes following injection. (*Right*) Adult female with a BMI of 78.3. Lymphoscintigram shows delayed transit of tracer to

inguinal nodes 3 hours following injection, tortuous collateral lymphatic channels, and dermal backflow consistent with lymphedema. Arrows indicate inguinal nodes, black arrowheads show tortuous lymphatic channels and dermal backflow, and white arrowheads mark the feet where the radiolabelled tracer was injected.

72
Keratinocytes Gene Expression of Innate and Adaptative Proinflammatory Cytokines and Members of the Toll-Like Receptor Pathways in Severe Burned

Alfredo Gragnani, Jr, MD, PhD; Silvana Aparecida Alves Correa de Noronha, PhD; Sarita Mac Cornick, master; Larissa Elias Lanziani, student; Marcus Vinicius Boaretto Cezillo, student; Samuel Ribeiro de Noronha, PhD; Lydia Masako Ferreira, MD, PhD, Full Professor
Universidade Federal de São Paulo, São Paulo, Brazil

PURPOSE: Burn injuries caused by various types of agents occur in average around one percent of world population annually. There are more than one million burns in the United States every year and about 5,000 of these injuries are fatal, making of burns the fourth leading cause of death from unintentional injuries in that country. No data about gene expression of skin cells of burned patients. The objective was to assess the expression profile of genes related to Innate and Adaptative Immune System (IAIS) and Toll-Like Receptors (TLR) in cultured primary human epidermal keratinocytes from patients with severe burns.

METHODS: Isolation and culture of human epidermal keratinocytes were performed with normal marginal-devitalized-skin fragments removed by the surgeon from burn injuries at day 4 after injury (n=6). Control group was patient undergoing to aesthetic surgery (n=3). The collected tissue was immediately immersed in sterile DMEM medium supplemented with penicillin and streptomycin. The culture was initiated by enzymatic method using dispase and then collagenase. Cells in the third passage were homogenized in Trizol reagent (Invitrogen). Total RNA extracted was dried and dissolved in RNase-free water, purified with Qiagen RNeasy Mini kit and subjected to DNAse treatment. The quantity and quality of extracted RNA were assessed by spectrophotometry using Nanodrop. Samples from each group were processed to perform PCR Array plates (SA Biosciences) containing 84 genes related to IAIS or to TLR pathways. The experiments were made in technical triplicates.

RESULTS: After the expression analysis of the 84 studied genes for each pathway, we observed, for IAAS pathway, that 63% of these genes were differentially expressed, among these 77% were down-regulated and 23% were up-regulated. Moreover, we could also observe for TLR pathways, that 21% of these genes were differentially expressed, and all of these genes (100%) were down-regulated. Among significant differentially expressed genes, we highlight the following ones (fold change): IAAS pathway= IL8 (41), IL6 (32), TNF (-92), HLA-E (-86), LYS (-74), CCR6 (-73), CD86 (-41) and HLA-A

(-35); TLR pathway= HSPA1A (-58), HRAS (-36), MAP2K3 (-23), TOLLIP (-23), RELA (-18), and FOS (-16).

CONCLUSIONS: These results provide a new insight into the potential role played by keratinocytes to drive inflammatory responses in severe burned patients. These epithelial cells play a key role in triggering the formation of several innate and adaptative proinflammatory cytokines and in activating members of the toll-like receptor pathway that might be disrupted by extensive lesions of the skin. Therefore, this study aims to contribute to understanding the molecular mechanisms underlying wound infection in severe burned patients and to provide new strategies that would restore the normal expression of these genes to enhance the inflammatory process and drive these patients to a better outcome.

73
MicroRNA Regulates Hemangioendothelioma Growth by Targeting the Nox-4/MCP-1 Pathway

Gayle M Gordillo, MD; Ayan Biswas, PhD; Savita Khanna, PhD; Sashwati Roy, PhD; Xueliang Pan, PhD; Mithun Sinha, PhD; Chandan K Sen, PhD

The Ohio State University, Columbus, OH

PURPOSE: MicroRNA (miR) are emerging as biomarkers to identify aberrant signaling pathways and potential therapeutic targets in tumors. Endothelial cell tumors are the most common soft tissue tumors in infants yet little is known about the role of miR in promoting their growth. A validated mouse endothelial cell (EOMA) tumor model was used to demonstrate that post-transcriptional gene silencing of dicer, the enzyme that converts pre-miR to mature miR, can prevent tumor formation in vivo. We also sought to determine how dicer activity regulates the nox-4/monocyte chemoattractant protein-1 (MCP-1) pathway, which we have previously shown is required for hemangioendothelioma formation.

METHODS: EOMA cells were transfected with either control or dicer lentiviral shRNA particles and injected (5×10^6 cells/100 ul PBS) subcutaneously into 6 week old 129 P3 mice. For in vitro experiments EOMA cells were transfected with control or dicer siRNA and samples collected 72 hours after transfection for measurement of miR, mRNA, or protein. Sybr green real-time PCR was used to measure miR and mRNA. Western blots and ELISA were used to measure protein. Plasmid transfections were done with reporter vectors containing firefly luciferase and co-transfected with a renilla luciferase vector as a transfection efficiency control. Luciferase levels were measured using a dual luciferase reporter assay. At least three independent replicates were conducted for all experiments. Two-sided 2 sample t-test was used to compare the difference between two groups, and ANOVA for comparison among more than 3 groups with Tukey's adjustment for the multiple pairwise comparisons among groups. Non-parametric procedures were used when normality assumption of the data was violated even after proper data transformation. A p-value of ≤ 0.05 was considered statistically significant.

RESULTS: Tumors formed in 4/4 mice injected with EOMA cells transfected with control short hairpin RNA (shRNA), but only formed in 1/5 mice injected with EOMA cells transfected with dicer shRNA and the single tumor in the dicer knockdown group was 91% smaller than the average size of tumors in the control group. This response to dicer knockdown was mediated by enhanced miR 21a-3p targeting of the nox-4 3'UTR. EOMA cells were transfected with miR 21a-3p mimics and luciferase reporter plasmids containing either intact nox-4 3'UTR or with mutation of the proposed 3'UTR miR21a-3p binding sites. Mean luciferase activity was decreased by 85% in the intact versus the site mutated vectors ($p<.01$). Loss of

nox-4 activity resulted in decreased hydrogen peroxide production and decreased production of oxidant inducible monocyte chemoattractant protein-1.

CONCLUSIONS: These are the first reported results to demonstrate the significant contribution of dicer activity and miR production in promoting hemangioendothelioma growth in vivo. These are also the first reported results of miR21a-3p targeting nox-4 mRNA and inhibiting reactive oxygen species production in endothelial cells. Collectively, these results indicate that targeting microRNA and specifically, miR-21a-3p, represent potential therapeutic strategies for the treatment of endothelial cell tumors including hemangioma and hemangioendothelioma.

74
Characterization of The Koliber Mutant: A New Model for Craniosynostosis Research

Yen-Yen S Gee, MMus[1]; Ramy A Shoela, MD[2]; Rebecca Anderson, PhD[3]; Jacek Topczewski, PhD[3]; Arun Gosain, MD[2]; Jolanta M Topczewska, PhD[2]

[1]Lurie Children's Hospital Research Center, Chicago, IL, [2]Lurie Children's Hospital Research Center, Department of Surgery, Chicago, IL, [3]Lurie Children's Hospital Research Center, Department of Pediatrics, Chicago, IL

PURPOSE: Zebrafish (Danio rerio) is an established model for craniofacial development studies. Here, we investigated cranium development in a recently identified kolibernu7 mutant. The kolibernu7 is characterized by a misshapen body, reduced length, and malformed skull as a result of hyperossified endochondral bones, bone fusions, and loss of cartilage (Anderson, in preparation). In this project, we investigated development of intramembranous calvaria bones and cranial sutures in kolibernu7 mutant and wildtype siblings. Our lab has established baseline biostatistical data for cranial vault development through progressive developmental stages (Shoela, in preparation). Here we expand on this method by using landmark-based morphometric analysis, with an aim to quantify the growth of individual bones of the cranial vault, the cranium as a whole, and the asymmetrical positioning of bilateral structures in kolibernu7 mutants.

METHODS: Wildtype (WT) (n=25) and kolibernu7 (n=23) zebrafish were collected at different developmental stages and double-stained with Alizarin Red and Alcian Blue to visualize bone and cartilaginous structures, respectively. Images of whole fish and isolated cranial vaults were taken using standard light microscopy. Following initial measurements of cranial width and length, total area, and overlapping areas of the anterior frontal, posterior frontal, parietal, and supraoccipital bones, the calvaria were enzymatically cleared using a trypsin solution with sodium borate. Individual bones were separated and photographed and similar measurements to those described above were taken. Morphometric analysis was conducted using landmarks and allowed for the creation of deformation grids of wildtype versus kolibernu calvaria. Similar analysis was conducted for individual cranial bones.

RESULTS: The ossification pattern and developmental schedule of cranial sutures are noticeably different between wildtype and kolibernu7 mutant. In contrast to the wildtype, where we observed a strong linear correlation between size of individual calvaria bones, total calvaria size, and standard length, in the

kolibernu7 mutant such correlation was lost. Interestingly, we observed a loss of coordinated growth resulting in asymmetric bone shapes as well as accelerated growth of frontal and parietal bones toward the midline in the kolibernu7 mutants.

CONCLUSION: Our research indicates that kolibernu7 is an interesting model to study membranous bone overgrowth and cranial sutures malformations.

75
Expression of Follicle-Stimulating Hormone Receptor in Vascular Anomalies

Reid A Maclellan, MD, MMSc; Matthew P Vivero, BA; Patricia Purcell, PhD; Harry P Kozakewich, MD; Amy D DiVasta, MD, MMSc; John B Mulliken, MD; Steven J Fishman, MD; Arin K Greene, MD, MMSc
Boston Children's Hospital / Harvard Medical School, Boston, MA

INTRODUCTION: The mechanism for the growth of infantile hemangioma and vascular malformations is unknown. Follicle-stimulating hormone secretion mirrors the life-cycle of infantile hemangioma, and increases during adolescence when vascular malformations often progress. The purpose of this study was to determine if vascular anomalies express the receptor for follicle-stimulating hormone.

METHODS: Human vascular tumors (infantile hemangioma, congenital hemangioma, kaposiform hemangioendothelioma, pyogenic granuloma) and vascular malformations (capillary, lymphatic, venous, arteriovenous) were subjected to immunofluorescence for follicle-stimulating hormone receptor. Tissues were co-stained with DAPI and CD31 antibodies to identify nuclei and blood vessels, respectively. Control specimens included normal skin/subcutis, mucosa, liver, spleen, Crohn disease, granulation, pancreatitis, rheumatoid arthritis, and synovitis. Receptor expression and microvessel density were quantified using imaging software.

RESULTS: Follicle-stimulating hormone receptor was expressed in the endothelium of all vascular anomalies, but was not present in control specimens. Receptor staining was greater in proliferating infantile hemangioma (6.0%) compared to the other vascular tumors [congenital hemangioma (0.61%), kaposiform hemangioendothelioma (0.55%), pyogenic granuloma (0.56%)] ($p<0.0001$), despite similar microvessel density ($p=0.1$). Follicle-stimulating hormone receptor expression in arteriovenous malformations (2.65%) was elevated compared to the other types of vascular malformations [capillary (1.02%), lymphatic (0.38%), venous (0.76%), ($p<0.0001$)].

CONCLUSIONS: Vascular anomalies express follicle-stimulating hormone receptor on their endothelium, in contrast to vascular control tissues. Vascular anomalies are the only benign, pathological tissue known to express this receptor. Because the secretion of follicle-stimulating hormone correlates with the growth pattern of infantile hemangioma and vascular malformations, follicle-stimulating hormone might be involved in the pathogenesis of these lesions.

76
Modeling Craniosynostosis in Zebrafish using the Genome Editing Technique CRISPR

Tatiana Favelevic, BS Pending[1]; Rebecca Anderson, PhD Candidate[2]; Jacek Topczewski, PhD Candidate[1]; Arun K Gosain, MD[3]; Jolanta M Topczewska, PhD[1]

[1]Ann & Robert H Lurie Children's Hospital of Chicago Research Center, Chicago, IL, [2]Northwestern University, Chicago, IL, [3]Ann & Robert H Lurie Children's Hospital of Chicago, Chicago, IL

Craniosynostosis (CS), or premature fusion of the cranial bones, represents a clinically and genetically heterogeneous illness, with multifactorial etiology. More than a hundred mutations within the *TWIST1* gene are associated with autosomal dominant disorders of CS in humans, a consequence of *TWIST1* haploinsufficiency. Moreover, *Twist1* heterozygote mice develop similar defects as humans, including coronal suture synostosis. To test the feasibility of a zebrafish model for the study of CS and to assess the degree of similarity between rodents and fish in the molecular mechanisms that control cranium development, we have employed new technology of genome editing (CRISPR/Cas) to mutate the *twist* homologue. We selected zebrafish *twist3* based on strong expression in the suture mesenchyme as revealed by in situ RNA hybridization. The CRISPR/Cas system uses CRISPR guided RNA (gRNA) working in a complex with Cas endonucleases to target and cleave target DNA. When a double stranded break is introduced into the target DNA, a non-homologous end joining repair mechanism creates a mutation. We anticipate that mutagenesis of *twist3* using CRISPR technology will result in a novel zebrafish model of craniosynostosis. Moreover, it will provide us with the possibility of rapid genetic manipulations of CS related genes to better understand the molecular mechanisms controlling normal and pathological development of cranial sutures.

METHODS: The CRISPR-*twist3* construct was created by PCR method, the gRNA, transcribed *in vitro*, and all constructs including *cas9* mRNA were injected into zebrafish embryos. For diagnostic reasons, the CRISPR/Cas cleavage site was designed next to a *Msp*I restriction site, permitting easy identification of genome editing events through the creation of restriction enzyme polymorphisms. This diagnostic digestion will be used for genotyping of the progeny of injected fish when testing for the inheritance of the *twist3* mutation. CRISPR^{twist3} injected fish, aged 2–3 months, will be out crossed with wild type. The germ line transmission of the *twist3* mutation would ensure a stable line. We predict that 3–5 founder fish will be isolated. The *twist3* gene will be sequenced to define the mutation.

RESULTS: Randomly selected, CRISPR/Cas RNAs-injected and non-injected embryos were genotyped as described above. We detected incomplete digestion of PCR product for ~30% of the injected embryos (n=76), while the controls were fully digested by *Msp*I, indicating that 30% of injected fish may carry the mutation within *twist3*. We expect this is sufficient to recover stable mutant strain in the next generation.

CONCLUSION: The present study demonstrates the effectiveness of the CRISPR/Cas method in editing the zebrafish genome. We predict that within 6 months, stable mutant strains can be established, providing the possibility of examining genetic interaction among genes and signaling pathways.

SATURDAY, MARCH 8, 2014

SCIENTIFIC SESSION 6 GROUP B
CRANIOFACIAL/BONE
4:00 PM – 5:30 PM

SATURDAY, MARCH 8, 2014

77
TGF Beta is a Potent Inhibitor of BMP2 Mediated Osteogenic Differentiation in a Primary Murine Muscle Cell in vitro Model of Heterotopic Ossification

S Alex Rottgers, MD; Laurie B Meszaros, PhD; Anand R Kumar, MD
University of Pittsburgh, Pittsburgh, PA

INTRODUCTION: Heterotopic ossification (HO) is pathologic bone formation in extremity muscles. Alterations in inflammatory mediators and bone morphogenetic proteins acting on muscle derived progenitor cells (MDCs) are thought to be critical for HO formation. The aim of this study is to evaluate the effects of bone morphogenetic protein (BMP2) and inflammatory mediators (TNFα, TGFβ1) on MDC osteogenic differentiation.

METHODS: Primary mouse muscle cells were isolated from 8-week-old C57B/6J mice. Hindlimb muscles were sterilely processed, followed by pre-plating on collagen-coated flasks for 2 hours to remove fibroblast. 100,000 cells per well were cultured in DMEM-based proliferation medium (PM) alone or with 50ng/mL of BMP2, with 1 ng/ml TNFα, with 5 ng/ml of TGFβ1 alone or in various combinations. Samples were collected after 3 days. RNA was isolated and reverse transcribed to cDNA. Quantitative PCR for Osx, Alp and Runx2 was performed. Changes in target gene expression were expressed relative to untreated MDCs with expression normalized to GAPDH.

RESULTS: FACS analysis revealed a mixed population of cells, with high Sca-1 and CD34 expression and low CD31, CD 56, CD144 and CD146 expression. Muscle cells cultured with BMP2 demonstrated increased expression of Osx (36.6±25.8), Alp (19.0±4.16) and Runx2 (2.26±0.61) relative to untreated cells. TNFα decreased expression of Osx (0.19±0.002), Alp (0.360±0.15) and Runx2 (0.75±0.18 fold). TGFβ1 demonstrated decreased expression of Osx (0.01±0.07), Alp (0.004±0.0005) and Runx2 (0.59±0.01). Cells cultured with BMP2/TNFα demonstrated increased expression of Osx (19.1±4.39) relative to untreated cells but significantly less than BMP alone (p=0.001). BMP-2 mediated expression of Alp (15.9±2.13) and Runx2 (1.64±0.10) was maintained. BMP2/TGFβ1 treatment demonstrated decreased expression of Osx (0.003±0.001), Alp (0.004±0.0005) and Runx2 (0.56±0.05) from baseline. Combined BMP2/TNFα/TGFβ1 treatment also decreased expression of Osx (1.58±0.52), Alp (0.021±0.006) and Runx2 (0.92±0.10).

DISCUSSION: Using a mixed population of primary MDCs we have demonstrated in vitro osteogenic differentiation following application of BMP2. TNFα significantly decreased BMP2 mediated osteogenic changes. We have demonstrated a more robust osteogenic inhibition of BMP2 mediated changes using TGFβ1. TGFβ1 and TNFα agonist therapy may represent a novel therapy for HO. Future studies evaluating changes within the intracellular SMAD pathway may elucidate the mechanism of inhibition.

78
An Experimental Study of Particulate Bone Graft for Secondary Inlay Cranioplasty over Scarred Dura

Reid A Maclellan, MD, MMSc; Aladdin H Hassanein, MD, MMSc; John B Mulliken, MD; Gary F Rogers, MD, JD, MBA, MPH; Arin K Greene, MD, MMSc
Boston Children's Hospital / Harvard Medical School, Boston, MA

BACKGROUND: Inlay cranioplasty in children is difficult because autologous bone is limited. Cranial particulate bone graft effectively closes defects when placed over normal dura. The purpose of this study was to determine if particulate bone graft will heal when used for secondary cranioplasty over scarred dura.

METHODS: A 17mm x 17mm critical-sized defect was made in the parietal bone of 12 rabbits and allowed to heal. Sixteen weeks post-operatively the 17mm x 17mm critical-sized defect was recreated and managed in two ways: Group I (no implant) (n=6) and Group II (particulate bone graft) (n=6). Particulate graft was obtained using a brace and bit from the frontal bone and placed over the scarred dura. Gross analysis and micro-computed tomography were performed 16 weeks following the cranioplasty to determine the: (1) area of critical-sized defect ossification and (2) thickness of the healed bone graft.

RESULTS: Critical-sized defects treated with particulate bone graft grossly exhibited superior ossification (96.0%; range, 86.5%-100%) compared to those managed without an implant (49.9%; range, 42.6%-54.6%) ($p < 0.0001$). MicroCT examination showed critical-sized defects treated with particulate bone graft healed 91.1% (range, 79.0–97.2%) of the area, while control defects demonstrated inferior ossification 56.9% (range, 40.0–68.3%) ($p < 0.0001$). Critical-sized defects treated with particulate bone graft exhibited thinner bone (2.42mm; range, 1.69–3.30mm) compared to the normal adjacent parietal cranium (4.33mm; range, 3.28–6.20mm) ($p < 0.0001$).

CONCLUSIONS: Particulate bone graft ossifies inlay calvarial defect area over scarred dura, although the bone is thinner than the normal cranium. Clinically, particulate bone graft may be efficacious for secondary inlay cranioplasty.

79

Deferoxamine in Combination with Adipose-Derived Stromal Cells Rescues Mineralization and Improves Union Rate in the Treatment of Established Radiotherapy Induced Non-Unions

Jordan T Blough; Alexis Donneys, MD, MS; Noah S Nelson, BS; Sagar S Deshpande, BS; Peter A Felice, MD; Erin E Page; Joseph E Perosky, MS; Kenneth M Kozloff, PhD; Steven R Buchman, MD

University of Michigan, Ann Arbor, MI

PURPOSE: Radiotherapy induced non-unions occurring in the head and neck cancer patient population are a devastating morbidity that can cause significant functional deficits, persistent pain and often have a dreadful impact on quality of life. Twenty-three percent of patients with advanced osteoradionecrosis proceed to develop pathologic fractures and associated non-unions. Unfortunately, clinicians have few efficacious treatment options for this catastrophic problem. Previously, we have demonstrated a reproducible non-union rate of approximately 75–80% in a non-treated, rat model of pathologic fracture healing after radiotherapy. Here, we report the utilization of a therapeutic strategy, combining adipose-derived stromal cells (ADSCs) with deferoxamine (DFO) to treat established non-unions in this validated model. Our hypothesis is that ADSCs will act to replenish cellular volume, while DFO will function to augment angiogenesis at the site of the non-union, thereby improving mineralization metrics and union formation after treatment.

METHODS: Thirty-six Lewis rats were administered a bioequivalent dose of radiotherapy two weeks prior to mandibular osteotomy and external fixation. Rats were assessed radiographically for bony union formation following a 40-day healing period. Only rats exhibiting non-unions (83%) were further utilized and divided into two groups: radiated fracture with surgical debridement (surgical debridement; n=15) and radiated fracture with both surgical debridement and combination therapy (combination therapy; n=15). The second surgery consisted of non-union confirmation and debridement of necrotic tissue for both groups. The mandibular defects in treatment animals were implanted with scaffolds loaded with ADSCs, and multiple DFO injections were delivered after surgery as previously described in the literature. ADSCs were harvested from the flanks of isogenic Lewis rats and allowed to reach confluence prior to implantation. After a second 40-day healing period, mandibles were dissected, assessed for bony union and imaged with micro-CT for mineralization outcomes. Groups were compared with an independent t-test and $p<0.05$ was considered statistically significant.

RESULTS: Enhanced mineralization metrics were found for the combination therapy group in comparison to the surgical debridement group. Improvements were found for bone volume fraction (0.78±0.069 versus 0.85±0.073; p=0.034), bone mineral density (665.64±56.23 versus 722.08±65.20; p=0.038) and tissue mineral content (16.18±4.14 versus 20.42±3.29; p=0.013). Perhaps even more clinically significant, the combination therapy group demonstrated a 65% improvement in the remediation of non-unions compared to the surgical debridement group. Specifically, the combination therapy group displayed a 7% incidence of non-union, while the surgical debridement group exhibited a 20% incidence of non-union.

CONCLUSION: Our results support the contention that combined ADSC and DFO therapy is superior to surgical debridement alone in the treatment of radiotherapy induced non-unions. The combination therapy of cellular replacement and angiogenic stimulation functions to significantly improve mineralization, as well as demonstrate a substantial increase in bony union rate. Our goal is to further explore this novel treatment option in an effort to take this treatment paradigm from the bench to the bedside, providing an attractive alternative to the current inadequate treatment strategies for non-unions caused by adjuvant radiotherapy.

80
Parathyroid Hormone Remediates Radiation Damage in a Murine Model of Distraction Osteogenesis via Histological Evaluation

Sagar S Deshpande, BS[1]; Steven Y Kang, MD[1]; Alexis Donneys, MD, MS[1]; Peter A Felice, MD[2]; Rodriguez J Jose, MD[1]; Noah S Nelson, BS[1]; Samir S Deshpande[3]; Steven R Buchman, MD[1]

[1]University of Michigan, Ann Arbor, MI, [2]Medical University of South Carolina, Charleston, SC, [3]Kalamazoo College, Kalamazoo, MI

PURPOSE: Radiation is known to be detrimental to bone and soft tissue repair, resulting in an unacceptably high incidence of devastating wound healing complications. This is effected through a mechanism of both direct cellular and vascular depletion. We sought to utilize an anabolic regimen of parathyroid hormone (PTH), an FDA-approved bone therapeutic, to remediate this deficiency. The purpose of this study was to allow for the successful utility of distraction osteogenesis in an irradiated field utilizing an intermittent regimen of PTH for the purpose of craniofacial reconstruction in head and neck cancer victims.

METHODS: 20 male Lewis rats were randomly split into three groups, DO (n=5), XRT/DO (n=10), and XRT/DO/PTH (n=5). XRT/DO and XRT/DO/PTH underwent 5 day fractionated XRT of the left mandible at 7 Gy per day and were allowed to recover for two weeks. All groups underwent mandibular distractor placement. Groups were distracted at 0.3mm every 12 hrs to a 5.1mm (a critical-sized defect for an irradiated, distracted mandible), and sacrificed on post-operative day (POD) 40. XRT/DO/PTH received 60mg/kg of PTH daily for 3 weeks, starting on POD 4. Coronal sections were obtained and stained using Hematoxylin Eosin (H&E), Safranin O, and Gomori Trichrome. Statistical analysis was performed with ANOVA and subsequent Tukey or Games-Howell post-hoc tests, dependent on data heterogeneity.

RESULTS: Gomori Trichrome demonstrated a significantly increased osteocyte number (133.44 ± 10.25 vs 67.86 ± 9.47, p=0.000) and significantly decreased empty lacunae (2.50 ± 1.20 vs 15.64 ± 7.79, p=0.000) in XRT/DO/PTH compared to XRT/DO. There were no significant differences between DO and XRT/DO/PTH. Safranin O demonstrated no cartilage presence. H&E staining demonstrated more woven bone within the regenerate of DO as well as XRT/DO/PTH specimens.

CONCLUSION: PTH has been previously shown to remediate radiomorphometrics, vascular analysis, and biomechanical strength in an irradiated model of distraction osteogenesis. This study has demonstrated both qualitative and quantitative metrics of radiation-induced remediation of cellularity utilizing parathyroid hormone, demonstrating its potential for use in irradiated fields. PTH therapy was able to remediate the detriments to osteocyte number as well as prevent empty lacunae formation. Furthermore, PTH stimulated new osteoid growth, as established by H&E. Finally, PTH maintains the intramembranous healing mechanism intrinsic to DO, as the Safranin O stain showed no evidence of a cartilaginous intermediate. As such, this abstract has demonstrated that anabolic regimens of PTH are a powerful tool for remediating the damage of radiation and allowing for successful utilization of distraction osteogenesis.

81
BMP2 Stimulation of Adipose, Bone Marrow, and Muscle-Derived Stromal Cells Fails to Augment Calvarial Repair

Sameer Shakir, BS; Dan Wang, DMD; Melissa A Shaw, BS; Darren M Smith, MD; Sanjay Naran, MD; James R Gilbert, PhD; Zoe M MacIsaac, MD; Joseph E Losee, MD; Gregory M Cooper, PhD

University of Pittsburgh, Pittsburgh, PA

PURPOSE: Tissue engineering is becoming a viable adjunct - or even alternative - to autologous bone grafting in craniofacial reconstruction. Current methods focus on implantation of bioresorbable scaffolds seeded with proteins and/or osteogenic progenitor cells, although it remains unclear whether specific stromal cell types are better suited for use in craniofacial reconstruction. This study aims to determine the healing capacity of adipose (ADSC), bone marrow (BMDSC), and muscle-derived (MDSC) stromal cell populations in a calvarial defect model when this environment is optimized using bone morphogenetic protein 2 (BMP2). We hypothesize that BMP2 will augment stromal cell engraftment and differentiation within calvarial defects.

MATERIALS AND METHODS: Bone marrow, muscle, and adipose tissues were harvested from 10-week old wildtype mice (n=8). Cells were seeded overnight onto 5mm acellular dermal matrix (ADM) discs (1×10^5 cells/disc) and were osteoinduced with 150ng (30ng/mm^2) BMP2. Unseeded ADM discs treated with either BMP2 or vehicle served as controls. Discs were subsequently placed into 5mm circular calvarial defects in 10-week old wildtype mice. Mice were euthanized 4 weeks postoperatively. Regenerate tissue was analyzed by 3D microCT and histology to assess percent healing and tissue morphology.

RESULTS: Differences in percent healing (mean ± SE) were observed between vehicle control (31.5%±8.8), BMP2 control (71.9%±7.0), ADSC + BMP2 (31.4%±1.8), MDCS + BMP2 (21.9%±4.9), and BMDSC + BMP2 (38.5%±20.2) groups. One-way ANOVA revealed a statistically significant main group effect ($F=3.988$, $p<0.02$). Percent healing was significantly decreased in osteoinduced stromal cell constructs and in vehicle control when compared to unseeded, BMP2 therapy. Pentachrome staining revealed histological evidence of endochondral ossification in all treatment groups. BMP2 treated defects regenerated vascularized, thick woven bone with large marrow spaces. Osteoinduced stromal cell-treated defects regenerated less bone that was also less thick when compared to BMP2-regenerated bone. However, regenerated bone was consistently limited to the region of interest in these treatment groups.

CONCLUSIONS: Low-dose BMP2 potently stimulates local osteoprogenitors to heal osseous deficiencies within the calvaria. We observed significant modulation of BMP2-induced osteogenesis with the addition of stromal cells; unlike BMP2 therapy alone, osteoinduced stromal cell therapies do not improve defect healing beyond that of vehicle control in this model. These observations collectively call into question the role of progenitor cells in tissue engineering strategies for calvarial repair, and suggest that engrafted cells may be susceptible to environmental influences that determine their ability to contribute to cranial regeneration. Based upon these findings, we suggest that the inherently heterogeneous population of cells within the stroma of adipose, bone marrow, and muscle tissues may restrict BMP2-induced calvarial defect healing.

82
What is the Optimal Age for Cranial Vault Remodeling in Syndromic Craniosynostosis? Insights from the Johns Hopkins Experience

Alan F Utria, BA[1]; Gerhard S Mundinger, MD[1]; Joy Zhou, Undergraduate Student[2]; Ali Ghasemzadeh, BS[1]; Robin Yang, MD DDS[3]; Amir H Dorafshar, MBChB[1]

[1]Johns Hopkins School of Medicine, Baltimore, MD, [2]Johns Hopkins University, Baltimore, MD, [3]University of Maryland School of Medicine, Baltimore, MD

PURPOSE: Optimal timing of cranial vault remodeling in syndromic patients with craniosynostosis is controversial. The purpose of this study was to gain insight into the impact of age at repair on relapse rates through the Johns Hopkins experience.

METHODS: Retrospective chart review was performed for 58 patients surgically treated for syndromic craniosynostosis at Johns Hopkins Hospital between 1990–2013. Patient demographics, suture involvement, age at surgery, syndrome, surgical management, hospital course, and complications were recorded. Surgical procedures were assigned a Whitaker category based on need for reoperation as follows: Category I signified no additional surgery required, Category II signified soft tissue and lesser bone contouring revisions required, Category III signified major alternative osteotomies or bone grafting required, and Category IV signified the need for major surgical revision essentially duplicating the original surgery. Multivariable logistic regression analysis was performed to determine the relationship between age at surgery and need for reoperation as categorized by the Whitaker scale, and to assign odds ratios (OR) for need for surgical revision by operative timepoint. Covariates included suture involvement, syndrome, race and gender.

RESULTS: 58 patients undergoing a total of 71 cranial vault remodeling procedures for syndromic craniosynostosis were identified. Average follow up was 6 years (SD 5 years). Patient demographics were as follows: 32 male (55%), 26 female, 39(45%) Caucasian, 10 Black, and 9 of another race. Syndromes were comprised of Crouzons (n=14), Aperts (n=12), other (n =12), Pfiffers (n=10), undiagnosed (n=6), and Seathre-Chotzen (n=4). Average number of sutures involved was 2.4 (range 1 to 5) as follows: right coronal (n=37), left coronal (n=38), sagittal (n=18), metopic (n=11), left lambdoid (n=7), and right lambdoid (n=6). Whitaker category for the 71 procedures was as follows: 31 in category I, 10 in category II, 3 in category III, and 27 in category IV. Multivariable logistic regression analysis for the effect of age on reoperation revealed a greater odds of major reoperation (category IV) in patients with less than 3 months of age (OR 5.6, p=0.015, 95% CI: 1.4–24.7) and 3–6 months of age (OR 4.3, p=0.03, 95% CI: 1.2–16.1), and a greater odds of no reoperation necessary (category I) in patients 6–9 months of age (OR 7.0, p=0.006, 95% CI: 1.7–27.9). Patients older than 12 months of age had a greater odds (OR 8.4, p=0.011, 95% CI: 1.6–43.2) of requiring minor operative revisions (category II).

CONCLUSION: Timing of surgery is an important factor to consider when planning vault remodeling in syndromic craniosynostosis. We found that operating before 6 months of age had greater odds of requiring a complete revision, and that patients undergoing remodeling after 12 months of age were more likely to require minor revisions. In our experience, the ideal operative window that demonstrated the greatest odds of requiring no additional surgery was 6–9 months of age.

83
Improved Biomechanical Metrics in the Treatment of Radiotherapy-Induced Non-Unions with a Novel Combination Therapy

Noah S Nelson, BS; Alexis Donneys, MD, MS; Jordan T Blough; Sagar S Deshpande, BS; Peter A Felice, MD; Erin E Page; Joseph E Perosky, MS; Kenneth M Kozloff, PhD; Steven R Buchman, MD

University of Michigan, Ann Arbor, MI

PURPOSE: Radiation-induced non-unions are complex morbidities with limited management solutions. In prior studies we have utilized a rat model of mandibular fracture healing after a Human Equivalent Dose of Radiotherapy (HEDR), and have established a reproducible non-union rate of approximately 75–80%. In this study, we sought to combine adipose-derived stem cells (ADSCs) with deferoxamine in order to treat established non-unions in our model. We posit that ADSCs will act as a cellular replacement, while DFO will function to enhance angiogenesis at the non-union site, resulting in improvements in biomechanical metrics after treatment.

METHODS: Thirty-six Lewis rats were administered a HEDR two weeks prior to osteotomy of the mandible and external fixation. Following a 40-day healing period, the rats were assessed radiographically for bony union. Those exhibiting non-unions (30/36) were further utilized and divided into two groups: surgical debridement (non-treatment; n=15) and surgical debridement with combination therapy (treatment; n=15). The second surgery consisted of debridement of necrotic tissue for both groups. The mandibular defects in treatment animals were implanted with scaffolds loaded with previously harvested ADSCs and were administered multiple DFO injections after surgery, as described in the literature. After a second 40-day healing period, mandibles were harvested for biomechanical testing (BMT). In the non-treatment group, two animals died, and two mandibles exhibited complete non-unions (no fibrous bridging) making BMT impossible. Groups were compared with an independent t-test and $p<0.05$ was considered statistically significant.

RESULTS: Upon harvesting our specimens, BMT analysis demonstrated a statistically significant increase in the combination therapy group in comparison to the surgical debridement group. Specifically, significant differences were found in the biomechanical metrics of Yield (65.39±28.55 vs 35.06±14.91; p=.015) and Energy (16.96±11.78 vs 6.67±4.45; p=.026). Additionally, results trending toward significance were observed for Ultimate Load (75.82±32.03 vs 50.17±22.93; p=.066), Failure Load (73.99±33.82 vs 50.17±22.93; p=.095), and Elastic Energy (10.70±10.92 vs 2.96±3.38; p=.057).

CONCLUSION: Consistent with our hypothesis, our results demonstrate that combined ADSC and DFO therapy is superior to surgical debridement alone in the treatment of radiation induced non-unions. The combination therapy of cellular replacement and angiogenic stimulation functions to significantly improve the biomechanical properties of the mandibles. Further experimentation with this novel treatment option will hopefully enable us to take this or a similar therapy to the clinic in order to mitigate the deleterious effects of radiation-induced non-unions and their related pathologies.

84
Fractures of the Mandibular Condylar Base Are Associated With Severe Blunt Internal Carotid Artery Injuries

Neil M Vranis, BA[1]; Gerhard S Mundinger, MD[2]; Justin L Bellamy, BS[3]; Abhishake Banda, MD, DDS[2]; Robin Yang, MD, DDS[2]; Amir H Dorafshar, MBChB[2]; Eduardo D Rodriguez, MD, DDS[2]

[1]University of Maryland School of Medicine, Baltimore, MD, [2]Division of Plastic, Reconstructive and Maxillofacial Surgery, R Adams Cowley Shock Trauma Center, University of Maryland Medical Center, Baltimore, MD, [3]The Johns Hopkins University School of Medicine, Baltimore, MD

PURPOSE: Fractures of the mandibular condyle at the head, neck, and base are common following blunt facial trauma. Patients with these fractures have also been shown to be at increased risk for concomitant blunt carotid artery injuries (BCAI), though this relationship remains poorly understood. Further elucidation of the relationship between specific condylar fracture patterns and BCAI may improve vascular injury screening criteria and treatment for craniofacial trauma patients.

METHODS: A retrospective cohort study was performed for all patients that presented to the R Adams Cowley Shock Trauma Center with mandibular condyle fractures from 2000 to 2012. In addition to demographic information, authors reviewed computed tomographic (CT) imaging to confirm and codify condylar fracture location, displacement, and comminution. Additional facial fractures were also systematically recorded. Condyle fractures were classified according to the Strasbourg Osteosynthesis Research Group (SORG) classification system as follows: fracture of the condylar head (SORG 1), fractures of the condylar neck (SORG 2), and fractures of the condylar base (SORG 3). Cerebrovascular injuries were confirmed by review of CT and magnetic resonance imaging (MRI) angiography, and were graded according to the Biffl scale from 1 (vessel with less than 25% intimal stenosis) to 5 (vessel transection). Severe BCAI was defined as a Biffl score greater than 1. Adjusted relative risk estimates were obtained using multivariable regression with STATA 12 software.

RESULTS: We identified 527 consecutive patients with 657 condyle fractures. Of these fractures, 150 (22.8%) were SORG 1, 203 (30.9%) were SORG 2 and 304 (46.3%) were SORG 3. 32 (6.1%) patients sustained 44 BCAI's, with 21 (4.0%) patients suffering a severe BCAI. Severe BCAI occurred in 2 (1.3%) of SORG 1, 2 (1.0%) of SORG 2 and 17 (5.6%) of SORG 3 fractures. After accounting for the effect of age, mechanism of injury, and concurrent LeFort I, II and III fractures, adjusted multivariable regression analysis found that SORG 3 fractures were independently associated with a 4.03 -fold increased risk of severe BCAI (p-value <0.01).

CONCLUSION: In blunt trauma patients with mandibular condyle fractures, there is an increased risk of severe BCAI with involvement of the condylar base compared to condylar head or neck. We hypothesize that base fractures constitute a relatively longer condylar moment arm that may displace and injure the internal carotid artery. Given the urgent nature of treating BCAI, the presence of a condylar base fracture should heighten suspicion for a severe internal carotid artery injury.

85
The Role of Distraction Osteogenesis in the Surgical Management of Craniosynostosis: A Systematic Review

Owen Johnson, III, MD, FACS; Anne Tong, MBBS; Christopher Wallner, BS; Amir H Dorafshar, MBChB

Johns Hopkins University School of Medicine, Baltimore, MD

PURPOSE: Distraction osteogenesis (DO) has been proposed as an alternative to cranial remodeling surgery (CRS) for craniosynostosis, but technique descriptions and outcome analyses are limited to small case series. This systematic review summarizes operative characteristics and outcomes of DO for craniosynostosis. A secondary aim is to identify advantages and disadvantages of this approach and formulate guidelines for recommending its use over CRS.

METHODS: Two independent assessors undertook a systematic review of the literature using Cochrane, PubMed, Scopus, Google Scholar, and Web of Science databases. Studies that reported descriptive analysis, operative technical data, outcomes, or post-operative complications of DO for craniosynostosis were included. Studies that reported concomitant midface or mandibular distraction were excluded.

RESULTS: Twenty-two eligible manuscripts, totaling 292 cases, were identified. In 267 cases DO was the primary procedure while 25 had previous operations. There were 93 cases of syndromic craniosynostosis, most frequently Apert (38) and Crouzon (21) syndromes. The remaining 199 were non-syndromic, the most common deformities being plagiocephaly (56), scaphocephaly (40), and brachycephaly (23). All comparison studies found mean operative time, blood loss, and intensive care unit (ICU) length of stay to be less than CRS, some with statistical significance. Only 19 patients (6.5%) required any blood transfusion whereas in CRS transfusion is almost universal. Treatment protocols included: latency period of 4.7 ± 1.6 d, distraction rate of 1 millimeter/d, distraction period of 20.4 ± 6.1 d, and consolidation period of 59.6 ± 22.8 d. Final distraction length was 22.9 ± 9.7 millimeters. There were complications in 46 (16%) cases, but most of these were minor, such as superficial infections, cerebrospinal fluid leaks requiring no intervention, or hardware issues. Footplate loosening or hardware malposition was highly variable and dependent on surgical technique. There were no post-operative deaths. Serious complications associated with CRS such as meningitis, epidural abscess, or significant resorption were not observed after DO. With reasonable follow-up (23.6 ± 21.6 months, range 6 to 130), there have been zero reports of bony relapse, including when DO was used to treat relapse after CRS. DO required at least two surgeries, and prolonged in-patient hospitalization was sometimes employed to manage the distraction process. In 291 cases, post-operative improvement was observed in the form of decreased intracranial pressure, resolved headache or papilledema, improved aesthetic appearance, increased cranial volume, or other measurements of endocranial angulation or proportion. In one case intracranial hypertension failed to completely resolve.

CONCLUSIONS: DO is a useful adjunct to treat craniosynostosis with low morbidity and durable results. Compared to CRS, DO is performed with decreased operative time, blood loss, need for transfusion, and need for intensive care. While DO can be labor-intensive and requires at least two procedures, its efficacy and safety profile suggest it can be considered an efficacious alternative method for the treatment of craniosynostosis. DO may be particularly advantageous in posterior vault expansion or to salvage cases of previous failure/relapse following CRS.

SATURDAY, MARCH 8, 2014

SCIENTIFIC SESSION 6 GROUP C
TISSUE ENGINEERING
4:00 PM – 5:30 PM

SATURDAY, MARCH 8, 2014

86
Lymph Node Transplantation Generates Spontaneous Lymphatic Reconnection and Restoration of Lymphatic Flow

Seth Z Aschen, BS; Gina T Farias-Eisner, BS; Daniel A Cuzzone, MD; Swapna Ghanta, MD; Nicholas J Albano, BS; Walter J Joseph, BS; Ira L Savetsky, MD; Jason C Gardenier, MD; Babak J Mehrara, MD
MSKCC, New York, NY

PURPOSE: Although lymph node transplantation has been shown to improve lymphatic function in patients with lymphedema, the mechanisms regulating lymphatic vessel reconnection and the functional status of lymph nodes (LNs) remains poorly understood. In this study we developed a novel reporter mouse that allowed us to determine the origin of lymphatic endothelial cells (LECs) and vessels forming functional connections with transferred LNs.

METHODS: We developed tamoxifen-induced Flt4-Cre/LacZ-LoxP lymphatic reporter mice to examine the lineage of lymphatic vessels infiltrating transferred LNs. The expression of Cre recombinase was driven by the promoter for the lymphatic specific gene vessel endothelial growth factor receptor 3 (VEGF-R3). These mice served as LN transplant recipients from donor wild-type C57/B6 mice. Five days prior to sacrifice, animals received daily doses of tamoxifen to activate Cre expression. Lymphatic function following LN transfer was analyzed with lymphoscintigraphy (LS) using Tc99 and ferritin injections. The anatomic localization of lymphatic vessels and high endothelial venules (HEVs) was analyzed by co-staining for LYVE-1 (specific to lymphatics) and MECA32 (specific to HEVs).

RESULTS: Reporter mice were specific and highly sensitive in identifying lymphatic vessels, such that tamoxifen treatment resulted in high-level expression of Cre recombinase with more than 90% of lymphatic vessels (LYVE-1+) demonstrating B-gal staining. Transferred LNs demonstrated near-normal levels of Tc99 uptake 28 days after transfer as compared to control (non-operated) contralateral lymph nodes. This uptake corresponded to a massive infiltration of recipient mouse lymphatics with putative connections to donor lymphatics, as evidenced by anastomoses between B- gal+/LYVE-1+ (i.e., recipient) and B-gal /LYVE-1+ (i.e., donor) vessels. This spontaneous reconnection was associated with high level expression of lymphangiogenic cytokines (VEGF-C) in the perinodal fat and infiltrating lymphatics. Newly formed lymphatic channels in transferred lymph nodes were in close anatomic proximity to HEVs (demonstrated by LYVE-1 and MECA32 co-staining) with histologic evidence of interstitial fluid exchange between lymphatics and HEVs. Importantly, we found that T and B cell populations in the lymph node were preserved suggestive of preserved lymph node function.

CONCLUSION: The lymphatic reporter mice we developed show a high fidelity for identifying lymphatic vessels. Using these mice we found that transferred lymph nodes have rapid infiltration of functional host lymphatic vessels and spontaneous return of interstitial fluid drainage function. These findings suggest that even in the absence of exogenous growth factors, transferred LNs are capable of generating functional lymphatic connections with recipient lymphatic vessels and that this process is related to endogenous expression of VEGF-C in the perinodal fat and infiltrating lymphatics. Additionally, considering the finding that LECs and HEVs exist in close proximity in transferred LNs, it is possible that an exchange of interstitial fluid occurs between these vessels, thereby increasing lymphatic flow and drainage. Lastly, the transferred LNs remain immunologically competent because T and B cell populations are maintained.

87
Beyond Cotton Candy: Fabrication of Capillary Networks within Biocompatible Tissue- Engineered Constructs from Kerria Lacca Resin (Shellac)

Adam Jacoby, BA; Rachel C Hooper, MD; Jeremiah Joyce, BA; Remco Bleecker, BA; Jason A Spector, MD, FACS
Weill Cornell Medical College, New York, NY

PURPOSE: Creation of synthetic tissues with microvascular networks, which adequately mimics the size and density of capillaries found in vivo, remains one of the foremost challenges in the field of tissue engineering. In our previous work, we utilized a sacrificial microfiber technique whereby 1.5 mm Pluronic F127 microfibers were embedded within a collagen matrix, leaving a patent internal channel, which was subsequently seeded with endothelial and smooth muscle cells forming a neointima and neomedia respectively. Here we describe two approaches to synthesize a tissue-engineered construct with macro-inlet and outlet vessels, bridged by a dense network of microvessels, which recapitulates the hierarchical organization of an arteriole, venule, and capillary bed found in vivo.

METHODS: 1.5 mm longitudinal Pluronic F127 macrofibers were created using pre-formed polydimethylsiloxane (PDMS) molds. Dense three dimensional matrices were fabricated using one of two techniques: 1) manual extrusion of 100–500 μm Pluronic F127 "mesh" or "checkerboard" 2) melt-spinning 10–400 μm Shellac (SSB 55 Astra FL) microfiber "cotton candy" or "fluff," both of which are FDA approved materials. Microfibers were melt-fused with Pluronic F127 macrofibers to complete the circuit. Pre-vascular networks were embedded in type I collagen, sacrificed and intraluminally seeded with 5x10^6 cells/mL human aortic smooth muscle cells (HASMC) followed by 5x10^6 cells/mL HUVEC 24 hours after. Constructs were prepared for 7 day static culture and a subset underwent dynamic culture via gravity driven perfusion. Architecture and cell viability were confirmed via histology and imaging.

RESULTS: Pluronic and Shellac/Pluronic three-dimensional constructs were successfully embedded and sacrificed in type I collagen, leaving behind patent microchannels ranging in size from 10 to 500 μm. Patency was confirmed via perfusion with colored buffer solution, whole rat blood, and gadolinium injection during microMRI. Hematoxylin and eosin staining after 7 days of static culture confirmed patency and the presence of a dense tangle of interconnecting microchannels with adherent cells along the luminal surfaces of both micro and macro channels. Additionally, following dynamic pressure-gradient driven perfusion, cells remained adherent along the luminal surfaces of the macro- and microchannels.

CONCLUSION: We have modified our previously described sacrificial approach for in vivo application and have developed two novel techniques to create dense, three-dimensional microvascular networks within tissue-engineered constructs using Pluronic F127 and Shellac sacrificial microfibers. Both techniques leave micro/macro channels that support adhesion and growth of endothelial cells crucial to providing thrombosis-free flow through the network. These results represent significant progress towards the fabrication of constructs with a hierarchical vascular network analogous to that seen in vivo, a necessity for the production of human-scale engineered tissues.

88
Microvascular Integration into Versatile Tissue Engineering Platforms

Eugenia H Cho, BS[1]; Alina Boico, BS[1]; Natalie A Wisniewski, PhD[2]; Kristen L Helton, PhD[2]; Janna K Register, PhD[3]; Andrew M Fales, BS[3]; Gregory M Palmer, PhD[1]; Tuan Vo-Dinh, PhD[3]; Thies Schroeder, PhD[1]; Bruce Klitzman, PhD[1]

[1]Duke University Medical Center, Durham, NC,
[2]PROFUSA, San Francisco, CA,
[3]Duke University, Durham, NC

PURPOSE: To maximize mass transport into biomaterial scaffolds for regenerative medicine, *in vivo* diagnostics, therapeutics, and cell delivery. We utilized matrix morphology to encourage long-term vascularization.

METHODS: We implanted 1cm-diameter poly-hydroxyethylmethacrylate (polyHEMA) disks with 40 and 80μm nominal interconnected pores into rat subcutis. Solid polyHEMA, silicone, and cotton disks were also implanted. We also investigated a minimally-invasive trocar-assisted delivery of ribbon-shaped porous polyHEMA implants and a suspension of polyHEMA microparticles. Microvessel density was quantified in 50μm-wide zones both into the implants and into the adjacent tissues.

RESULTS: One week after implantation, the microvessel (mv) density closest to the interface was 74±8 mv/mm^2 (mean±SEM) for the 80μm polyHEMA and 28±8 mv/mm^2 for the 40μm polyHEMA. The rate of vascularization was greater in 80μm polyHEMA, with higher vascular density in the material and adjacent tissues one week and one month post-implantation ($p<0.001$). After two months, vascular ingrowth was similar for both 40 and 80μm polyHEMA (maximum = 155±32 mv/mm^2 and 182±43 mv/mm^2, respectively). Solid polyHEMA and silicone exhibited no vascular ingrowth. Notably, despite similar levels of vascularization into both porous materials at two months, the 80μm polyHEMA elicited greater vascularization in the critical 100μm margin of tissue around the implant, compared to other materials. At two months, the microvessel density in the 0–50μm and 50–100μm skin tissue margins was 203±11 mv/mm^2 and 317±19 mv/mm^2, respectively, compared to 101±15 mv/mm^2 and 136±24 mv/mm^2 for the 40 μm polyHEMA; 60±16 mv/mm^2 and 212±45 mv/mm^2 for the solid polyHEMA; and 24±7 mv/mm^2 and 116±43 mv/mm^2 for silicone. All materials (except 80μm polyHEMA) showed a narrow margin of significantly reduced vascularity at the implant-tissue interface, and convergence to normal microvessel density values at further distances away from the interface (control skin = 242 mv/mm^2). Microvessel diameters (99th percentiles) were 16.3μm in 40μm polyHEMA, 14.5μm in 80μm polyHEMA, and 11.8μm in control tissue. Microvessel diameters were similar for the two pore sizes after two months, but were significantly greater than in the sham wound ($p<0.001$). Vascularization into ribbons supported our findings in the disks; more microvessels were detected inside and around porous polyHEMA ribbons than for solid materials at all timepoints. Vascularization into porous polyHEMA microparticles was highly variable. Using real-time ultrasonic microscopy, the microshearing that can disrupt microvessel formation was observed to decrease as tissue integrated into the pores.

CONCLUSION: Rigorous evaluation metrics to assess long-term mass transport capabilities are key to successful tissue engineering platforms since poorly vascularized scaffolds have limited utility. Robust vascularization, particularly at the critical implant-tissue interface, makes open interconnected-pore polyHEMA an excellent morphology for scaffolds in regenerative medicine.

89
Novel Targeting of the Alk-2 Receptor Using the Cre/lox System to Enhance Osseous Regeneration by Mesenchymal Stem Cells

Cameron Brownley, BS; Shailesh Agarwal, MD; Jonathan Peterson, BS; Eboda Oluwatobi, BS; Kavitha Ranganathan, MD; Stewart C Wang, MD, PhD; Yuji Mishina, PhD; Steven R Buchman, MD; Benjamin Levi, MD

University of Michigan, Ann Arbor, MI

PURPOSE: There is a significant need for readily available autogenous tissue to aid in bone regeneration without causing a donor-site defect. Most studies focus on the ability of bone morphogenetic protein ligands (BMP-2 and 7) to stimulate the Bmpr1b receptor (ALK-6). The *ACVR1* gene is often overlooked, but provides instructions for making the activin receptor type I protein (ALK-2), a protein member of the Bmpr1 family. When the ALK-2 receptor is overexpressed globally, patients develop fibrodysplasia ossificans progressive. We believe this highly osteogenic phenotype can be harnessed in adipose derived stem cells (ASCs) to improve bone tissue engineering. Our goal here was to demonstrate that ALK-2 may serve as a novel target to 1) improve in vitro ASC osteogenic differentiation and 2) enhance in vivo bone regeneration and calvarial healing.

METHODS: Transgenic mice were designed using the Cre/lox system to express constitutively active ALK2 (ca-ALK2) after exposure to tamoxifen. Exposure to tamoxifen results in expression of the Cre enzyme, which splices out a floxed nucleotide sequence in the regulatory domain of the ALK-2 receptor, resulting in constitutive activation. ASCs were collected from these mice, seeded and cultured in osteogenic differentiation medium +/- tamoxifen. These wells were assessed for markers of osteogenic differentiation including histologic staining for mineral and bone deposition (alkaline phosphatase and alizarin red) and transcription of pro-osteogenic genes (alkaline phosphatase, osteocalcin, osteopontin, Runx2, and collagen-1). Next, ASCs collected from these transgenic mice were cultured in osteogenic differentiation medium +/- tamoxifen and impregnated into 4mm hydroxyapatite-coated PLGA scaffolds (200,000 cells/scaffold). 4mm-diameter calvarial defects were created in the parietal bone of C57BL/6 mice; the impregnated scaffolds were then implanted into the defect. The defects were monitored by serial micro-CT scans.

RESULTS: We found that ASCs from our transgenic mice with ALK-2 over-expression had 4 times as much early bone signaling (alkaline phosphatase staining) as ASCs with normal ALK-2 expression ($n=4$, $p<0.05$). We similarly found that ALK-2 overexpressing ASCs had 5 times as much bone deposition (Alizarin red stain) compared to control. Transcription of pro-osteogenic genes at day 7 was significantly higher in ASCs from ALK-2 overexpressing mice: Alkaline phosphatase was 50 times higher, osteocalcin 4 times higher, osteopontin 10 times higher, Runx2 3 times higher, and collagen-1 2 times higher than from ASCs not over-expressing ALK-2 ($n=4$, $p<0.05$). Finally, based on in vivo micro-CT imaging and histology, we found that bone growth within the calvarial defect was significantly increased in mice which had received PLGA scaffolds impregnated with ALK-2 over expressing ASCs ($n=4$, $p<0.05$).

CONCLUSIONS: Using a novel transgenic mouse model, we show that constitutive activity of the ALK-2 receptor results in significantly increased osteogenic differentiation of ASCs. Furthermore, we show that this increased differentiation can be harnessed to improve calvarial healing. Future studies to target the ALK-2 receptor to enhance both endogenous and implanted tissues are underway to improve bone tissue engineering.

90
Donor-Recipient Chimeric Cell Transplantation as a Novel Rescue Therapy for Acute Radiation Syndrome: A Preliminary Report

Grzegorz Kwiecien, MD; Joanna Cwykiel, MSc; Maria Madajka, PhD; Adam Bobkiewicz, MD; Safak Uygur, MD; Maria Siemionow, MD, PhD, DSc
Cleveland Clinic, Cleveland, OH

PURPOSE: Victims of nuclear disasters present with acute radiation syndrome as a result of exposure to ionizing radiation. Impairment of immune system with subsequent sepsis is the most common cause of mortality. Following high exposure, stem cell transplantation is the only effective treatment but it carries several risks and access to stem cell sources is insufficient in case of extremely high demands. Therefore there is an urgent need to develop new effective therapies of acute radiation syndrome. The aim of this study was to test efficacy of ex-vivo created donor-recipient chimeric cells (DRCC) in reconstitution of bone marrow compartment following total body γ-irradiation (TBI).

METHODS: Sixteen Lewis ($RT1^l$) rats were exposed to sublethal dose (7Gy) of Cs-137 TBI. Irradiated rats were divided into 4 experimental groups (n=4 each) based on therapeutic approach: Group 1 - no intervention; Group 2 - normal saline injection; Group 3 - allogeneic bone marrow transplantation (BMT) [ACI ($RT1^a$)]; and Group 4 - DRCC transplantation [ACI/LEW ($RT1^a$/$RT1^l$]. Saline as well as cellular therapeutics were delivered into the femoral bone at 6 hours following TBI. DRCC were created by ex-vivo fusion of bone marrow cells derived from fully MHC mismatched LEW ($RT1^l$) and ACI ($RT1^a$) donors. Briefly, donor and recipient cells were isolated, separately stained with the PKH26 and PKH67 fluorescent dyes, fused with polyethylene glycol (PEG) and sorted by flow cytometry. Cells presenting double staining were transplanted in a dose 10–12 x 10^6. All animals received supportive treatment with prophylactic antibiotics, fluids, and softened food during 90-days follow-up. Blood samples were evaluated using hemocytometer at 0, 5, 10, 20, 30, 40, 60 and 90 days after TBI. Reconstitution of CD3, CD4, CD8a, CD45RA, CD90 and CD11b/c positive cell populations was assessed by flow cytometry and donor specific chimerism was detected by PCR.

RESULTS: We have successfully created DRCC by ex-vivo fusion of bone marrow derived cells. Survival rates in groups without cellular therapy (Groups 1–2) was 75%, in Group 3 treated with BMT was 50%, and in Group 4 treated with DRCC was 100%. Clinical signs of graft versus host disease (GVHD) were observed in 50% of animals that received BMT. Hematologic analysis revealed markedly increased peripheral leukocyte counts in DRCC treated animals between day 20^{th} and 60^{th} following transplantation, whereas red blood cell and platelet counts did not differ between groups. Differential counts confirmed regenerative effect of DRCC on both the lymphocyte and polymorphonuclear cell lineages. Evaluation of CD3, CD4, CD8a, CD45RA, CD90 and CD11b/c positive cells by flow cytometry as well as PCR assessment of donor-specific chimerism are currently in progress.

CONCLUSION: Transplantation of DRCC after ionizing radiation exposure proved to be the most effective rescue therapy against acute radiation syndrome, as confirmed by 100% of recipients' survival and expedited recovery of the hematopoietic system without developing GVHD. Our novel approach of DRCC transplantation may act as a bridging therapy supporting hematopoietic recovery and ameliorating injuries in patients exposed to the harmful effects of radiation.

91
Engineering Primary Schwann Cells using Lentiviruses to Control GDNF Expression

Yuewei Wu-Fienberg, BS; Laura Marquardt, BS; Piyaraj Newton, BS; Philip J Johnson, PhD; Susan E Mackinnon, MD; Shelly E Sakiyama-Elbert, PhD; Amy M Moore, MD; Matthew D Wood, PhD
Washington University, St Louis, MO

PURPOSE: Glial cell-line-derived neurotrophic factor (GDNF) is a potent neurotrophic factor known to increase axonal regeneration. Recent studies found that prolonged excess GDNF production from transgenic cells caused sequestering of motor axons at the site of GDNF expression and prevented improved distal nerve regeneration, a phenomenon called the "candy-store effect." In the present study, we attempted to capitalize on the beneficial effects of GDNF delivery and limit the "candy store effect" by engineering transgenic Schwann cells (SCs) in which constitutive GDNF overexpression can be downregulated using a tetracycline-inducible Cre/lox excision mechanism. The purpose of this study was to create transgenic SCs that could provide temporally-controlled, local GDNF delivery to be used in peripheral nerve injuries to enhance axonal regeneration.

METHODS: Lewis rat SCs were transduced with 2 distinct lentiviral vectors: a GDNF FUIV vector in which full-length rat GDNF cDNA is flanked by two loxP sites under the control of an ubiquitin promoter, and a Cre vector based on the pSLIK platform in which Cre recombinase is expressed in a Tet-On fashion. Cells were transduced using our 2 vectors at a multiplicity of infection (MOI) of 20 for each vector. Successful transduction was assessed by visualization of a red fluorescent protein reporter. GDNF expression was quantified by enzyme-linked immunosorbent assay (ELISA) of cell medium samples collected daily and normalized to corresponding daily cell counts. Cre recombinase expression was visualized qualitatively using immunohistochemistry. Biological activity of the GDNF produced by engineered SCs was measured by neurite extension assays.

RESULTS: Engineered SCs allowing temporally-controlled GDNF expression were produced by lentiviral transduction of 2 unique viral vectors. These SCs expressed and secreted significantly more GDNF as compared to untransduced controls, as measured by ELISA. Further, the SCs produced biologically active GDNF as demonstrated by neurons extending neurites. To demonstrate control of GDNF expression, engineered SCs were exposed to doxycycline (a tetracycline analog) to excise the GDNF transgene. The addition of doxycycline to SC culture medium demonstrated a marked increase in Cre recombinase staining as visualized by immunohistochemistry and produced significantly lower levels of GDNF on ELISA in comparison to engineered SCs that were not exposed to doxycycline.

CONCLUSION: We have engineered SCs that constitutively overexpress GDNF, and in which expression can be controlled, i.e."turned off," by exposure to tetracycline-family antibiotics using a tetracycline-inducible Cre/lox excision mechanism.

92
Skeletal Muscle Regeneration in a Rat Model with Extracellular Matrix and Adipose Derived Stem Cells

Tiffany Sarrafian, DVM[1]; Sue Bodine, PhD[1]; Susan Stover, DVM, PhD[1]; Kevin Grayson, DVM, PhD[2]; Hakan Orbay, MD, PhD[1]; David E Sahar, MD[1]; Daren Danielson, MD[2]

[1]University of California, Davis, Davis, CA, [2]Clinical Investigation Facility, David Grant USAF Medical Center, Fairfield, CA

PURPOSE: This study aims to address the important clinical need for repair of volumetric muscle loss by employing an extracellular matrix (ECM; decellularized porcine small intestinal submucosa) in a rat gastrocnemius muscle regeneration model. We hypothesize that ECM, either as a sheet or emulsification, will stimulate a muscle regenerative response in a rat skeletal muscle volumetric loss model, and the combination will provide synergistic benefit. Muscle healing will be further enhanced when the matrix is seeded with rat syngeneic adipose derived stem cells (ASCs).

METHODS: A 7mm full thickness volumetric muscle loss defect was surgically created under anesthesia in the medial head of the rat gastrocnemius muscle, utilizing a specially designed muscle biopsy clamp. Study groups include using a 4-ply sheet of ECM and an emulsified matrix suspension, with or without ASCs seeded onto the matrix to repair the muscle defect. In group I muscle was repaired with ECM only. In group II the ECM was sutured to bridge the muscle gap, with emulsification injected into the gap (0.2 ml). In group III ECM was seeded with ASCs, prior to repair, with a seeding density of 300,000 cells / cm^2. In group IV the defect was repaired with emulsified matrix only. Defects in the control group were left unrepaired. Rats were sacrificed at 3 and 6 months for histologic evaluation and immunohistochemistry to evaluate muscle healing.

RESULTS: The animal model described here was shown to be reproducible and the specially designed muscle biopsy clamp helped to standardize the size of muscle defects. ASCs attached to the ECM scaffolds after 3 days of incubation and were visualized with DiI labeling. ECM sheet and emulsified matrix were successfully implanted to bridge the gap in study animals. No visible wound related complications, gait deficits or pain were observed in animals post-operatively. At 3 and 6 months post-operatively, there was histologic and immunohistochemical (myosin and desmin positivity) evidence of angiogenesis and new striated muscle formation. A minimal degree of inflammation was observed in the regenerated tissue within the ECM tube along with a compensatory increase in soleus muscle mass in response to defect creation.

CONCLUSION: Herein, we present a novel model for evaluation of muscle regeneration. ECM shows promise to regenerate skeletal muscle, opening a therapeutic avenue for patients with devastating traumatic injury and irreparable volumetric muscle loss. We anticipate that future study will reveal more ingrowth and functionality of repaired muscle at later time points.

93
Optimized Repopulation of Extracellular Matrix Hydrogel: Synergistic Effects of Combinations of Growth Factors and Adipoderived Stem Cells

Simon Farnebo, MD, PhD; Maxwell Kim, MSC; Lovisa Farnebo, MD, PhD; Hung Pham, MSC; James Chang, MD
Stanford Medical University, Palo Alto, CA

BACKGROUND: Poor healing of acute and chronic tendon injuries is a common and unsolved problem in plastic and hand surgery. We have previously described how tendon healing can be augmented by the addition of a tendon-derived, extracellular matrix (ECM) hydrogel. In a rat tendon injury model, an accelerated healing with a more mature collagen composition, and improved biomechanical strength was observed. We now hypothesized that reseeding of the gel with adipose-derived stem cells (ASC's) could further assist repopulation of the gel. Also, we aimed at investigating if combinations of growth factors (GF) - basic fibroblast growth factor (bFGF), insulin-like growth factor (IGF)-1, and platelet-derived growth factor (PDGF)-BB would improve the growth survival of these cells.

METHODS: Lyophilized decellularized tendons were milled and enzymatically digested. The resulting ECM solution was then supplemented with or without fetal calf serum (FCS) and varying concentrations of bFGF, IGF-1, and PDGF-BB, both individually and in combinations. The different gel conditions were then seeded with ASC's transfected with a GFP and luciferin construct. After 3 and 5 days in vitro, cell proliferation was determined using the MTT assay and histology. When the optimal condition for cell proliferation was established, gels were supplemented with the selected combination of GF, or no GF and injected into the back of immune competent Wistar rats. Bioluminescence of seeded gels was continuously followed up to 14 days after re-seeding in vivo. Histology and cell counts were performed after the gels were explanted at 14 days. Scanning electron microscopy was used to study difference in ultrastructure. Statistical analysis of biomechanical data was performed using a paired Student's T-test.

RESULTS: There was enhanced proliferation of ASC's in gels supplemented with all individual growth factors in vitro. Among single growth factors, PDGF-BB at 100 ng/ml was the most efficient stimulator of proliferation. With multiple growth factors (combinations), the optimal concentration was determined to be 10 ng/ml bFGF, 100 ng/ml IGF-1, and 100 ng/ml PDGF-BB (increase 2.9-fold; $p < 0.05$). In vivo, bioluminescence showed an improved initial survival of cells in gels supplemented with the optimal concentration of GF compared with the control group (increase -fold at 8 days; $p < 0.05$). After 8 days a decline in cells was seen, and most replanted cells were not detectable by day 14. Cell counts of explants, however, showed a dramatic endogenous re-population of gels supplemented by GF+ASC's compared to both gels with GF but no ASC's (7.6-fold increase) and gels with ASC's but no GF (1.6-fold increase).

CONCLUSION: Synergistic effects of bFGF, IGF-1, and PDGF-BB can be used to improve cellular proliferation and repopulation of ASC's seeded to a tendon ECM gel. Reseeding with ASC's, with or without GF drastically stimulates endogenous repopulation of the gel in vivo and may be used to further augment tendon healing through this system.

94
Decellularized Porcine Stomach Extracellular Matrix for Tissue Engineering and Repair

Lina Wang, PhD; Joshua Johnson, MS; Qixu Zhang, MD, PhD
MD Anderson Cancer Center, Houston, TX

PURPOSE: Repair of large size musculofascial defects, such as ventral hernia, is still a challenge for reconstructive surgery. This study aims to develop a new platform - decellularized porcine smooth muscle-fascia-based matrix (PDSM) system - for musculofasical defect repair and regeneration.

METHODS: Musculafasical layer from porcine stomach, composed of a thin fascia layer, three layers of smooth muscle tissues, and a thin loose connective tissue layer, was processed by decellularization. Resultant PDSM was comprehensively characterized with respect to its biochemical component by immunohistochemistry, three-dimensional (3D) structure by scanning electron microscope, mechanical properties by mechanical test, cytotoxicity by live cell staining, cell-substrate interaction by immunofluorescent staining, and *in vivo* immunoresponse by immunohistochemistry. PDSM and combination of PDSM and multiple cells (i.e. human adipose-derived stem cells [hASCs] and human umbilical vein endothelial cells [HUVECs]) were applied to repair full thickness abdominal wall defect *in vivo*.

RESULTS: PDSM maintained intact 3D structure of extracellular matrix and biochemical components such as collagen, laminin, vascular endothelial growth factor, and sulfated glycosaminoglycan, but lacked major histocompatibility complex antigen 1. PDSM presented strong ultimate tensile strength (UTS) (5.52 ± 0.32 MPa) and elastic modulus (E) (6.76 ± 1.35 MPa), and showed high strain at failure (1.07 ± 0.12). PDSM provides a suitable microenvironment for hASC integration, proliferation, and patterning. In addition, *in vitro* studies showed that PDSM induced HUVECs formed vascular structure formation in the presence of hASCs. *In vivo* animal test demonstrated that PDSM did not cause immunogenic response (a few CD68+, CD4+ and CD8+) in Fischer rats. *In vivo* studies also showed that cell treatment promoted neovascularization within PDSM after implantation. The DPSM underwent tissue remodeling and muscle regeneration, and provided strong mechanical properties to successfully repair full thickness abdominal wall defect up to 3 month (UTS = 6.6 ± 2.1 MPa and E = 21.4 ± 2.3 MPa at the tissue-implant interface, UTS = 29.4 ± 8.4 MPa and E = 90.5 ± 18.1 MPa at the implant).

CONCLUSION: This study may lead to a new promising platform for large size of musculofascial tissue engineering and repair.

SUNDAY, MARCH 9, 2014

SCIENTIFIC SESSION 7 GROUP A
OUTCOMES
8:30 AM – 9:30 AM

SUNDAY, MARCH 9, 2014

95
Results of Primary Repair of Submucous Cleft Palate with Furlow Palatoplasty in Both Syndromic and Non-Syndromic Children

Zhi Yang Ng, MBChB; Selena Young, PhD; Yong Chen Por, FAMS (Plast Surg); Vincent Yeow, FAMS (Plast Surg)

Cleft and Craniofacial Centre, KK Women's and Children's Hospital, Singapore, Singapore

PURPOSE: Submucous cleft palate (SMCP) is an often-missed diagnosis until the child has developed abnormal speech. This often results as a consequence of aberrant anatomy, leading to velopharyngeal insufficiency and/or articulation errors. While the latter can usually be corrected with speech therapy, much controversy persists with regard to the optimal technique for surgical repair in the former. Moreover, when SMCP occurs as part of a syndrome, surgery has yielded mixed results. This study therefore aims to investigate outcomes of primary SMCP repair with Furlow palatoplasty in both syndromic and non-syndromic children.

METHODS: Records of patients with SMCP who underwent primary repair with Furlow palatoplasty by the two senior authors (YCP, VY) at our institution between 2004 and 2012 were reviewed. Data for age at surgery, follow-up duration, presence of concomitant hearing loss, diagnosis of syndrome type, pre- and post-operative nasopharyngoscopy, perceptual and nasometry assessments, and secondary surgery rates were collected and analyzed using standard statistical methods; patients who were less than 4 years old at the time of surgery and with less than 6 months' follow-up were excluded.

RESULTS: Of 46 patients identified, 34 (15 males, 44%) satisfied our inclusion criteria. Patient demographics include: mean age at surgery = 7.7 years (range 4.5–14), syndromic patients = 50% (velocardiofacial syndrome, n = 13), associated hearing loss = 11 patients (32%), and a mean follow-up period of 48 months (range 9–80). All patients underwent primary Furlow palatoplasty and there were no post-operative complications such as wound dehiscence or fistula; two patients (one syndromic, one non-syndromic) however required secondary procedures (revision Furlow palatoplasty ± pharyngeal flap). Post-operative nasopharyngoscopy revealed an increase in the number of patients with a coronal velopharyngeal closing pattern and greater velar closing ratios for all patients ($p<0.05$). Velar closing ratios on nasopharyngoscopy also approached normal at an average of 1.3 years (range 1–4) after surgery for all patients but nasometry values did not improve significantly for syndromic patients.

CONCLUSION: At our institution, Furlow palatoplasty is the technique of choice for primary SMCP repair, regardless of velar closing ratios or the presence of associated syndromes. Pre- and post-operative speech therapy has a vital role to play in both the initial assessment and rehabilitation of patients who have undergone surgery for SMCP. Further studies with greater patient numbers are necessary to achieve population statistical significance. As well, future research to elucidate the optimal timing of primary SMCP repair is warranted in both syndromic and non-syndromic patients.

96
The Venous Anastomotic Flow-Coupler for Free Flap Monitoring: A Prospective Analysis of 85 Microsurgical Breast Reconstruction Cases

Steve J Kempton, MD; Jenny Chen, MD; Samuel Poore, MD; Ahmed Afifi, MD
University of Wisconsin-Madison Division of Plastic Surgery, Madison, WI

PURPOSE: The venous anastomotic flow-coupler has recently been developed for clinical use, contributing to a multitude of flap monitoring devices and techniques. To date, only one published small retrospective series (19 patients) reported this device to be both reliable and accurate for use in head and neck reconstruction; however, no data exists in the setting of abdominal based free flaps for breast reconstruction. The authors present a prospective analysis of the venous anastomotic flow coupler in 85 microsurgical breast reconstruction cases.

METHODS: Prospective data was collected on patients undergoing post-mastectomy free flap breast reconstruction from May 2012 to May 2013. Data obtained included patient age, BMI, flap type (DIEP, MS TRAM, SIEA), flow-coupler size, incidence of intraoperative and postoperative signal loss, anastomotic problems, coupler problems, flap take back, and flap failure. Proportion data was compiled and analyzed.

RESULTS: Eighty-five consecutive abdominal based free flaps for breast reconstruction were performed from May 2012 to May 2013 by two co-surgeons at the University of Wisconsin Hospital. The average patient age was 49.3 years and average BMI was 28.4. There were 53 MS-TRAM, 31 DIEP, and 1 SIEA flaps performed. The venous anastomotic flow coupler (FC) was used in all cases. The overall flap failure rate was 4.7% and flap take back rate was 7.1%. The flow-coupler was analyzed in both intraoperative and postoperative settings. Flap type and flow-coupler size were not found to be associated with flow-coupler problems. The intraoperative and postoperative sensitivity of the flow-coupler was found to be 100% (signal presence correlated well with flap viability). However, intraoperatively, the flow-coupler had a false positive rate of 75% and a positive predictive value of 0.25. Postoperatively, the flow-coupler had a 36% false positive rate and a positive predictive value of 0.64.

CONCLUSIONS: If the flow-coupler Doppler signal is audible, it becomes extremely fast, reliable, and efficient to confirm patency of a microsurgical anastomosis. However, there is a high false positive rate in both the intraoperative and postoperative setting. This led to a high incidence of intraoperative maneuvers to diagnose and amend the cause of signal loss. In 13% of cases, the flow-coupler Doppler signal was completely ignored and flaps were monitored more traditionally with external doppler or clinical exam.

97
Timing and Technical Implications of Breast Reconstruction in Anemic Women: The Advantages of Staged (Delayed-Immediate) Breast Reconstruction

Pablo A Baltodano, MD[1]; José M Flores, MPH[2]; Nicholas B Abt, BS[1]; Karim A Sarhane, MD, MSc[1]; Francis M Abreu, BS[2]; Karen K Burce, MHS[1]; Carisa M Cooney, MPH[1]; Damon S Cooney, MD, PhD[1]; Justin M Sacks, MD[1]; Gedge D Rosson, MD[1]
[1]Johns Hopkins University School of Medicine, Baltimore, MD, [2]Johns Hopkins Bloomberg School of Public Health, Baltimore, MD

PURPOSE: Anemia, a common finding in breast cancer patients, is independently associated with adverse outcomes after breast reconstruction. If treating anemia before surgery is not possible due to urgency of breast cancer treatment, anemic women undergoing mastectomy should be offered the reconstruction strategy associated with the lowest morbidity. In the present study, we sought to determine the safest reconstructive approach to anemic women undergoing mastectomy.

METHODS: We analyzed women undergoing mastectomy with or without reconstruction from 2005–2011 using the American College of Surgeons National Surgical Quality Improvement Program (ACS-NSQIP) databases. All anemic females (hematocrit <36%, WHO definition) were identified and multivariable logistic regression was used to compare 30-day postoperative morbidity between patients undergoing mastectomy-only vs. immediate breast reconstruction. Subgroup analysis compared morbidity within the immediate breast reconstruction groups: tissue expanders (TE), implants, and flaps. Morbidity events included: wound, prosthesis/flap failure, cardiac, respiratory, neurological, urinary, and venous thromboembolism complications.

RESULTS: 77,902 women underwent mastectomy with or without immediate reconstruction: 11,770 (15.1%) anemic, 52,943 (68.0%) non-anemic women, while 13,189 (16.9%) had missing hematocrit data. Among anemic women, mastectomy-only had lower morbidity (11.13%) than immediate breast reconstruction (13.25%, p=0.015). Subgroup analysis of anemic women undergoing immediate reconstruction revealed that TE had significantly lower morbidity (9.83%) than both, implant (13.10%, p=0.019) or flap reconstructions (24.63%, p=0.001).

CONCLUSION: For anemic women undergoing immediate reconstruction, staged (delayed-immediate) reconstruction (using TE) carries lower morbidity than implant or flap-based reconstructions. Future studies should investigate the effect of treating preoperative anemia on reconstruction morbidity profiles

98
Nipple-Sparing Mastectomy in Patients with Previous Breast Surgery: Comparative Analysis of 123 Immediate Reconstructions

Alex Lin, BS; Eric Liao, MD; Jonathan Winograd, MD; Curtis Cetrulo, MD; Rong Tang, MD; Barbara L Smith MD, PhD; William G Austen, Jr., MD; Amy S Colwell, MD
MGH, Boston, MA

PURPOSE: An increasing number of women are candidates for nipple preservation with mastectomy. It is unclear how previous breast surgery impacts the ability to perform nipple-sparing mastectomy (NSM) and reconstruction.

METHODS: Single institution retrospective review was performed between June 2007-December 2012.

RESULTS: 104 patients with prior breast surgery (PBS) underwent 123 NSM with immediate reconstruction. The PBS included 105 lumpectomies, 14 breast augmentations, and 4 breast reductions. A group of 222 patients and 462 NSM reconstructions without prior breast surgery (no PBS) served as the control group. The group with PBS were older (49.6yrs vs. 45.4yrs, $p<0.001$) but had similar BMI and smoking status. PBS reconstructions were more often unilateral, therapeutic, and associated with preoperative radiotherapy ($p<0.001$ for each). There were similar percentages of single-stage vs. two-stage reconstruction between the groups. The most frequent incision for PBS was use or extension of a pre-existing scar while the most frequent incision for no PBS was the infero-lateral IMF incision ($p<0.001$). There was no significant difference in total complications or individual complications of skin necrosis, nipple necrosis, or implant loss in the group with PBS compared to no PBS ($p>0.2$ for each). There was a trend toward increased risk of infection in the PBS reconstructions (5.69% vs. 2.38%, $p=0.059$). When stratifying by type of prior breast surgery, the lumpectomy group had a higher number of patients with preoperative radiotherapy (31 vs. 11, $p<0.05$) and therapeutic mastectomy (76.2% vs. 40.7%, $p<0.05$). The breast augmentation patients had a higher number of single-stage reconstructions (92.9% vs. 61.5%, $p<0.05$) but also an increased risk of total complications (35.7% vs. 13.6%, $p<0.05$) and a trend toward increased mastectomy skin flap necrosis (14.3% vs. 3.90% $p=0.112$). There was a trend toward infection and implant loss (25.0% vs. 2.16% $p=0.091$) in patients with breast reduction.

CONCLUSIONS: NSM and immediate reconstruction can be performed in patients with prior breast surgery with no significant increase in nipple loss. Larger series are warranted to determine if breast augmentation or breast reduction patients have higher rates of complications following mastectomy compared to patients without prior breast surgery.

99
Reducing Unplanned Reoperations for Mastectomy Skin Flap Necrosis - A Multidisciplinary Approach

Valerie Lemaine, MD, MPH; Tanya L Hoskin, MS; Judy C Boughey, MD; David R Farley, MD; Clive S Grant, MD; Steven R Jacobson, MD; James W Jakub, MD; Tiffany T Torstenson, DO; Ryan D Reusche, MD; Amy C Degnim, MD
Mayo Clinic, Rochester, MN

PURPOSE: Necrosis of breast skin and/or nipple areolar complex (NAC) following skin-sparing mastectomy (SSM) or nipple-sparing mastectomy (NSM) and immediate breast reconstruction (IBR) can result in delayed adjuvant therapy, prosthetic infection and reconstruction failure. A multidisciplinary quality improvement (QI) project was undertaken using the DMAIC (Define, Measure, Analyze, Improve, Control) framework in an attempt to reduce mastectomy skin flap necrosis. This study's goal was to assess the impact of the QI initiative in improving surgical outcomes, specifically by reducing unplanned reoperations for mastectomy skin flap necrosis in mastectomy patients undergoing IBR.

METHODS: Consecutive cases of SSM or NSM followed by IBR were reviewed retrospectively for mastectomy skin flap necrosis and unplanned reoperation for necrosis. Plastic and breast surgeons reviewed medical records and postoperative photographs for details of mastectomy skin flap necrosis and its management. Reoperations specifically performed for management of mastectomy skin flap necrosis were recorded. Reoperation rates were compared for time periods BEFORE initiating the QI project (Nov 2009-Oct 2010) and AFTER (Nov 2010-Dec 2011).

RESULTS: 344 patients underwent 594 breast procedures (397 SSM and 197 NSM). Of these, 296 procedures were performed BEFORE the QI project was initiated (201 SSM and 95 NSM). AFTER the QI project began, 298 procedures were performed (196 SSM and 102 NSM). Overall, reoperation rates decreased significantly from the BEFORE group (22/296 = 7.43%) to the AFTER group (10/298=3.36%, $p=0.026$). The rate of reoperation of SSM cases decreased in the BEFORE vs AFTER group, but this was not statistically significant (4.98% vs 3.06%, respectively; $p=0.330$). For NSM cases, reoperations decreased significantly from the BEFORE group (12/95=12.63%) vs AFTER group (4/102=3.92%, $p=0.023$).

CONCLUSIONS: This multidisciplinary QI initiative to improve outcomes after SSM and NSM with IBR resulted in substantial reductions in unplanned reoperations for mastectomy skin flap and/or NAC necrosis in NSM. Further work is ongoing to identify factors that contributed to the reduction.

100
Comparison of the Histological Characteristics of ADM Capsules to No-ADM Breast Capsules in ADM-Assisted Breast Reconstruction

Deborah Yu, MD; Kasandra Hanna, MD; Robin LeGallo, MD; David Drake, MD
University of Virginia, Charlottesville, VA

INTRODUCTION: Acellular dermal matrices (ADM) have been proposed to have several advantages in implant-based breast reconstruction over traditional techniques. The goal of this study was to compare histological characteristics between areas of the capsule containing a novel decellularized regenerative matrix and areas without the ADM in ADM-assisted breast reconstruction.

METHODS: Women undergoing implant-based breast reconstruction at the University of Virginia Health System using a Matracell™ decellularized regenerative matrix were enrolled in this IRB-approved study. Forty-eight non-ADM and ADM breast capsule biopsy specimens were collected from fifteen women and analyzed for several histological parameters: inflammation, vascular proliferation, capsule fibrosis, foreign body giant cell inflammatory reaction, and myofibroblasts. A semi-quantitative scoring system was used for evaluation. The presence or absence of an inflammatory capsule and of suture granulomas were also assessed. The evaluator of the specimens was blinded to the tissue source.

RESULTS: There was significantly less inflammation in the ADM capsule biopsy samples compared with the no-ADM capsule biopsy samples (ADM: 0.83±0.70; no-ADM 1.83±0.82; $p<0.001$). There was significantly less fibrosis in the ADM samples (ADM: 0.92±0.58; no-ADM: 1.29±0.62; $p=0.037$). There was a significantly higher likelihood of presence of an inflammatory capsule in the no-ADM biopsy samples ($p=0.005$). There were significantly less myofibroblasts in the ADM group (ADM: 0.79±0.66; no-ADM: 1.46±0.51; $p<0.001$). There was significantly less vascular proliferation in the ADM samples compared with the no-ADM samples (ADM: 0.75±0.61; no-ADM: 1.42±0.58; $p<0.001$). There were no significant differences in the amount of giant cell reaction (ADM: 0.50±0.83; no -ADM: 1.00±1.10; $p=0.083$) or the presence of suture granuloma ($p=0.128$).

CONCLUSION: When used for staged breast reconstruction, this novel decellularized regenerative matrix processed using Matracell™ technology appears to induce less inflammation and less myofibroblasts. These results may explain the observed decreased capsular contracture in ADM-assisted breast reconstruction.

SUNDAY, MARCH 9, 2014

SCIENTIFIC SESSION 7 GROUP B
CTA
8:30 AM – 9:30 AM

SUNDAY, MARCH 9, 2014

101
Intrathymic in Vivo Two-photon Microscopy Reveals the Interaction of Donor Bone Marrow-Derived Dendritic Cells and Host Thymocytes in a Model Of VCA Central Tolerance

Wensheng Zhang, MD, PhD; Yang Yang, MD, PhD; Yang Li, MD, PhD; Kia M Washington, MD; Vijay S Gorantla, MD; Xin Xiao Zheng, MD; Mario G Solari, MD
University of Pittsburgh, Pittsburgh, PA

PURPOSE: We have demonstrated that vascularized composite allografts (VCA) containing viable vascularized bone morrow offer the inherent potential for establishment of stable mixed chimerism (MC) and robust tolerance. Studies also showed that dendritic cells (DC) contribute critically to central tolerance-induction by elimination of developing thymocytes. In this study, we track donor bone marrow-derived DCs (BM-DCs) in a mouse VCA model, and visualized their dynamic communication with the recipient thymocytes in the chimeric thymus environment related to VCA tolerance induction.

METHODS: Syngeneic or allogeneic hind-limb transplantation was performed from B6.CD11c-YFP or BALB/c.CD11c-DTR/GFP transgenic donor mice, whose DCs expresses enhanced fluorescent protein, to wild-type B6 recipient mice. MHC-mismatched recipients were treated with the combined immunosuppressive regimen of rapamycin, CTLA4/Fc and anti-CD40L mAb. In a control group, diphtheria toxin (DT) was administered after transplantation for deletion of DCs from BALB/c.CD11c-DTR/GFP donors. 90 days after transplantation, the long-term surviving chimeric B6 recipients were sacrificed as donors, and B6 nude mice served as recipients of the secondary thymus transplantation. Nude mice were gamma-irradiated and reconstituted with BM from B6.DsRed.MST transgenic mice 3 weeks before thymus transplantation under the renal capsule. After thymus acceptance, the kidney containing the transplanted thymus was exposed for in vivo imaging by two-photon microscopy. The MC and DCs profiles were also studied by flow cytometry and immunofluorescence analysis.

RESULTS: 1) Long-term survival of hind-limb allografts was achieved in the BALB/c to B6 strain combination under comstimulation blockade plus rapamycin treatment. 2) Donor derived DCs were detected in peripheral blood of the recipient from 2 weeks post limb transplantation and over a sustained period of time. 3) Donor BM-DCs presented in the thymus of VCA recipients for an extended period as determined by flow cytometry and immunofluorescence analysis. 4) The functional interaction between donor BM-DCs and the new developing thymocytes were visualized in vivo in the transplanted chimeric thymus from living mice that lack an endogenous thymus.

CONCLUSION: Donor BM-DCs migrate to the host thymus and are implicated in the clonal deletion process by presenting donor-derived antigens. This intravital imaging study provides further insights into the activities of DCs in VCA tolerance induction.

102
Inflammatory Mediators Modulate Alloreactive T Cell Susceptibility to Immune-Regulation in Reconstructive Transplantation

Saami Khalifian, BA[1]; Yawah Nicholson, BS[2]; Cordelia Ziraldo, PhD[2]; Ravi Starzl, PhD[3]; Stefan Schneeberger, MD[1]; Angus Thomson, PhD, DSc[2]; Gerald Brandacher, MD[1]; Yoram Vodovotz, PhD[2]; Giorgio Raimondi, PhD[1]

[1]Johns Hopkins University School of Medicine, Dept of Plastic & Reconstructive Surgery, Baltimore, MD, [2]University of Pittsburgh Medical Center, Starzl Transplantation Institute, Pittsburgh, PA, [3]Language Technologies Institute, Carnegie Mellon University, Pittsburgh, PA

PURPOSE: Tolerance induction to allografts in reconstructive transplantation remains an elusive goal, partly due to limitations in understanding the interplay between inflammatory mediators and activation/regulation of T lymphocytes. We believe specific inflammatory mediators contribute to the activation of alloreactive T cells via previously unappreciated mechanisms: i), direct costimulation, ii) simultaneous reduction of Treg suppressive activity, thereby limiting the effectiveness of tolerogenic regimens. We aimed to identify these inflammatory mediators that diminish T cell regulation and identify strategies to blunt their effect.

METHODS: In vitro assessment of inflammatory mediators and Treg activity on T cell activation and proliferation was determined via CFSE-suppression assay. The expression of 22 cytokines in the supernatant of maturing dendritic cells was quantified using Luminex. Bioinformatics analysis was used to determine which cytokines most significantly contributed to modulation of Treg suppression, and resultant cytokines were then tested in the CFSE-suppression assay. The immunomodulatory activity of specific cytokines in vivo was tested in a mouse model of inflammatory bowel disease (outcome measure=weight loss). Specifically, Rag-knockout mice were adoptively transferred with T cells (+/- Tregs), followed by injections of anti-IL-6R mAb or IL-1R antagonist (IL-1RA). To further dissect the role of IL-1 family members (e.g. IL-18), the experiment was repeated with T and Treg from MyD88 knockout mice. Production/accumulation of inflammatory cytokines in various tissues was also investigated after orthotopic hindlimb transplantation (OHTx) using Luminex at various timepoints.

RESULTS: Bioinformatics identified IL-6 and IL-1α/β as potential modulators of Tcell/Treg activity. In vitro analysis confirmed that all three cytokines directly promoted T cell proliferation; however, IL-1α/β also directly inhibited Treg suppressive activity. In vivo analysis in Rag-/- mice confirmed that blockade of IL-6R after adoptive transfer of Tcells/Treg resulted in significantly delayed weight loss in this model (not observed without Treg injection), suggesting that blockade of IL-6 signaling sufficiently slowed activation of T cells permitting Treg to effectively control disease development. Unexpectedly, blockade of IL-1R did not delay disease progression, likely due to redundant function of IL-1 with IL-18. Therefore, the experiment was repeated using T and Treg from MyD88-/- mice (IL-1 and IL-18 use MyD88 for intracellular signaling) and only when MyD88 was absent from both injected populations (Tcells and Tregs) was there a significant delay in weight loss, corroborating our in vitro observations that IL-1α/β (and now IL-18) have a counter-regulatory effect on Tregs/Tcells. IL-6, IL-1α/β, and IL-18 were all confirmed to accumulate in various tissues after OHTx--further evidence of their role in the rejection response.

CONCLUSION: Specific inflammatory cytokines promote activation of alloreactive T cells and reduce T cell susceptibility to suppression. We have identified the synergistic activities of IL-6, IL-1α/β, and IL-18, which must be taken into consideration when designing novel therapeutic modalities. Furthermore, our VCA model provides clear evidence that these cytokines play an important role in promoting rejection. Targeting these inflammatory mediators should translate into improved immunological outcomes post-VCA, and elucidation of the intracellular mechanisms used by these cytokines to prevent T cell suppression will aid in identifying targets that promote immuneregulation.

103
Primed Mesenchymal Stem Cells Prevent Endothelial Activation and Improve Allograft Perfusion Following Transplantation

Jessica B Chang, BS; Marc A Soares, MD; Jonathan P Massie, BS; April Duckworth, MD; Nakul Rao, MD; Camille Kim, BS; Karan Mehta, BS; Amanda Hua, BS; Piul Rabbani, PhD; Pierre B Saadeh, MD; Daniel J Ceradini, MD

NYU Department of Plastic Surgery, New York, NY

PURPOSE: Endothelial activation following ischemia-reperfusion injury (IRI) in transplantation triggers the inflammatory cascade, compromising allograft perfusion. Additionally, IRI is a critical factor that contributes to the incidence and severity of both acute and chronic rejection. We have previously demonstrated that mesenchymal stem cells (MSCs) can be seeded into allografts ex vivo where they take up residence in the perivascular space. While conventional expansion of MSCs produces an innate immunomodulatory phenotype, conditions that enhance this phenotype may be utilized to attenuate endothelial failure following ischemic insult during transplantation. We hypothesized that expansion under hypoxic conditions or with inflammatory cytokines primes the immunosuppressive functions of MSCs and improves allograft perfusion subsequent to ex vivo delivery.

METHODS: MSCs were expanded during exposure to hypoxia (5% O2) or inflammatory cytokines IFNγ and/or TNFα prior to assessment of the immunomodulator indoleamine 2,3-dioxygenase (IDO) expression. MSC-only, endothelial cell (EC)-only, and MSC-EC co-cultures were exposed to IRI and analyzed for changes in expression of pro-inflammatory (MCP-1), anti-inflammatory (IDO), and permeability (Cadherin 5) markers by quantitative real-time RT-PCR. Results were normalized to 18s rRNA expression and expressed as arbitrary units (a.u.). Leukocyte-endothelium adhesion and endothelial permeability assays were also performed to determine functional modulation of MSCs on endothelial activation. In an ex vivo allogeneic transplant model, donor Brown-Norway rat allografts were seeded with recipient Lewis rat MSCs prior to transplantation into Lewis rats. Postoperative perfusion was then assessed via clinical inspection and Doppler imaging.

RESULTS: Hypoxic conditions significantly increased expression of IDO (2.81E+04 a.u.) by MSCs compared to normoxia (1.24E-03 a.u., $p < 0.01$). Co-culture with ECs further increased IDO expression (8.59E+04 a.u., $p < 0.01$). Exposure to inflammatory cytokines IFNγ and TNFα also markedly increased IDO expression (2.77E-02 and 5.38E-03 a.u. compared to 1.24E-03 a.u. untreated, or 4.33- and 22.3-fold change, respectively). Co-cultured MSC-ECs demonstrated a 49.8% reduction in endothelial MCP-1 (1.23 vs. 2.45 a.u.) and 230% increase in Cadherin 5 expression compared to ECs alone ($p < 0.05$) following IR injury. Enhanced immunomodulation was functionally demonstrated in diminished leukocyte adhesion to ECs (49%, $p < 0.01$) and mitigated IRI-related permeability through an endothelial barrier. MSCs perfused in the ex vivo period were identified in the perivascular space throughout the allograft and improved postoperative perfusion (normalized perfusion index of 83±12 compared to 42±8 in controls; $p < 0.01$) consequent to increased eNOS expression (3.66 vs. 1.48 a.u. in controls, $p < 0.01$) and vasodilation.

CONCLUSION: Here we demonstrate that ex vivo MSC therapy can attenuate IRI in a composite tissue transplant model. MSCs primed with a hypoxic environment and/or exposure to inflammatory cytokines exhibit enriched immunoregulatory and vasoprotective functions that mitigate activation of the endothelial barrier, which significantly improves post-operative allograft perfusion. This strategy is clinically feasible and may reduce IRI in composite tissue allotransplantation.

104

Mhc Class I Sharing Influences the Fate of the Epidermal Component of Vascularized Composite Allografts in Mixed Chimerism Based Tolerance Protocols in Miniature Swine.

Kumaran Shanmugarajah, MCRS; Christopher Mallard, Bachelor of Science; David A Leonard, MRCS; Alex Albritton, Bachelor of Science; Harrison Powell, Bachelor of Science; Edward Harrington, Bachelor of Science; Mark A Randolph, Master of Science; David H Sachs, MD; Josef M Kurtz, PhD; Curtis L Cetrulo, Jr, MD

Massachusetts General Hospital, Charlestown, MA

PURPOSE: While skin remains one of the most difficult tissues for induction of transplant tolerance, the precise mechanisms that govern skin tolerance/rejection remain poorly understood. Skin-containing vascularized composite allograft (VCA) transplants, including face, hand, lower extremity and abdominal wall transplants, have emerged as a treatment option in patients with severe tissue loss. The induction of robust VCA transplant tolerance, including tolerance of the skin component, would obviate the need for chronic immunosuppression and allow broader application of this reconstructive modality. Disparate results with regards to skin tolerance have been observed in two related large animal experiments in our laboratory using MGH miniature swine. Long-term tolerance to VCAs (>600 days), including the skin component, has been achieved across a single haplotype MHC-mismatch barrier using a mixed chimerism-based protocol. However, when a similar protocol was used across a full MHC-mismatched combination, the outcome was tolerance to all components of VCAs except the skin epidermis. This result suggested that sharing of MHC at class I and/or class II may be required for stable skin tolerance in a mixed chimerism model.

METHODS: Using a non-myeloablative protocol (CD3 T-cell depletion, 100 cGy total body irradiation and 45 days of cyclosporine) with hematopoietic stem cell transplantation (HSCT), mixed chimeras were generated across either a MHC Class I (n=2) or a MHC Class II mismatch (n=2). VCAs consisting of primarily vascularized fasciocutaneous flaps were transplanted at the time of HSCT. VCA outcomes were monitored by clinical inspection and histology and peripheral blood chimerism was assessed in multiple cell lineages using flow cytometry. In vitro immune responsiveness was assessed using mixed lymphocyte reaction (MLR) and cell-mediated lymphocytotoxicity (CML) assays.

RESULTS: Regardless of the MHC mismatching, all animals displayed high-level chimerism at all time points in lymphoid (50–70%), myeloid (40–80%) and granulocyte (40–80%) lineages. MHC Class II-mismatched chimeras remained tolerant of VCAs, without significant histological or clinical features of rejection at any time-point. In contrast, both MHC Class I-mismatched animals experienced acute rejection crises of the epidermal component of the VCAs following tapering of immunosuppression, with one of these animals mounting recurrent rejection episodes. Histological visualization confirmed that rejection was confined to skin epidermis. In vitro assays in all animals demonstrated donor-specific non-responsiveness at all points, including after rejection crises, suggesting that the epidermal rejection in the MHC class I-mismatched animals was a local effect.

CONCLUSIONS: The identification of MHC Class I sharing as a determinant of skin tolerance may have important immunological as well as clinical implications. These data suggest that local regulation of immune tolerance is critical in long-term acceptance of all components of the VCA, and that sharing of MHC class I may be necessary for establishing and maintaining tolerance of epidermal tissue. In the clinic, MHC matching of recipient and donor has not been taken into consideration in VCA transplants under cover of conventional immunosuppression. But with the goal of developing tolerance-inducing approaches in the future, these results suggest that sharing of class I antigens could have a beneficial effect in mixed-chimerism-based clinical tolerance protocols.

105
A Non-Suture Cuff Technique for Lymph-Vein Anastomosis in a Rat Model

Dedi Tong, MD[1]; Shan Zhu, MD[1]; Yong Huang, PhD[2]; Lehao Wu, MD[1]; Zuhaib Ibrahim, MD[1]; Qi Mao, MD[1]; Jin Li, MD[1]; Damon S Cooney, MD[1]; W P Andrew Lee, MD[1]; Gerald Brandacher, MD[1]

[1]Johns Hopkins University School of Medicine, Baltimore, MD, [2]Department of Electrical and Computer Engineering, Johns Hopkins University, Baltimore, MD, Baltimore, MD

PURPOSE: Lymph-vein anastomosis has been an effective way to treat lymphedema. However, the extremely thin and fragile wall of both the lymphatic vessels and vein impose great technical microsurgical challenges. In this pilot project we explored a novel cuff-based non-suture technique for lymph-vein anastomosis in a rat model, aiming to improve the success rate and reduce operation time.

METHOD: A total of 15 Lewis rats (age: 6–8 weeks, body weight: 252.8±3.78g) underwent lymph-vein anastomosis. The left cervical branch of the lymphatic duct that commence into the thoracic duct and the facial vein were freed and dissected. Lymph-vein anastomosis was performed in an end-to-end fashion using a polyimide tube (0.368361mm as inner diameter, 0.41148mm as outer diameter), which was prepared into a wedge-like cuff. After the cuff was mounted on the lymph duct, the duct was then inverted and held in place with a circular tie. Next the facial vein was pulled over the lymph stent and anastomosis was completed with a second nylon tie over the cuff. All anastomoses were evaluated by histology on post-op day 7.

RESULTS: Total operating time averaged about 2.3±0.28 hours. Lymph-vein anastomosis could be completed within 16.8±4.3 minutes. All 15 procedures in this series were successful. Histology on post-operative day 7 showed patent anastomosis in all cases with both vein and lymph endothelia smooth and intact, no evidence of thrombus formation.

CONCLUSION: This novel non-suture cuff based technique is a safe, efficient and reliable method for lymph-vein anastomosis, which might offer a promising approach that could be utilized in clinical lymphedema surgery.

106
Development of a Chimeric Free Flap Allograft Using the LGR6+ Epithelial Stem Cell

Denver M Lough, MD, PhD[1]; Damon Cooney, MD, PhD[2]; Shaun Mendenhall, MD[3]; Joel Reichensperger, BS[3]; Lisa Cox, BS[3]; Nicole Cosenza, MS[3]; Nathan Wetter, MD[3]; Carrie Harrison, BS[3]; Michael Neumeister, MD[3]

[1]SIU School of Medicine/Johns Hopkins, Springfield, IL, [2]Johns Hopkins, Baltimore, MD, [3]SIU School of Medicine, Springfield, IL

PURPOSE: Reconstructive Transplantation (RT) and Reconstructive Microsurgery have seen enormous growth over the last decade with regards to both surgical technique and post operative monitoring and therapy. Understanding the nature of the chronic cellular rejection cascade seen in RT, in that it primarily initiates with the epithelium, we seek to apply our knowledge of the LGR epithelial stem cell (ESC) system, an epithelial stem cell capable of developing the skin, hair shaft and sweat gland, in developing the first chimeric free flap allograft. From this LGR recipient seeded chimeric allograft free flap, we intend to determine if the slow repopulation of the recipient epithelium from its own autologous stem cell niche, while in the presence of donor tissues, can lead to more successful transplantation as well as enhanced tolerance and freedom from rejection.

METHODS: Using populations of age matched Sprague Dawley and Lewis rat species within a DIEP based abdominal wall transplant model, we transplanted a donor partially de-epithelialized (reticular dermis) composite tissue allograft containing abdominal wall to a recipient abdominal wall defect. Following inset of the flap, a recipient-derived LGR GFP+ ESC seeded acellular matrix was grafted onto the flap's exposed dermis and bolstered in place. Recipients received either LGR6+ ESC graft, standard skin grafts and either rapamycin-based mono-therapy or normal saline as control. Specimens were examined for histological signs of rejection using published protocols as well as additional assays utilizing: immunofluorescent up-regulation of apoptosis, tunnel assay augmentation and recipient T-cell infiltrate. Additionally high-throughput gene arrays examining mTOR, cytokine, adhesion molecules, WNT, NFKB and NOTCH pathways were utilized to determine alterations in key markers ie: IL-12 IFN-γ, IL-4, and IL-10, IL-1, IL-4, and TNF-α etc.

RESULTS: Recipients receiving the LGR6+ ESC seeded graft when compared to skin graft controls had significantly lower levels of inflammatory markers and augmented levels of freedom from rejection. Additionally, LGR6+ ESC chimeric flaps were able to develop nascent hair follicles, which the skin controls were not capable of producing.

CONCLUSION: We hope that these preliminary findings can provide initial insight to the potential therapeutic benefit for the development of chimeric free flap allografts via the utilization of the LGR6+ ESC for tolerance induction, graft survival and hair growth. From this basic data it appears that epithelial chimerism appears to down-regulate the induction of chronic rejection.

SUNDAY, MARCH 9, 2014

SCIENTIFIC SESSION 7 GROUP C
MICROSURGERY
8:30 AM – 9:30 AM

SUNDAY, MARCH 9, 2014

107
Deferoxamine Mitigates Radiation-Induced Hypovascularity and Improves Tissue Elasticity in a Rat Irradiated TRAM Flap Model

Alexander F Mericli, MD; Anusuya Das, PhD; Ryan Best, PhD; Pamela Rodeheaver, BS; George Rodeheaver, PhD; Kant Y Lin, MD
University of Virginia, Charlottesville, VA

PURPOSE: The beneficial effects of radiation therapy for the treatment of breast cancer are indisputable, however irradiation also results in permanent damage to the microvasculature, leading to dermal damage and inelastic tissue. Clinically, therapeutic radiation after autologous breast reconstruction is associated with an elevated complication rate and distortion of the soft tissue. Deferoxamine (DFX) is an FDA-approved iron-chelating medication that has also been shown to increase angiogenesis. We hypothesize that the application of DFX will result in increased vascularity and improved tissue elasticity in a rat irradiated TRAM flap model.

METHODS: Fifteen Sprague-Dawley rats were randomized to three groups: control, XRT, and XRT+DFX. All rats underwent a right pedicled TRAM flap. After recovering from surgery, the flaps in the XRT and XRT+DFX groups were radiated with 35 Gy in a single dose. Four weeks after radiation, rats in the XRT+DFX group were treated with DFX injected subcutaneously into the flap every other day for ten days. Rats were euthanized and perfused; flaps were imaged with micro computed-tomographic angiography (mCTA). Vascular radiomorphometrics were calculated and statistical comparison was conducted. Flap creep and stress relaxation was assessed using an Instron tensiometer. H&E, picrosirius red, and Verhoeff Van Gieson stains were performed.

RESULTS: Radiated flaps demonstrated gross stigmata of cutaneous radiation injury within four weeks: transient erythema followed by alopecia, and a shiny/waxy appearance. Histologically, the epidermis in the XRT flaps was thicker than in the XRT+DFX and control flaps - a finding well described in irradiated skin (control = 42 μm; XRT = 79 μm; XRT+DFX = 34 μm; $p<.001$). Using picrosirius red staining, the scar index was calculated: the greatest scar index was associated with the XRT flaps, followed by the XRT+DFX and control flaps (2.4 vs 1.8 vs 1.8; $p=.01$). mCTA demonstrated increased vascularity in the XRT+DFX flaps compared to XRT alone. Similarly, histologic analysis revealed an increased number of blood vessels per high-powered field (vHPF) in the XRT+DFX flaps (control=2 vHPF; XRT=1.25 vHPF; XRT+DFX=2.4 vHPF; $p=.04$). The creep curve was indicative of increased elasticity in the XRT+DFX flaps compared to XRT flaps. Additionally, the Verhoeff Van Gieson stain for elastin indicated a greater elastin content in the dermis of the XRT+DFX flaps compared to XRT flaps.

CONCLUSIONS: Flaps in the XRT group were quantifiably different than the control (thicker epidermis, greater scar index, less vasculature). The subcutaneous administration of DFX is associated with increased vascularity after radiation, as measured by mCTA and histologic analysis. Additionally, radiated flaps that received DFX demonstrated a lower scar index, greater elasticity and higher elastin content. DFX appears to mitigate radiation-induced hypovascularity and improve tissue elasticity in a rat model of soft tissue reconstruction.

108
Photochemical Tissue Passivation for Prevention of Vein Graft Intimal Hyperplasia

Harry M Salinas, MD; Justin Fernandes, MD; Felix Broelsch, MD; Michael C McCormack, MD; Amanda Meppelink, MD; Michael Watkins, MD; William G Austen, Jr, MD

Massachusetts General Hospital, Boston, MA

PURPOSE: Vein grafts are frequently used as conduits for coronary bypass, peripheral arterial revascularization, and microsurgical reconstruction of the upper extremities. For coronary revascularization, saphenous vein grafts (SVG) are the most commonly used conduit. However, they have poor long term patency rates compared to arterial grafts due to accelerated atherosclerosis in the venous grafts. Accelerated atherosclerosis begins as intimal hyperplasia (IH), which is a consequence of the intimal injury that results from excessive stretching of the vein graft as it is exposed to arterial pressures. Limiting the stretch of the graft reduces the degree of IH. To date, every modality to prevent stretch has been through the application of external sheaths over the vein graft. Photochemical Tissue Passivation (PTP) is a technology that crosslinks surface proteins by a light activated process. PTP offers a simple approach to stiffen venous conduits, thus limiting excessive stretch and the resulting intimal injury.

METHODS: Porcine jugular veins were used to evaluate the effect of PTP on the elasticity of venous tissues. Veins harvested from 5 pigs were divided in half. One segment served as control, the other was treated with 0.1% Rose Bengal and a 532 nm laser. The veins were cut into 0.5x2cm strips (N=33; 16 control, 17 treated). Stress-strain curves were generated for each with a tensiometer and the modulus of elasticity calculated as the slope of the initial linear portion of the curve. Collagenase digestion was performed on treated and untreated rat epigastric vein segments to demonstrate crosslinking. An animal model of IH was then adopted for in-vivo testing. An interposition graft was placed in the femoral artery of Sprague-Dawley rats using a reversed segment of epigastric vein. Animals were euthanized for graft harvest after 4 weeks.

RESULTS: The modulus of elasticity (Young's modulus) was 587±288 and 1008±555 KPa for untreated and treated samples respectively ($p=0.01$). Collagenase digestion took 66±8 and 300±0 min for untreated and treated samples respectively ($p<0.001$). Our in-vivo model showed that after four weeks, intimal thickness was 80±56 and 24±22 μm in untreated and treated grafts ($p=0.03$). Medial thickness was 216±69 and 141±40 μm in treated and untreated grafts ($p=0.04$). All grafts were patent.

CONCLUSION: PTP stiffens venous conduits, increasing the modulus of elasticity by nearly 2-fold. The collagenase digestion assay demonstrated significant collagen cross-linking of venous conduits after treatment with PTP. Our animal model showed 70% reduction in intimal thickness and 35% reduction in medial thickness of treated grafts. Therefore, PTP may improve the long term patency rates of venous grafts used for coronary revascularization and peripheral arterial reconstruction without the need for cumbersome external sheaths.

109
Venous Flow Monitoring Using an Entirely Implanted, Wireless Doppler Sensor

Michael L Gimbel, MD; Michael A Rothfuss, MS; Jignesh V Unadkat, MD; Marlin H Mickle, MSEE, PhD; Ervin Sejdic, PhD
U Pittsburgh, Pittsburgh, PA

PURPOSE: Successful salvage of the threatened free flap is dependent upon prompt diagnosis of vascular occlusion and timely restoration of blood flow. Many monitoring systems can be used to augment clinical exam, but all suffer from drawbacks. The implantable venous Doppler offers rapid diagnosis of vascular compromise, but has a cumbersome transcutaneous wire and is reported to have high false positive rates largely due to inadvertent internal probe dislodgement. A wireless device would avoid these problems. This study describes the implementation of an entirely implanted Doppler sensor with wireless transmission of flow data in a pig femoral vein model.

METHODS: An encapsulated implantable Doppler sensor with self-contained power source and wireless data transmission capability was developed. Four 6 month old 30kg Hanford swine underwent femoral vein dissection bilaterally. Femoral veins were skeletonized and affixed with wireless Doppler probes and skin was closed, with no transcutaneous wires. After equilibration, femoral vein flow was monitored (via wireless transmission to a receiver connected to a computer running custom software) for 1 minute of uninterrupted **Flow**, followed by 1 minute of venous Occlusion, followed by 1 minute of Release (restored flow). Four iterations of this cycle were performed on each femoral vein of each animal, a total of 32 cycles. Transmitted digital flow data was recorded in millivolts (mV) and filtered for noise reduction. Paired t-test analyses were performed comparing signal strength in Flow vs Occlusion periods and Occlusion vs Release periods.

RESULTS: Successful implanted, wireless venous flow monitoring was achieved for all femoral veins in this study. Mean signal strength during Flow, Occlusion, and Release were 0.103 mV (SD 0.139), 0.018 mV (SD 0.029), and 0.105 mV (SD 0.185), respectively. Signal strengths were significantly greater in the Flow period vs the Occlusion period ($p < 0.001$) and during the Release period vs the Occlusion period ($p = 0.006$).

CONCLUSION: While clinical exam remains the gold standard for free flap monitoring, many microsurgeons find added value using flap monitoring sensors for their reconstructions. The currently available implantable Doppler devices suffer from problems largely related their cumbersome transcutaneous wires, including inadvertent wire probe removal, false positive signals from unrecognized internal probe dislodgement, and the necessity of potentially harmful probe withdrawal. This proof-of-concept study is the first description of an entirely implanted blood flow monitor with wireless data transmission capability. Our device successfully distinguished between venous flow and occlusion and between occlusion and release with statistical significance. Importantly, these differences in flow waveforms are obvious to the untrained eye. Future work will include device miniaturization through integrated circuit technology.

110
The Impact of Deferoxamine on Vascularity and Soft Tissue Biomechanics in a Rat TRAM Flap Model

Alexander F Mericli, MD; Anusuya Das, PhD; Pamela Rodeheaver, BS; George Rodeheaver, PhD; Kant Y Lin, MD
University of Virginia, Charlottesville, VA

PURPOSE: Flap ischemia is a worrisome complication in reconstructive surgery and can lead to partial or total flap necrosis, tissue fibrosis and stiffness, infection, and a poor aesthetic result. Deferoxamine (DFX) is an FDA-approved iron chelating medication which has also been shown to increase the growth of new blood vessels through its ability to upregulate HIF-1a, a key transcription factor for several genes important for angiogenesis. DFX has been shown to augment bone vascularity, however its use in soft tissue has not been fully evaluated. We hypothesize that the application of DFX will result in improved vascularity and tissue elasticity in a rat TRAM flap model.

METHODS: Two groups of Sprague-Dawley rats (n =10) underwent a right pedicled TRAM flap. Twenty-one days after surgery, the experimental group (n = 5) was treated with deferoxamine injected subcutaneously into the flap every other day for ten days. The control group underwent TRAM flap creation only. Ten days after the last dose of deferoxamine the rats were perfused and imaged with micro computed-tomographic angiography (mCTA). Vascular radiomorphometrics were calculated and statistical comparison was conducted. Flap tissue biomechanics were assessed in both groups using an Instron tensiometer. Stress-strain, creep, and stress relaxation curves were created. Histologic analysis was performed using H&E and Verhoeff Van Gieson stains.

RESULTS: mCTA demonstrated significantly increased vascularity in the DFX TRAM flaps compared to the control. Similarly, histologic analysis revealed an increased number of blood vessels per high-powered field (vHPF) in the DFX flaps (3.24 vHPF - DFX vs 2 vHPF - control; p = .03). The DFX flaps demonstrated greater creep and stress-relaxation compared to control, findings consistent with a more elastic tissue. Additionally, the Verhoeff Van Gieson stain for elastin indicated a greater elastin content in the dermis of the DFX flaps compared to control.

CONCLUSIONS: These results suggest that the subcutaneous administration of DFX is associated with increased TRAM flap vascularity, as measured by mCTA and histologic analysis. Additionally, flaps that received DFX demonstrated greater elasticity and higher elastin content.

111
An Alternative to the SGAP Flap in Autologous Breast Reconstruction: The Gluteal Upper Lateral Flap (GULF)

Alexis Laungani, MD; Nirusha Lachman, PhD; Michel Saint-Cyr, MD, FRCS(C)
Mayo Clinic, Rochester, MN

BACKGROUND: Many flaps have been described in autologous breast reconstruction, among which include; DIEP, SGAP/IGAP, LD, TUG and PAP flaps. Nevertheless, depending on body habitus or history of previous surgery, some of these flap donor sites may not be possible. The ascending branch of the lateral circumflex femoral artery (LCFA) provides vascularity to the upper lateral thigh and overlaps with the perforasome of the SGAP flap.

PURPOSE: The purpose of this study was to investigate the feasibility of using the upper lateral gluteal tissue as a potential flap donor site for autologous breast reconstruction. Methodology: An anatomical study was performed using 6 fresh cadavers acquired at the department of anatomy at Mayo Clinic, Rochester, Minnesota. Two flaps were harvested from each cadaver for a total of 12 flaps. Two flaps were injected with red latex at the level of the profunda femoris artery for the purpose of gross anatomy description in situ. Ten flaps were harvested, cannulated with a 24 Gauge catheter and flushed with warm saline. A dilute methylene blue solution was infiltrated into the flap to identify vascular leaks, which were ligated. The flaps were then injected with Omnipaque 180 and scanned through a 64-slices CT-Scanner (Siemens). Analysis included a 3D reconstruction and assessment of flap vascularity. All donor sites were closed primarily. A retrospective study of 50 CT-scans was also performed to characterize perforator course, and vascular anatomy relative to source artery and perforator entrance into the flap.

RESULTS: Based on our CT-scan study, we have constantly found a perforator artery and vein that are the cutaneous terminal branches of the ascending branch of LCFA (aLCFA). The aLCFA coursed towards the greater trochanter and passed underneath the rectus femoris and tensor fascia late muscles. The anatomical findings confirmed the CT-scan radiologic study and showed an average pedicle length of 8cm. The perforasome (perforator vascular territory) related to this perforator was defined during the injection studies and extended from the greater trochanter to the upper posterior aspect of the thigh and buttock.

CONCLUSION: We describe a flap that could become a good alternative to the SGAP flap for breast reconstruction. This potential new flap option presents many advantages. These include a less tedious pedicle dissection, conservation of the buttock contour and a dissection in a supine position, thus allowing a two-team approach in autologous breast reconstruction.

112
Hydrogen Peroxide Priming of Cadaveric Veins Reveals the Underlying Anatomical Basis for Venous Complications of DIEP, TRAM and Other Flaps of the Anterior Torso

Kwok Hao Lie, MA MB BChir; G Ian Taylor; AO MD FRACS FACS; Mark W Ashton, MD FRACS
University of Melbourne, Parkville, Melbourne, Australia

INTRODUCTION AND PURPOSE: Previous studies of venous anatomy lack the detail of their arterial counterparts due to (i) the technical challenge of retrograde perfusion against competent valves and (ii) anterograde venous perfusion that fails to capture significant portions of the area of interest. A novel technique is presented that uses retrograde hydrogen peroxide priming in order to dilate veins and render valves incompetent, thereby facilitating full cadaveric venous perfusion.

MATERIALS AND METHODS: The superficial and deep venous systems of 41 hemiabdomens and 20 hemi-chests of fresh human cadavers were cannulated and primed by retrograde injection with 6% hydrogen peroxide. After 24 hours, the specimens were injected with lead oxide contrast, radiographed and dissected. In 3 hemiabdomens, the veins were dissected to map valve sites and orientation. Results were compared with our archival venous studies of 6 total body injections, 6 abdominal lipectomy specimens and 2 in vivo studies of patients undergoing delayed TRAM flap operations.

RESULTS: Studies demonstrated venous filling with unprecedented detail of the anterior abdomen and chest wall. Two types of superficial-to-deep venous connections were defined - large caliber venae communicantes and small caliber venae comitantes. Venae communicantes (>2mm) formed major connections between large superficial and deep veins. They were found most frequently within 5cm of the umbilicus in the abdomen and beside the sternum, the fifth or sixth intercostal space and the axilla in the chest. Such veins typically accompany large arterial perforators, although in 26% of studies they were found with arteries <0.5mm in diameter. Four major longitudinal valved subcutaneous pathways of the SIEV and SCIV were defined bilaterally in the abdomen with large caliber avalvular transverse supraumbilical, subumbilical and suprapubic connections in the midline and small caliber connections laterally that help explain venous complications seen sometimes in DIEP and other abdominal flaps.

CONCLUSIONS: Retrograde hydrogen peroxide priming of veins in unembalmed cadavers renders valves incompetent and facilitates highly detailed venous injection studies. This information explains the aetiology of zone IV, hemiabdominal and diffuse venous congestion in transverse abdominal flaps, and also helps inform and refine flap design.

SUNDAY, MARCH 9, 2014

SCIENTIFIC SESSION 8 GROUP A
OUTCOMES
10:00 AM – 12:00 PM

SUNDAY, MARCH 9, 2014

113
Comparison of Outcomes for Patients Undergoing Free Flap Autologous Breast Reconstruction Utilizing a Multimodal Enhanced Recovery Pathway versus Traditional Care

Niles J Batdorf, MD; Ronnie Mubang, MD; Goede Whitney, PharMD, RPh; Karla Ballman, PhD; Jenna Lovely, PharMD, RPh; Pamela Grubbs, RN, CNS; Bungum Lisa, RN; Andria Hinckley, RN, CNP; Valerie Lemaine, MD; Michel Saint-Cyr, MD
Mayo Clinic, Rochester, MN

PURPOSE: Enhanced recovery after surgery pathways (ERAS) have been utilized in other surgical specialties and been shown to reduce length of hospital stay after surgery, but they have not been described for patients undergoing free flap breast reconstruction. The purpose of this study was to develop an ERAS pathway specific to plastic surgery free flap breast reconstruction.

METHODS: An enhanced recovery after surgery pathway (ERAS) was developed through multidisciplinary collaboration between a plastic surgeon, anesthesiologists, pharmacists, and nursing staff. The ERAS pathway included preoperative analgesia, use of intraoperative liposomal bupivacaine in the surgical site, avoidance of postoperative opioids, pre-emptive nausea and vomiting treatment, avoidance of routine intensive care unit monitoring, immediate resumption of diet, and early ambulation. All patients were treated using the ERAS pathway once it was instituted. Postoperative outcomes were retrospectively analyzed and compared to a historical cohort of patients treated in a traditional care after surgery (TRAS), non-pathway manner. All patients in the study were operated on and under the care of a single staff surgeon within a 12 month period. Patients were excluded from the study if they had a pre-operatively diagnosed coagulopathy or a chronic pain syndrome.

RESULTS: A total of 48 patients were analyzed, 17 treated with TRAS, and 31 patients with ERAS. The total number of flaps in the cohort was 83. Flaps were either deep inferior epigastric perforator flaps (n=71), muscle sparing transverse rectus abdominis flaps (n=7), or transverse upper gracilis flaps (n=5). The hospital stay averaged 4.4 days with TRAS, but decreased to 3.0 days with ERAS (p=0.0007). None of the ERAS patients were admitted to the ICU post-operatively. Total inpatient postoperative opioid usage for the first three days, calculated in oral morphine equivalents, was 321.3 mg for TRAS, but decreased to 142.3 mg with ERAS (p=0.005). Pain goal and scores (from 1–10) were analyzed for the first 3 days at 8 time points. At 24 hours postoperatively, pain scores in the ERAS cohort were significantly better than TRAS (p=0.014), however, this was the only time point with a statistically significant difference. The observed 30 day complication rate between ERAS and TRAS cohorts was not statisitically significant (p=0.28).

CONCLUSIONS: The initiation of an Enhanced Recovery after Surgery pathway for breast free flap reconstruction significantly reduced hospital stay in our study. The pathway also significantly decreased the amount of opioids used post-operatively by more than 50% without a consequent increase in patient reported pain score. A free flap breast reconstruction ERAS pathway is a powerful tool to deliver high-value, quality care and decrease costs.

114
Use of Morphomic Analysis for Preoperative Risk Stratification in Patients Undergoing Major Head and Neck Cancer Surgery

Jacob Rinkinen, BA; Shailesh Agarwal, MD; Michael Terjimanian, BS; Jeffrey Beauregard, MS; Kavitha Ranganathan, MD; Matthew Benedict, BS; David Hiltzik, BS; Isaac Stein, BA; Jeffrey Lisiecki, BS; Stewart C Wang, MD, PhD; Steven R Buchman, MD; Benjamin Levi, MD
University of Michigan, Ann Arbor, MI

INTRODUCTION: Post-operative complications following major head and neck cancer surgery (MHNCS) are associated with significant morbidity and mortality. The ability to stratify pre-operative risk based on already available objective measures could improve pre-operative counseling and decision making. Currently, pre-operative risk is assessed based on comorbidities. Traditionally, patient assessment has been performed using comorbidities. However, an emerging field of patient assessment involves the evaluation anatomic morphology to measure patient frailty. We hypothesize that the morphologic characteristics of the temporalis region in patients undergoing MHNCS can serve as a reliable marker for risk of complications.

METHODS: Patients who underwent MHNCS from 2004 to 2012 with available pre-operative CT scans were included in this study. All CT scans were performed as part of routine pre-operative planning, and were not initially ordered to evaluate the temporalis region. Archived images were extracted and the three-dimensional characteristics of the bilateral temporalis regions were mapped from both sides using a previously validated method to determine the zygomatic arch thickness and TFPV. Charts were reviewed for patient characteristics (age, gender, BMI, diabetes history, smoking status, and ASA score) and post-operative complications (*e.g.* MI, VTE, wound breakdown, hematoma, infection). Univariate and multivariate statistical analysis was performed to determine the relationship between risk of complications and zygomatic arch thickness and/or temporal fat pad volume. We then developed receiver-operator curves (ROC) to determine the reliability of arch thickness and TFPV for evaluating complication risk.

RESULTS: A total of 70 patients undergoing MHNCS had available CT scans. Mean zygomatic arch thickness was 2.7 mm (s.d. 0.6 mm) and mean TFPV was 1.37 cm^3 (s.d. 0.92 cm^3). Major post-operative complications were noted in 28% (20/70) of our patients. Patients with post-operative complications had 33% less TFPV (1.50 v. 1.01 cm^3, $p<0.02$), and 13% smaller zygomatic arch thickness (2.82 v. 2.46 mm, $p<0.02$); interestingly, we noted no significant differences in other characteristics (*e.g.* age, BMI, diabetes history, smoking status, or ASA score), between patients which did or did not experience complications. The area-under-the-curve (AUC) for zygomatic arch and temporal fat pad ROCs were 0.709 and 0.674 respectively, suggesting a slightly better test for complications using zygomatic arch thickness. Multivariate analysis showed that the odds of complications was 0.43 for each cm^3 increase in TFPV, and 0.24 for each mm increase in zygomatic bone thickness.

CONCLUSION: Head and Neck Morphomics is a powerful technique which can provide pre-operative risk assessment for major complications in Head and Neck Cancer patients based on anatomic variables as a proxy for frailty and fitness. Specifically, we demonstrated that MHNCS patients with significantly lower zygomatic arch thickness and fat pad volume had higher major complication rates. These data, either alone, or in combination with co-morbidities hold the promise of more accurately determining pre-operative risk stratification in order to better council patients and prepare surgeons to deliver the best possible clinical care.

115
Combined Free Tissue Transfer For The Management Of Composite Achilles Defects: Functional Outcomes And Patient Satisfaction Following Vascularized Reconstruction With A Neo-tendon Construct

Michael DeFazio, MD; Kevin D. Han, MD; Christopher Attinger, MD; Karen K Evans, MD; Chrisovalantis Lakhiani, MD
Georgetown University Hospital, Washington, DC

PURPOSE: Free tissue transfer with a vascularized tendon construct permits single-stage reconstruction of composite Achilles/posterior leg defects. While this approach appears to offer a solution to high rates of recurrent infection and tendon failure, long-term functional outcomes and quality-of-life measures following salvage reconstruction are limited. We present our experience and outcomes following combined Achilles defect reconstruction utilizing vascularized neo-tendon constructs.

METHODS: A series of six patients underwent vascularized reconstruction of Achilles tendon and soft tissue defects, by a single surgeon (K.K.E.), between October 2011 and June 2012. Mechanism of injury, range of motion, calf circumference, and tiptoe ambulation were assessed for each patient. Subjective evaluation and quality-of-life measures were obtained pre- and postoperatively using the AOFAS Ankle-Hindfoot and SF-36 scores. Early and late complications were noted for each case.

RESULTS: Achilles defects were reconstructed using an anterolateral thigh/vascularized fascia lata flap in five cases. For one patient with inadequate anterolateral skin perforators, a free rectus femoris/posterior rectus fascial flap was used. The average soft tissue defect was 76.7 cm2 (r, 40 - 90 cm2) with a tendon gap of 7.8 cm (r, 5 - 10 cm). Mean follow-up was 17 months (r, 15 - 23 months). Flap survival was 100%, and all patients returned to pre-injury level of activity by 1 year postoperatively. Overall range of motion of the reconstructed side was 82% of the unaffected side (48.2° vs. 59°, $p = 0.004$). Average percent increase in AOFAS and SF-36 scores were 71% (54 vs. 93, $p = 0.0005$) and 22% (86 vs. 104, $p = 0.003$), respectively. Operative revision was required for 2 patients with delayed-onset soft tissue infections and 1 donor site hematoma. Distal flap ischemia was managed with hyperbaric oxygen therapy in 1 patient. Functional and aesthetic outcomes were judged good to excellent by all patients.

CONCLUSION: Free tissue transfer with vascularized tendon reconstruction is a viable option for patients with combined Achilles tendon/posterior leg defects, as both functional and quality-of-life measures were significantly improved at one year postoperative follow-up.

116
The Rate of Oronasal Fistula Formation Following Primary Cleft Palate Surgery: A Meta-Analysis

Michael R Bykowski, MD; Sanjay Naran, MD; Daniel F Winger, BS; Joseph E Losee, MD
University of Pittsburgh, Pittsburgh, PA

PURPOSE: The purpose of this study was to perform a meta-analysis to answer the questions: What is the rate of oronasal fistula formation following primary cleft palate repair, and what risk factors are associated with their development?

METHODS: The Medline database was reviewed for English-written papers published between 2000 and 2012 with the search items: “cleft palate fistula” and “cleft palate surgery”. Inclusion criteria included: 1) primary cleft repair; 2) average or median age at time of surgery of 3 months; and 4) a clear description of an oronasal fistula as a communication between oral and nasal cavities. Exclusion criteria included: 1) preclinical animal studies; 2) case reports; 3) patients with a type V-VII fistula, as defined by the Pittsburgh Fistula Classification System; and 4) repair of submucous cleft palates. A random effects meta-analysis of proportions and exact confidence intervals was performed. For Veau classifications, an extension of the Cochran-Mantel-Haenszel Test for a series of 2x4 tables was utilized.

RESULTS: Of the 17 studies that met our inclusion criteria, 6 more were rejected because they were deemed to be statistical outliers. This resulted in 11 studies, comprising 2505 children, which were incorporated into our analysis. These studies were found to be statistically comparable to each other, meeting the homogeneity assumption with an acceptable I-squared value of 25.3% and a non-significant heterogeneity chi-squared p-value (0.203). The primary outcome targeted for analysis was the occurrence of an oronasal fistula, which we found to be 4.9% (95% CI 3.8–6.1%). There was a significant relationship between Veau classification and the occurrence of a fistula ($p<0.001$) with fistulae most prevalent in patients with a Veau IV cleft. The rate of fistula occurrence did not correlate to the surgical technique utilized for palate repair. The location of fistula, based upon the Pittsburgh Fistula Classification System, were as follows: Type I, 0.0%; Type II 12.7%; Type III, 54.0%; Type IV, 27.0%; with the remaining reported as a combination of locations not otherwise specified.

CONCLUSION: Evaluation of the rate of occurrence of oronasal fistulae following primary cleft palate repair is hindered by inconsistency of reporting surgical outcome details, inclusion or exclusion of submucous cleft palate repair, a wide range of patient populations, and differing surgical techniques. Utilizing 11 studies comprising 2505 children, we find the rate of fistula occurrence, defined as a true communication between the oral and nasal cavities, to be 4.9%. Furthermore, patients with a Veau IV cleft are significantly more likely to

develop an oronasal fistula but use of decelluarized dermis may be protective. When fistulae do occur, they do so most often at the junction of the primary and secondary palate. A deeper understanding of fistula formation will help cleft palate surgeons improve their outcomes in the operating room and will allow them to effectively communicate expectations with patients' families in the clinic.

117
Preoperative Anemia Increases the Risk of Adverse Outcomes in Patients Undergoing Free Tissue Transfer: a Critical Analysis of 2135 Patients from the ACS-NSQIP Database

Sashank Reddy, MD, PhD; Karim Sarhane, MD; Jose Flores, MPH; Pablo Baltodano, MD; Gedge D Rosson, MD
Johns Hopkins University, Baltimore, MD

PURPOSE: Perioperative anemia is associated with adverse outcomes in general surgery, vascular surgery, cardiac surgery, and breast surgery. Perioperative anemia increases complications in patients undergoing extensive surgical procedures and procedures with major blood loss. Since free tissue transfers are among the most lengthy and complicated plastic surgery procedures, we hypothesized that patients undergoing free tissue transfer would be particularly susceptible to the effects of preoperative anemia. This study examines the effects of preoperative anemia on free flap outcomes.

METHODS: Patients who underwent free tissue transfer from 2008 to 2011 were identified from the American College of Surgeons National Surgical Quality Improvement Program (NSQIP). De-identified data on patient demographics, perioperative risk factors, and incidence of complications were obtained. Pre-defined outcomes included overall morbidity, flap failure, surgical site infection, wound breakdown, and repeat operation. Logistic regression was used to assess the crude and adjusted effect of anemia (defined as a hematocrit concentration <36% in women or <39% in men) on postoperative 30-day morbidity.

RESULTS: The study population included 2135 patients, among whom 653 (30.6%) had preoperative anemia. Compared to patients with normal hematocrit levels, anemic patients had 2.16 times higher odds of experiencing overall morbidity within 30-days of their operation (OR = 2.16, $p < 0.005$). Patients with anemia were significantly more likely to have wound breakdown (OR 2.20, $p < 0.005$) and were more likely to return to the operating room (OR 1.54, $p < 0.005$). However, preoperative anemia was not associated with a significantly increased risk of flap loss or surgical site infections.

CONCLUSIONS: Preoperative anemia is associated with an increased incidence of overall morbidity and is specifically associated with wound healing difficulties and repeat operations. However, anemia may not predispose patients to flap loss. As many patients undergoing free flap reconstruction are chronically ill, screening for preoperative anemia should be strongly considered. If found, preoperative anemia is often easy to correct. Additional prospective studies should clarify whether treating preoperative anemia can improve outcomes in microsurgical procedures.

118
Mastectomy Weight and Tissue Expander Fill Volume Predict Skin Necrosis and Increased Costs Associated with Breast Reconstruction

Georgia C Yalanis, MSc, BS[1]; Shayoni Nag, BA[1]; Jakob R Georgek, BS[2]; Carisa M Cooney, MPH[1]; Michele A Manahan, MD[1]; Gedge D Rosson, MD[1]; Justin M Sacks, MD[1]

[1]The Johns Hopkins School of Medicine, Baltimore, MD, [2]Rensselaer Polytechnic Institute, Troy, NY

PURPOSE: Impaired vascular perfusion in breast reconstruction following mastectomy and tissue expander (TE) placement can result in skin necrosis, infection, and implant loss. Increased mastectomy weight, TE fill volume, and patient comorbidities may impair mastectomy flap perfusion. We investigated factors associated with mastectomy flap necrosis in TE breast reconstruction as well as the actual cost to patients who experienced adverse sequelae.

METHODS: A retrospective review of 169 women who underwent immediate TE placement following mastectomy between May 2009 and May 2013 was performed. Patient demographics, comorbidities, mastectomy weight and type, intraoperative TE fill volumes, and postoperative outcomes were collected. Logistic regression analysis on individual variables and outcomes was performed. For breast-dependent outcomes, standard errors were adjusted for within-patient correlation using clustering for bilateral operations. Billing data was obtained to determine the additional financial burden associated with mastectomy flap necrosis.

RESULTS: 251 immediate TE placements with acellular dermal matrix for 169 women were analyzed. Skin necrosis occurred in 20 mastectomy flaps for 15 patients (8.9%). Patients with hypertension (HTN) had 8 times the odds of developing skin necrosis compared to patients without (OR: 8.10, $p<0.001$). When adjusted for HTN, patients with intraoperative fill volumes greater than 300cc had 10 times greater odds of developing skin necrosis (OR: 10.13, $p=0.012$). Fill volumes greater than 400cc resulted in a 14 times greater odds of developing skin necrosis (OR: 14.78, $p=0.003$). Mastectomy specimens weighing over 500g had a 10 times higher odds of skin necrosis and flaps weighing over 1000g had an 18 times higher odds of skin necrosis (OR: 9.91 and OR: 18.00, respectively; $p<0.001$). Body Mass Index (BMI) >30 was associated with skin necrosis ($p=0.0034$). Race, smoking status, and diabetes mellitus showed no association in multivariate regression analysis and should be studied in a larger population. Patients with skin flap necrosis had 15 times higher odds of developing a post-operative infection (OR: 15.12, $p<0.001$) and almost 16 times higher odds of requiring their TE to be prematurely removed (OR: 15.83, $p<0.001$). 10/15 patients with skin necrosis required re-admission with intravenous antibiotics, surgical debridement, and removal of the TE (67%). The remaining patients were treated conservatively with oral antibiotics. Patients with flap necrosis were matched to patients in the same sample without mastectomy flap necrosis by race, age, year of surgery, type of mastectomy, BMI, smoking status, and HTN status. Patients with mastectomy flap necrosis requiring surgical debridement suffered an average additional inpatient cost 49% higher than patients who did not require reoperation.

CONCLUSIONS: Mastectomy flap necrosis is associated with hypertension, increased intraoperative TE fill volume, and mastectomy weight. Conservative TE fill volumes should be considered for patients with HTN, larger BMI's, and larger mastectomy specimens. Reoperation due to mastectomy flap necrosis poses a significant financial and emotional burden to the patient. Clinical outcomes can be improved using these parameters as guidelines in staged breast reconstruction.

119
Validation of Clinical Criteria for Obtaining Maxillofacial CT in Trauma Patients

Nyama Sillah, MD[1]; Thomas Sitzman, MD[2]; Summer Hanson, MD, PhD[3]; Lindell Gentry, MD[1]; John Doyle, DDS[1]; Karol Gutowski, MD[4]

[1]University of Wisconsin, Madison, WI, [2]Cincinnati Children's Hospital Medical Center, Cincinnati, OH, [3]University of Texas MD Anderson Cancer Center, Houston, TX, [4]Glenview, IL

PURPOSE: Each year over 180,000 patients present to emergency departments in the United States with facial trauma. Of these, approximately one-third will have a facial fractures. While maxillofacial computed tomography (CT) has become the gold standard in identifying facial fractures, the indiscriminate use of CT brings increased cost and unnecessary radiation exposure. In a previous study, the authors developed a set of clinical criteria (decision instrument) that identified patients at low risk of facial fracture who could avoid CT imaging. The present study aims to internally validate that instrument.

METHODS: A retrospective observational study was conducted on all patients evaluated at a Level I trauma center over a one year period. Inclusion criteria were maxillofacial physical exam, head CT, and maxillofacial CT at presentation. The decision instrument used five criteria: bony stepoff or instability, periorbital swelling or contusion, Glasgow Coma Scale less than 14, malocclusion and tooth absence. The presence of any one finding placed the patient at high risk for fracture.

RESULTS: A total of 179 patients met enrollment criteria. Fracture of the maxillofacial skeleton occurred in 81% of patients (n=145). The decision instrument was 97.4% sensitive (95% CI, 93.8–99.3) for the presence of facial fracture. The negative predictive value was 81.3% (95% CI, 55.0–95.0). Application of the instrument to the study population would have missed three patients with facial fractures, for a missed injury rate of 2.6%. All missed fractures were non-displaced and managed non-operatively. If only patients meeting the criteria obtained imaging, CT use would have decreased by 8.9%.

CONCLUSIONS: The proposed decision instrument may assist providers in identifying patients that need maxillofacial CT. Patients with any of the five clinical criteria are at high risk for facial fracture and should undergo CT imaging. Application of the instrument may reduce maxillofacial CT use without missing fractures requiring operative intervention.

120
Neoadjuvant Radiotherapy is not associated with Increased Post-Mastectomy/Reconstruction Morbidity Events: A Critical Analysis of 85,851 Patients from the ACS-NSQIP Database

Pablo A Baltodano, MD[1]; José M Flores, MPH[2]; Lyonell Kone, MHS[1]; Nicholas B Abt, BS[1]; Karim A Sarhane, MD, MSc[1]; Danielle H Rochlin, BA[1]; Francis M Abreu, BS[2]; Richard C Zellars, MD[1]; Martin A Makary, MD, MPH[1]; Gedge D Rosson, MD[1]

[1]Johns Hopkins University School of Medicine, Baltimore, MD, [2]Johns Hopkins School of Public Health, Baltimore, MD

PURPOSE: Neoadjuvant radiotherapy (NRT) is a novel therapeutic approach to breast cancer that reduces local recurrences and increases overall survival. However, its effect on postoperative morbidity remains ill defined. We sought to assess the impact of NRT on 30-day postoperative morbidity after mastectomy.

METHODS: We analyzed all females undergoing mastectomy with and without immediate breast reconstruction from 2005–2011 in the American College of Surgeons National Surgical Quality Improvement Program (ACS-NSQIP) databases (a prospective, risk adjusted, outcomes-based registry). De-identified data were obtained for demographics and perioperative factors. Outcomes included morbidity and surgical site occurrences (SSO, i.e., wound infections and dehiscence). Morbidity variables included flap/graft/prosthesis, cardiac, respiratory, neurological, urinary, and venous thromboembolism outcomes. Logistic regression was used to estimate the crude and adjusted effect of NRT on postoperative 30-day morbidity and SSO. Our analysis adjusted for 21 perioperative variables.

RESULTS: The study population included 85,851 women: 61,039 (71.1%) mastectomy-only and 16,863 (19.6%) immediate breast reconstruction patients. A total of 266 (0.4%) mastectomy-only and 75(0.4%) immediate breast reconstruction patients received NRT. In the mastectomy-only population, no significant differences in the odds of morbidity (ORAdjusted_Morbidity: 0.75; P=0.34) or SSO (ORAdjusted_SSO: 1.61; P=0.22) were observed between NRT and no NRT groups on multivariable analysis. In the immediate breast reconstruction population, the odds of morbidity (OR_Adjusted_Morbidity: 0.21; P=0.059) or SSO (OR_Adjusted_SSO: 0.81; P=0.79) between NRT and no NRT groups on multivariable analysis were also similar.

CONCLUSIONS: This large retrospective study revealed that NRT is not associated with increased 30-day postoperative

morbidity or SSO in breast cancer patients undergoing mastectomy with or without immediate reconstruction. This results suggest that NRT is not a contraindication to immediate breast reconstruction, and provide a strong basis for future prospective studies to assess long-term morbidity and survival associated with NRT.

121
Evaluation of Otology Outcomes After Surgical Treatment of Symptomatic Pierre Robin Sequence: A Cohort Comparison Study Between Furlow Palatoplasty vs. Radical Intravelar Veloplasty

Lino F Miele, MD, MS; Kavita Dedhia, MD, MS; David Chi, MD; Deepak Mehta, MD; Anand R Kumar, MD
University of Pittsburgh, Pittsburgh, PA

PURPOSE: Comparative outcome studies of otology outcomes (hearing loss, middle ear disease, and myringotomy rates with or without tube placement)after treatment of wide cleft palate defects seen with severe Pierre Robin Sequence (PRS) are currently limited. This study aims to compare otology outcomes in PRS patients requiring early neonatal/infant airway surgery (Tongue Lip Adhesion (TLA) vs. Mandible Distraction (DOG)) and later treated with Furlow palatoplasty (FP) or radical intravelar veloplasty (IVV).

METHODS: A retrospective cohort study of symptomatic PRS patients (n=23) treated over 81 months was performed using clinical data to compare hearing loss, middle ear disease, and myringotomy rates with or without Armstrong tube placement rates between FP (Group 1) and IVV (Group 2) treatment groups. Statistical analysis between groups using a Wilcoxen signed-rank and Chi Square test was performed using SPSS 2.0.

RESULTS: In Group 1, the FP cohort, 10 patients were identified from September 2005- November 2009, (4 male and 6 female patients, average age at palatoplasty 1.30 years, 1 syndromic). In Group 2, the IVV cohort, 13 patients were identified from July 2007 - June 2012 (5 male and 8 female patients, average age at palatoplasty 1.57 years, 10 syndromic). The average age at oldest speech sample for FP was 3.96 years and for IVV was 2.48 (0.84 - 4.02) years ($p>0.05$ for all demographic variables except syndromic status $p=0.003$). In Group1 (FP), n=10 (100%) vs. Group 2 (IVV), n=9 (69%) ($p=0.002$) were treated with tympanostomy with venting tubes at an average age of 1.03 years (0.33–1.63) vs. 1.01 years (0.45–1.44) respectively. The serous otitis, mucoid otitis, suppurative otitis media rates were 20%, 60%, and 20% in Group 1 (FP) and 11%, 78%, and 11% in Group 2 (IVV) respectively. The otorrhea rate was 30% in Group 1 and 31% in Group 2. The revision tube placement was in 20% in Group 1 and 30% in Group 2. Average hearing test score was 19.2db in Group 1(n=8) vs. 20.75 db in Group 2 (n=8). No patients required mastoidectomy during the study period. Delayed speech acquisition, velopharyngeal incompetence, and adequate speech in group 1 was n=2 (20%), n=1 (10%), and n=5 (50%) respectively and in group 2 was n=11 (85%), n=1, (7.5%), n=1(7.5%) respectively.

CONCLUSION: Symptomatic effusions were present during the first year of life in the majority of patients with severe symptomatic Pierre Robin Sequence. Typanostomy tube

placement rate was reduced in our study in patients treated with IVV when compared to Furlow palatoplasty. Hearing outcomes were similar for patients requiring typanostomy tubes in either group. Speech acquisition and subsequent speech delay was associated with syndromic status rather than type of palate repair or rate of tympanostomy tube placement.

122
Prevalence and Management of Preoperative Depression and Anxiety Disorders in Patients Undergoing Mastectomy Reconstruction

Tiffany N S Ballard, MD[1]; Jennifer B Hamill, MPH[1]; Randy S Roth, PhD[1]; Andrea L Pusic, MD, MHS[2]; Edwin G Wilkins, MD, MS[1]
[1]University of Michigan, Ann Arbor, MI, [2]Memorial Sloan Kettering Cancer Center, New York, NY

PURPOSE: Although 20–40% of newly diagnosed cancer patients report significant levels of psychological and emotional distress, fewer than 10% are routinely screened for these problems using evidence-based measures.[1,2] Starting in 2015, the American College of Surgeons Commission on Cancer will require that accredited cancer centers screen all patients for distress and offer appropriate support services.[3] As part of a multi-center prospective outcome study, we sought to identify the prevalence of depression and anxiety disorders in patients undergoing post-mastectomy breast reconstruction and to develop a response system for at-risk patients.

METHODS: The Mastectomy Reconstruction Outcomes Consortium Study is an NCI-funded, 11 center prospective outcome study comparing the results of common techniques of mastectomy reconstruction. Patients undergoing first-time, immediate or delayed breast reconstruction are eligible and are administered a panel of validated surveys pre- and post-operatively. The surveys include the Patient Health Questionnaire (PHQ-9), a widely used depression assessment, and the Generalized Anxiety Disorder (GAD-7) Scale. Preoperative rates of depression and anxiety disorders were calculated using the global scores of the two instruments.

RESULTS: To date, 1841 patients are enrolled in the study. Preoperatively, the PHQ-9 has been completed by 1417 patients and the GAD-7 by 1455. Overall, 92.5% of study patients received immediate reconstruction. Expander-implant procedures were performed in 64.1% and autogenous tissue procedures in 35.9% of patients. On the PHQ-9, 15.9% of patients indicated moderate to severe depression. Seventeen percent reported moderate to severe anxiety on the GAD-9. In our most concerning finding, 14 patients indicated significant suicidal ideation on the PHQ-9. Although our study is observational, we recognized a responsibility to protect at-risk study patients: Each of the study sites has implemented an IRB-approved protocol in which patients reporting suicidal ideation are automatically identified in the database and are immediately contacted for psychological support services.

CONCLUSIONS: Our findings confirm the high prevalence of psychological distress reported by previous studies in other cancer populations. Rates of depression and anxiety disorders

observed in our study far exceed those of the general adult population (6.7% and 3.1%, respectively). Based on these findings, we recommend that providers (including plastic surgeons) implement protocols to screen new breast cancer patients for these issues and that psychological support services be readily available as part of routine care.

REFERENCE CITATIONS: 1. Derogatis LR, Morrow GR, Fetting J et al. The prevalence of psychiatric disorders among cancer patients. JAMA 1983;249(6):751–7. 2. Kadan-Lottick NS, Vanderwerker LC, Block SD, et al. Psychiatric disorders and mental health services use in patients with advanced cancer: a report from the coping with cancer study. Cancer 2005;104(12):2872–81. 3. American College of Surgeons Press Release, August 31, 2011.

123
Early Surgical Site Infection Following Tissue Expander Breast Reconstruction With And Without Acellular Dermal Matrix: National Benchmarking Using NSQIP

Sebastian Winocour, MD, MSc; Elizabeth B Habermann, PhD; Kristine M Thomsen, BA; Valerie Lemaine, MD, MPH
Mayo Clinic, Rochester, MN

PURPOSE: Surgical site infections (SSI) following immediate tissue expander breast reconstruction (ITEBR) with and without acellular dermal matrix (ADM) result in significant patient morbidity and health care costs. Using the American College of Surgeons National Surgical Quality Improvement Program (ACS-NSQIP) database, institutions are now able to query their results and conduct national benchmarking analyses. The purpose of this study is to determine a single institution's 30-day SSI rate and benchmark it against participating national institutions for quality improvement purposes.

METHODS: Women who underwent mastectomy followed by ITEBR with and without ADM were identified using the ACS-NSQIP database between 2005–2011. The subset of patients treated at our institution was also identified. Patient demographics, including BMI (<25 vs 25–29.9 vs 30+), smoking status, age 18 and greater, operative time quartiles, preoperative radiation and steroid-use, were evaluated in addition to postoperative SSI rates. Multivariable logistic regression was used to determine patient characteristics predictive of 30-day SSI rate and to identify differences in SSI rates between our institution and the national database.

RESULTS: Between 2005 and 2011, a total of 12,498 patients underwent ITEBR in the ACS-NSQIP database; of these 264 were at our institution. Of the 12,234 patients outside of our institution, 1894 patients received ADM (15.5%). The percentage of cases with ADM consistently increased nationally from 4.4% in 2005 to 22.5% in 2011. At our institution, 140 patients (53.0%) received ADM, with an increase in ADM use from 57.7% to 86.4% of cases between 2008 and 2011. In the nation, SSI occurred in 419 patients (3.4%) compared to 5 patients (1.9%) at our institution. SSI were significantly more common in ADM-ITEBR patients (4.3%) compared to non-ADM patients (3.2%) ($p<0.011$) nationally, while this trend was also observed at our institution (2.1% vs. 1.6%, $p=0.75$). Patient characteristics that were univariately significantly associated with increased rates of SSI in the entire ACS-NSQIP database included age 50 and older ($p<0.001$), increasing BMI ($p<0.001$) and greater total operative time ($p<0.001$). In addition, not currently smoking and absence of steroid-use trended towards lower rates of SSI but were not statistically significant. In a multivariable logistic regression model of the ACS-NSQIP database, age greater than 50 (OR 1.5, CI 1.1–1.7), BMI greater than 30 vs less than 25 (OR 3.4, CI 2.6–4.4), and operative time greater than 4.25 hours (OR 2.1, CI 1.5–2.8)

were significant risk factors for SSI. Overall, our institutional rate of SSI was lower than the nation (OR 0.4, CI 0.17–1.05), although not statistically significant (p=0.06).

CONCLUSION: The 30-day SSI rate at our institution in women undergoing mastectomy followed by ITEBR was lower than the ACS-NSQIP database. 30-day SSI was more common in the presence of ADM nationally and at our institution. Further work is ongoing to confirm if risk factors for the development of SSI at our institution are similar to those across the nation. Institutional quality improvement initiatives to reduce 1-year SSI rates in this patient population are currently ongoing.

124
Outcomes of Total Skin-Sparing Mastectomy and Reconstruction in 924 Breasts Over 11 Years

Frederick Wang, MD; Anne Peled, MD; Robert Foster, MD; Eric Wang, MD; Cheryl Ewing, MD; Michael Alvarado, MD; Laura Esserman, MD, MBA; Hani Sbitany, MD
University of California, San Francisco, San Francisco, CA

PURPOSE: Total skin-sparing mastectomy (TSSM) with preservation of the nipple-areolar complex (NAC) has become increasingly accepted and offered to women for both therapeutic and prophylactic indications.

METHODS: This retrospective study from October 2001 to January 2013 evaluates the outcomes of 599 patients who underwent TSSM for both therapeutic and prophylactic indications. Postoperative complications and recurrences were obtained from a prospectively maintained database. Outcome measures included postoperative infections, ischemic skin and nipple necrosis, implant loss, and tumor recurrence.

RESULTS: TSSM was performed on 924 breasts with a mean follow-up time of 24 months. The mean age was 47±10 years with a range of 18–74 years. TSSM was performed prophylactically in 320 cases (34.6%). Tissue expander and implant based reconstruction was performed in 813 cases (87.9%) while autologous reconstruction was performed in the remaining 111 cases (12.1%). A total of 195 patients (32.6%) received neoadjuvant chemotherapy and 99 patients (16.5%) received adjuvant chemotherapy. Post mastectomy radiation therapy was performed in 114 breasts (12.3%). Ischemic complications included 19 cases (2.1%) of nipple necrosis and 98 cases (10.6%) of skin flap necrosis. A total of 69 expanders/implants were removed secondary to infection (8.5%). Factors contributing to postoperative infections included radiation therapy (RR 2.27, p<0.001), smoking history (RR 1.53, p<0.01), and undergoing chemotherapy (RR 1.37, p<0.03). Factors contributing to loss of expanders/implants included radiation therapy (RR 3.76, p<0.001), diabetes (RR 3.45, p=0.02), and smoking history (RR 1.81, p=0.018). Overall locoregional recurrence rate was 1.5% and distant recurrences occurred in 1.3% of breasts.

CONCLUSION: In this large cohort of patients with breast cancer, TSSM was associated with a low rate of ischemic complications and recurrences. In addition, smoking history, diabetes, chemotherapy, and radiation therapy were all associated with an increased risk of postoperative complications.

SUNDAY, MARCH 9, 2014

SCIENTIFIC SESSION 8 GROUP B
FAT STEM CELLS
10:00 AM – 12:00 PM

SUNDAY, MARCH 9, 2014

125
Adipogenesis by External Volume Expansion

Jorge R Lujan-Hernandez, MD[1]; Luca Lancerotto, MD[1]; Christoph Nabzdyk, MD[1]; Kazi Z Hassan, BS[1]; Roger K Khouri, Jr, BS[1]; Hamed Zartab, MD, MSc[1]; Michael S Chin, MD[2]; Franco Bassetto, MD[3]; Janice F Lalikos, MD[2]; Dennis P Orgill, MD, PhD[1]

[1]Brigham and Women's Hospital- Harvard Medical School, Boston, MA, [2]University of Massachusetts Medical School, Worcester, MA, [3]Institute of Plastic Reconstructive and Aesthetic Surgery, University of Padova, Padova, Italy

PURPOSE: External Volume Expansion (EVE) has emerged as an adjuvant to improve the survival of fat grafting to the breast. We have previously described in an experimental animal model how EVE by mechanical stimulation, edema, hypoxia and inflammation improves vascularity and increases cellular proliferation of the potential recipient site. However, some have suggested an increase of adipose tissue in EVE-treated subjects even prior to fat grafting. Adipogenesis studies have shown that hypoxia and inflammation can stimulate differentiation of pre-adipocytes into mature adipocytes, yet no studies have evaluated this effect when preparing the recipient site.

METHODS: 28 SKH1 hairless mice were stimulated with a miniaturized model of EVE for 2 hours/day for 1 (Group 1) or 5 (Group 2) consecutive days. A rubber dome with an inner diameter of 1cm was applied to the skin on the dorsum of the mouse, 1cm lateral to the spine, and was connected to a suction pump set at 25mmHg. In each mouse, the contralateral non-stimulated site was used as control (NS). Tissue samples were harvested immediately after stimulation (n=7/group) or 48hr after stimulation (n=7/group). Paraffin-embedded samples stained with H&E were examined for gross morphology and edema. IHC staining and quantification was performed for CD45 (inflammatory cells) and Perilipin-1 (marker of metabolically active adipocytes). Western Blot was performed for PPAR-gamma expression (transcription factor inducing adipogenesis).

RESULTS: Immediately after stimulation, tissues were edematous and enriched in CD45+ cells in both groups. 48hr after the last stimulation, edema had regressed and inflammation was decreased in both 1-day and 5-day stimulated tissues. The number of adipocytes/mm of tissue increased 2.1-fold in group 1 and 3-fold in group 2 compared to NS ($p<0.05$). WB showed significant up-regulation of PPAR-gamma immediately after five days of stimulation compared to NS.

CONCLUSION: EVE induces a significant increase in number of adipocytes/mm of tissue, CD45+ cells and PPAR-gamma expression compared to NS skin. These changes are immediate, even after short periods of stimulation. Inflammation and hypoxia are known adipogenic cues that might be responsible for this finding. Further studies are needed to better understand the mechanisms of action of these elements separately.

126
Complication Rates of Fat Grafting Associated with Various Modalities of Breast Reconstruction

Zaahir Turfe, BS[1]; Alan Davis, PhD[2]; Ewa Komorowska-Timek, MD[3]

[1]Michigan State University College of Human Medicine, Grand Rapids, MI, [2]Grand Rapids Medical Education Partners, Grand Rapids, MI, [3]Michigan State University College of Human Medicine, Advanced Plastic Surgery, Grand Rapids, MI

PURPOSE: Fat grafting is gaining popularity as a solo or adjunct treatment modality in breast reconstruction. Complication rates of this procedure, however, have not been clearly elucidated. The current study reviews a large single surgeon cohort of fat grafting procedures to define complication rates of this technique in various reconstructive scenarios.

METHODS: All breast fat grafting procedures conducted by a single surgeon from 2010 to 2013 were included in the study. The patients' demographics, comorbidities, indications for fat grafting, technique of fat preparation, volume of transferred fat, and complications resulting from each procedure were noted. Indications for fat grafting were defined as follows: 1. contour deficiency over prosthetic or autologous flap 2. Breast reconstruction after mastectomy and/or implant failure 3. Post lumpectomy 4. Attempt to alter the skin after radiation 5. Congenital or cosmetic. Complications included infection, fat necrosis, cyst formation, wound dehiscence, sterile collection of necrotic fat, and abscess formation.

RESULTS: A total of 123 patients with average age of 50.8 ± 10.2 years underwent 173 fat grafting procedures. The average BMI of our patients was 26.5 ± 6.0. Seventeen of 123 (13.8%) were smokers, 5/123 (4%) were diabetic, and 17/123 (13.8%) were hypertensive. The indications for fat grafting were distributed as follows: countour deficiency over a prosthetic or autologous flap in 141/173 (81.5%) of cases, breast reconstruction after mastectomy and/or implant failure in 7/173 (4%) of cases, lumpectomy defect in 8/173 (4.6%) of cases, attempt to alter the skin after radiation in 9/173 (5.2%) of cases, and correction of congenital or cosmetic defects in 3/173 (1.7%) of cases. Five of 173 (2.9%) procedures were conducted due to a combination of 2 of the aforementioned indications. The mean follow up was 535 ± 34 days. Overall, complications occurred following 55/173 (32.3%) of the procedures. Majority of procedures were associated with prosthetic reconstruction (118/173, 68%), and there was no significant difference in complication rates of fat grafting as an adjunct to either prosthetic or autologous reconstruction (37/118 [31.4%] vs. 18/55 [32.7%], p=0.86). Furthermore, 68/173 (39%) procedures were conducted in association with radiation therapy, but there was no significant difference in complication rates in radiated vs non-radiated breasts (24/68 [35.3%] vs 31/102 [30.4%] p=0.5, respectively). The technique used to graft the fat (centrifugation vs straining) and the volume of transferred fat did not yield any statistically significant difference in outcomes irrespective of radiation history.

CONCLUSION: Fat grafting is an important modality utilized in cosmetic and reconstructive that offers great versatility in multiple clinical scenarios. Our data suggests that fat grafting can be performed in the setting of prosthetic breast reconstruction or radiation therapy without increasing post-procedural morbidity.

127
Expression of SDF-1alpha in Skin Can be Upregulated by Mechanical Stretch and Induce Migration of Bone Marrow-Derived Stem Cells into Expanded Skin

Shuangbai Zhou, MD; Jing Wang, MD; Chengan Chiang, MD; Qingfeng Li, MD, PhD
Shanghai Jiao Tong University, Shanghai Ninth People's Hospital, Shanghai, China

PURPOSE: Skin and soft tissue expansion is a procedure that stimulates skin regeneration by applying continuous mechanical stretching of normal donor skin for reconstruction purposes. We have reported that topical transplantation of bone marrow-derived mesenchymal stem cells (MSCs) can accelerate mechanical stretch induced skin regeneration. However, it is unclear how circulating MSCs respond to mechanical stretch in skin tissue.

METHODS: MSCs from luciferase-Tg Lewis rats were transplanted into a rat tissue expansion model and tracked *in vivo* continuously by luminescence imaging to observe MSCs migration during skin expansion. Expression levels of chemokines including MIP-1α, TARC, SLC, CTACK, and SDF-1α were evaluated in mechanically stretched tissues, as were their related chemokine receptors in MSCs. Chemotactic assays were conducted in vitro and in vivo to assess the impact of chemokine expression on MSC migration. Expanded skin sections were stained with anti-luciferase antibody, to mark migrated MSCs, and anti-K19, CD31 antibodies, to analyze differentiation of migrated MSCs.

RESULTS: MSC migration was observed in mechanically stretched skin during in vivo cell tracking. Mechanical stretching induced temporal upregulation of chemokine expression. Among all the tested chemokines, SDF-1α showed the most significant increase in stretched skin, suggesting a strong connection to migration of MSCs. The in vitro chemotactic assay showed that conditioned medium from mechanically stretched cells induced MSC migration, that could be blocked with the CXCR4 antagonist AMD3100, as effectively as medium containing 50 ng/ml rat recombinant SDF-1α. Results from in vivo study also showed that MSC migration to mechanically stretched skin was significantly blocked by AMD3100. Moreover, migrating MSCs expressed differentiation markers, suggesting a contribution of MSCs to skin regeneration through differentiation. Expanded skin from MSC Group had significant advantage in area and epidermal thickness than that from AMD-MSC Group. More proliferating cells were found in skin sections from MSC Group.

CONCLUSION: Mechanical stretching can upregulate SDF-1α in skin and recruit circulating MSCs through the SDF-1α/CXCR4 pathway. Migrated MSCs can promote skin regeneration by differentiating into structural cells and accelerating skin cell proliferation.

128
Developing Tumor-Suppressing Autologous Fat Grafts for Breast Cancer Survivors

Jolene Valentin, PhD; Wakako Tsuji, MD, PhD; Chris Chung, BS; Meghan McLaughlin, BS; Kacey Marra, PhD; Vera Donnenberg, PhD; Albert Donnenberg, PhD; J Peter Rubin, MD
University of PIttsburgh Medical Center, Pittsburgh, PA

PURPOSE: Autologous fat grafting is widely carried out in breast cancer patients, although there is a risk that fat tissues or adipose-derived stem cells (ASCs) may promote breast cancer progression. The incorporation of tumor-suppressing agents into fat grafting may represent an ideal method to reconstruct a natural appearing breast while minimizing local recurrence risk. We studied the differential sensitivities of ASCs and breast cancer cells to anti-breast cancer drugs. We also studied tumor development using estrogen receptor-positive BT-474 and triple-negative MDA-MB-231 breast cancer cell lines in Matrigel, and are currently developing a tumor-forming fat graft model using human adipose tissue.

METHODS: To study the sensitivity of ASCs when exposed to chemotherapeutic agents, human ASCs were isolated from non-diabetic female patients between 35 and 60 years of age (n=3). BT-474 and MDA-MB-231 breast cancer cell lines were obtained from ATCC. ASCs, BT-474, and MDA-MB-231 were exposed to various concentrations of paclitaxel or 4OH-tamoxifen. Proliferation, viability, and differentiation ability were assessed with CyQuant, MTT, and AdipoRed assays, respectively. To create a tumor containing graft, viable DAPI-exclusing BT-474 and MDA-MB-231 cancer cells were sorted directly into Matrigel containing 10000 irradiated feeder cells or into lipoaspirate at doses of 10, 100, 1000, 10000, or 100000 cells per injection. 50uL of Matrigel + cells or 300uL of lipoaspirate + cells were injected subcutaneously in NSG immunodeficient mice and sacrificed at 6 weeks. After sacrifice, the grafts were explanted and volumes were measured using gas pycnometry. The grafts were prepared for H&E, cytokeratin, and Ki-67 staining.

RESULTS: Dose-dependent inhibition was observed for paclitaxel and 4OH tamoxifen in ASCs and both breast cancer cell lines. IC_{50s} of paclitaxel were 15.7, 3.5 and 31.9 μM for BT-474, MDA-MB-231, and ASCs, respectively. IC_{50s} of 4OH tamoxifen were 4.4, 3.2×10^4 and 28.5μM on BT-474, MDA-MB-231, and ASCs, respectively. 4OH tamoxifen is known to be effective against ER+ cells, such as BT-474. ASCs differentiation into mature adipocytes was not inhibited by anti-breast cancer drugs exposure. The tumor volumes followed a dose-dependent trend for the Matrigel groups. Histology showed that cancer cells resided in Matrigel and in lipoaspirate grafts

containing higher doses of cancer cells at 6 weeks. These cells stained positive for human cytokeratin and Ki-67, verifying that cancer cells survived and are proliferative. Results are pending for BT-474 in lipoaspirate grafts.

CONCLUSION: Our findings suggest that incorporating paclitaxel in fat grafts for breast reconstruction following primary breast surgery is a viable option for decreasing the risk of local recurrence. 4OH tamoxifen can also be incorporated in fat grafting with ER-positive breast cancer patients. An in-vivo model employing lipoaspirate and cancer cells to test encapsulated chemotherapeutics is currently being developed with encouraging results. Taken together, incorporating encapsulated chemotherapeutic drugs in autologous fat grafts for breast reconstruction procedures is a feasible therapeutic option for breast cancer survivors.

129
Phosphodiesterase Type 5 Inhibition Enhances The Angiogenic Profile Of Adipose-derived Stem Cells

Marc Soares, MD; Piul S Rabbani, PhD; Clarence Ojo, MD; April Duckworth, MD; Hersh Patel, BS; Lukas Ramcharran, BS; Camille Kim, BS; Amanda Hua, BS; Jessica Chang, BS; Karan Mehta, BS; Nakul Rao, MD; Pierre B Saadeh, MD; Daniel J Ceradini, MD

New York University Department of Plastic Surgery, New York, NY

PURPOSE: Autologous fat grafting is a powerful clinical technique limited by unpredictable long-term retention of transplanted fat. We have previously reported that the use of phosphodiesterase type 5 inhibitors (PDE5i) markedly increases long term fat graft survival and improves predictability of the technique. Here, we investigate the underlying cellular and molecular mechanisms that impact adipose-derived stem cells (ASCs) in hypoxic engraftment conditions, and potentially contribute to graft durability. We hypothesize that targeted inhibition of PDE5 using FDA approved compounds will enhance ASC function in ischemic conditions, which may contribute to graft survival.

METHODS: We harvested ASCs from wild type adult mice and maintained them in vitro as previously described. We treated ASCs with PDE5i and incubated the cells in either normoxia or hypoxia, along with untreated controls. We monitored the cells over several timepoints spanning 14 days. At each time point, we assayed cell numbers using MTT assays. We also performed RT-PCR to examine changes in expression of the angiogenic marker, vascular endothelial growth factor (VEGF), and inducible nitric oxide synthase (iNOS). Using a well described preclinical model of autologous fat grafting, we analyzed ASC number and survival in transplanted grafts using flow cytometry ($CD45^- CD31^- CD36^+ CD105^+$).

RESULTS: ASCs demonstrated at least 20% increase in cell number and viability when cultured in hypoxic conditions compared to normoxia. Specifically, at 10 days in culture hypoxic ASCs demonstrate a 100% increase in cell viability. Treatment with PDE5i further emphasized this difference as early as 1 day after induction and resulted in at least 25% increase in hypoxic ASCs. VEGF expression in hypoxic ASC ($1.78 \times 10^{-3} \pm 3.64 \times 10^{-04}$ units) is significantly increased, as compared to normoxic ASCs ($5.60 \times 10^{-04} \pm 3.69 \times 10^{-04}$ units, $p<0.01$). Similar to the pattern seen with cell numbers, PDE5i treatment increases VEGF expression 2x in hypoxic ASCs ($p<0.01$). iNOS expression follows a similar trend where hypoxia alone provides an advantage, and PDE5i-treated hypoxic ASCs express 3 times more iNOS than that in hypoxia alone ($p<0.01$). In vivo, PDE5i treated grafts demonstrated

statistically significant increase in survival of donor derived $CD45^{-}$ $CD31^{-}$ $CD36^{+}$ $CD105^{+}$ ASCs, and a nearly two-fold increase in volume retention at three months.

CONCLUSIONS: Here we demonstrate that targeted PDE5 inhibition significantly increases ASC survival in transplanted grafts, while promoting a more angiogenic and vasoprotective phenotype. The strategy of targeted protection of both the donor vasculature and the function of ASCs in preserving this vasculature is a novel approach to improve reliability of autologous fat grafting. Use of FDA approved PDE5i is a rapidly translatable approach to increase predictability of clinical fat graft survival and modulate ASC function.

130
Platelet-Rich Plasma Promotes Fat Graft Survival via Stemness and Angiogenesis on Adipose-derived Stem Cells

Han-Tsung Liao, MD, PhD; Kokai Lauren, PhD; Kacey G Marra, PhD; J Peter Rubin, MD
UPMC, Pittsburgh, PA

PURPOSE: Platelet-rich plasma (PRP) containing multiple growth factors has been documented to enhance bone regeneration, wound healing and muscle or tendon healing. Recently, platelet-rich plasma (PRP) is reported to promote fat graft survival in both animal and clinical studies. However, the molecular mechanism is still not clear. The aim of this study is to determine the possible mechanism via in-vitro and in-vivo nude mice study.

MATERIALS AND METHODS: Human Platelets were purchased from HEMOCARE for the production of PRP. Human adipose-derived stem cells were isolated as per laboratory protocol. The ASCs were cultured under four conditions: 1. Regular DMEM medium, 2. Regular DMEM medium with PRP 3. Adipogenic medium 4. Adipogenic medium with PRP. The cell proliferation was assessed by CYQUANT and the adipogenesis were evaluated by AdipoRed stain and the qPCR of PPAR-gamma and FABP4 gene expression. The mRNA of stemness gene expression of ASCs was compared by qPCR of SOX-2, Nanog and Oct-4.The angiogenesis of ASCs was evaluated by qPCR of VEGF gene expression and endothelium tube formation assay. The nude mice were implant with fat graft with PRP as experiment and fat graft only as control group. The survival rate was analyzed by volume retention, the histomophometry of mature adipocyte area and vessel density assay by CD31 immunohistochemical stain.

RESULTS: Proliferation of ASCs was enhanced dramatically both in regular DMEM and adipogenic medium with PRP. The PRP-treated ASCs appeared smaller and more spindle in shape than ASCs in regular medium. The up-regulation of Sox-2, Nanog and Oct-4 further proved the more stemness of PRP-treated ASCs. In contrast, intra-cytoplasmic lipid accumulation was decreased after treatment with PRP. The qPCR also confirmed the down-regulation of adipogenesis on both PPAR-gamma and FABP4 gene expression in PRP-treated cells under adipogenic medium. The up-regulation of VEGF expression and the tube formation assay indicated angiogenesis of PRP-treated cells under regular medium. The in-vivo nude mice showed more fat graft retention in the PRP-treated group than fat graft only group ($p<0.05$). Histology indicated the greater adipocyte survival and more vessel formation in PRP-treated group.

CONCLUSION: Taken together, PRP may promote fat graft survival via proliferation of ASCs and its angiogenic

effect. The angiogenic effect of PRP itself and PRP-treated ASCs will enhance the vascular supply to maintain the adipocyte survival within fat graft. Furthermore, the stemness effect of PRP increases the renewal and differentiation capabilities of ASCs which can be the cell depot required in fat graft survival.

131
Adipose Derived Stem Cell Count is Influenced by Receipt of Chemotherapy in Breast Cancer Patients

Brian Mailey, MD[1]; Jennifer Baker, MD[1]; Ava Hosseini, MD[1]; Zeni Alfonso, PhD[2]; Paula Strasser, BS[2]; Kevin Hicok, PhD[2]; Steven R Cohen, MD[3]; Amanda Gosman, MD[1]; Marek Dobke, MD, PhD[1]; Anne M Wallace, MD[1]

[1]UCSD, San Deigo, CA, [2]Cytori Therapeutics, San Deigo, CA, [3]Faces+, San Deigo, CA

PURPOSE: The identification of mesenchymal stem cells (MSC) in adult human fat was first described in 2001. The clinical significance and therapeutic utility of these cells is still unclear. We sought to determine the relationship of MSC to receipt of previous systemic chemotherapy.

METHODS: All patients undergoing fat grafting to the breast after cancer reconstruction were offered participation in study. Patients were imaged with volumetric three-dimensional stereophotogrammetry preoperative and at selected time-points up to 6-months postoperative. Additional fat harvested in the operating room (mean 64 ± 38 grams) was analyzed for stromal vascular fraction cells per gram (c/g), colony forming units (CFU), percent viability and by flow cytometry for CD45, CD34, CD31 and CD146 markers. Patients were categorized by percent fat retention and by receipt of systemic and hormonal chemotherapy.

RESULTS: Between September 2012 and July 2013, 28 patients were accrued to study. The average age and BMI of the patients were 54, SD ± 10 years and 27.8, SD ± 5, respectively. Of these, 54% (N=15) previously received chemotherapy and 46% (N=13) did not. The mean cell count, c/g and percent viability for patients who received chemotherapy was higher than those who did not (2.27 x 106 vs. 1.06 x 106, p=0.01; 1.8 x 105 vs. 3.0 x 105, p=0.001; and 88% (SD ± 3.5), and 84% (SD ± 5), p=0.03, respectively). Stratified by timing of chemotherapy, c/g was higher for patients who received chemotherapy in a more distant past (3.1 x 105, vs. 2.8 x 105 vs. 1.8 x 105 for >18 months, ≤18-months and no chemotherapy, respectively, p=0.006).

CONCLUSION: Receipt of chemotherapy affects number of MSC present in fat. This finding may represent a response of fat-derived MSC to meet physiologic needs. The role these cells contribute to tissue repair and regeneration remains undefined, however their increase after systemic chemotherapy might indicate a rebound effect of the body shifting from a catabolic to an anabolic state.

132
The Key Components of Schwann Cell Differentiation Medium and the Effects on the Gene Expression Profile of Adipose Derived Stem Cells

Hakan Orbay, MD, PhD; Chris Little, BS; Brittany Busse, MD; Lee Lankford, MS; David E Sahar, MD
UCDavis Medical Center, Sacramento, CA

PURPOSE: Multiple protocols have been used in the past for differentiation of adipose-derived stem cells (ASCs) towards Schwann cells (SC) lineage with variety of growth factors. However the role of growth factors and chemokines in the differentiation medium are not well known. Our aim in this study is to define the importance of each component of a previously published ASCs-SC differentiation protocol.

METHODS: ASCs were isolated from rat inguinal fat pads and characterized with fluorescence assisted cell sorting (FACS). Multilineage differentiation potency of ASCs was confirmed with adipogenic, osteogenic and chodrogenic differentiation. Cells in culture flasks were divided into 6 groups. Cells in control group were supplemented with cell growth medium. Cells in group I were treated with 1 mM β-mercaptoethanol for 24 hours and 35 ng/ml all-*trans*-retinoic acid for 72 hours. Subsequently, SC differentiation medium [cell growth medium supplemented with 5 ng/ml platelet-derived growth factor (PDGF), 10 ng/ml basic fibroblast growth factor (bFGF), 14 μM forskolin and 252 ng/ml glial growth factor (GGF)] was added into cell culture flasks. These components were removed from differentiation medium sequentially to detect the changes in gene expression profile of ASCs towards SC differentiation. In group II differentiation medium lacked GGF. Group III lacked forskolin, group IV lacked bFGF, and group V lacked PDGF in the differentiation medium. Cells were cultured for 2 weeks in all groups. Fresh medium was added every 72 hours. The fold changes in the expression levels of genes S100, integrinβ4, and NGFR were evaluated with qRT-PCR and immunofluorescence (IF) staining.

RESULTS: Harvested ASCs were negative for CD31 and CD45, but positive for CD90. ASCs were successfully differentiated into adipogenic, osteogenic, and chodrogenic lineages as confirmed by oil O red, Alizarin red and Alcian blue staining respectively. Undifferentiated ASCs expressed a certain level of S100 gene but no integrinβ4 or NGFR. The highest expression of SC characterizing genes was observed in groups III and IV that lacked forskolin and bFGF respectively. The cells treated with complete differentiation medium showed a 3.2 fold increase in the expression of S100 but the expression of integrinβ4 and NGFR was significantly lower in comparison to groups III and IV. Without GGF, cells did not express significant levels of SC characterizing genes as observed in group II. Overall the gene expression profile of cells from group IV was the most compatible with SC differentiation in comparison to other groups. Our results suggested that bFGF does not have a significant role in the differentiation of ASCs into SC. Moreover, GGF has a key role in SC differentiation process. IF staining yielded parallel results with qRT-PCR.

CONCLUSION: Differentiation of ASCs into SC-like cells can be possible with a modified method utilizing a smaller number of growth factors. This study was the first step of a study to define a more clinically relevant and cost-effective SC differentiation protocol.

133
Gender Differences in Heterotopic Ossification

Kavitha Ranganathan, MD; Jonathan Peterson, BS; Oluwatobi Eboda, BS; Shailesh Agarwal, MD; Steven Buchman, MD; Paul Cederna, MD; Stewart Wang, MD, PhD; Benjamin Levi, MD

University of Michigan Health Systems, Ann Arbor, MI

PURPOSE: The ectopic formation of bone within soft tissue structures, or heterotopic ossification (HO), has been shown to occur most commonly in patients suffering from burn injuries, prolonged periods of immobilization, and trauma. Previous studies have quoted male gender as a risk factor in the development of HO. It remains unclear why males are more predisposed to this pathology as compared to females. In this study, we explore differences in ectopic bone formation between male and female mice in the setting of burn and non-burn models to quantify and characterize differences in heterotopic ossification.

METHODS: An Achilles tenotomy and burn model was used to study the in vivo and in vitro relationship between gender and heterotopic ossification. Mice were divided into burn and non-burn groups with 3 male or 3 female mice in each of the four groups. All mice received an Achilles tenotomy and micro-CT scans were performed at 5, 7, and 9 weeks to quantify the extent of heterotopic ossification in each group. Histology was performed following the course of uCT scans. In vitro, adipose-derived mesenchymal cells (MSCs) capable of forming bone were harvested from both male and female mice in burn and non-burn control groups. Each cell type was exposed to osteogenic differentiation media (ODM) and the osteogenic potential assessed by alkaline phosphatase and alizarin red stain and quantification. Osteogenic transcripts and proteins were assessed by qRT PCR and Western Blot analyses.

RESULTS: 3 male and 3 female mice were utilized in each burn and non-burn group. Female mice in the burn group formed less bone as compared to male mice in the burn group as quantified on CT scan at 5, 7, and 9 weeks. An average of 4.9 mm3 of ectopic bone formed following burn injury in female mice compared to 6.6 mm3 in male mice with burn injury ($p<.05$). Similarly, MSCs derived from male mice in the burn group were much more osteogenic in comparison to MSCs derived from female mice in the burn group at 2 hours ($p<.05$). A similar relationship between male and female quantities of bone formation was noted in the non-burn group at this time point.

CONCLUSIONS: We demonstrate that male mice form quantitatively more bone as compared to female mice based on data from micro-CT scans and histology immediately after Achilles tenotomy. Furthermore, MSCs derived from male mice in the burn group were more osteogenic than MSCs derived from their female counterparts. Going forward, we aim to identify the exact mechanism behind differences in HO formation between males and females so that such differences can be exploited to develop novel therapeutics.

134
Adipose Derived Stem Cells Express von Willebrand Factor and Factor VIII

Maricel Miguelino, MD; David Sahar, MD; Jerry Powell, MD
University of California, Davis, Davis, CA

PURPOSE: Hemophilia A is an x-linked recessive bleeding disorder due to a mutation of the coagulation Factor VIII (FVIII) gene that manifests as a deficiency or complete absence of FVIII. Patients with severe HA (FVIII levels <1%) experience severe bleeding in the joints that may result in debilitating hemarthroses, oropharygneal bleeds or fatal intracranial hemorrhage. Monogenic disorders such as HA is highly attractive for stem cell based therapy due to its broad therapeutic window were an increase in plasma clotting FVIII levels above 5% converts disease phenotype from severe HA to moderate HA reducing episodes of spontaneous bleeds, improving the patient's quality of life and may provide a permanent cure for the disease. Putative adipose derived stem cells (ASCs) represent an abundant and readily available source of stem cells that possess the ability to undergo multi-lineage differentiation analogous to mesenchymal stem cells (MSCs) from the bone marrow [1]. MSCs from bone marrow have been reported to contribute to endogenous FVIII production and to phenotypically correct hemophilia in murine and sheep[2].The aim of this study is to demonstrate that ASCs may contribute to endogenous production of FVIII and after ex vivo transduction, ectopically express sustained Factor VIII.

METHODOLOGY: ASCs were isolated from murine stromal vascular fraction (*n=6)*, and characterized via flow cytometry. Osteogenic, adipogenic, chondrogenic and endothelial differentiation was assessed in lineage-specific induction media after passage three. Identification of von Willebrand factor (vWF) and FVIII was conducted through immunocytochemistry. Lentiviral vector transduction of the ASCs with B-domain deleted FVIII tagged with green fluorescent protein (GFP) was performed. 72 hours after transduction, transgene FVIII expression was examined via immunofluorescence imaging and flow cytometry.

RESULTS: Isolated ASCs showed spindle shaped morphology after 5–7 days in culture. Flow cytometry showed that majority of ASCs were from mesenchymal origin. Adipogenic differentiation was characterized by microscopic observation of intracellular lipid droplets by Oil Red O staining. Osteogenic differentiation potential was confirmed by Alizarin red staining. Intense Alcian blue staining confirmed presence of proteoglycans in chondrogenic differentiation. Immunocytochemistry is positive for both vWF and Factor VIII. About 70% of the cells were GFP positive.

CONCLUSION: ASCs exhibit similar differentiation and multi-functional abilities as bone marrow MSCs. After endothelial differentiation and transduction with FVIII, ASCs express FVIII and vWF which stabilizes FVIII in circulation. ASCs may provide a novel approach and a valuable cell source for establishing cell-based gene therapy for hemophilia A.

1. Zhu, Y., et al., *Adipose-derived stem cell: a better stem cell than BMSC.* Cell Biochem Funct, 2008. **26**(6): p. 664–75.
2. Porada, C.D. and G. Almeida-Porada, *Treatment of Hemophilia A in Utero and Postnatally using Sheep as a Model for Cell and Gene Delivery.* J Genet Syndr Gene Ther, 2012. **S1**.

135
Improved Engraftment of Autologous Skin Grafts in Diabetic Mice with Adipose-Derived Stem Cells

Michael Hu, MD, MPH, MS; Wan Xing Hong, MS; Kshemendra Senarath-Yapa, MA, MBBChir, MRCS; Andrew Zimmermann, BS; Michael Chung, BS; Mikaela Esquivel; Adrian McArdle, MB, BCh, BAO(NUI), MRCSI; Graham Walmsley, AB; Zeshaan Maan, MBBS, MS, MRCS; Rebecca Garza, MD; H Peter Lorenz, MD; Michael Longaker, MD, MBA

Stanford, Stanford, CA

PURPOSE: Non-healing diabetic wounds are a major health concern in the US, affecting over 1 in 10 diabetic patients. With the increasing prevalence of diabetes, a significant rise in the number of diabetic patients suffering from non-healing wounds is also expected to occur. However, therapies currently available to diabetics are often insufficient to ensure satisfactory wound healing. Thus there is an urgent need for novel therapeutic strategies to address non-healing diabetic wounds. Autologous full thickness skin grafts are one of the most common procedures used for wound closure in both diabetic and nondiabetic patients. However, in diabetic patients skin graft rejection is common because of poor circulation around the graft and surrounding wound areas. One strategy that has been identified as particularly promising has been a cell-based therapeutic approach utilizing adipose-derived stem cells (ASCs). ASCs are an abundant and easily accessible population of adult pluripotent stem cells present in stromal tissue. They can be readily isolated from patients through minimally invasive techniques, potentially allowing for autologous transplantation. ASCs have been shown to promote wound healing in hypoxic environments by releasing various cytokines and growth factors at the wound to promote neovascularization. However, whether ASCs can increase the success of autologous full thickness skin grafts in a diabetic setting remains unclear. In this study we examine the ability of ASCs to mediate acceptance of autologous skin grafts in both wild-type and diabetic mice.

METHODS: Therapeutic ASCs were isolated from fat harvested from the inguinal fat pads of transgenic FVB-L2G mice. A 6mm full thickness excisional wound was created on the dorsum of wild-type FVB mice. The right ear of each mouse was harvested and the epithelial layer used as an autologous skin graft. Skin grafts were then placed over the cutaneous wounds. Wounds were treated with or without ASCs (5 x 10^5) in PBS cell suspension via injection under the wound bed. As the ASCs from the L2G transgenic mice luminesce when interacting with injected luciferin, this enabled the quantification of ASC survival *in vivo* through bioluminescent imaging (BLI). The effectiveness of the treatments was recorded over a period of two weeks via quantification of wound healing.

RESULTS: ASCs were found to promote acceptance of the autologous skin grafts in diabetic mice. All wild-type mice demonstrated successful engraftment of the autologous full thickness skin graft with or without ASC treatment. Diabetic mice with ASC treatment achieved 100% engraftment whereas only 20% of grafts were taken in control diabetic mice (*$p<0.03$). BLI revealed survival of ASCs when assessing for engraftment two weeks following wounding.

CONCLUSIONS: We demonstrate complete engraftment of all full thickness skin grafts in diabetic mice with therapeutic ASCs. This cell-based application may improve the efficacy of skin grafting in both diabetic and nondiabetic patients.

ACKNOWLEDGMENT: Support for this research was provided by the Sarnoff Cardiovascular Foundation and the California Institute for Regenerative Medicine (CIRM).

136
Centrifugation Compared to a Combined Mesh/telfa Technique for Fat Grafting: Mechanism, Outcomes and Effect on ADSCs

Harry M Salinas, MD; Felix Broelsch, MD; Justin Fernandes, MD; Saiqa Khan, MD; Michael C McCormack, MBA; Amanda Meppelink, BSc; Mark Randolph, MSc; William G Austen, Jr, MD
Massachusetts General Hospital, Boston, MA

PURPOSE: Fat grafting involves lipoaspirate harvest, isolation of adipocyte fraction, and subsequent injection of processed fat. Centrifugation is cumbersome and the mechanism by which it improves outcomes remains unclear. Hypotheses include fat concentration, reduction of inflammatory response by removal of nonviable components and concentration of adipose-derived stem cells (ADSCs). We performed a series of experiments to compare the process of centrifugation to a faster, simpler, processing method that combines mesh and telfa techniques.

METHODS: The mesh/telfa technique involves placing lipoaspirate on a 0.149mm nylon mesh, which sits on top of a thick layer of gauze. A 1:1 wash is performed with normal saline. Tumescence and debris are absorbed by the gauze through capillary action. Lipoaspirate was collected from nine females. In-vitro experiments included: 1.Quantification of lipoaspirate components by centrifugation at increasing speeds, 2.Quantification of components after processing with mesh/telfa, 3.Quantification of ADSCs in fat after centrifugation at 1,200g and mesh/telfa technique. ADSCs were identified as CD90/73+ and CD105/45- by FACS analysis of the stromal vascular fraction. In-vivo experiments were performed by grafting 1g aliquots into the flank of nude mice and harvesting after 4–6 weeks. Experiments included: 1.Graft survival at increasing centrifugation speed, 2. Survival of fat graft only and fat grafts mixed with various spin-off products, 3.Graft survival after centrifugation at 1,200g and mesh/telfa. Endpoints included weight and histology.

RESULTS: In-vitro: The infranatant remains constant above 1,200g. Oil separate out at 1,200g and increased linearly with higher speeds. The volume of fat remained constant above 5,000g. High-speed centrifugation of fat previously processed with mesh/telfa results in 90% fat and 10% infranatant. The total number of ADSCs in one gram of centrifuged fat was 1,603±2020 and 1,857±1832 cells in the mesh/telfa grafts. ($p = 0.86$). In-vivo: Weight at explantation after centrifugation at 50g, 1,200g, 5,000g, 10,000g, 23,000g were 0.58±0.11, 0.68±0.09, 0.72±0.13, 0.81±0.19, and 0.76±0.09 grams respectively. Histologically, 5,000g samples appeared healthiest with reduced injury. Five "add-back" groups were tested: 1.Fat plus oil, 2.Fat plus surgical tumescence, 3.Fat plus fresh tumescence, 4.Fat plus cell pellet and fresh tumescence, 5.Fat plus cell pellet. There were statistically significant differences between the fat only group (0.66 g ± 0.08) and groups mixed with tumescence (Groups 2–4: 0.56±0.12, 0.58±0.09, and 0.50±0.11 grams). Mixing with oil did not affect graft take (0.62±0.08 grams). In fact, fat plus oil superior histology scores, similar to control. Graft weight and histology after centrifugation at 1,200g and mesh/telfa was equivalent (0.73±0.12 and 0.72±0.13 grams).

CONCLUSION: The fat volume remains constant after 5,000g. Fat isolated by increasing centrifugation results in a linear increase in graft take up to 10,000g. The mesh/telfa technique results in similar fat graft volume, while the washing step removes blood and cellular components. ADSC content is equivalent after both processing techniques. The add-back data suggests that the mechanism by which centrifugation improves graft take is concentration of fat. Fat processed by the mesh/telfa technique results in equivalent results without a costly and time-consuming centrifuge.

SUNDAY, MARCH 9, 2014

SCIENTIFIC SESSION 8 GROUP C
WOUND HEALING
10:00 AM – 12:00 PM

SUNDAY, MARCH 9, 2014

137
Negative Pressure Wound Therapy with Instillation Accelerates the Granulation Response with Gene Expression Variations While Maintaining Comparable Tissue Quality Compared to Continuous and Non-Continuous Negative Pressure Wound Therapy in a Porcine Model

Diwi Allen, MS; Chris Lessing, PhD; Kathleen Derrick, MS; Roberta James, MS; Shannon Ingram; PE
KCI, San Antonio, TX

PURPOSE: Negative pressure wound therapy (NPWT*) can be coupled with automated delivery and removal of topical wound treatment solutions and suspensions (NPWTi[†]) or delivered in either continuous or non-continuous modes. This porcine study compared the granulation response, genomic response, and resulting tissue quality of NPWTi using normal saline with instillation foam dressing[‡] to NPWT using standard foam dressing[§] in continuous and non-continuous modes. The quality of the resulting granulation tissue was assessed using these key measures: collagen content, angiogenesis, extracellular matrix components, and cellular energetics.

METHODS: Full-thickness dorsal excisional wounds in pigs were treated with continuous NPWT, intermittent NPWT, dynamic (controlled variable) NPWT, and NPWTi with saline. Wound dimensions were determined from 3-D images collected on Days 0, 2, 5, and 7. On Day 7, animals were euthanized and specimens were collected for histopathological review and downstream processing for RNA and total protein. Gene expression was measured by quantitative real-time PCR. Tissue quality was assessed via enzyme-linked immunosorbent assays evaluating the following porcine-specific proteins: collagen type 1, vascular endothelial growth factor (VEGF), fibronectin, vitronectin, and cytochrome C oxidase.

RESULTS: Average granulation thickness of NPWTi with saline wounds was statistically greater ($p<0.05$) by 44%, 57%, and 40% than continuous, intermittent, and dynamic NPWT wounds, respectively. Per 3-D image analysis, NPWTi wounds revealed greater reduction in wound area and perimeter compared to all NPWT wounds ($p<0.05$) with a faster wound fill rate than continuous (40%; $p<0.05$), intermittent (25%; $p>0.05$), and dynamic (65%; $p<0.05$) NPWT wounds. Regarding gene expression, NPWTi was similar to that of continuous NPWT with some key differences. Genes for Tenascin C (an extracellular matrix, or ECM, glycoprotein) and urokinase plasminogen activator receptor (a mediator of ECM remodeling) were expressed 1.88 and 1.55 times greater, respectively, in NPWTi wounds than intermittent NPWT. Similarities in gene expression included collagen type I alpha 1 and colony stimulating factor 2 (over-expressed 2 times in both NPWTi and continuous NPWT compared to intermittent and dynamic NPWT). Regarding tissue quality, collagen type 1 content for NPWTi was comparable to NPWT in continuous and non-continuous modes and similar to unwounded tissue (~2000pg/ml per µg total protein). No difference was found between NPWTi and NPWT wounds regarding VEGF content, ~600pg/ml per mg. Vitronectin and fibronectin levels were also similar when comparing NPWTi to NPWT (~8000pg/ml per µg, and ~1225pg/ml per mg, respectively). Analysis of cytochrome C oxidase content also revealed similar levels, at ~12500pg/ml per mg, comparing NPWTi and NPWT wounds.

CONCLUSION: These porcine data suggest that NPWTi with saline may stimulate a faster rate of wound granulation than NPWT in continuous and non-continuous modes. This study also suggests that NPWTi may positively influence the expression of genes associated with wound healing and stimulate wound granulation with comparable vascular and matrix quality as continuous or non-continuous NPWT. *V.A.C.® Therapy, [†]V.A.C. VeraFlo™ Therapy, [‡]V.A.C. VeraFlo™ Dressing, [§]V.A.C.® GranuFoam™ Dressing (KCI USA, Inc., San Antonio, TX)

138
Staphyloccocus aureus Biofilms Impair Reepithelialization and Granulation Tissue Deposition in Cutaneous Wounds via a MyD88-Dependent Mechanism

Eugene Park, MD; Seok J Hong, PhD; Claudia Chavez-Munoz, MD, PhD; Wei Xu, PhD; Thomas A Mustoe, MD; Robert D Galiano, MD

Northwestern University Feinberg School of Medicine, Chicago, IL

PURPOSE: Toll-like receptors (TLRs) have mainly been studied for their role in the innate immune response, but they have also been shown to affect wound healing. The effects of TLR function on wound healing in the presence of bacterial biofilms have not been previously studied. In this study, we investigate the role of MyD88, an adaptor protein critical to the function of multiple TLRs, in the impairment of wound healing caused by *Staphylococcus aureus* biofilms.

METHODS: *In vivo* wound healing was analyzed using a murine model of *S. aureus* biofilm previously developed by our group. Six mm excisional wounds were created on the backs of MyD88 -/- mice and analyzed over time using a splinted wound model to minimize wound contraction. Wound healing was quantified by photo planimetry and by measuring epithelial gaps and granulation tissue thickness in cross-section using paraffin sections with immunohistochemical staining. *In vitro* scratch assays to measure cell migration were performed using the HaCat keratinocyte cell line and *S. aureus* biofilm exudate collected using a flow chamber model of bacterial biofilm formation.

RESULTS: MyD88 -/- mice (n=10) displayed delayed wound healing compared to wild-type C57bl/6 (WT) mice (n=9) as measured by the ratio of final wound size to initial wound size on both post-operative day (POD) 6 (WT: 0.710.16 vs. MyD88 -/-: 0.950.25; $p<0.05$) and POD 8 (WT: 0.510.23 vs. MyD88 -/-: 0.800.21; $p<0.0001$). Wound reepithelialization in WT mice (n=5) was delayed in the presence of *S.aureus* biofilm compared to non-biofilm controls on both POD 7 ($p<0.05$) and POD 10 ($p<0.05$). In MyD88 -/- mice (n=5), there was no significant difference in reepithelialization between biofilm and non-bioflim wounds on either POD 7 or POD 10. Granulation tissue deposition in non-biofilm wounds (n=5) was greater in WT mice compared to MyD88 -/- mice ($p<0.001$). In the presence of biofilm, this difference was no longer seen. Cell migration was delayed in MyD88-knockdown HaCat cells compared to WT (n=5) at both 16 hours ($p<0.01$) and 32 hours ($p<0.05$). In the presence of *S. aureus* biofilm exudate, migration was further impaired in WT ($p<0.05$) but not MyD88-knockdown cells. On immunofluorescence staining, WT biofilm wounds displayed 4-fold greater macrophage recruitment at POD 3 than MyD88 -/- biofilm wounds ($p<0.001$). Gross examination of immunofluorescence staining on POD 7 revealed greater M1-phase activation of macrophages in WT biofilm wounds compared to MyD88 -/- biofilm wounds. Transcription analysis revealed a higher upregulation of iNOS ($p<0.01$) and CCL2 ($0<0.05$) in WT biofilm wounds compared to MyD88 -/- biofilm wounds. Col1A1a expression was more highly upregulated in MyD88 -/- biofilm wounds ($0<0.05$).

CONCLUSIONS: In the presence of a *S. aureus* biofilm, MyD88 influences wound healing impairment by affecting keratinocyte migration, granulation tissue deposition, and the regulation of inflammation. By targeting the innate immune system, we may one day be able to develop therapeutics that control the host response to bacterial biofilms and improve biofilm wound healing.

139
Macrophages Regulate Tissue Fibrosis in Lymphedema

Swapna Ghanta, MD; Daniel A Cuzzone, MD; Nicholas J Albano, BS; Seth Z Aschen, BS; Ira L Savetsky, MD; Jason C Gardenier, MD; Walter J Joseph, III, BS; Babak J Mehrara, MD
MSKCC, New York, NY

PURPOSE: Lymphedema is a morbid condition that is characterized by fibrosis and progressive lymphatic dysfunction. We have previously shown that modulation of inflammatory responses not only decreases fibrosis but also prevents the onset of lymphedema suggesting that tissue remodeling and lymphatic function are related. In previous studies, we have found that lymphedema is associated with massive increases in the number of infiltrating macrophages. This is important because macrophages are known to be critical regulators of lymphangiogenesis and tissue remodeling implying that these cells may play a crucial role in regulating the link between these processes in lymphedema. The purpose of these experiments was, therefore, to use conditional ablation of macrophages after lymphatic injury to determine how these cells contribute to fibrosis and lymphatic function.

METHODS: Wild-type C57B6 mice were lethally irradiated and then reconstituted with bone marrow cells harvested from transgenic mice that express the simian diphtheria receptor (DTR) under the regulation of Cd11b (a macrophage specific gene). Mosaic mice created in this manner express the simian DTR gene on circulating/bone marrow derived macrophages enabling selective depletion of these cells after administration of minute amounts of diphtheria toxin. Bone marrow transplanted mice were allowed to recover and then underwent surgical ablation of the superficial and deep lymphatic vessels of the mid-portion of the tail to induce lymphedema. Experimental animals underwent macrophage depletion using DT beginning either immediately after surgery for 3 weeks, or for 3 weeks after lymphedema had become established (i.e. 3 weeks postoperatively). Control animals were treated with PBS. Tissue fibrosis and lymphatic function were then analyzed using histology, lymphoscintigraphy, and immunohistochemistry.

RESULTS: Treatment of mosaic-DTR mice with DT was well tolerated and resulted in significant depletion of macrophages systemically (>60% depletion in peripheral lymph nodes and tissues; $p<0.05$) as compared with controls. However, we did not note a significant decrease in overall inflammation as analyzed by CD45 staining (all leukocytes). Interestingly, we found that depletion of macrophages immediately after surgery improved lymphatic function as analyzed by Tc99 lymphoscintigraphy ($p<0.001$). In contrast, depletion of macrophages after lymphedema had become established (i.e. 3-weeks after surgery) was associated with increased fibrosis and impaired Tc99 lymph node uptake. Interestingly, there was no significant change in other hallmarks of lymphedema, such as adipose deposition or T-cell infiltration.

CONCLUSIONS: Our findings suggest that macrophages play an important role in the regulation of tissue fibrosis and lymphatic dysfunction in a mouse model of lymphedema. The finding that macrophage depletion immediately after surgery has different effects from depletion after lymphedema has become established suggests that these effects are complex, temporally regulated, and modulated by other tissue responses. Understanding these temporal changes is important for developing novel therapies for lymphedema and is a long-term goal of our lab.

140
Identification, Characterization, and Prospective Isolation of a Fibroblast Lineage Contributing to Dermal Development, Cutaneous Scarring, Radiation Fibrosis, and Cancer Stroma

Graham G Walmsley, BA[1]; Yuval Rinkevich, PhD[1]; Michael S Hu, MD[1]; Adrian McArdle, MB, BCh, BAO, MRCSI[2]; Zeeshan N Maan, MBBs, MS, MRCS[2]; Hermann P Lorenz, MD[1]; Irving L Weissman, MD[1]; Michael T Longaker, MD, MBA[1]

[1]Stanford University School of Medicine, Stanford, CA, [2]Stanford University, Stanford, CA

PURPOSE: Fibroblasts represent a heterogeneous population of cells with diverse functional and phenotypic features. Such diversity remains largely undefined due to phenotypic drift in vitro and a lack of unique surface markers for functional subclasses of fibroblasts. Here we track the contributions of two distinct fibroblast lineages, defined by embryonic expression of Engrailed-1 (En1) and Wnt1, to connective tissue formation in the context of dermal development, cutaneous wounding, radiation fibrosis, and cancer stroma.

METHODS: $En1^{Cre}$ and $Wnt1^{Cre}$ transgenic mice were crossed with $ROSA26^{mTmG}$ mice, which harbor a double-fluorescent reporter that replaces the expression of membrane-bound tomato red with membrane-bound green fluorescent protein following Cre-mediated recombination. The resulting offspring were used to trace En1- and Wnt1-derived fibroblasts, defined by their GFP positivity, into the dorsal and oral dermis respectively. Flow cytometry allowed for the isolation of En1-derived fibroblasts from the dorsal dermis of wild type mice on the basis of highly expressed surface molecules. Transplantation methodologies functionally corroborated these surface markers in the context of wounding healing, radiation fibrosis, and cancer stroma formation. Finally, we performed reciprocal transplantation of FACS-sorted fibroblast lineages between the dorsal back and oral cavity to assess whether differences in the outcomes of wound repair between cutaneous and oral dermis are a consequence of cell intrinsic vs. environmental properties.

RESULTS: Here we examined a distinct cellular lineage in the dorsal dermis, defined by embryonic expression of Engrailed-1, and characterized its contribution to connective tissue deposition during dermal development, cutaneous wound healing, radiation fibrosis, and cancer stroma formation. Using flow cytometry and in silico approaches, we identified CD26 as a surface marker that enables the prospective isolation of this fibrogenic lineage from the dorsal dermis. Microarray analysis of FACS-isolated En1- and Wnt1-derived fibroblasts revealed significant differences in their transcriptional programs that were otherwise masked by conventional harvesting/culturing methodologies. Reciprocal transplantation experiments further identified En1- and Wnt1-derived fibroblasts as functionally distinct lineages in terms of their migratory/secretory programs, and revealed that site-specific differences in scar formation between oral and cutaneous dermis are a consequence of lineage-intrinsic fibrogenic potential rather than extrinsic environmental effects.

CONCLUSION: These studies demonstrate that distinct tissue-resident fibroblast lineages are responsible for the majority of connective tissue deposition during dermal development, wound healing, radiation fibrosis, and cancer stroma formation. Furthermore, we define unique fibrogenic properties intrinsic to each lineage that explain differences in the scarring/fibrosis of cutaneous vs. oral dermis. These studies demonstrate that distinct fibroblast lineages represent unique cell types and hold promise for translational medicine aimed at in vivo modulation of fibrogenic behavior.

141
Influence of MAPK Signaling on Ischemic Wound Healing in the Elderly

Ran Ito, MD; Qixu Zhang, MD, PhD
MD Anderson Cancer Center, Houston, TX

PURPOSE: The majority of chronic wounds occurs in people over age 60 and is increasing at a rate of approximately 10% per year. However, there is still no effective treatment method for such wounds because the mechanism has not been fully elucidated. We have found both high ROS production and MMPs expression in the ischemic wound of young animal, which correlated with high levels of MAPKs. The present study aimed to test the hypothesis that the ROS/MAPK/MMPs signaling axis plays an important role in pathobiological process of chronic wound in elderly by using small interference RNA (siRNA) approach in a novel ischemic wound model.

METHODS: The delayed wound healing model based on an axial ischemic flap on the abdomen was created in 12 month-old male Fischer 344 rats. 80 μg DY547 labeled Non-targeting control siRNA and SMARTpool AP-1-siRNA was administered to ischemic wound tissue by injecting into superficial inferior epigastric artery (SIEA) of the animal for both control and experimental group respectively. The closure of the wounds was monitored and the wound tissue was analyzed on days 7 & 14 respectively (n=6).

RESULTS: The ischemic wounds showed significantly impaired closure compared to the normal acute wounds. 3-nitrotyrosine, a marker of oxidative stress, is markedly increased in ischemic wounds. IL-1, HIF-1α and VEGF receptor 2 were significantly decreased in ischemic wound tissue. The MMP9 and Cleaved Caspase 3 protein were increased dramatically, correlated with more collagen degradation. These data of control group suggested severe oxidative stress with excessive collage breakdown and increased apoptosis leading to wound closure impairment. The fluorescently labeled siRNA was successfully delivered and detected in the wound tissue. AP-1 siRNA treatment significantly improved ischemic wound healing and reversed the effects of oxidative stress on such wounds.

CONCLUSIONS: Specific agents can be selectively and accurately delivered to the wounds via an arterial pedicle in the novel model, enhancing the ability to study wound healing mechanisms. Blockage of ROS/MAPK/MMPs signaling axis with MAPKs- siRNA could be an important therapeutic approach for chronic non-healing wounds.

142
Prevention of Seroma and Post-operative Wound Complications Using Negative Pressure Wound Therapy Devices Following Panniculectomy in Massive Weight-Loss Patients

Marc E Walker, MD, MBA[1]; Victor Z Zhu, BA[1]; Matthew L Webb, AB[1]; Tracy Sturrock, MSN, NP-C[1]; Reuben Ng, BSc, MSc[2]; J Grant Thomson, MD[1]; P Niclas Broer, MD[1]; Stephanie L Kwei, MD[1]
[1]Yale University School of Medicine, New Haven, CT, [2]Yale University School of Public Health, New Haven, CT

PURPOSE: To compare the immediate application of continuous negative pressure wound therapy (NPWT) versus standard, closed-suction drains (CS) in prevention of seroma in body-contouring patients.

METHODS: In a prospective, randomized-controlled, single-surgeon study, patients seeking panniculectomy were randomized to NPWT or CS drains. Patients were compared on multiple demographic criteria including age, gender, BMI, incision length, pannus weight, nutritional status, comorbidities, prior surgery and duration of drain placement. Abdominal ultrasound was performed 2 weeks following drain removal to objectively quantify persistent fluid collections. Statistical analysis using T-test and logistic regression was performed.

RESULTS: The NPWT (n=12) and CS (n=10) groups showed no statistically significant differences in age (p=0.407), BMI (p=0.151), incision length (p=0.528), pannus weight (p=0.743), smoking status (p=0.594), diabetes (p=0.293), nutritional status (p>0.05), history of prior surgeries (p=0.378), or drain duration (p=0.429). Both BMI (r=0.679, p=0.001) and pannus weight (r=0.536, p=0.010) showed strong positive correlations with presence of seroma. No significant correlations were identified between age, incision length, and drain duration and presence of seroma (p>0.05). Following drain removal, the mean fluid volumes on ultrasound were 44.6cm3 (0–166) and 11.2cm3 (0–45) for CS and NPWT, respectively. There is a statistically significant difference is seroma presence in CS vs NPWT groups (p=0.037). Controlling for age, BMI, incision length, and drain duration, NPWT drain systems confer a 96.7% risk reduction in seroma presence when compared to standard, closed-suction drains in panniculectomy patients.

CONCLUSIONS: Negative pressure wound therapy drain systems reduce the risk of seroma presence in panniculectomy patients compared to standard, closed suction bulb drains. Increases in BMI and increases in pannus weight correlate with increases in presence of seroma formation. Continuous negative pressure wound therapy connected directly to drains may impact the post-operative outcomes in massive weight loss patients undergoing panniculectomy and other body-contouring procedures.

143
Morphologic and Histological Comparison of Hypertrophic Scar in Nude and Knockout Mice Deficient in T, B and Natural Killer Cells

Moein Momtazi, BSc, MSc, MD
University of Alberta, Edmonton, AB, Canada

PURPOSE: Xenotransplantation of human skin onto nude mice results in proliferative scars with morphologic and histological similarities to human hypertrophic scar (HSc). These observations prompted us to consider strains of knockout mice to investigate the effects of deleting subsets of immune cells on proliferative scar formation.

OUR OBJECTIVES ARE:
1. Demonstrate that grafting human skin onto TCR (T-cell receptor) αβ-/-γδ-/-, RAG (recombination activating gene)-1-/- and RAG-2-/-γc-/- mice results in scars morphologically and histologically consistent with human HSc.
2. Characterize histologic and cellular changes that occur in scars with removal of specific immune cell subsets.
3. Compare scar response over time nude and knockout mice.

METHODS: Nude, TCRαβ-/-γδ-/-, RAG-1-/- and RAG-2-/-γc-/- mice (n=20 per strain) were xenografted with split thickness human skin and euthanized at 30, 60, 120 and 180 days post-operatively. Control animals (n=5 per strain) were autografted with full thickness mouse skin. Scar biopsies and normal skin were harvested at each time point. Sections were stained with hematoxylin and eosin (H&E), Masson's trichrome and toluidine blue. Immunohistochemistry included anti-human HLA-ABC, α-smooth muscle actin (SMA), decorin and biglycan staining.

RESULTS: At 30 days post-operatively, xenografted nude, TCRαβ-/-γδ-/-, RAG-1-/- and RAG-2-/-γc-/- mice developed shiny, firm, elevated scars consistent with human. This scar morphology is in contrast to the flat, supple, inconspicuous scars observed in autografted controls. In nude mice, the average percent increase in scar thickness compared to the original skin graft was 254.0 ±7.4% ($p<-0.01$). Average percent increase in scar thickness for knockout animals was 265.3 ±10.8% for TCRαβ-/-γδ-/-, 164.7 ±10.2% for RAG-1-/- and 208.0 ±12.8% for RAG-2-/-γc-/- mice ($p<0.01$). Histologically, scars from all four strains of mice are hypercellular, hypervascular, possess an abundance of disorganized, whorl-like collagen fibers and express less decorin compared to normal skin. Positive staining for α-SMA expressing myofibroblasts, a pathognomonic feature of HSc was seen in all four strains over time. Compared to nude mice, knockout animals demonstrated a greater capacity for scar remodeling manifested by decreasing average scar thickness and alteration in α-SMA staining patterns over time.

CONCLUSION: Split thickness xenografts transplanted onto TCRαβ-/-γδ-/-, RAG-1-/- and RAG-2-/-γc-/- mice result in murine scars with morphologic and histologic features of human HSc. Remodeling of murine scars generated in knockout animals is analogous to changes known to occur in human HSc and suggests scars in these animal models may better represent the natural history of HSc.

144
Cd4+ Cells Are Key Regulators of Pathologic Changes in Lymphedema

Daniel A Cuzzone, MD; Nicholas J Albano, BS; Swapna Ghanta, MD; Seth Z Aschen, BS; Ira L Savetsky, MD; Jason C Gardenier, MD; Walter J Joseph, BS; Jeremy S Torrisi, BA; Gina T Farias-Eisner, BA; Babak J Mehrara, MD
Memorial Sloan Kettering Cancer Setting, New York, NY

PURPOSE: Lymphedema is a common complication of cancer treatment afflicting about 1 in 3 women who undergo lymph node dissection for breast cancer. We have previously shown that the absence of CD4+ cells either by antibody depletion or in transgenic CD4 knockout mice prevents development of lymphedema after lymphatic injury suggesting that CD4+ inflammation is necessary for this process. However, it remains unclear if CD4+ cells alone are sufficient to induce the pathologic changes that occur after lymphatic injury. This distinction is important since it implies that CD4+ cells play an active role in the pathology of this disease. The purpose of this study was therefore to determine how adoptive transferred CD4+ cells differentiate and regulate development of lymphedema in transgenic mice lacking CD4 cells (CD4KO).

METHODS: Adult female CD4KO mice underwent microsurgical excision of the superficial and deep lymphatics of the mid portion of the tail. Beginning two weeks postoperatively and weekly thereafter, experimental animals (n=8) were adoptively transferred using retro-orbital injections with 10e7 CD4+ cells harvested from the spleens of syngeneic female C57B6 mice using negative magnetic selection and expanded in vitro. Control animals (n=8) received retro-orbital injections of PBS. Tail volumes were recorded weekly using caliper measurements and calculated using the truncated cone formula. Lymphatic function (uptake of Tc99) as well as histological changes in the tail were analyzed using a variety of techniques 6-weeks postoperatively based on our previous studies demonstrating onset of lymphedema changes at this time point.

RESULTS: In vitro expanded CD4+ cells maintained CD4+ markers but did not demonstrate evidence of T cell maturation or activation as analyzed by flow cytometry. Adoptive transfer of 10e7 cells resulted in significantly increased numbers of these cells in the spleens and lymph nodes of recipient mice (554 and 75 fold change respectively). Adoptively transferred experimental mice had significantly greater tail volume and decreased lymphatic transport capacity (Tc99) as compared with controls (both $p<0.001$) 6 weeks after tail surgery. In addition, consistent with histological changes noted in clinical lymphedema, we found that CD4+ cell adoptive transfer promoted significant subcutaneous adipose deposition in the regions of the tail distal to the zone injury ($p<0.05$). Moreover, using flow cytometry and immunohistochemistry we found

that there was significant accumulation of CD4+ cells in the dermis/subcutaneous fat ($p<0.001$) and that this response was associated with a significant fibrotic response (type I collagen deposition; $p<0.03$ compared with controls). Interestingly, our preliminary studies have not demonstrated differences in Th1/ Th2 differentiation, however, these studies are ongoing.

CONCLUSION: We have shown that the adoptive transfer of CD4+ cells into CD4KO mice recapitulates the histopathologic findings associated with wild type mice following ablation of tail lymphatics. Specifically, adoptive transferred CD4+ cells home to and are sufficient to induce fibrosis, chronic inflammation, and adipose deposition in the regions of the tail distal to the zone of injury. These findings therefore suggest that CD4+ cells play an active role in the pathology of lymphedema. Future studies will determine how CD4+ cell differentiation contributes to this process.

145
Human Keratinocytes Have Two Distinct Cell Proliferation Patterns on Timelapse Imaging in Vitro with 8-Cell Microarrays Revealing Early Molecular Identifiers

Amit Roshan, MRCS(Eng)[1]; Benjamin D Simons, PhD[2]; Kasumi Murai, PhD[3]; Philip H Jones, PhD, FRCP[3]

[1]Departments of Plastic Surgery and Oncology, University of Cambridge, Cambridge, United Kingdom, [2]Cavendish Laboratory, TCM, University of Cambridge, Cambridge, United Kingdom, [3]Hutchison/ MRC Research Laboratories, Cambridge, United Kingdom

PURPOSE: Human keratinocytes are commonly used during reconstruction either as sheet grafts or passaged in vitro cultures, but direct evidence for the drivers of proliferation after transplantation are limited. Recent genetic lineage tracing studies in vivo have defined the cellular behavior in homeostatic mouse epidermis. Here, the inter-follicular epidermis is renewed by stochastically dividing progenitors and also contains a smaller second population of slow cycling stem cells which self renew and generate progenitor cells. Slow cycling cells do not participate in homeostasis but proliferate extensively following wounding. We examine the proliferation patterns in primary and cultured human keratinocytes to inform regenerative strategies.

METHODS: Using in vitro timelapse imaging, we observed primary adult and cultured neonatal keratinocytes at single-cell resolution over 7 days. We recorded spatial and division outcome for related cells. Monte Carlo simulations and combinatorial statistics were used to predict population colony size distributions. Supplementation or withdrawal of growth factors(Epidermal Growth factor(EGF) or R-Spondin) were used to assess environmental responses to proliferation. Microarrays of 8-cell clones at 60 hours post-plating were performed on Affymetrix GeneChip® Human Gene 1.0ST Array.

RESULTS: Two distinct growth patterns emerged from 2335 divisions in 83 colonies. The first group of cells showed behaviour similar to murine progenitors, dividing to generate two differentiated daughters, two progenitor daughters or one progenitor and one differentiated daughter. Division outcome in cell pairs were independent in neighbours or closely related cells. The probabilities of generating two progenitor daughters or two differentiated daughters were similar(38±3% or 34±2%), as in vivo. In consequence, colonies derived from these progenitor-like cells increasingly accumulated differentiated cells and eventually stopped dividing. The second group exhibited no divisions producing two differentiated daughters in the first four rounds of division, with 90% of divisions

producing two dividing cells and 10% one differentiated and one proliferating cell. Here too, division outcomes were independent of neighbours or close relations. These stem-like cells generated colonies containing hundreds of cells, mostly proliferating.

Combinatorial statistics using the timelapse data predicted the distribution of clone sizes in a large sample of cells (n=1462) cultured for 7days, indicating the probabilities of each type of division were balanced as in vivo. Hypersupplementation (20ng/mL) or withdrawal (0ng/mL) of EGF, or addition of R-Spondin to the culture imbalanced the generation of proliferating or differentiating cells indicating that the fate of the progenitor-like cells was subject to external regulation. Transcriptional analysis revealed a distinct pattern of gene expression in 8-cell colonies derived from stem and progenitor-like cells. Validation of these results by immunostaining revealed the proportion of cells expressing differentiation associated genes in progenitor-derived colonies in accordance with the timelapse data.

CONCLUSION: In summary, this is the first direct observation of two modes of cell proliferation in human keratinocytes, revealing a stem-like and progenitor-like population similar to mouse in vivo. We identify potential therapeutic targets for patients with large area skin loss or with systemic healing impairments. This also provides mechanistic insights why EGF supplementation in skin grafting has been of limited benefit after promising initial human trials.

146
Diet-Induced Obesity Results in Lymphatic Dysfunction and Impaired T Cell Function

Nicholas J Albano, BS; Daniel A Cuzzone, MD; Swapna Ghanta, MD; Seth Z Aschen, BS; Gina T Farias-Eisner, BA; Ira L Savetsky, MD; Jason C Gardenier, MD; Walter J Joseph, BS; Jeremy S Torrisi, BA; Babak J Mehrara, MD

Memorial Sloan-Kettering Cancer Center, New York, NY

INTRODUCTION: Obesity induced inflammation is a major contributor to morbidity from a variety of disorders including atherosclerosis, cancer, and metabolic syndrome. Although many studies have focused on the cardiovascular effects of obesity, the negative effects of dietary changes on the lymphatic system remain largely unknown. This gap in our knowledge is important since the lymphatic system is a critical physiologic regulator of inflammatory responses, a key mechanism by which the negative effects of obesity are exerted. We have previously shown that obesity results in significant architectural changes in peripheral lymph nodes. The purpose of these experiments was to determine the functional effects of these changes on immune responses.

METHODS: We used a well-described diet induced obesity (DIO) model in which adult male C57BL/6J mice were fed a high fat (60%) and compared with control mice fed a normal chow diet for 10 weeks. To test humoral immunity, we vaccinated DIO or control mice with ovalbumin (OVA) and analyzed serum anti-OVA IgG1 titers 3 weeks after vaccination. Additionally, B and T cells were isolated from peripheral lymph nodes, cultured, and re-stimulated in vitro to analyze cytokine responses using ELISA. To assess cellular immunity, we induced contact hypersensitivity responses in the ear using 1-fluoro-2,4-dinitrobenzene (DNFB). Responses were measured using caliper measurements, immunohistochemistry and flow cytometry to analyzed gross and cellular inflammatory responses, respectively. Finally, we analyzed inflammatory lymph node lymphangiogenesis in obese and control animals to determine how draining lymph nodes respond to inflammatory stimuli.

RESULTS: Consistent with our previous studies, we found that DIO mice had significantly smaller lymph nodes as compared with controls; however, despite these changes, DIO mice demonstrated comparable anti-OVA IgG1 titers and B cell cytokine production as compared with controls. In contrast, T cells isolated from DIO mice demonstrated a significant decrease in both interferon gamma (IFN-g) and IL4 production after stimulation in vitro ($P<0.05$ for both). Further supporting changes in T cells in response to obesity was our finding of increased contact hypersensitivity responses to DNFB. In these experiments, obese mice displayed a significant increase in peak

inflammation (160% increase) as compared to controls. More importantly, we found that obese mice required a much longer period of time to clear inflammatory responses as compared with controls (11.75 vs. 8.2 days; $p<0.05$). Finally, although we found only modest changes in inflammatory lymph node lymphangiogenesis, we found significant changes in T cell populations in DIO mice as compared to controls (P=0.0003).

CONCLUSIONS: This study is the first to show that DIO results in significant architectural and functional changes in lymph nodes and lymphatic regulation of inflammation. Although the B cell responses were relatively unchanged by obesity, we found that DIO results in exaggerated T cell inflammation and impaired T cell memory responses. These changes not only increase the intensity of inflammation but, more importantly for the pathology of obesity, impair its resolution. This finding is critical and suggests that pathologic changes in the lymphatic system may exacerbate and contribute to the wide-ranging pathologic responses to obesity.

148
Use of Bmp Type I Alk-3 Knockout Mice to Develop Novel Treatment Strategies for Trauma-Induced Heterotopic Ossification

Benjamin Levi, MD; Shailesh Agarwal, MD; Jonathan Peterson, BS; Eboda Oluwatobi, BS; Kavitha Ranganathan, MD; Yuji Mishina, PhD; Stewart C Wang, MD, PhD; Steven R Buchman, MD, PhD; Paul S Cederna, MD

University of Michigan, Ann Arbor, MI

PURPOSE: Heterotopic ossification (HO) is a debilitating process characterized by the formation of ectopic bone following trauma, burn injury, and amputations. HO formation in trauma and burn patients is poorly understood at a mechanistic level, contributing to the lack of therapeutic options. In this study, we demonstrate the role of BMP type I receptor Alk3 in HO development and target downstream Alk3 signaling with a novel small molecule to prevent HO.

METHODS: Conditional Alk3 knockout (KO) mice were engineered using a C57BL/6 background; these mice are no longer able to express Alk3 upon exposure to the AdCre adenovirus. Mesenchymal stem cells (MSCs) from bone marrow and adipose tissue were harvested from these mice (N=4/group). These MSCs were then exposed to AdCre or AdLac (control virus) with subsequent assessment of osteogenic differentiation using qRT-PCR. A separate set of wild type and conditional Alk3 KO mice underwent Achilles tenotomy with 30% total body surface area partial thickness burn (N=4/group). Mice underwent injection of AdCre or AdLac (control) at the tenotomy site. An additional set of wild type mice underwent injection of the small molecule LDN-193189, a known Alk3 pathway inhibitor. Serial micro-CT scans were completed 1–9 weeks post injury and HO volume was assessed. Functional impairment was assessed by ankle range of motion (ROM).

RESULTS: AdCre-mediated knockout of Alk3 resulted in significantly decreased osteogenic capacity of MSCs as demonstrated by reduced alkaline phosphatase (ALP) stain, ALP enzymatic activity, and a three fold decrease osteoid deposition by alizarin red stain ($p<0.05$). In vivo ectopic bone formation was significantly reduced after 9 weeks in ALK-3 KO mice which received the AdCre injection at the tenotomy site by μCT scan ($n=4$, $p<0.05$). Ankle range of motion was similarly significantly enhanced in mice with introduction of AdCre in ALK-3 KO mice ($p<0.05$). Small molecule inhibition of downstream Alk-3 signaling with a novel small molecule LDN-193189 resulted in a dramatic decrease in osteogenic differentiation of MSCs in vitro and abrogated HO formation and ROM in vivo.

CONCLUSION: Alk3a plays a vital role in the osteogenic response to burn injury with respect to MSC osteogenic differentiation and HO development. Introduction of AdCre in conditional KO Alk3 mice reduces HO and joint contractures. Novel small molecule inhibitors such as LDN-193189 may be used to inhibit Alk3 signaling and prevent the formation of HO in patients in the future.

SUNDAY, MARCH 9, 2014

SCIENTIFIC SESSION 9 GROUP A
ISCHEMIA, REPERFUSION & TUMOR BIOLOGY
1:00 PM – 2:00 PM

SUNDAY, MARCH 9, 2014

149
Effect of Low Energy Laser on Skin Flap Survival: A Study in Murine Dorsal Skin Flap Model

Dhaval Bhavsar, MBBS[1]; Mayer Tenenhaus, MD FACS[2]

[1]University of Kansas Medical Center, Kansas City, KS, [2]University of California San Diego, School of Medicine, San Diego, CA

INTRODUCTION: Random pattern skin flaps are commonly employed in reconstructive surgery. Despite general dimensional design guidelines, distal flap necrosis occurs with some regularity. The application of Low energy LASER (LEL) at 635 nm has been shown to augment mitochondrial activity and ATP production. We studied effects of LEL on tissue perfusion, tissue survival and cytokine response in a murine skin flap model.

MATERIALS AND METHODS: A caudally based skin flap, 1.5 cm x 4 cm was designed over the dorsum of mice (n=28). Study group (n=14) received 635 nm Laser irradiation, 2 min. every day for up to 4 days, beginning immediately after surgery. Control group (n=14) did not receive LEL treatment. All other care was identical. Six animals in each group were sacrificed 24 hrs after surgery to obtain tissue samples for TNF-alpha. Laser Doppler measurements were performed immediately before and after surgery and on post-operative days 1, 4, and 7 for rest of the 8 animals in both groups. These animals were euthanized on day 7 and digital photos of flaps were taken. Flap necrosis was calculated with image analysis software. Six animals received anesthesia but did undergo surgery and served as SHAM subjects for skin biopsy for TNF-alpha levels.

RESULTS: The mean flap loss in control and study animals was 54.6% and 23.7% respectively ($P<0.01$, ANOVA). The mean TNF-alpha levels for control and study groups were 11.72 and 1.92 ($p=0.014$, t-test) fold higher respectively when compared to SHAM animals. Animals in both groups demonstrated uniform pattern of increased perfusion and vasodilatation at the base of the flap peaking on day 4 but study groups showing significantly less vasodilatation. Study animals demonstrated higher tissue perfusion at the distal end of the flap compared to control animals after day 1 lasting through day 7.

CONCLUSION: LEL improved flap survival in this murine dorsal skin flap model. Study animals demonstrated improved tissue survival and perfusion at the distal end in presence of less vasodilatation at the base and reduced inflammatory response. We plan to study the metabolic effects of LEL on tissues in ischemic and hypoxic environment.

150
Local Mild Hypothermia (30–32°C) is Effective in Protection of Ex Vivo Human Skeletal Muscle from Hypoxia/ Reoxygenation Injury

Anne O'Neil, MD, PhD, FRCS (C)[1]; Stefan Hofer, MD, PhD, FRCS (C)[2]; Homa Ashrafpour, BSc[1]; Ning Huang, MD[1]; Toni Zhong, MD, FRCS (C)[2]; Christopher Forrest, MD, MSc, FRCS (C)[1]; Cho Y pang, PhD[1]

[1]Hospital for Sick Children, Toronto, ON, Canada, [2]Toronto General Hospital, Toronto, ON, Canada

INTRODUCTION: In reconstructive surgery, skeletal muscle may endure protracted ischemia before reperfusion which may lead to significant ischemia/reperfusion injury. Other investigators reported that low local hypothermia (local cooling at 4–10°C) significantly reduced ischemia/reperfusion injury in skeletal muscle of different species of laboratory animals. However, this range of severe low local hypothermia is known to induce capillary damage. More recently, other investigators reported that low local mild hypothermia at 32–34°C significantly reduced ischemia/reperfusion injury in rabbit rectus femoris muscle in vivo. However, this infarct protective effect of low local hypothermia has not been tested in human skeletal muscle. The objective of this study was to use our established ex vivo human skeletal muscle culture model to study the efficacy of low local mild hypothermia (30–32°C) in salvage of human skeletal muscle from hypoxia (ischemia)/ reoxygenation (reperfusion) injury.

METHODS: Human rectus abdominus muscle strips (~ 0.5 X 0.5 X 15mm) derived from muscle biopsies were cultured in Krebs buffer bubbled with 95% N_2 / 5% CO_2 (hypoxia) or 95% O_2/5% CO_2 (reoxygenation). Control muscle strips underwent 6h normoxia at 37°C (normal thermia). Other skeletal muscle groups underwent 4h hypoxia/2h reoxygenation in normal thermia at 37°C or in low local hypothermia at 32°C, 30°C or 10°C. Skeletal muscle viability, injury, and energy content were assessed by measuring 3-(4,5-dimethylthiazol-2-yl)-2-5-diphenyl-2H-tetrazolium bromide (MTT) reduction, lactate dehydrogenase (LDH) release, and adenosine triphosphate (ATP) content, respectively.

RESULTS: The MTT reduction in the skeletal muscle of the normoxic control group was 0.66 ± 0.08 optical density (OD)/ mg wet wt. This MTT reduction was significantly reduced to 0.24 ± 0.03 OD/mg wet wt. ($n=6$; $p<0.05$) in the treatment group subjected to 4h hypoxia/2h reoxygenation at 37°C. Importantly, this MTT content was significantly ($p<0.05$) increased in the treatment groups (n=6) subjected to 4h

hypoxia/2h reoxygenation at 32°C (0.42 ± 0.04 OD/mg wet wt.; n=6), at 30°C (0.44 ± 0.42 OD/mg wet wt.; n=6) and at 10°C (0.39 ± 0.05 OD/mg wet wt.; n=6). There was no significant difference in MTT content among these three hypothermial treatment groups. The skeletal muscle contents of LDH and ATP are being analyzed at the present time, and will be ready for presentation at the meeting.

CONCLUSION: The data which we have generated thus far indicate for the first time that local mild hypothermia between 30°C to 32°C is effective in salvage of ex vivo human skeletal muscle from hypoxic/reoxygenation injury compared with the severe 10°C hypothermia. The mechanism of local mild hypothermia (30°C to 32°C) is being studied in our laboratory. Our results support the design of clinical study of local mild hypothermia (30–32°C) for prevention and/ or salvage of skeletal muscle from ischemia/ reperfusion injury in transplantation or replantation surgery.

151
Short Hairpin RNA Interference Therapy for Diabetic Murine Wound Closure and Hindlimb Ischemia

Kevin J Paik, AB[1]; Robert Rennert, BS[1]; Michael T Chung, BS[1]; Michael Sorkin, MD[1]; Dominik Duscher, MD[1]; David Atashroo, MD[1]; Hsin-Han Chen, MD[1]; Shane D Morrison, MS[1]; Andrew Zimmermann, BS[1]; Allison Nauta, MD[1]; Sae-Hee Ko, MD[1]; Ruth Tevlin, MD[1]; Elizabeth Zielins, MD[1]; Michael S Hu, MD[1]; Adrian McArdle, MD[1]; Graham Walmsley, BS[1]; Kshemendra Senarath-Yapa, MD[1]; Wan Xing Hong, MS[1]; Rebecca M Garza, MD[1]; Christopher Duldulao, BS[1]; Taylor Wearda, BS[1]; Arash Momeni, MD[1]; Joseph C Wu, MD, PhD[2]; Geoffrey C Gurtner, MD[1]; Michael T Longaker, MD, MBA[1]; Derrick C Wan, MD[1]

[1]Hagey Laboratory for Pediatric Regenerative Medicine, Department of Surgery, Plastic and Reconstructive Surgery Division, Stanford, CA, [2]Department of Radiology and Department of Medicine, Division of Cardiology, Stanford, CA

PURPOSE: The transcription factor hypoxia-inducible factor 1-alpha (HIF1A) is responsible for the downstream expression of over 60 genes that affect cell survival and metabolism in hypoxic conditions, including angiogenic growth factors. However, under normoxic circumstances, HIF1A is hydroxylated by prolyl hydroxylase 2 (PHD2), ubiquitinated, and degraded with a biological half-life of only 5 minutes. The present study investigated the therapeutic potential of inhibiting HIF1A degradation through short hairpin RNA (shRNA) knockdown of PHD2 for the treatment of diabetic wounds and ischemic hindlimbs in a murine model.

METHODS: PHD2 and control shRNAs were used to transfect mouse fibroblasts in vitro. Protein and RNA were harvested for Western blot and for qRT-PCR to evaluate PHD2 knockdown. qRT-PCR was also used to measure subsequent expression of downstream angiogenic genes. For assessment of plasmid function in vivo, six-millimeter full thickness wounds were created on the dorsa of diabetic db/db mice. Wounds were then injected with either PHD2 shRNA or control shRNA. Sample protein and RNA were collected from wounds for Western and qRT-PCR confirmation of in vivo PHD2 knockdown. Wound healing was then monitored and measured photometrically every two days till closure. Finally, ischemic hindlimbs were perfused with PHD2 or control shRNAs. Muscle ischemia

was analyzed histologically and distal digit tip necrosis was evaluated.

RESULTS: PHD2 knockdown in diabetic mouse fibroblasts resulted in enhanced expression of multiple angiogenic factors compared to control shRNA-treated fibroblasts. Diabetic skin wounds treated with PHD2 shRNA were observed to close within 14 ±0.47 days while control shRNA-treated wounds closed at 18 ±1.36 days. Finally, perfusion of ischemic hindlimbs with PHD2 shRNA resulted in decreased muscle necrosis histologically and no distal digit tip necrosis.

CONCLUSION: Nonviral shRNA treatment holds significant promise as a future avenue for gene therapy. This study demonstrates that knockdown of regulatory factors involved in angiogenesis, as explored here with PHD2, might present new opportunities for wound healing treatments.

152
Pharmacologic Inhibition of Phosphodiesterase 5 as a Strategy to Improve Outcomes in Microvascular Surgery

Marc Soares, MD; Piul Rabbani, PhD; April Duckworth, MD; Nick Rao, MD; Jessica Chang, BA; Pierre B Saadeh, MD; Karan Mehta, BA; Amanda Kua, BA; Daniel Ceradini, MD

NYU, New York, NY

PURPOSE: Ischemic microvascular injury compromises the endothelial barrier that maintains tissue homeostasis and initiates the inflammatory cascade. Following reperfusion, vascular injury is exacerbated and poses a critical clinical challenge to microsurgery, particularly with regards to vascularized composite allotransplantation. Phosphodiesterase 5 inhibitors (PDE5i), most commonly represented by the FDA-approved drug sildenafil citrate (trade-name Viagra), can potentiate vasodilation in ischemic vasculature and suppress inflammatory pathways. If ischemic injury to the endothelium initiates a pathologic cascade leading to impaired revascularization, persistent tissue hypoxia, and accelerated inflammation, then we hypothesize that pharmacologic treatment microvascular flaps with sildenafil will improve tissue physiology and survival in the context of prolonged ischemia.

METHODS: Using in vitro and in vivo models of ischemia-reperfusion injury (IRI), we characterized the effect of FDA-recommended doses of sildenafil (10nM and 100nM) on vascular inflammatory markers. Functionally, an adhesion assay was performed to assess the effect of PDE5i on the ability of the vascular endothelium to reduce allogenic lymphocyte adherence. In vivo, using an established rat model of VCA, composite flaps were perfused with sildenafil-containing perfusate and transplanted into allogenic rats. Laser doppler assess tissue perfusion in the immediate post-operative period.

RESULTS: PDE5-inhibition decreased endothelial expression of vascular inflammatory markers ICAM-1 and MCP-1 following ischemia reperfusion injury (3.4-fold, and 8.1-fold reduction from non-treated controls, respectively $p<0.01$), while increasing vasculoprotective expression of VEGF and eNOS (2-fold & 4.5-fold respectively compared to non-treated controls $p<0.05$). Functionally, PDE5i-treatment correlated with a 23% decrease in allogenic lymphocyte adhesion compared to non-PDE5i controls ($p =0.04$). In the immediate post-operative period, PDE5i-allografts demonstrated a 3-fold increased vascular perfusion compared to non-treated allografts (310 FU v.s. 117 FU, $p=0.01$). Ongoing studies are evaluating the role of PDE5 inhibition on graft survival and rejection.

CONCLUSION: PDE5 inhibition using an FDA-approved compounds can attenuate vascular inflammation associated with ischemia-reperfusion injury and may be a rapidly-translatable therapy to improve outcomes in microvascular surgery and allotransplantation.

153
A Novel 3D Platform to Investigate Neoangiogenesis, Transendothelial Migration and Metastasis of Breast Cancer Cells

Rachel C Hooper, MD[1]; Karina A Hernandez, DO[1]; Jeremiah Joyce, BA[1]; Adam Jacoby, BA[1]; Ope Asanbe, MD[1]; Ross Weinreb[1]; Claudia Fischbach, PhD[2]
[1]Weill Cornell Medical College, New York, NY, [2]Cornell University, Ithaca, NY

PURPOSE: Breast cancer remains the most common cancer afflicting women and is the second leading cause of death from cancer. A crucial step in the progression of this disease is the transendothelial migration of tumor cells into the blood stream or lymphatic system. The factors guiding this process remain poorly understood. The development an *in vitro* biomimetic platform to further investigate these factors is under intensive investigation. In previous work we synthesized a tissue-engineered scaffold containing an endothelialized internal loop microchannel for microsurgical anastomosis and *in vivo* perfusion utilizing a sacrificial microfiber technique. Here we design a novel 3D platform to investigate tumor cell behavior in the presence of vascular cells in order to better understand the cell-cell and cell-matrix interactions that drive neoangiogenesis, invasion, metastasis and ultimately tumor progression.

METHODS: Pluronic F127 microfibers were sacrificed in neutralized type I collagen with 1 x10^6 cells/mL MDA-MB231 breast cancer cells suspended in the bulk of the hydrogel creating a central loop microchannel, 1.5 mm in diameter. A 5 x10^6 cells/mL cell suspension of human umbilical vein endothelial cells (HUVEC) or HUVEC and human aortic smooth muscle cells (HASMC) was seeded into the microchannel. Scaffolds without microchannel seeding served as controls. Following 7, 14, and 28 days of culture specimens were fixed and processed for histology.

RESULTS: After 7, 14, and 28 days of culture, MDA-MB 231 cells had performed significant matrix remodeling and migrated extensively toward the surface of the hydrogel or "lumen" of HUVEC/HASMC seeded microchannels. At 14 and 28 days dense MBA-MB231 tumor nests were seen within the collagen hydrogel bulk of HUVEC and HUVEC/HASMC-seeded microchannel constructs. After 7,14, and 28 days MDAMB demonstrated transendothelial migration into the central 'neovessel' of HUVEC-only seeded microchannels resulting in HUVEC apoptosis. After 7, 14, and 28 days, the endothelial lining of HUVEC/HASMC appeared thinner and somewhat destabilized, without the elaboration of additional matrix proteins as had been seen in previous constructs without breast cancer cells in the bulk. Immunohistochemical staining demonstrated adherence of both CD31 and VWF expressing endothelial cells and α-SMA positive-smooth muscle cells along co-culture seeded microchannels. Epithelial cell adhesion molecule (EpCAM) positive staining of MDA-MB231 cells confirmed tumor cell migration toward HUVEC- and HASMC/HUVEC- seeded microchannels as well as breast cancer tumor aggregates within the bulk after 14 and 28 days. MDA-MB231 cells demonstrated no distinct pattern of tumor formation or transmigration within the hydrogels containing unseeded microchannels.

CONCLUSION: We have successfully created an *in vitro* 3D biomimetic platform to analyze the progression, transendothelial migration, and metastasis of MDA-MD231 breast cancer cells within tissue-engineered constructs containing endothelialized microchannels. Using our platform, we have demonstrated that signaling between tumor cells and endothelial cells plays a critical role in tumor invasiveness and metastatic potential. Such a model can be utilized to examine the efficacy of therapeutic interventions in the treatment of various malignancies and prevention of metastasis, shedding light on these incompletely understood phenomena.

154
The Anti-Neoplastic Effect of Aminosterol Squalamine on Melanoma

Denver M Lough, MD, PhD[1]; Damon Cooney, MD, PhD[2]; Shaun Mendenhall, MD[3]; Joel Reichensperger, BS[3]; Lisa Cox, BS[3]; Nicole Cosenza, MS[3]; Nathan Wetter, MD[3]; Carrie Harrison, BS[3]; Michael Neumeister, MD[3]

[1]SIU School of Medicine/ Johns Hopkins, Springfield, IL, [2]Johns Hopkins, Baltimore, MD, [3]SIU School of Medicine, Springfield, IL

PURPOSE: Squalamine, a recently discovered aminosterol, has notably been shown to be effective as both an antibiotic and an inhibitor of angiogenesis. This intrinsic anti-angiogenic effect of squalamine has been studied in the literature for its clinical capacity to reduce cancer progression. Here, we suggest an additional role of squalamine in inducing melanoma destruction via induction of apoptosis and or necrosis of melanotic cells through angiogenic inhibition.

METHODS: We utilized three model systems: (1) Application of the aminosterol squalamine to a A375 melanoma cell line (2) Application an organotypic 3D melanoma skin model tissue system and to a melanoma murine model in order to determine squalamine's potential against melanoma viability and progression.

RESULTS: The addition of squalamine to A375 melanoma cell lines, organotypic 3D melanoma skin model tissue and to a full murine melanoma model showed significant destruction of neoplastic cells with upregulation of both apoptosis and necrosis pathway markers.

CONCLUSION: Carcinoma of the skin is the most common type of cancer diagnosed in the United States, with the most deadly type being malignant melanoma. The incidence of this disease has continued to rise for the last three decades, with an estimated 70,000 individuals expected to receive a new diagnosis of malignant melanoma in 2014. Using three melanoma models we have shown that this aminosterol is capable of significantly reducing melanoma cell viability and propose a potential therapeutic property in squalamine.

SUNDAY, MARCH 9, 2014

SCIENTIFIC SESSION 9 GROUP B
ASSORTED
1:00 PM – 2:00 PM

SUNDAY, MARCH 9, 2014

155
Do Unclothed Images Affect Decision Making in a Conjoint Analysis?

Malik Mossa-Basha, MD 2014[1]; Peter Ubel, MD[2]; Lillian Burdick, BA[3]; Lillie Williamson, BA[2]; Clara Lee, MD[3]

[1]Wayne State University, Detroit, MI, [2]Duke University, Durham, NC, [3]University of North Carolina, Chapel Hill, NC

PURPOSE: Conjoint analysis is a powerful technique for eliciting preferences, which enables consumers to make multiple simultaneous trade-offs in choosing a product. Recently, health service researchers have been using conjoint analysis to learn more about which attributes patients' value when making health care choices. Prior research in marketing has demonstrated strong effects of images on consumers' choices, but the effect of images within conjoint questionnaires is unknown. For the medical decision about reconstruction after mastectomy, images of breasts could be particularly relevant. We aim to evaluate the effects of adding unclothed or clothed images to a questionnaire on breast cancer reconstruction surgery choices.

METHODS: We enrolled adult women ages 40 to 70 who had no history of breast cancer through online sampling sources. Participants complete an online conjoint analysis questionnaire consisting of 13 questions with a choice between two treatment breast cancer surgeries that varied according to 4 different attributes_appearance, complication rate, number of surgeries and recovery time. Participants were randomized into one of four groups different only by what images they were shown. The images were realistic computer generated representations of what patients would look like after surgery. The groups included unclothed images, clothed images, both or no images. We analyzed the responses using Sawtooth Software. The outcome of interest was the average importance of the appearance attribute.

RESULTS: 105 participants completed the study. Two were excluded_one for being a male and the other for leaving multiple questions blank. The unclothed, clothed, both and no images groups had average importance ratings of 25.49, 16.90, 27.95, and 20.88 respectively ($p<.05$). 19% of subjects in the unclothed group ranked the appearance attribute as most important while 12% of the clothed group ranked appearance as most important. The group with both images had the most participants ranking appearance as most important at 33%. The no-images group had 13% of subjects ranking appearance as the most important attribute.

CONCLUSION: The presence of images was associated with a greater appearance rating. The impact of images was greater in the unclothed than in the clothed group. Unclothed images had a greater emotional impact on subjects. As a result, the method by which healthcare providers present patients with information on surgeries could impact decision making.

156
Plastic Surgery - Quo Vadis? Current Trends and Future Projections of Aesthetic Plastic Surgical Procedures in the United States of America

P Niclas Broer, MD PhD[1]; Sabrina Juran, MSc[2]

[1]Bogenhausen Teaching Hospital Technical University Munich, Germany, München, Germany, [2]United Nations Population Fund (UNFPA), New York, NY

PURPOSE: Aesthetic plastic surgery has witnessed a steady growth over the past. The objective of this study is to evaluate past trends regarding aesthetic surgeries in the USA and to project future changes in such procedures. The results aim to alert the medical community about these trends in order to plan and prepare in advance.

METHODS: Cosmetic surgery statistics from 1997 to 2012 from the American Society for Aesthetic Plastic Surgery were analyzed by sex, age and ethnic group. Then, utilizing the national population projections from the U.S. Census Bureau based on the 2010 census, two projection scenarios of the expected number of aesthetic plastic surgery procedures by 2030 were generated, based on the assumption of the occurrence and non-occurrence of another economic crisis during this time period of similar degree to the crisis that set in in 2007.

RESULTS: Based on trends in procedures over the past years and the changing age and ethnic structure of the U.S. population, in the absence of an economic crisis, aesthetic procedures are expected to grow from 1,688,694 in 2012 to 3,847,929 by 2030. Should another economic crisis of a similar degree occur, procedures would only increase to 2,086,994 over the same time. Since the age distribution of the patient population, preferences for specific procedures according to age will also influence, and thus are reflected in, future demand. Further, the ethnic profile of the patient population will be altered as well, with 32% of all procedures being performed on patients other than Caucasians by 2030.

CONCLUSION: Demand for aesthetic plastic surgical procedures is expected to continue to grow, with its future path heavily depending on the economic performance at the macro level as well as the changing population dynamics of the US population. This study breaks new ground since it is the first non-profit effort to analyze trends in, and project future demand for, such procedures in the United States of America, with a time horizon up to 2030.

157
In Vivo Evaluation of a Novel Suture Design for Abdominal Wall Closure

Jason M Souza, MD; Gregory A Dumanian, MD
Northwestern University, Chicago, IL

PURPOSE: Plastic surgeons have become increasingly involved in the field of abdominal wall reconstruction. Here we present a novel suture design aimed at minimizing the early laparotomy dehiscence that drives ventral hernia formation. We hypothesized that modulation of the suture-tissue interface through use of a macroporous structure and increased aspect ratio (width-to-height ratio) would decrease the suture pull-through that leads to laparotomy dehiscence.

METHODS: We produced incisional hernias in 30 animals according to an established rat hernia model. This model has been shown to produce predictable hernia recurrence when repaired with conventional suture. On postoperative day (POD) 28, the mature hernia rings were dissected and standardized photographs were taken. The animals were then randomized to repair with either two 5-0 polypropylene sutures (Group 1) or two mid-weight polypropylene mesh sutures (Group 2) placed in similar fashion. On POD 56, we completed necropsies, during which the recurrent hernia rings were again dissected and photographed. Waterproof 2mm grid graph paper was placed intra-abdominally to serve as a reference for all photographs. To minimize the investigator bias introduced in defining and measuring defect areas, edge-detection software was used to define the border of the hernia defect and calculate the area. All calculations were calibrated based on the 2mm grid present in each photograph. In addition to these measurements, histology was performed on all mesh suture specimens. In-growth was graded according to a 4-point scale adapted from the American Society for Testing and Materials (ASTM) guidelines, as previously described.

RESULTS: Seventeen hernias were repaired with mesh sutures, while 13 hernias were repaired with conventional 5-0 polypropylene sutures. Despite randomization, the defects repaired with mesh suture were significantly larger than those undergoing conventional suture repair (391.9 ± 33.4 mm^2 vs. 255.4 ± 23.3 mm^2; $P<.0025$). The mean area of the recurrent defects following repair with the mesh suture was 177.8 ± 27.1 mm^2, compared to 267.3 ± 34.1 mm^2 following conventional suture repair. This correlated to a 57.4% reduction in defect area after mesh suture repair, compared to a 10.1% increase in post-repair defect area following conventional suture repair ($p<.0007$). Notably, none (0/34) of the mesh sutures pulled-through the surrounding abdominal wall tissue, while 65% (17/26) of the conventional sutures used for repair demonstrated complete pull-through. With regard to histology, Excellent (ASTM 3) in-growth was observed in 13/17 mesh suture specimens, while the remaining 4 specimens demonstrated Good (ASTM2) in-growth.

CONCLUSION: The mesh sutures better resisted suture pull-through than conventional polypropylene sutures of comparable tensile strength. To our knowledge, this is the first laboratory investigation to highlight the importance of increased aspect ratio and macroporous structure with regard to suture design. By more evenly distributing distracting forces across the suture-tissue interface and permitting tissue integration into the substance of the suture, a suture incorporating these design elements would better prevent the early laparotomy dehiscence that leads to incisional hernia formation.

158
Identification of BMP-Responsive Long Noncoding RNAs in Pluripotent Cells

Kevin J Paik, AB[1]; Kun Qu, PhD[2]; Brian Hsueh, AB[1]; Eduardo A Torre, BS[2]; Ryan A Flynn, BS[2]; Michael T Chung, BS[1]; Andrew Spencley, BS[3]; Kevin C Wang, MD, PhD[3]; Joseph C Wu, MD, PhD[4]; Michael T Longaker, MD, MBA[1]; Howard Y Chang, MD, PhD[2]; Derrick C Wan, MD[1]

[1]Hagey Laboratory for Pediatric Regenerative Medicine, Department of Surgery, Plastic and Reconstructive Surgery Division, Stanford, CA, [2]Howard Hughes Medical Institute and Program in Epithelial Biology, Stanford, CA, [3]Department of Dermatology, Stanford, CA, [4]Department of Radiology and Department of Medicine, Division of Cardiology, Stanford, CA

PURPOSE: Pluripotent stem cells hold tremendous promise for the study of human diseases and for the treatment of various tissue deficits in regenerative medicine. A key challenge in controlling cell fate toward lineage-specific differentiation, however, is minimizing the risk of teratoma formation. Previous research has highlighted the important role that epigenetic regulation plays in the specification and maintenance of cell fate. Furthermore, a growing body of literature has shown that a novel class of long noncoding RNAs (lncRNAs) are capable of effecting changes to the chromatin landscape through histone modification, thus being able to render genes transcriptionally active or silent. As Bone Morphogenetic Proteins (BMPs) have been found to be closely involved in the regulation of differentiation among pluripotent cells, the present study sought to identify specific lncRNAs responsive to BMP-2 in order to gain a clearer understanding of the epigenetic machinery responsible for controlling cell fate toward osteogenic differentiation.

METHODS: Human induced pluripotent stem cells (iPSCs) were cultured on Matrigel-coated tissue culture dishes with mTeSR™1 medium. Cells were treated with BMP-2 (200ng/ml) and total RNA was harvested with Trizol at 0, 6, 12, 18, 24, and 48 hours. Samples were treated with Turbo DNase followed by Ribo-Zero magnetic beads for DNA and rRNA depletion respectively. Fragmentation with alkaline hydrolysis buffer and first strand synthesis and second strand synthesis were performed. 3'-A tailing and ligation to Illumina linkers allowed for gel size selection and sequencing with the Illumina HiSeq System. Paired-end reads were mapped to the human genome reference sequence hg19. Transcriptome assembly was performed with Cufflinks and transcriptomes were merged. Reads per kilobase of transcript per million mapped reads (RPKM) for known transcripts was calculated, and significantly differentially expressed transcripts were identified. Differentially expressed transcripts were then further narrowed down by Gene Ontology (GO) term analysis to identify functional transcripts related to modulation of pluripotency and skeletal development.

RESULTS: To visualize genome-mapped data, results were uploaded to the UCSC Genome Browser. Importantly SOX2 expression was found to decrease with longer exposure to BMP-2, confirming decreased pluripotency. From 5566 significantly differentially expressed transcripts (protein-coding: 78%, lncRNAs: 4%, other: 18%), twelve annotated transcripts were determined following GO term analysis. Of these, the lncRNA at LOC100505806 showed unidirectional upregulation in response to BMP-2, which was confirmed by qRT-PCR. Subsequent studies will be done to manipulate this transcript and to assess for changes to pluripotent cells similar to BMP-2 exposure.

CONCLUSION: The precise role of lncRNAs in regulating differentiation remains undefined, but with a better understanding the potential exists to redirect the developmental process in iPSCs, facilitating their use in regenerative medicine. By defining lncRNAs that effect BMP-mediated changes to chromatin states, it may be possible to manipulate regulatory networks of pluripotent cells to promote osteogenic differentiation.

159
SPY Imaging Use in Post-mastectomy Breast Reconstruction Patients: Preventative or Overly Conservative?

Gennaya L Mattison, BS[1]; Priya G Lewis, BA[1]; Subhas C Gupta,MD, CM, PhD, FACS, FRCSC[2]; Hahns Y Kim, MD[2]

[1]Loma Linda University School of Medicine, Loma Linda, CA, [2]Loma Linda University Medical Center, Loma Linda, CA

PURPOSE: SPY imaging technology utilizes an injectable fluorescing agent to intra-operatively assess the perfusion and viability of tissue, including skin flaps during post-mastectomy reconstruction for breast cancer patients. This study sought to compare the surgeon's assessment of flap viability with that of the SPY imaging perfusion, analyzing the clinical outcomes including necrosis and expander/implant viability post-operatively.

METHODS: In this study, the intra-operative difference between the plastic surgeon's assessment of skin viability and the SPY imaging assessment was analyzed by the skin flap area preserved in a total of sixteen breasts undergoing mastectomy. Following the mastectomy, the operating surgeon marked the area of the skin flap to excise then the SPY imaging was performed and photos and videos of the perfusion collected. The skin flap was resected prior to implant or tissue expander placement according to the plastic surgeon's assessment. The patients were then routinely followed up in clinic post-operatively.

RESULTS: A total of sixteen breasts were analyzed and compared. During the study, there was one incidence of necrosis with a return to the OR for debridement along with tissue expander removal and replacement. In one of the sixteen cases, SPY imaging indicated a greater area of viability than the surgeon's assessment. For the remaining fifteen breasts, however, resecting the area of diminished perfusion as indicated by the SPY imaging would have resulted in a statistically significant increased area of resection ($t=0.038$). In addition, three of the fifteen cases were nipple-sparing mastectomies; none of the nipples were well-perfused by SPY imaging, but no post-operative necrosis occurred.

CONCLUSION: SPY imaging has a great deal of potential for use in reconstructive procedures. In this study, it was found to be conservative in its estimation of viability and, if followed, would result in a more aggressive resection than the area deemed viable by the human eye. It is possible that the case of necrosis with a return to the operating room for a tissue expander removal and replacement might have been prevented following the SPY imaging guidance for the tissue viability. Overall, SPY imaging is a valuable tool to assist in the evaluation of skin flap viability following a mastectomy. If some future returns to the operating room can be prevented by following the conservative estimation by SPY imaging and filling the tissue expander more slowly, that is clearly the most appropriate course to pursue. Though it should not be used as the only determining factor of viability, SPY imaging has a great deal of potential as a complementary tool to be integrated with the experienced surgeon's analysis during post-mastectomy breast reconstruction.

160
Biomechanical Considerations in Abdominal Wall Reconstruction using the Extended Component Separation Technique

Henrik O Berdel, MD; Mirza Mujadzic, Medical Student; Nina Yoo, Medical Student; Jack C Yu, MD, DMD, ME Ed, FACS; Mirsad Mujadzic, MD; Edmond Ritter, MD

Medical College of Georgia, Augusta, GA

PURPOSE: Large midline abdominal wall hernias are challenging surgical problems with no optimal solution to date. The Component Separation Technique (CS), initially described by Ramirez in 1990, provides an effective alternative to mesh reconstruction. Although Ramirez reported a 0% recurrence rate in a series of 11 patients, other authors observed higher recurrence rates, as well as complications including wound infection, skin necrosis, dehiscence, and abdominal compartment syndrome. In order to increase efficacy and safety by further reducing tension, the Extended Component Separation (ECS) was introduced. To our knowledge the load-displacement characteristics of the human abdominal fascia in either technique, though critically important, have not been determined. The aim of this study is to measure such tensile behaviors, as well as to establish possible differences in load-displacement characteristics between CS and ECS in a human cadaver model.

METHODS: 10 fresh human cadavers were dissected first with conventional CS, followed by ECS. Advancement toward the midline was measured in millimeters at preset tensions of 0, 22, 44, and 65 Newtons (N) using a tension gauge applied to the middle abdominal fascial edge with Kocher clamps. The advancements were recorded in millimeters, and statistical analysis was performed using a 2-tailed student's t-test to compare the load-displacement data of CS and ECS. A P-value of less than 0.05 was considered as statistically significant.

RESULTS: With ECS, a statistically significant increase in advancement could be achieved in comparison to CS at all preset tensions. In the conventional CS the advancement of the mid-abdomen was 37.10 +/- 8.08 mm (Mean +/- SD) at 0N, 49.90 +/-10.61 mm at 22N, 59.30 +/- 11.06 mm at 44N, and 67.67 mm at 65N. The advancement in the mid abdomen with ECS resulted in 58.70 +/-9.20 mm at 0N, 74.40 +/-10.62 mm at 22N, 82.40 +/- 11.32 mm at 44N, and 89.67 mm at 65N. P-values comparing these means were 0.00006 at 0N, 0.00012 at 22N, 0.00046 at 44N, and 0.04 at 65N. The average net gain at a tension of 0N was 46mm in the middle abdomen.

CONCLUSION: Autologous reconstruction of large abdominal wall defects necessitates tissue re-deployment under force. However, the quantitative measure of this force, though obviously important, has not been reported. We describe a method of such quantitative measurement, and show that, in a cadaver model, ECS indeed increased mobilization of fascial edges without increasing tension. The key observations from this study are: 1. The theoretical maximum defect that can be closed without a mesh is 18 cm in the mid abdomen. 2. After ECS, the human abdominal wall fascia advances 1–3 mm/N.

SUNDAY, MARCH 9, 2014

SCIENTIFIC SESSION 9 GROUP C
TISSUE ENGINEERING
1:00 PM – 2:00 PM

SUNDAY, MARCH 9, 2014

161
Identification of Cell-Intrinsic Mechanisms and Differentially Regulated Genetic Pathways Responsible for the Age-Related Functional Decline in Aged Skeletal Stem Cells

Adrian McArdle, MB, BCh, BAO, MRCSI; Charles Chan, PhD; Jun Seita, MD, PhD; Kshemendra Senarath-Yapa, MBBChir, MA, MRCS; Michael Hu, MD, MPH; Graham G Walmsley, BS; Elizabeth Zielins, MD; David Atashroo, MD; Ruth Tevlin, MB, BCh, BAO, MRCSI; Irving Weissman, MD; Michael T Longaker, MD, MBA, FACS
Stanford University, Stanford, CA

PURPOSE: Aging is associated with a gradual loss of homeostatic mechanisms that maintain the structure and function of adult tissues. Most adult tissues contain resident stem cells, which proliferate to compensate for tissue loss throughout the life of the organism. It is believed that both chronological aging and replicative aging of adult stem cells negatively affects their functional capacity for tissue regeneration. Natural aging has a profound effect on skeletal healing, evidenced by the reduced healing ability with advancing age, and an increased incidence of osteoporosis. In mice, we have identified a resident stem-cell pool in skeletal tissue. We can successfully isolate a highly-purified population of skeletal stem cells that have the ability of forming bone, cartilage, stroma and a functioning bone marrow cavity at the clonal level. This study examines the cell-intrinsic mechanisms, and the role of the extrinsic stem cell niche on influencing skeletal stem cell aging. The aim of this study is to identify potential pathways that could be manipulated to reverse the effects of skeletal stem cell aging.

METHODS: Highly-purified populations of skeletal stem cells were prospectively isolated by fluorescence-activated cell sorting (FACS) using a novel panel of cell surface markers. Microarray analysis was performed to identify genetic pathways that are differentially regulated with aging. Cell intrinsic function was assayed using isochronic and heterochronic transplantations beneath the kidney capsule to assess their bone-forming ability at an ectopic location. To determine if exposure of aged bone to a young, healthy circulation would improve bone health, we surgically paired mice, creating isochronic and heterochronic parabiosis to determine if it is possible to manipulate the niche and rescue an age-related functional decline in stem cell function.

RESULTS: The ability of skeletal stem cells to form colonies in vitro declined significantly with age (*$p<0.05$). Isochronic and heterochronic ectopic skeletal stem cell transplantation assays demonstrated a functional decline in the ability of aged skeletal stem cells to form bone beneath the renal capsule. Aged mice demonstrated a significant reduction in bone mineral density using microCT analysis (*$p<0.05$). Fracture healing was also delayed in this group, as measured by the callus index. The ability of a young, systemic microenvironment to rejuvenate aged stem cells remains to be seen. Microarray data analysis of skeletal stem cell populations comparing early post-natal to aged mice, has identified differentially regulated genes that may be responsible for the functional decline in the ability of aged skeletal stem cells to form bone.

CONCLUSION: Aging is associated with changes in cell-intrinsic mechanisms that underlie the functional decline in the ability of skeletal stem cells to form bone. Microarray analysis has identified differentially regulated genes that may be responsible for this functional decline. Manipulation of these pathways may allow us to reverse the effects of skeletal stem cell aging and improve bone healing in vivo.

162
In Vivo Microanastomosis of Microvessel Containing Tissue-Engineered Constructs: The Final Frontier

Rachel C Hooper, MD, FACS; Karina A Hernandez, DO; Tatiana Boyko, MD; Jeremiah Joyce, BA; Adam Jacoby, BA; Jason A Spector, MD, FACS
Weill Cornell Medical College, New York, NY

PURPOSE: Although autologous tissue transfer has been established as a reliable approach to the reconstruction of complex defects, there are associated consequences including donor site pain, functional loss, paresthesias, dysthesthia, and scarring. The ability to synthesize vascularized constructs for the management of these complex wounds would represent a quantum leap in the field of tissue engineering. In previous work we synthesized and performed an in vivo microvascular anastomosis of a collagen construct containing an unseeded internal longitudinal microchannel with inlet and outlet. Here we fabricate and microsurgically anastomose collagen constructs containing an internal endothelialized microchannel.

METHODS: Pluronic F127 microfibers were embedded in neutralized type I collagen, then sacrificed leaving a central "loop" microchannel, 1.5 mm in diameter. Constructs contained an inlet and outlet and were reinforced with polyglactone mesh for tensile strength at the anastomotic site. Microchannels were seeded with 5 x106 cells/mL human umbilical vein endothelial cells (HUVEC) or a co-culture of HUVEC and human aortic smooth muscle cells (HASMC) and cultured for 7 days with daily media changes. Seeded and unseeded constructs were microsurgically anastomosed to the femoral artery and vein of RNU 316 nude rats. Following completion of anastomoses, patency was evaluated via venous strip tests and in vivo microdoppler assessment. Unseeded constructs were perfused for 2.5 and 5 hours. Seeded constructs were perfused for up to 24 hours. Following perfusion, all constructs were fixed in 10% formalin, embedded, stained and analyzed.

RESULTS: Polyglactone mesh provided the necessary tensile strength, allowing microchannel-containing constructs to be successfully anastomosed to the femoral artery and vein of nude rats. In vivo gross inspection and H&E staining of seeded and unseeded constructs following harvest revealed intact microchannels capable of withstanding physiologic perfusion pressures. Patency was confirmed via venous strip tests and auscultation of continuous pulsatile blood flow via microdoppler. Post-perfusion analysis of unseeded constructs demonstrated microchannels with adherent host inflammatory cells along the luminal surface. Post-harvest histology following perfusion of HUVEC-seeded microchannels demonstrated areas of delamination whereas HUVEC/HASMC-seeded microchannels maintained concentric confluent "neointimal" and "neomedial" layers comprised of endothelial and smooth muscle cells respectively. Immunohistochemical analysis of HUEVC-only seeded microchannels revealed CD31 expressing cells whereas the co-culture-seeded microchannels demonstrated both CD31 and α-SMA expressing HUVEC and HASMC.

CONCLUSION: We have successfully created custom vascularized biodegradable, biocompatible constructs that support microchannel endothelialization and microsurgical anastomosis in vivo. Constructs with their own inherent vascular network can be directly anastomosed to host vasculature providing immediate perfusion, thus increasing the survival of cellular constituents within the scaffold as well as the rate of incorporation into the host. This represents a major advance in tissue engineering and opens the door to the creation and application of larger, more complex surgically relevant constructs.

163
Regional Inflammation Following Lymph Node Transfer Improves Spontaneous Lymphatic Reconnection and Functional Drainage

Walter J Joseph, BS; Seth Z Aschen, BS; Gina Farias-Eisner, BS; Daniel A Cuzzone, MD; Swapna Ghanta, MD; Nicholas J Albano, BS; Ira L Savetsky, MD; Jason C Gardenier, MD; Babak J Mehrara, MD
MSKCC, New York, NY

PURPOSE: Lymph node (LN) transplantation has been clinically shown to improve lymphatic function and decrease lymphedema in selected cases. However, the results of these reports have been inconsistent as a consequence of inadequate lymphatic regeneration in some patients. Therefore, developing novel strategies that improve lymphatic regeneration after LN transplantation is clinically relevant and important. We have previously shown that lymphatic vessels spontaneously reconnect and restore lymphatic function after LN transplantation in a mouse model. In addition, we have previously shown that sterile inflammation massively increases lymphangiogenesis. Therefore, the purpose of the current study was to determine if sterile inflammation before or after LN transplantation can be used as a means to improve spontaneous lymphatic reconnection and lymphatic function.

METHODS: To test the hypothesis that sterile inflammation can improve lymphatic reconnection after LN transplantation, we performed LN transplants in adult male mice using lymphatic reporter mice (express B-gal in lymphatic vessels) as recipients and wild-type mice as LN donors. The axillary contents of recipient mice including LNs and perinodal fat were replaced with tissues from the donor mice. Animals were divided into 2 experimental groups. In group I, we induced sterile inflammation in draining LNs by injecting Freund's Complete Adjuvant (CFA)/OVA in the distal extremity of the donor mouse 14 days prior to transplantation. In group 2, we performed LN transplantation and then injected CFA/OVA in the distal extremity of the recipient mouse 14 days following transplantation. A third group of animals served as inflammation controls and were not treated with CFA/OVA before or after surgery. Four weeks after surgery, we compared lymphatic vessel regeneration, VEGF-C expression, and lymphatic function with sham operated control animals that had undergone axillary incision without lymph node removal.

RESULTS: Sterile inflammation prior to LN transplantation resulted in signification donor LN enlargement and lymphangiogenesis. However, unexpectedly we found that inflammation prior to LN transplantation was associated with markedly impaired lymphatic regeneration as compared with animals that did not have inflammation or those in which inflammation was induced after transplantation. For example, analysis of lymphatic function using Tc99 lymphoscintigraphy demonstrated that induction of inflammation after LN transplantation resulted in a 1.68-fold increase in Tc99 uptake in the transplanted node as compared with pre-inflammation transplanted lymph nodes ($p=0.0002$). Lymphatic vessel staining corroborated these findings demonstrating a massive ingrowth of lymphatics into the post-transfer inflammation LNs as compared to pre-transfer inflammation group. These findings also corresponded to increased lymphangiogenic cytokine expression in the post-transfer inflammation group. Post-transplant inflammation animals had virtually normal lymphatic function as compared with sham-operated controls.

CONCLUSION: This study demonstrates that sterile inflammation after LN transplantation can be used as a means of augmenting lymphatic regeneration and function. Interestingly, we found that inflammation prior to transplantation markedly impairs lymphatic regeneration (despite increasing the size and level of lymphangiogenesis in the transplanted LN). Our findings also suggest that post-transplantation sterile inflammation increases the endogenous expression of lymphangiogenic cytokines and that this effect increases lymphatic vessel ingrowth in the transplanted LN.

164
Repair of Critical Size Bone Defects Using Bone Marrow Stromal Cells a Histomorphometric Study in Rabbit Calvaria

Antonio C Aloise, PhD; André Antonio Pelegrine, PhD; Lydia Masako Ferreira, PhD
Federal University of Sao Paulo, Sao Paulo, Brazil

PURPOSE: Therapies involving bone marrow may be helpful in the bone repair of critical defects because this tissue possesses cell populations that play an important role in bone homeostasis, namely bone marrow stromal cells (BMSCs). To date, no consensus has been reached on the best methodology for using BMSCs. Relevant literature has reported three main alternatives: (1) fresh bone marrow ("in natura") (Pelegrine et al. 2010; Costa et al. 2011; Oliveira et al. 2012), (2) bone marrow mononuclear cell (BMMC) concentrate, also called bone marrow mononuclear fraction (BMMF) (Sakai et al. 2008; Yoshioka et al. 2011; Pelegrine et al. 2013) and (3) cultivated bone marrow mesenchymal stem cells (BM MSCs) (Quarto et al. 2001; Cerruti Filho et al. 2007).

OBJECTIVES: The aim of this study was to evaluate the bone healing observed after the use of a scaffold enriched with bone marrow mesenchymal stem cells (Group 3) and to compare it with scaffold enriched with bone marrow aspirate (Group 1), scaffold enriched with bone marrow mononuclear fraction (Group 2), and scaffold alone (control group)

MATERIAL AND METHODS: Twenty-four rabbits were operated, and bilateral defects 12 mm in diameter were created in the animals' parietal bones. The bilateral defects were filled with a xenograft enriched with bone marrow mesenchymal stem cells (Group 3), one of the bilateral defects was randomly covered with a barrier membrane. The rabbits were sacrificed 8 weeks after surgery, and their parietal bones were harvested and analyzed histomorphometrically. The Wilcoxon test and Friedman test for paired data were used for intra-group comparisons (with and without membrane coverage) and the Kruskal-Wallis test was used for inter-group comparisons

RESULTS: The sides in which the defects were covered with the barrier membrane did not show improved bone healing ($p > 0.05$) The percentage of non-vital mineralized tissue (NVMT), represented by remaining Bio Oss® particles, was 27.79% ± 2.72% and 27.23% ± 6.8% for the defects with and without membrane coverage, respectively, whereas the percentage of vital mineralized tissue (VMT) was 28.24% ± 6.17% and 27.9% ± 5.79% for the defects with and without membrane coverage, respectively. .

CONCLUSIONS: Both methods using bone marrow mesenchymal stem cells, with and without membrane coverage, contributed to enhancing bone healing. The use of a barrier membrane seemed to have a synergistic effect on bone healing.

165
Enhanced Adipose-Derived Stromal Cell Osteogenesis through Surface Marker Enrichment and BMP Modulation using Magnet-assisted Transfection

Michael T Chung, BS; Shane D Morrison, MS; Kevin J Paik, AB; Adrian McArdle, MD; Graham Walmsley, BS; Kshemendra Senarath-Yapa, MD; Michael S Hu, MD; Ruth Tevlin, MD; Elizabeth Zielins, MD; David Atashroo, MD; Wan Xing Hong, MS; Christopher Duldulao, BS; Taylor Wearda, BS; Rebecca M Garza, MD; Arash Momeni, MD; Michael T Longaker, MD, MBA; Derrick C Wan, MD
Hagey Laboratory for Pediatric Regenerative Medicine, Department of Surgery, Plastic and Reconstructive Surgery Division, Stanford, CA

PURPOSE: Stem cell-based bone engineering is a promising approach for the clinical treatment of skeletal defects. Fluorescence-activated cell sorting (FACS) has identified CD90+ ASCs as a more osteogenic subpopulation than unsorted ASCs. More recently, inhibition of Noggin (NOG) has been shown to facilitate higher levels of endogenous bone morphogenetic proteins (BMPs), also resulting in enhanced osteogenesis. The present study investigated the concept of a concerted approach, employing both an isolation of CD90+ ASCs via FACS and modulation of BMP signaling, to optimize bone regeneration.

METHODS: Magnet-assisted transfection was used to deliver minicircle (MC) NOG shRNA into CD90+ and unsorted cells. These cells were then cultured in ODM in vitro. Alkaline phosphatase staining was performed on Day 7, and alizarin red staining and quantification on Day 14. Osteogenic gene expression was assessed by qRT-PCR. For evaluation of in vivo osteogenesis, critical-sized calvarial defects in nude mice were treated with a novel MC-releasing HA-PLGA scaffold. MC plasmids were labeled with magnetic nanoparticles, and an external magnet was used to transfect ASCs seeded onto the scaffold. Healing of the defects was followed using micro-CT scans for eight weeks. Calvaria were harvested at Week 8, and sections were stained with Movat's Pentachrome.

RESULTS: Suppression of NOG through magnet-assisted transfection resulted in increased osteogenic gene expression and in vitro osteogenic differentiation, as demonstrated by alkaline phosphatase and alizarin red staining. In vivo, over the course of eight weeks, defects with the NOG-suppressed CD90+ subpopulation were found to heal faster than defects treated with the NOG-suppressed unsorted cells.

CONCLUSION: Our findings indicate that the use of CD90-selected ASCs may facilitate more rapid regeneration of skeletal defects. Furthermore, NOG knockdown may serve to augment bone differentiation through an increase in BMP signaling. The integration of these two strategies through magnet-assisted transfection may lead to the development of promising, temporospatially controlled treatments for clinical translation.

166
Electrospun Synthetic Scaffolds: A Biomimetic Approach to Prevent Hypertrophic Scar Contraction

Kyle J Miller, BA[1]; Elizabeth R Lorden, BS[2]; Ellen Hammett[2]; Mohamed M Ibrahim, MD[1]; Carlos Quiles, MD[1]; Angelica Selim, MD[3]; Kam W Leong, PhD[2]; Howard Levinson, MD[1]

[1]Division of Plastic Surgery, Department of Surgery, Duke University School of Medicine, Durham, NC, [2]Department of Biomedical Engineering, Duke University, Durham, NC, [3]Department of Pathology, Duke University School of Medicine, Durham, NC

PURPOSE: Over 2.4 million Americans and tens of millions of patients worldwide suffer from hypertrophic scar contraction (HSc) following serious thermal injury. HSc is a debilitating condition that results in disfigurement and decreased range of motion in affected joints. In unwounded skin, native collagen is arranged randomly, myofibroblasts are absent, and matrix stiffness is low. Conversely, in HSc, collagen is arranged in linear arrays while myofibroblast density and matrix stiffness are high. The current standard of care for HSc involves skin grafting with or without the placement of a collagen based bioengineered skin equivalent (BSE). Present BSEs assist in tissue regeneration but do not target Hsc because they are brittle and rapidly degrade prior to completion of the remodeling phase of repair. To overcome this significant unmet medical need, we have created an elastomeric biomimetic BSE which will persist through the remodeling phase of repair.

METHODS: Electrospun scaffolds were created with randomly-oriented fibers akin to collagen fiber alignment in unwounded human skin. Mechanical properties were characterized via microstrain analysis. Human dermal fibroblast ingrowth and matrix contraction were compared in vitro between scaffolds and fibroblast populated collagen lattices (FPCL, a 3-dimensional in vitro model of wound healing that is the progenitor for present-day BSEs). To test HSc reduction in vivo, scaffolds were surgically placed beneath skin grafts in an immune competent murine HSc model. In vivo statistics utilized student's t-test and ANOVA. In vitro statistics utilized Tukey's HSD. All pairings tested, significance judged as $p<0.05$.

RESULTS: Scaffolds demonstrated a lower (but not statistically significant) elastic modulus than human skin and a collagen-based clinical BSE (Integra™), suggesting scaffolds will not prohibit movement in vivo. Ultimate tensile strength of scaffolds was greater than human skin, while Integra™ was significantly weaker, making the scaffolds tougher than their surrounding environment and giving them the ability to withstand forces experienced by skin in vivo. Scaffolds supported fibroblast ingrowth and proliferation analogous to the FPCL,

but prevented nuclear alignment observed in FPCL. After seven days of culture, the scaffold contracted only 8 +/- 1.5% whereas the FPCL contracted 66 +/- 9%, with significantly fewer activated myofibroblasts in the scaffold. To confirm that the scaffolds reduce HSc in vivo, scaffolds were surgically inserted beneath skin grafts in a validated immune competent murine HSc model. The scaffolds limited HSc contraction to 6 +/- 0.2%, whereas wounds treated with Integra™ contracted 65 +/- 5% and control scars contracted 68 +/- 4%. Skin grafts were healthy and scaffolds were found to promote fibroblast invasion, angiogenesis, and macrophage recruitment.

CONCLUSION: The data demonstrate that biomimetic electrospun scaffolds provide mechanical support to prevent wound bed contraction during healing and prevent fibroblast alignment and myofibroblast activation associated with HSc. These findings suggest the importance of mechanical properties in the prevention of HSc contraction, and will help guide the rational design of future generations of BSEs in treating the millions of patients who suffer from burns each year.

MARCH 7 – 9, 2014

POSTER DISPLAYS

MARCH 7 – 9, 2014

P1
Bioprinted Vascularized Tissue-Engineered Constructs for In Vivo Perfusion

Rachel C Hooper, MD[1]; Duan Bin, BS[2]; Alice Harper, BS[1]; Adam Jacoby, BA[1]; Anya Laibangyang[2]; Jonathan T Butcher, PhD[2]; Jason A Spector, MD, FACS[1]
[1]Weill Cornell Medical College, New York, NY, [2]Cornell University, Ithaca, NY

PURPOSE: The greatest challenge to contemporary tissue engineers remains the difficulty associated with creating vascular networks within the engineered tissue. Furthermore, any vascularized construct must be designed to allow for anastomosis to the host vascular system. In previous work we synthesized a tissue-engineered scaffold containing an endothelialized internal loop microchannel for microsurgical anastomosis and in vivo perfusion utilizing a sacrificial microfiber technique. Bioprinting is an emerging technology that allows for the consistent and rapid fabrication of three-dimensional constructs comprised of any combination of extrudable polymers and cells with a precise predetermined microarchitecture. Here we describe the fabrication of bioprinted hydrogel constructs for cell seeding and in vivo microanastomosis.

METHODS: 15mm x 15mm x 5mm "loop" or "diamond" internal microchannel containing poly(ethylene glycol) diacrylate/ methacrylated gelatin/ alginate hydrogels were bioprinted using the Fab@Home ™ platform based upon a custom designed stereolithography (STL) file. Briefly, the STL file was divided into layers generating fill-paths for each layer of the scaffold; the hydrogel formulation was loaded and extruded along the X-Y paths for each layer at a rate of 5 mm/s. Constructs for microsurgical anastomosis were modified with polyglactin mesh at the inlet and outlet following printing to allow for suture fixation. To confirm cell compatibility with the chosen "bioink", 8 mm discs were topically seeded with 2.5 x 10 4 cells/mL porcine aortic smooth muscle cells (SMC) and 2.5 x 10 4 cells/mL aortic endothelial cells (EC) and cultured for 7 days. Fixed constructs were processed for histology and immunohistochemical staining

RESULTS: Bioprinted loop and diamond shaped constructs were successfully fabricated. Patency was confirmed via perfusion of colored buffer solution. Biocompatibility was established via Live/Dead ™staining and revealed adhesion and proliferation of SMC and EC. Immunohistochemical staining demonstrated smooth muscle actin and myosin heavy chain expressing SMC. Polyglactin mesh-modified constructs were successfully anastomosed to the femoral artery and vein of nude rats.

CONCLUSION: We have successfully created custom bioprinted biocompatible vascularized constructs that support cell adhesion, growth and microsurgical anastomosis for in vivo perfusion. These proof of concept flaps provide a starting point towards the further development of bioprinted vascularized tissues which has the potential to revolutionize the field of tissue engineering.

P2
Short-term Electrophysiological Changes in Muscle After Injury by Tenotomy and Partial Sectioning: A Pilot Study

Shoshana L Woo, MD; Melanie G Urbanchek, PhD; Paul S Cederna, MD; Nicholas B Langhals, PhD
University of Michigan, Ann Arbor, MI

PURPOSE: In amputation victims, partial muscle grafts will be required to create stable bio-artificial interfaces that can connect severed nerves to the electronics of a neuroprosthetic device. The purpose of this study was to examine the structural and electrophysiological changes in muscles three weeks following tenotomy and partial sectioning in the *in vivo* rat model.

METHODS: In twelve F344 adult male rats, the extensor digitorum longus (EDL) muscle was isolated, and the proximal and distal EDL tendons were transected. Three experimental groups were defined by "muscle cut": (1) whole EDL *("Whole")*; (2) EDL divided in half longitudinally *("Half-Longitudinal")*; and (3) EDL divided in half transversely *("Half-Transverse")*. The neurovascular pedicle to each muscle was left intact. All muscles were then wrapped in small intestinal submucosa (SIS) and either left "free-floating" (no tendon anchoring) or anchored at the proximal and distal tendons to the underlying fascia at resting length. At three weeks, all EDL constructs were isolated. Electrophysiological tests were performed on six muscle constructs using a stimulating hook electrode on the common peroneal nerve and a recording needle electrode in the EDL. To minimize signal interference, the lateral compartment musculature was denervated, and the remaining muscles of the anterior compartment were excised. The remaining six muscle constructs were sent for histological examination.

RESULTS: Muscle construct mass ranged from 69.6 to 211.4 mg (SD 49.0; n=12). Stimulation of the common peroneal nerve produced visible contractions and detectable compound muscle action potentials (CMAPs) in all tested muscle constructs (100%; n=6). Peak-to-peak amplitudes ranged from 6.8 to 20.7 mV (SD 5.7), with latencies ranging from 2.91 to 4.36 msec (SD 0.59) and threshold stimulation currents from 110 to 450 μA (SD 114). Whole muscle and non-anchored constructs displayed higher peak-to-peak amplitudes compared to their half-sized and anchored counterparts, respectively. Histological examination demonstrated intact healthy muscle fibers in all muscle constructs regardless of muscle cut or anchoring status.

CONCLUSIONS: Partial muscles, or muscles injured by both tenotomy and partial excision, demonstrated electrophysiological and contractile function in the short-term *in vivo* rat model. Tendon fixation, or anchoring, was not required. These

findings support the novel use of partial muscles in the construction of bio-artificial interfaces necessary for the surgical integration of robotic devices with the residual limbs of amputees. As this was a short-term pilot study, longer-term studies with larger sample sizes are warranted to determine how the effects of muscle cut and anchoring can be used for signal optimization in prosthetic control.

ACKNOWLEDGEMENTS: This work was supported by DARPA (N66001-11-C-4190) and the Plastic Surgery Foundation.

P3
A Ceiling Effect Exists for the Number of Nerves That Will Neurotize a Regenerative Peripheral Nerve Interface Device

Nicklaus S Carrothers, HS[1]; Zachary P French, HS[2]; Ziya Baghmanli, MD[2]; Cheryl A Hassett, BS[2]; Theodore A Kung, MD[2]; Jana D Moon, BS[2]; Nicholas B Langhals, PhD[2]; Paul S Cederna, MD[2]; Melanie G Urbanchek, PhD[2]

[1]University of Rochester, Rochester, NY,
[2]University of Michigan, Ann Arbor, MI

PURPOSE: The regenerative peripheral nerve interface (RPNI) has potential for facilitating innate peripheral nerve signal transduction to microcomputers for control of motorized prosthetic limbs. Regenerated RPNI devices recover 20–30% of normally innervated muscle signaling capacity. We reported this for RPNI devices constructed with extensor digitorum longus (EDL) muscle neurotized by the entire peroneal nerve. Our purpose is to determine if providing more nerve fibers for RPNI neurotization increases RPNI signaling capacity.

METHODS: Rat peroneal nerve has 6,000 nerve fibers, with 600 (10%) classified as myelinated motor while tibial nerve has 13,600 fibers with 1000 (7%) myelinated motor fibers. Fifty-seven rats were assigned to one of six groups varying density of nerve fibers neurotizing RPNI devices. Control EDL and SOL muscles remained innervated by native nerve. RPNI groups were: EDL muscle transfers with entire peroneal neurotization (EDL-RPNI) or SOL muscle transfers neurotized by the entire tibial nerve (SOL-RPNI). Negative controls were denervated EDL muscle (EDL-Den) and SOL muscle (SOL-Den). Recovery times were three to five months. Evoked maximal twitch compound muscle action potentials (CMAP) and maximal muscle contractile force were measured. Control and RPNI group muscles were digested to determine muscle fiber length to whole muscle length (Lf/Lo). Lf/Lo ratios are a factor in calculating physiologic cross sectional area (CSA).

RESULTS: Muscle Lf/Lo increased for EDL-RPNIs but not SOL-RPNI. Dividing measured CMAP and force values by CSA normalizes data for comparing EDL and SOL muscles. Though SOL-RPNI devices were neurotized with 40% more motor axons than were implanted in the EDL-RPNI devices, the RPNI signal transduction represented by CMAP, specific CMAP, force and specific force measurements did not differ from EDL-RPNI device signaling (power >0.63). CMAP and specific CMAP signaling for the EDL-RPNI devices were 20% and 17% the Control EDL signals. CMAP and specific CMAP signaling for the SOL-RPNI devices were 27% and 25% the Control SOL signals. Specific CMAP and force deficits usually adjust for muscle atrophy seen with denervation. Muscle atrophy or loss of muscle mass was not observed in

this study. CMAP and force measurements correlate strongly ($\geq r=0.73$, $p<0.01$).

CONCLUSION: Providing 40% more neurotizing nerve fibers during RPNI implant did not improve signaling capacity of the RPNI following at least three months of recovery. We believe this represents a ceiling effect on number of nerve fibers needed to neurotize RPNI devices. Both tibial and peroneal nerves contain 10 to 100 times more nerve fibers than innervate native EDL or SOL muscles.

ACKNOWLEDGMENTS: This work was sponsored by the Defense Advanced Research Projects Agency, Grant/Contract No. N66001-11-C-4190.

P4
Head and Neck Reconstruction Utilizing Free Tissue Transfer, Does Training in Otolaryngology or Plastic Surgery have an Effect on Outcomes?

Ian C Hoppe, MD; Anthony M Kordahi, BA; Edward S Lee, MD

Rutgers, The state university of New Jersey - New Jersey Medical School, Newark, NJ

PURPOSE: The reconstruction of defects resulting from the extirpation of head and neck neoplasms is performed by both otolaryngology and plastic surgery services, mostly dependent on the institution. Very little, if any, literature exists comparing differences between these two services and their reconstructions, specifically outcomes. The American College of Surgeons' National Surgical Quality Improvement Project (NSQIP) provides a unique opportunity to examine a predefined set of variables with regards to free vascularized tissue transfers performed by each service.

METHODS: Following institutional review board approval the NSQIP Participant Use Files for 2005 - 2011 were examined for all Current Procedural Terminology codes regarding free tissue transfer. The results were further refined to include only primary ICD-9 codes involving a neoplasm of the head or neck. Each record was examined to determine which service performed the free tissue reconstruction. Outcome variables examined included total operative time, total hospital stay, wound complications, flap failures, and other selected outcomes.

RESULTS: During this time period a total of 534 flaps were performed, 213 by plastic surgery and 321 by otolaryngology. The average age was 61.8, with 367 males and 166 females (sex of 1 patient not provided). The average operative time was 578 and 567 minutes for plastic surgery and otolaryngology, respectively ($p = 0.52$). When further refining the analysis to resections performed by otolaryngology, there was no difference in operative time when the same surgical team performed the flap, or when another team performed the reconstruction. Total hospital length of stay was 12.9 and 11.2 days for plastic surgery and otolaryngology, respectively ($p < 0.05$). There were no significant differences noted between surgical site infections, wound dehiscence, and flap failure between flaps performed by plastic surgery and otolaryngology. In addition there were no significant differences noted between blood transfusion, return to operating room, postoperative pneumonia, and myocardial infarctions between the two services. Patients undergoing flaps performed by plastic surgery were significantly more likely to be on a ventilator 48 hours postoperatively ($p < 0.005$).

CONCLUSION: This study shows similar results with regards to free vascularized tissue transfers when performed by plastic surgery and otolaryngology. Plastic surgeons may be

less familiar with airway management than otolaryngologists, possibly explaining the increased likelihood of the patient being ventilated for more than 48 hours postoperatively. The similar outcomes between the two services indicate that each specialty receives adequate training in microsurgery.

P5
Systemic Application of Adipose Derived Stem Cells Accelerates Functional Peripheral Nerve Regeneration in a Rodent Transection and Repair Model

Jonas T Schnider, MD[1]; Paolo M Fanzio, MD[2]; Wakako Tsuji, MD[2]; Natalya Kostereva, PhD[2]; Mario G Solari, MD[2]; Kacey Marra, PhD[2]; Jan A Plock, MD[3]; Vijay S Gorantla, MD, PhD[2]

[1]University Hospital Bern, Bern, Switzerland, [2]University of Pittsburgh Medical Center, Pittsburgh, PA, [3]University Hospital Zurich, Zurich, Switzerland

PURPOSE: Complete disruption of peripheral nerves represents a severe injury leading to total loss of motor or sensory function and often results in unsatisfactory regeneration. The improvement of nerve regeneration after local application of adipose derived stem cells (ASCs) has been described recently. Possible mechanisms include transdifferentiation of ASCs into Schwann cells (SC) as well as paracrine effects. The aim of this study was to evaluate the functional outcome after systemic application of ASCs.

METHODS: Lewis rats underwent resection of the sciatic nerve (Res, n=10), transection and repair (TSR, n=10), TSR + ASCs (TSRA, n=12), or reconstruction with 15mm PCL conduits (CC, n=12) or 15mm PCL conduits + ASCs (CA, n=12). ASCs (1 million) were administered intravenously on postoperative day one. Functional outcome was evaluated on a weekly basis with a swim test, static sciatic index (SSI), and CatWalk XT during 6 weeks (TSR, TSRA) or 8 weeks (CC, CA). Sciatic nerve and gastrocnemius muscle was harvested at 2, 4, (n=2 per group) and at 6 weeks (Res / TSR n=6; TSRA, n=8) or 8 weeks (CC, n=6; CA, n=8) for histological and histomorphometrical analysis.

RESULTS: TSRA showed a clear improvement in SSI, as well as the swim test compared to TSR. The swim test showed improved functional recovery for TSRA at week 2 followed by further improvement over 4 weeks. A superior outcome could be observed at the 6 weeks endpoint. On the contrary, the CatWalk was only able to detect a postoperative decline due to the trauma, but did not exhibit sensitivity for differences between the groups. CC and CA remained at the same levels as Res and no functional recovery was monitored during 8 weeks.

CONCLUSION: We conclude that systemic administration of ASCs after peripheral nerve transection and repair has the potential to enhance motor functional recovery and can be detected by static and functional tests. Systemic application of ASCs appears to be a promising approach in cases where multiple peripheral nerves are involved or in order to avoid direct access to the nerve as necessary in local application.

P6
A Photochemical Tissue Bonding Approach for Sutureless Microvascular Anastamosis in an Arterial Graft Model

Joanna H Ng-Glazier, MD; Neil G Fairbairn, MD; Amanda M Meppelink, BS; Hatice Bodugoz-Senturk, PhD; Mark A Randolph, MS; Orhun K Muratoglu, PhD; Jonathan M Winograd, MD; Robert W Redmond, PhD
Massachusetts General Hospital, Boston, MA

PURPOSE: Microvascular repair with suture remains the gold standard, but can lead to inflammation and thrombosis, especially in small peripheral vessels. Use of clips, couplers, and rings can assist with technical difficulties but do not minimize risk of thrombosis or endothelial damage. Photochemical tissue bonding (PTB) is a technique that covalently links protein to create an immediate watertight bond, and has been employed by our group for wound closure in several tissues including cornea, skin, tendon, and peripheral nerve. We hypothesize that use of PTB in conjunction with a biocompatible intraluminal stent would result in a watertight seal with minimal endothelial inflammation.

METHODS: 14 New Zealand white rabbits underwent unilateral femoral artery transection with contralateral 1.5cm graft harvest, and were randomized to standard microsurgical repair with 10-0 nylon (SR) (n=6), SR+stent (n=3), or PTB+stent (n=6). For the PTB group, a 1mm overlapping cuff was stained with 0.1% Rose Bengal then illuminated with 532nm green light laser for 60 seconds on each side. One dose of heparin (100U/kg) was administered after vessel clamp removal in all animals. Repair time and vessel patency (immediate, 1 week, 4 weeks) were assessed by milk test and transcutaneous Doppler. Histology was performed at 4 weeks to assess for endothelial damage, intimal hyperplasia, and thrombus formation. Statistics were performed using one-way ANOVA with Bonferroni's comparison test.

RESULTS: Time to complete microvascular anastomosis in the PTB group was significantly faster compared with the SR ($p=0.008$) and the SR+stent groups ($p< 0.0001$). The SR and SR+stent groups were patent immediately and at 1 week. The PTB group was 100% patent immediately, with 80% patency rate at 1 week. At 4 weeks, the SR group was 100% patent, the SR+stent group was 66.6% patent, and the PTB group was 60% patent. Histologic analysis revealed qualitatively less intimal hyperplasia in the PTB group compared with other groups; quantitative measurements are currently in progress. There was grossly no hematoma or aneurysm formation at 4 weeks in any of the groups.

CONCLUSIONS: PTB induces minimal endothelial inflammation and creates a rapid, watertight and sutureless vascular anastomosis compared with standard microsurgical repair, but the use of a non-dissolvable intraluminal stent induces thrombus formation. Preliminary in-vivo studies (n=2) using a readily soluble biocompatible glass stent in a rodent model are currently in progress.

P7
Quantification of Extraneous Electromyographic Bio-Signal in the Anterior Compartment of the Rat Hind Limb

Shoshana L Woo, MD; Melanie G Urbanchek, PhD; Paul S Cederna, MD; Nicholas B Langhals, PhD
University of Michigan, Ann Arbor, MI

PURPOSE: High-fidelity signal acquisition is critical for the fundamental control of a neuroprosthesis. Our group has developed a bio-artificial interface consisting of a muscle graft neurotized by a severed nerve in the rat model. This regenerative peripheral nerve interface (RPNI) permits nerve signal transmission, amplification, and detection via *in situ* electromyography. This study examined the magnitude of extraneous bio-signal during needle electromyography in the anterior compartment of the rat hind limb.

METHODS: In six F344 rats, the extensor digitorum longus (EDL) muscle was isolated, and the proximal and distal tendons were transected. The EDL was then wrapped in small intestinal submucosa to fabricate a "simulated" RPNI construct, obviating the need for neurotization and revascularization by preserving the neurovascular pedicle. At three weeks post-implantation, all EDL constructs were isolated. A stimulating hook electrode was placed on the common peroneal nerve, a recording needle electrode in the EDL, and a grounding electrode in the contralateral toe web space. To minimize signal interference within the anterior compartment, the lateral compartment musculature was denervated. Electrophysiological tests were performed on each EDL construct (1) before and (2) after excision of the tibialis anterior (TA) and extensor hallucis longus (EHL) muscles, which comprise the remainder of the anterior compartment musculature.

RESULTS: Average EDL construct mass was 153.3 mg (range 104.7–211.4 mg; SD 44.8). Prior to TA/EHL excision, EDL compound muscle action potentials (CMAPs) displayed an average peak-to-peak amplitude (Vpp) of 23.4 mV (range 14.0–30.7 mV; SD 7.1) with an average threshold stimulation current of 192 μA (range 100–295 μA; SD 72). After TA/EHL excision, average Vpp was 14.1 mV (range 6.8–20.7 mV; SD 5.7), with an average threshold current of 239 μA (range 110–450 μA; SD 114). Vpp after TA/EHL excision was overall lower by 23.3 to 57.9% (SD 12.4) compared to Vpp prior to TA/EHL excision [paired $t(5) = 6.65$; $p=0.0012$].

CONCLUSIONS: Extraneous bio-signal from concomitant stimulation of the anterior compartment musculature was shown to contaminate needle electrode CMAP recordings from various EDL constructs. This signal interference was reduced by TA/EHL excision. Our findings prompt further investigation of CMAP recording methodology (e.g. electrode choice, multi-electrode configurations, and use of bioelectrical

insulators) to minimize signal interference from adjacent musculature. Larger studies are warranted to examine the relationship between signals-of-interest and extraneous bio-signal to develop tissue-specific noise-canceling technology in support of high-fidelity neuroprosthetic control.

ACKNOWLEDGEMENTS: This work was supported by DARPA (N66001-11-C-4190) and the Plastic Surgery Foundation.

P8
Nerve Gap Repair with Human Epineural Sheath Conduit Supported with Human Mesenchymal Stem Cells: A Preliminary Report

Grzegorz Kwiecień, MD[1]; Maria Madajka, PhD[1]; Safak Uygur, MD[1]; Adam Bobkiewicz, MD[1]; Arnold Caplan, PhD[2]; Maria Siemionow, MD, PhD, DSc[1]

[1]Cleveland Clinic, Cleveland, OH, [2]Case Western Reserve University, Cleveland, OH

PURPOSE: Peripheral nerve repair is often challenging and results in unsatisfactory outcomes. Based on our experience, rat epineural sheath conduit supported with rat bone marrow stromal cells demonstrates excellent neuroregenerative potential. Human mesenchymal stem cells (hMSC) modulate migration and replication of progenitor cells of the non-mesenchymal lineages including neurons, oligodendrocytes, and Schwann cells, with the capacity to improve neuronal regeneration. Thus, to bring this approach closer to clinical applications we have developed human epineural sheath (hES) conduit supported with hMSC as a new cellular therapy supporting nerve regeneration. The aim of this study was to assess the outcome of peripheral nerve repair using hES conduit supported with hMSC in the nude rat model.

METHODS: 20mm long sciatic nerve defect was created in 24 nude male rats. Animals were divided into four experimental groups (n=6 each): Group 1 - no repair; Group 2 - nerve autograft; Group 3 - hES filled with 0.1cc of normal saline; and Group 4 - hES supported with 3–4 x 10^6 hMSC suspended in 0.1cc of normal saline. hES conduit was created by fascicles removal using pull out technique. Bone marrow derived hMSC were cultured for 14 days and immunostained for cell surface antigens to ensure homogenicity prior to injection into the empty hES conduit. Outcome assessment included: sensory pinprick (PP) and motor toe-spread (TS) tests at 1, 3, 6, 12 weeks. Somatosensory evoked potentials (SSEP), gastrocnemius muscle index (GMI), histomorphometry, immunostaining for GFAP, NGF, S-100, HLA I / II, vWF and laminin B2 were performed 12 weeks after surgery.

RESULTS: Cultured hMSC expressed CD105, CD73 and CD90, and lacked expression of CD45, CD34, CD14, CD11b, CD79a, CD19 and HLA-DR surface molecules. No leakage of cells was observed at the time of injection during conduit implantation. hES conduit maintained its shape and integrity at 12 weeks following repair. No local inflammation or scarring was observed at the end of the follow up. Clinical evaluation and SSEP analysis confirmed sciatic nerve recovery in groups 3 and 4 with outcomes comparable to nerve autograft repair. Immunostaining showed presence of the hMSC in the conduit at 12 weeks post-implantation. Quantitative nerve and muscle histological analysis is currently in progress.

CONCLUSION: This study confirms feasibility of application of hES conduit for restoration of peripheral nerve defects. hES supported with hMSC demonstrated comparable functional outcomes to the autograft technique. The role of local hMSC application in nerve regeneration is currently under investigation.

P9
Non-Invasive Objective Evaluation of Peripheral Neuroregeneration Using Magnetic Resonance Diffusion Tensor Imaging

Nataliya Kostereva, PhD[1]; Vincent Lee, PhD Candidate[1]; Kimimasa Tobita, PhD[1]; Jignesh Unadkat, MD[1]; Jonas Schnider, MD[2]; Chiaki Komatsu, MD[1]; Mario Solari, MD[1]; Vijay Gorantla, MD, PhD[1]

[1]University of Pittsburgh, Pittsburgh, PA, [2]University Hospital Berne, Berne, Switzerland

PURPOSE: Objective, non-invasive, sequential monitoring of regeneration after peripheral nerve repair is critical for evaluation of the efficacy of re-innervation and treatment strategies that may have important implications in recovery and outcome. We investigated whether diffusion magnetic resonance imaging (MRI) can accurately assess neuroregeneration.

METHODS: We used sciatic nerve (SN) transection & repair model in Lewis rats. A wide range of treatment modalities (FK506, Schwann cells (SC), chondroitinase ABC (CH) and IGF-1, alone or in combination) was applied at the time of surgery. At the end points (2 and 5 weeks), SNs were excised and embedded in 1% agarose. Spin echo DTI was performed with following parameters: TE= 27msec, TR= 5000msec, 6 directions, 128 x 128 matrix with 300um resolution. MRI parameters such as fractional anisotropy (FA) was computed and compared with histomorphometry, expression of GAP43 (marker of regeneration), neurofilament M and myelin (nerve functionality).

RESULTS: The analysis of DTI images showed that injured nerves have lower FA values as compared to the naïve nerves. It suggests that in area distally to coaptation site of injured nerves water diffuses in various directions indicating low structural integrity whereas most of the water inside of the naïve nerve diffuses in the same direction. FA has increased or did not change in the proximal and transection segment of injured nerve across groups from 2 to 5 weeks post-surgery. In the distal segment, FA value has increased by a noticeable margin in IGF-1 group and to a lesser degree, in FK506 treated group. This correlated strongly with changes in GAP43 expression, neurofilament M and myelin expressions in the distal nerve fragment.

CONCLUSIONS: The results suggest that MRI analysis can be successfully employed as one of the methods for the assessment of neuroregeneration. Comparison of DTI data to validated measures like histomorphometry, immunohistochemistry, electrophysiology (EMG, NCV) and others can enable us to develop an accurate non-invasive evaluation of overall functional outcomes after nerve repair, reconstruction or transplantation.

P10
Targeted Nerve Implantation for Primary Prevention and Secondary Treatment of Neuromas in Amputees

Mitchell Andrew Pet, MD; Janna L Friedly, MD; Douglas G Smith, MD; Jason H Ko, MD
University of Washington, Seattle, WA

PURPOSE: Painful neuromas affect up to 25% of amputees, because axons sprouting from the proximal nerve stump are deprived of a distal target to reinnervate. This leads to a directionless and disorganized proliferation of neural and connective tissue. To address neuroma formation in this setting, we performed a surgical technique called Targeted Nerve Implantation (TNI), wherein the proximal amputated nerve stump is implanted onto a surgically denervated portion of nearby muscle at a secondary motor point, thereby providing regenerating axons with a distal target for organized reinnervation. We hypothesized that rather than forming a neuroma, sprouting axons enter the secondary motor point and arborize into the denervated muscle. In this study, we determined whether TNI was an effective strategy for primary prevention of neuroma in the setting of acute amputation and for secondary treatment of established neuromas in upper and lower extremity amputees.

METHODS: We retrospectively reviewed two groups of patients treated by a single surgeon at a high-volume trauma center between 2006 and 2012: 1) 14 patients who underwent primary TNI for neuroma prevention at the time of acute amputation; and 2) 24 patients with established neuromas who underwent neuroma excision with secondary TNI. The primary outcome examined was presence or absence of neuroma pain at the last post-operative follow-up visit.

RESULTS: Thirty-eight amputees underwent TNI for either primary neuroma prevention or secondary neuroma treatment. In the primary TNI group, 12 out of 14 patients were male, and 12 out of 14 were upper extremity amputees. In the secondary TNI group, 16 out of 24 patients were male, and 7 out of 24 were upper extremity amputees. After primary TNI in the setting of acute amputation, 13 of 14 (93%) patients were free of neuroma pain at a mean follow-up of 20 months. After secondary TNI for the treatment of established neuroma, 21 of 24 (88%) patients were free of neuroma pain after a mean follow-up of 19 months.

CONCLUSIONS: Targeted nerve implantation was effective for neuroma prevention when performed primarily at the time of acute amputation and for the treatment of established painful end-neuromas when performed secondarily. By providing a distal target for proximal axon sprouts to grow into, TNI may offer an effective strategy for the prevention and treatment of neuromas in upper and lower extremity amputees. However, additional research is necessary to confirm the proposed mechanism and to compare TNI to existing techniques.

P11
Plastic Surgery Closure of Craniotomy Incisions Reduces the Incidence of Wound Complications in Patients with Previous Neoadjuvant Bevacizumab (Avastin) and Radiation

Alyssa R Golas, MD; Tatiana Boyko, MD; John A Boockvar, MD; Theodore H Schwartz, MD; Philip E Stieg, MD, PhD; Jason A Spector, MD, FACS
Weill Cornell Medical Canter, New York, NY

INTRODUCTION: Craniotomy incisions are often associated with wound healing complications, particularly in the setting of re-operative craniotomy, radiation (XRT) and/or intra-arterial or intra-venous bevacizumab (Avastin) therapy. In the setting of these obstacles to wound healing, wound complication rates may be as high as 44%. As a result of these strikingly high complication rates, plastic surgeons have increasingly become consulted for management of craniotomy incisions in patients deemed to be at "high risk" for wound healing complications. We therefore hypothesized that plastic surgery closure following craniotomy in these patients would decrease the rate of postoperative wound complications.

METHODS: A retrospective review was performed of all patients who underwent craniotomy incision closure at a single institution by a single plastic surgeon between 2006 and 2013. Charts were reviewed for previous operative interventions, the presence of pre-existing infection, indication for plastic surgery involvement, neoadjuvant and adjuvant XRT and/or bevacizumab administration, and the need for surgical intervention following the index plastic surgery closure.

RESULTS: Forty-three patients (64 procedures) were included in the study. Forty-two patients (97.7%) underwent previous craniotomy for indications including intracranial neoplasia (n=32), intracranial hemorrhage (n=5), seizure disorder (n=4), and hydrocephalus (n=1). Average follow-up was 295d (range, 1-1715d; median, 124d). Nine patients (20.9%) required reoperation after their index plastic surgery intervention. Twenty-two patients (51.2%) received 24 "prophylactic" plastic surgery closures (i.e., in the absence of infection) for indications including previous craniotomy (n=22), XRT (n=19), and prior bevacizumab therapy (n=11). Three patients (13.6%) who underwent prophylactic closure (for indications including previous craniotomy +/- XRT) required further surgical intervention (12.5% of prophylactic procedures). Of note, none of the 11 patients who underwent prophylactic closure for previous craniotomy+neoadjuvant bevacizumab+XRT required repeat intervention. Fourteen patients (32.6%) in this series received neoadjuvant bevacizumab+XRT. Of these, only 2 patients (14.3%) required additional plastic surgical intervention for wound complications after their index plastic surgery procedure. Of the 7 patients who received neoadjuvant

XRT and adjuvant bevacizumab, 2 (28.6%) required reoperation for wound complications (both patients had also received neoadjuvant bevacizumab). Lastly, 25 patients in this series received neoadjuvant XRT, 5 of whom (20.0%) developed wound complications requiring intervention.

CONLCUSIONS: Plastic surgery involvement in "high risk" patients undergoing re-operative craniotomy and who received neoadjuvant bevacizumab+XRT reduces the incidence of wound complications. This is particularly true when plastic surgery closure is performed "prophylactically." As the cohort of "high risk" neurosurgery patients undergoing craniotomy continues to grow, further collaboration between the neurosurgical and plastic surgery teams is warranted.

P12
The Effect of CXCR4 Inhibition on Hindlimb Allograft Survival

Joani M Christensen, BA[1]; Lehao W Wu, MD[1]; Georg Furtmuller, MD[1]; Saami Khalifian, BS[1]; Michael Kimelman, MD[2]; Angelo Leto Barone, MD[1]; Nance Yuan, MD[1]; Justin M Sacks, MD[1]; W P Andrew Lee, MD[1]; Gerald Brandacher, MD[1]; Damon S Cooney, MD, PhD[1]

[1]Johns Hopkins University School of Medicine, Baltimore, MD, [2]Innsbruck Medical University, Innsbruck, Austria

PURPOSE: Wider application of vascularized composite allotransplantation (VCA) is hindered by need for chronic immunosuppression post-transplant Evidence suggests that autologous, bone marrow-derived CD34+ hematopoietic stem and progenitor cells (HSPCs) may promote induction of central and peripheral immunologic tolerance. Recipients of VCAs possess two sources of HSPCs, donor and recipient bone marrow, but the role of these cells in the immune response to a VCA is yet to be explored. Antagonism of the CXCR4 axis has been shown to mobilize bone marrow HSPCs to the periphery. Our objective was to investigate the effect of CXCR4 receptor antagonists AMD3100 and plerixafor on the ability to mobilize stem cells, promote peripheral chimerism, and prolong graft survival in a rodent hindlimb transplantation model.

METHODS: Lewis rats received orthotopic hindlimb transplants from Brown Norway (BN) donors. Treatments consisted of tacrolimus (0.5mg/kg) for 21 days, AMD3100 (5mg/kg) POD 0,1,2,3,7; or plerixafor (1mg/kg) POD 0,1,2,3,7. Groups included 1) tacrolimus; 2) tacrolimus + AMD3100; 3) tacrolimus + plerixafor; 4) AMD3100; 5) plerixafor. Mobilization of peripheral blood mononuclear cells was assessed by performing a colony forming unit (CFU) assay on day 7 and day 21 using peripheral blood mononuclear cells of rats (n=3) receiving the regimens above. Peripheral hematopoietic chimerism was detected using flow cytometry staining PBMCs with antibodies for RT1Ac, MHC class 1 marker for BN, on POD 7, 21, 28, and at the time of rejection. Clinical rejection was assessed according to Banff criteria.

RESULTS: CFU assays from day 7 peripheral blood revealed an average of 54.3 CFU in the AMD3100 group, 48.0 in the tacrolimus + AMD3100, 43.0 in the plerixafor group, and 49.8 in the tacrolimus + plerixafor group, all significantly elevated compared to control, 22.7 (all $p<0.05$). MHC-I chimerism was detectable in all experimental animals. Rats receiving combination treatment with tacrolimus + AMD3100 had average peripheral lymphoid chimerism of 4.1%, higher than that in treatment with tacrolimus alone, 0.84% ($p=0.23$) on POD 7. No significant difference in chimerism levels was found at any

other time point. Average rejection-free graft survival with conventional tacrolimus was 35 days, while it was 37.0 for those receiving tacrolimus + AMD3100, and 36.0 for those receiving tacrolimus + plerixafor. Average rejection free graft survival after AMD3100 treatment alone was 11.0 days, and 12.5 after plerixafor alone.

CONCLUSION: The results suggest that treatment with AMD3100 or plerixafor, alone or in combination with conventional tacrolimus therapy elevates the number of circulating HSPCs as expected. Additionally this treatment led to increases in circulating donor-derived cells in animals following hindlimb transplant. Despite the ability to increase circulating stem cells and peripheral chimerism these treatments did not significantly prolong graft survival. Further studies will explore this disconnect between chimerism and graft survival as well as explore whether variations in the dosing may be more successful in prolonging graft survival.

P13
Abdominal versus Thigh Based Reconstruction of Perineal Defects in Cancer Patients

Jens Berli, MD; John Pang, BS; Justin M Broyles, MD; Kate Buretta, MD; Sachin M Shridharani, MD; Danielle H Rochlin, BS; Jonathan E Efron, MD; Justin M Sacks, MD
Johns Hopkins Hospital, Baltimore, MD

INTRODUCTION: An abdominoperineal resection (APR) is a highly invasive procedure that leaves the patient with pelvic dead space and a large perineal defect. Traditionally the pedicled vertical rectus abdominus myocutaneous flap (VRAM) is used to reconstruct the perineal defect to improve functional outcomes and reduce complications. Oftentimes, the VRAM cannot be utilized due to previous abdominal surgery or need for multiple ostomy placement. Using the VRAM in this setting would create significant morbidity to the abdominal wall. The pedicled anterolateral thigh flap (ALT) is a described alternative to the VRAM and allows the perineum to be reconstructed sparing the abdominal wall. In the current study, we report complex perineal reconstruction in cancer patients using either the VRAM or the ALT flap when clinically appropriate.

METHODS: A retrospective chart review (2010–2012) of prospectively entered data was conducted to identify all VRAM and ALT flaps that were utilized for perineal reconstruction following APR. Complications were defined as: partial and complete flap failure, seroma, dehiscence, infection, abdominal or perineal herniation, necrosis, and bleeding. Patient demographics such as gender, race, prior surgery, tumor stage, body mass index (BMI), smoking status, alcohol consumption, medical comorbidities, chemoradiation status, oncologic margin status, need for re-operation, readmissions, time to initiation of chemotherapy, and time to complete healing were also recorded. A two-sided Fisher's exact test was used for categorical variables and a student's T-test for continuous variables.

RESULTS: We identified 19 patients of which 10 underwent an ALT and 9 underwent a VRAM. There were no significant differences in gender, age, BMI, race, or co-morbidities between patients receiving ALT or VRAM reconstruction ($p>0.05$). Surgical outcomes and complications of ALT versus VRAM demonstrated no significant differences in the rate of infection, hematoma, bleeding, or necrosis. No flap failures, either full or partial, occurred in any of the groups. The mean length of stay after reconstruction was 9.7 ± 3.4 days in the ALT group and 13.4 ± 7.7 days in the VRAM group ($p>0.05$).

CONCLUSION: Perineal reconstruction with the pedicled ALT or VRAM flaps can be performed safely, with acceptable complication rates in the presence of contamination, compromised soft-tissue vascularity, and radiotherapy.

Our results from a single surgeon suggest that the ALT is an acceptable alternative to the VRAM for the reconstruction of perineal defects when there are concerns of using the abdominal wall as a soft-tissue flap harvest site. The ALT flap for perineal reconstruction allows the armamentarium of the reconstructive surgeon to expand and offer patients robust vascularized tissue for restoration of form and function.

P14
In Vivo Real-time Ultra-fast 3D Fourier Domain Optical Coherence Tomography Imaging of Anastomoses for Super-microsurgical Research

Shan Zhu, MD[1]; Dedi Tong, MD[1]; Yong Huang, PhD[2]; Lehao Wu, MD[1]; Zuhaib Ibrahim, MD[1]; Qi Mao, MD[1]; John Pang, MD[1]; Damon S Cooney, MD[1]; W P Andrew Lee, MD[1]; Gerald Brandacher, MD[1]

[1]Department of Plastic and Reconstructive Surgery, Johns Hopkins University School of Medicine, Baltimore, MD, Baltimore, MD, [2]Department of Electrical and Computer Engineering, Johns Hopkins University, Baltimore, MD, Baltimore, MD

PURPOSE: The emergence of supermicrosurgery has enabled reconstructive surgery to enter into a new era by advancing a series of novel techniques including lymphaticovenous anastomosis, fingertip replantation, and perforator flap surgery. Nonetheless, super-microsurgery techniques impose great technical challenges. The instant monitoring and evaluation of the patency of the anastomosis, in particular of intraluminal structure, is critical to be able to predict the necessity of early re-intervention and thus reduce/avoid complications and improve surgical success rates. Real-time 3D fourier-domain optical coherence tomography (3D FD-OCT) is a powerful imaging system, which uniquely provides noninvasive, *in vivo* real-time images on a micrometer-scale, allowing intraoperative assessment of dynamic tissue microstructure of vessels at depths beyond those of standard microscopy. In this study, we evaluated 3D FD-OCT as an effective method for *in vivo* monitoring of various super-microsurgical anastomosis techniques.

METHODS: 40 C57BL/6 mice underwent end-to-end femoral artery anastomosis and *in vivo* monitoring by the 3D FD-OCT at various time points (pre-anastomosis, right before release of vessel clamp, and 60-minutes post anastomosis). 3D FD-OCT was running at 70,000 A-scans per second with lateral resolution of 12 μm and axial resolution of 3.6 μm was used for intravital imaging. In addition, all results from 3D FD-OCT imaging were correlated and confirmed by H&E histology.

RESULTS: Within the 40 femoral arteries (diameters averaged slightly less than 0.4 millimeter), 38 of them gained immediate patency after removing the clamp and had stable blood flow 1 hour after anastomosis. Two anastomoses were not patent because of suturing the back wall of the vessel and entangled adventitia respectively. In those cases, OCT images successfully exhibited the structures of all layers of the vessel wall, the vessel patency and continuity shown by tomographic section, 3D anatomic reconstruction and Doppler image, and

blood flow. In the 2 instances with anastomotic complications, thrombus formation and progression could be clearly visualized. Furthermore, OCT imaging was able to detect impaired endothelium continuity, evidence of technical error and compromised blood flow. Histology confirmed the respective OCT outcomes.

CONCLUSION: 3DFD-OCT is a valid method to evaluate vessel patency, hemodynamics and the structural changes of the anastomosed artery, as well as potential technical glitches during anastomosis. This real-time non-invasive method has tremendous potential for clinical applications and to improve outcomes of super-microsurgical procedures.

P15
The Effect of Torticollis on Helmet Therapy for Deformational Plagiocephaly

Emma M Kulig, BA; Chelsea R Horwood, BA; Sarah A Donigian, BA; Alexander Y Lin, MD

Saint Louis University School of Medicine, St Louis, MO

PURPOSE: Children with deformational plagiocephaly frequently have some degree of relative neck muscle imbalance, or torticollis. It is unclear whether torticollis leads to positional preference in sleeping, or the preferential sleep position limits neck flexibility, but it is commonly thought that concomitant torticollis makes deformational plagiocephaly treatment more refractory. It is therefore possible that torticollis could affect the age of diagnosis and treatment of deformational plagiocephaly, duration and effectiveness of helmet therapy, initial and final transcranial differences, or ultimate helmet therapy outcomes. Among patients undergoing helmet therapy for deformational head shape problems, we compared between those diagnosed with torticollis and those who did not have torticollis.

METHODS: Patients with deformational plagiocephaly who underwent helmet orthotic treatment from 2006 to 2013 were retrospectively reviewed. The helmet orthotist recorded standard cranial measurements at each helmet adjustment visit, and only patients who completed their treatment course with final measurements were included. Patients who were lost to followup before being discontinued from helmet therapy, or did not have explicit mention of presence or lack of torticollis, were excluded. Continuous variables were compared with parametric tests (t-tests), and categorical variables were compared with chi-square tests.

RESULTS: 155 patients met the inclusion and exclusion criteria. Torticollis (T) was seen in 60% (93/155), and no torticollis (NT) was found in 40% (62/155), p=0.151. Helmet therapy was initiated at age in months adjusted for prematurity (with range): T 6.13 (±1.4), NT 6.6 (±1.89), p=0.096. Asymmetry was measured by transcranial difference (TCD) between frontozygomatic-to-eurion diagonals in millimeters, with initial TCD: T 11.2 (±2.8), NT 8.4 (±4.3), ***$p < 0.001$; final TCD: T 4.2 (±2.3), NT 3.5 (±2.3), p=0.086; change in TCD: T 7.7 (±2.9), NT 4.9 (±4.3), ***p<0.001. The duration of therapy in months was: T 3.91 (±1.63), NT 3.73 (±1.67), p=0.516; with rate of TCD change (mm/month) being: T 2.3 (±1.2), NT 1.7 (±1.6), *p=0.006. 47% (69/146) of torticollis patients underwent physical therapy (PT) for neck exercises, and their average final TCD (in mm) was 4.4 (±2.6), compared to those who did not get PT at 3.7 (±2.1), p=0.069.

CONCLUSIONS: Our data suggest that torticollis does not significantly affect effectiveness or duration of helmet therapy. Although torticollis patients had greater initial transcranial

differences (TCD) as would be expected, they ended with similar final TCD measurements, and surprisingly, helmet therapy duration was similar despite the worse initial asymmetry. This greater rate of TCD change is not explained by the similar age at initiation of helmet therapy. In addition, infants with torticollis who received physical therapy did not have improved final transcranial differences as compared to those who did not receive physical therapy. These results suggest that although torticollis and deformational plagiocephaly often occur hand-inhand, once the decision to proceed with helmet therapy has been made, their outcomes appear to proceed independently. Therefore, treatment can remain independent, with helmeting for the deformational plagiocephaly, and physical therapy for the torticollis.

P16
Detailed Characterization and Functional Analysis of Skin-Resident Leukocytes from Vascularized Composite Allografts in Tolerant Miniature Swine Mixed Chimeras

Harrison Powell, BS; David A Leonard, MBChB, MRCS; Alexander Albritton, BS; Christopher Mallard, BS; Curtis L Cetrulo; Jr, MD, FACS; Josef M Kurtz, PhD
Massachusetts General Hospital, Boston, MA

PURPOSE: We have previously reported induction of vascularized composite allograft (VCA) tolerance across major histocompatibility (MHC) barriers by hematopoietic stem cell transplantation (HSCT) in MGH Miniature Swine, with stable mixed chimerism permitting indefinite immunosuppression-free survival of all components of the VCAs. While previous studies have primarily focused on peripheral blood leukocytes for analysis, the characterization of both lineage and function of the resident skin leukocyte populations remain to be investigated.

METHODS: Two animals underwent haplomatched HSCT and VCA. VCA and host skin were biopsied for FACS and mixed lymphocyte reaction (MLR) analysis. Biopsies were first incubated in Dispase II to separate epidermis from dermis, following which the tissue was further digested to produce single cell suspensions. Dermis was digested in collagenase D, while epidermis was digested with trypsin. For FACS analysis, dermal and epidermal cell suspensions were analyzed for lineage markers (CD3, CD4, CD8, g/d T cells, MHC Class 2, Langerin) and donor/host hematopoietic origin. For MLR, Langerhans cells were FACS sorted and plated in culture as stimulators to peripheral blood leukocyte responders.

RESULTS: Two weeks post-VCA and HSCT, host skin dermis contained distinct populations of donor derived T cells (CD4+ 18–30%, CD8+ 5–10%, and g/d 8–10%) cells, but no donor-derived Langerhans cells were detected within the epidermis. In contrast, the VCA contained a significant population of host-derived leukocytes; host derived T cells (CD4+ 20–30%, CD8+ 5–6%, and g/d 20–60%) cells were found within VCA dermal tissue. In the VCA epidermis, the majority of Langerhans cells remained of donor origin, but a small population (5–15%) of host derived Langerhans cells was detected. At later time points (150 days post-VCA/HSCT), skin chimerism levels reflected peripheral blood chimerism. The majority of leukocytes from the dermis were donor-derived in both host and VCA skin. While the majority of T cells in peripheral blood were donor-derived, a small but significant number of host T cells were found in the host and VCA dermis. Interestingly, at >150 days, 30–40% of the Langerhans cells in host skin epidermis remained host derived. This suggests that while donor derived Langerhans cells migrate into host epidermis, the turnover is slower compared to other cell lineages. Langerhans cells, of both donor and host origin, stimulated

proliferative responses in naive responders of host- and donor type as well as third party peripheral blood lymphocytes in MLRs. However, no proliferation was observed in responders from the chimeric VCA recipient, demonstrating tolerance of both host- and donor-derived lymphocytes to host- and donor-derived Langerhans cells in these animals. Furthermore, the ability to stimulate non-tolerant host and donor responders suggests that the Langerhans cells isolated were not suppressive in vitro, while their in vivo suppressive capability remains to be investigated.

CONCLUSION: Given the difficulty in achieving tolerance to skin in the transplant setting, these studies will contribute significantly to our understanding of the mechanisms of skin-specific immunobiology. Understanding the kinetics of cellular infiltrate and resident leukocyte turnover will enhance our understanding of the balance of rejection and tolerance in VCA transplantation research.

P17
Readability Assessment of Online Patient Resources for Breast Augmentation

Christina R Vargas, MD; Bernard T Lee, MD, MBA

Beth Isreal Deaconess Medical Center / Harvard University, Boston, MA

PURPOSE: Patients increasingly rely on internet resources in evaluating their medical concerns, deciding to seek care, and understanding elective procedures. Well-informed patients are more likely to be active participants in their healthcare, contributing to higher satisfaction and better overall outcomes. Access to online patient material, however, is limited for a significant portion of United States adults by inadequate functional health literacy. As such, the National Institutes of Health and American Medical Association recommend that patient educational content should be written at a sixth grade reading level. This study aims to assess the readability of the most popular online patient resources regarding breast augmentation in the context of average adult American literacy.

METHODS: A web search for "breast implant surgery" was performed using the two largest public search engines. After sponsored results were excluded, the twelve most accessed sites common to both searches were identified. Patient-directed information from all relevant articles immediately linked from the main site was downloaded and formatted in plain text. The readability of 110 articles was evaluated using 10 established analyses: Coleman-Liau Index, Flesch-Kincaid Grade Level, Flesch Reading Ease, FORCAST Formula, Fry Graph, Gunning Fog Index, New Dale-Chall, New Fog Count, Raygor Readability Estimate, and SMOG Readability Formula.

RESULTS: The overall average readability of the twelve most popular internet resources for breast augmentation was 13. The Raygor readability estimate for the 110 articles combined was 15th grade, with a range from 8th to 17th grade.

CONCLUSION: Online patient resources for breast augmentation exceed the recommended reading level, limiting their accessibility for a significant portion of American adults.

P18
Validating Regenerative Peripheral Nerve Interface Function in Relationship to Hind Limb Kinematics during Treadmill Locomotion

Daniel C Ursu, MS; Andrej Nedic, MSE; Cheryl A Hassett, BS; Jana D Moon, BS; Nicholas B Langhals, PhD; Richard B Gillespie, PhD; Paul S Cederna, MD; Melanie G Urbanchek, PhD
University of Michigan, Ann Arbor, MI

PURPOSE: Regenerative Peripheral Nerve Interfaces (RPNI) are neurotized autologous free muscle grafts equipped with electrodes to record myoelectric signals for prosthetic control. RPNI devices implanted into rats have been shown, using evoked responses, to be stable and viable for up to 2 years. In vivo characterization of RPNI signaling is critical for assessing their utility as a control modality for prosthetic devices. This work quantifies RPNI signal activation and relates it to gait; its ultimate purpose is to define signaling relationships between RPNI and native muscle during volitional control.

METHODS: Three experimental groups of two rats each were created: Control, RPNI, and Denervated. In the Control group, the soleus muscle remained intact; subjects in the Denervated and RPNI groups underwent soleus muscle neurotomy. The RPNI group received a free soleus muscle transfer to the ipsilateral thigh and reinnervation with the proximal end of the transected tibial nerve. In all groups, bipolar wire electrodes were positioned on the soleus surface. Evaluation was performed 4–5 months post-surgery. Rats were conditioned to walk on a treadmill at constant pace between 8.5 and 9.0 m/min. A synchronized 120 frames per second videography and 3 kHz data acquisition system identified hip, knee, ankle, and toe joint angle trajectories and myoelectric signals. Each gait cycle and corresponding conditioned myoelectric signal was temporally normalized to facilitate comparisons across gaits and subjects. Within each subject group, normalized trajectories and signals were averaged. Integrated myoelectric activity over each phase of gait was then compared between subject groups.

RESULTS: Per the kinematic analysis, ankle movement in the Control group was characterized as normal (according to published data), while the ankle movement of the RPNI and Denervated groups exhibited a marked inability to extend the ankle. Myoelectric activity was highly repeatable within subjects and within subject groups. The Control group's electromyographic signals were periodic with gait and reflected typical activation patterns. An altered electromyographic signal pattern was found for the RPNI group, but this pattern was also periodic with gait. A comparison of myoelectric activity integrated separately over stance and swing phases for the Control and RPNI groups indicates that RPNI signaling predicts firing of the tibial nerve that is lower, yet proportionally similar to Control. The Denervated group demonstrated low amplitude random myoelectric activity, unrelated to gait.

CONCLUSION: This study demonstrates that in vivo myoelectric RPNI activity is periodic and occurs during stance phase preceding push-off, when the tibial nerve is expected to be most active. Contamination from muscles adjacent to the RPNI is minimal, as demonstrated by the results obtained from the Denervated group. The periodicity recorded during RPNI firing suggests control governed by volitional or reflexive processes appropriate to an altered gait.

P19
Peripheral Nerve Repair Using a Novel Peptide Amphiphile Nanofibers: In Vitro and In Vivo Studies

Akishige Hokugo, DDS PhD; Andrew Li, MD; Anisa Yalom, MD; Luis A Segovia, MD; Reza Jarrahy, MD
David Geffen School of Medicine at UCLA, Los Angeles, CA

PURPOSE: Traumatic peripheral nerve injuries can result in lifelong disability. Primary nerve repair is used for short nerve defects. Autologous nerve can be used in longer defects but creates donor site morbidity. Nerve conduits lack an aligned internal scaffold to support and guide axonal regeneration. Peptide amphiphiles (PA) can self-assemble into aligned nanofibers and promote peripheral nerve regeneration in vivo. There are no studies to date that examine the ability of PA nanofibers to support the regeneration of injured nerves that supply the musculoskeletal system. In this preliminary study, we investigate the viability of rat Schwann cells after incorporation into PA gels.

METHODS: PA nanofibers were synthesized. PAs were aqueously dissolved, and rat Schwann cells (cell line RT4-D6P2T) were incorporated into the PA solution. The PA/cell suspension was then pipetted in aliquots into salt solution containing CaCl2, immediately forming a solid gel. Gelling solution was then replaced with Dulbecco's Modified Eagle's Medium (DMEM) with 10% fetal bovine serum, and changed every 3 days. Control collagen gels with incorporated Schwann cells were made at the same density. Cell proliferation assay was performed. To evaluate of peripheral nerve regeneration, PLGA conduit filled with PA gels were grafted in the critical sciatic nerve gap of rat. Control empty PLGA conduit or autologous nerve were also grafted in the nerve gap. Motor and sensory function tests were performed to evaluate the peripheral nerve regeneration.

RESULTS: Schwann cells demonstrated significantly increasing proliferation after embedding in PA gels from days 1–11. Control collagen gel and cell culture also demonstrated increasing growth from day 1 to day 11. Motor and sensory functions were improved by the PLGA conduit filled with PA gels similar to autologous nerve graft.

CONCLUSION: Schwann cells embedded in PA gels exhibit increasing proliferation within PA gel. PA gels were supported peripheral nerve regeneration in vivo. These findings support the idea that PA gel constructs are an effective candidate for an internal scaffold in nerve conduits.

P20
Tracheal Allotransplantation: The Next Step

Margot Den Hondt, MD; Pierre Delaere, MD, PhD; Jan Jeroen Vranckx, MD, PhD
KULeuven, Leuven, Belgium

PURPOSE: Key elements in tracheal allotransplantation are adequate vascularization, a stable framework withstanding respiratory forces and an inner mucosal lining, thus preventing healing by secondary intention and subsequent stenosis. Since we are dealing with allogenic tissues, rejection of the respiratory epithelium remains of great concern.

METHODS: We transplant an allogenic tracheal segment into the lateral thoracic fascia of the New Zealand White rabbit. Rabbits receive full dose immunosuppression, i.e. tacrolimus. Tapering of tacrolimus induces a silent rejection of the inner mucosal lining. By replacing donor epithelium with recipient mucosa, we eliminate the allogenic component. After a 14-day heterotopic prefabrication period, we perform an orthotopic transfer of the segment to the neck. We cultured ciliated epithelium from tracheal inner lining to subconfluence. Cells in passage three were used as a patch of neo-epithelium on an inner lining defect in the rabbit model. Gradually the size of defects was enlarged and cell migration observed on histological sections. We decellularized a rabbit trachea tube using controlled enzymatic digestion protocols. Aim was to preserve structural integrity while removing cellular components. Subsequently these trachea's were covered with the cultivated ciliated epithelium. Blood outgrowth endothelial cells (BOECs) were cultured from rabbit intravenous blood and added to the construct to enhance vascularization. In the human model, we observed an avascular necrosis of the posterior tracheal wall during heterotopic revascularization of the tracheal segment in the radial forearm fascia. Since little lumen is preserved by primary anastomosis of the cartilage rings, we perform an additional reconstruction of the membranous trachea with cartilage in the rabbit model.

RESULTS: As we demonstrated by creating a full thickness mucosal defect in the rabbit model, bare cartilage will lead to recurrent stenosis. After enzymatic decellularization, the rabbit trachea preserves its rigidity and the structural elements necessary for cellular adhesion. Ciliated epithelium could be efficiently cultivated and led to reepithelialization on decellularized tracheal tubes of various sizes. These 'cell-engineered ' tubes could be efficiently prefabricated using our lateral thoracic pedicle. BOECs could be cultivated from intravenous rabbit blood and led in vitro to the formation of vascular structures. In vivo, adding BOECs accelerated healing of the reepithelialized tracheal tubes. By cartilaginous reconstruction of the posterior wall, we preserved adequate diameter of the tracheal lumen to allow for normal breathing.

CONCLUSION: Up until now, five patients in our center received a tracheal allotransplantation with withdrawal of immunosuppression. To reconstruct a long segment tracheal stenosis, it is of utmost importance to provide a vascularized inner mucosal lining. We modified the time points in our protocol to reduce the adverse effects of immunologic rejection. Currently we are fine-tuning the enzymatic treatment of the inner lining and cultivation of mucosa in the rabbit model.

P21
Magnesium and Biological Hydrogel Degradation within a Polycaprolactone (PCL) Conduit for Peripheral Nerve Repair

Danielle M Minteer, BS[1]; Andrew Villasenor, BS[2]; Ricardo Andres-Nieves, BS[1]; Wesley Sivak, MD/PhD[1]; Sarah Pixley, PhD[3]; Kacey G Marra, PhD[1]

[1]University of Pittsburgh, Pittsburgh, PA, [2]Summer Premedical Academic Enrichment Program, Pittsburgh, PA, [3]University of Cincinnati, Cincinnati, OH

PURPOSE: The objectives of the study were to 1) observe Mg degradation, 2) assess hydrogel scaffold behavior within a PCL conduit over a period of 7 days at 37 °C, and 3) to evaluate the tissue engineered device as a potential solution to long-gap peripheral nerve repair. Peripheral nerve damage results from trauma, infection, or surgical procedures. While collagen nerve guides are commercially available, current solutions do not provide adequate mechanical support required by the growing axon nor provide promotion of axonal growth for defects larger than three centimeters.

Exposure to magnesium (Mg) ions has been shown to increase neural stem cell proliferation in vitro and in vivo testing has indicated replenishing Mg ions via blood delivery improves functional recovery following nerve damage. Keratin, after degrading into peptides, promotes Schwann cell migration and improves axonal elongation. Poloxamer-407 is a copolymer used in several biological applications, including as a drug delivery system.

METHODS: Keratin was isolated from freshly cut human hair, rinsed, extracted and freeze-dried and reconstituted with PBS to achieve hydrogel scaffold. Poloxamer-407 solution was reconstituted with PBS in order to achieve hydrogel scaffold. Salt-leeching fabrication of PCL conduits followed a previously established protocol. Next, 0.5 centimeter-Mg wire was placed within PCL conduits and keratin hydrogel, poloxamer-407, or phosphate buffered saline (PBS) was introduced to the lumen of the conduit via a 18G syringe and stored at 37°C. As a control for the PCL conduit, a Mg wire was also embedded within keratin, poloxamer-407, or PBS within a plastic cryotube, with no PCL conduit and stored at 37°C. To assess magnesium degradation in vitro after 7 days, scanning electron micrographs (SEM) were obtained.

RESULTS: SEM indicated that Mg degradation occurred over 7 days at 37°C with exposure to keratin and Poloxamer-407 hydrogels and, interestingly, as well as with PBS, either when incorporated within a PCL conduit, when embedded within hydrogels or with PBS only (no PCL). Magnesium embedded within the keratin scaffold appeared to have surface erosion, while Mg within PBS and poloxamer-407

appeared to have undergone bulk erosion, with less degradation of the Mg in PBS

CONCLUSION: To address the clinical need of a tissue engineered solution to long-gap peripheral nerve repair, degradation of metal magnesium wire within keratin and poloxamer-407 hydrogels was assessed in vitro over a 7-day period. Keratin and poloxamer-407 both contain potential to serve as scaffolds to maintain orientation of a Mg wire within a PCL conduit for peripheral nerve repair. Future directions include applying a coating to the Mg wire to tailor degradation, cytotoxicity studies in vitro and in vivo studies within a large defect rat sciatic nerve hind limb model.

P22
In Vitro Electrode Stability Protocols for Use in a Regenerative Peripheral Nerve Interface

Stephanie A Goretski; Jana D Moon, BS; Melanie G Urbanchek, PhD; Paul S Cederna, MD; Nicholas B Langhals, PhD
University of Michigan, Ann Arbor, MI

PURPOSE: A Regenerative Peripheral Nerve Interface (RPNI) is designed to intuitively control prostheses utilizing an electrode to record and stimulate activity from a free muscle graft reinnervated by a peripheral nerve. In order to achieve long term stability of the interface, the electrode must remain stable and produce minimal foreign body responses. Electrode stability can be measured by long term electrochemical impedance spectroscopy (EIS) and cyclic voltammetry (CV). Unstable electrodes will exhibit variations in impedance and decreases in cathodic charge storage capacity (CSCc). In this study, we examined readily available stainless steel pad electrodes as proposed materials for use within the RPNI.

METHODS: Stainless steel (SS) electrodes (n=4) were submerged in 37°C +/-0.5°C 1X phosphate buffered saline and incubated over ~200 hours during which EIS and CV were performed 3X daily using a three electrode system. During EIS, a sinusoidal stimulation with amplitude of 10 mV with respect to the open circuit potential was applied at frequencies from 1 Hz to 100 kHz. CV was completed by sweeping the potential on the working electrode from an initial voltage and upper limit of 0.8 V to a lower limit of -0.6 V using a scan rate of 1000 mV/s. The mean CSCc of the four experimental electrodes was then calculated and differences were quantified using a linear regression model. The initial 10 hours of incubation time during testing were excluded from models to focus on long term stability as opposed to initial electrode fluctuations.

RESULTS: A linear regression line with a 0.54 coefficient of determination and a -0.13 slope coefficient showed an overall decrease in CSCc of 15%. Average CSCc for all electrodes was 151.8 μC with standard deviation of 21.5 μC. Within the first five hours of testing, the impedance for three of the four electrodes was 2.5–7 times greater at 1 kHz than the average of the remaining measurements. During the remaining time points, impedance had a 10% standard deviation from the average impedance at 1 kHz.

CONCLUSION: Impedance and CSCc for SS pad electrodes were stable over time supporting the belief that SS electrodes may be reasonable candidates for use within a RPNI due to minimal degradation, retention of charge for stimulation, and preservation of non-faradaic charge transfer processes. Furthermore, we have developed instrumentation and a series of protocols for stability testing in vitro using EIS and CV. These developments will be used to explore other proposed electrode

materials including various electrode metals as well as electroconductive polymer coatings for use in RPNIs. *This work was sponsored by the Defense Advanced Research Projects Agency (DARPA) MTO under the auspices of Dr. Jack Judy through the Space and Naval Warfare Systems Center, Pacific Grant/Contract No. N66001-11-C-4190 and the University of Michigan Undergraduate Research Opportunity Program.*

P23
Standardizing the Use of Somatosensory Evoked Potentials in the Rat Hindlimb Model

Max C Herman
Vassar College, Poughkeepsie, NY

PURPOSE: The regenerative peripheral nerve interface (RPNI) consists of transferred skeletal muscle reinnervated by a peripheral nerve. A sensory RPNI must possess the ability to transmit viable electrochemical signals to the brain. Somatosensory evoked potentials (SSEPs) can provide information on peripheral nerve health as observed through averaged electrocorticograms (ECoGs) of the contralateral area of the somatosensory cortex following electrical stimulation of peripheral nerves. The purpose of this study was to establish an SSEP protocol for use in the rat hindlimb consisting of stimulation parameters and expected cortical responses for various peripheral nerve branches.

METHODS: One week prior to testing, nine subjects underwent cortical electrode placement surgery. An incision was made along the midline of the skull, skin and connective tissue were cleared to expose bregma. Two titanium microscrews (KLS Martin) were implanted over the hindlimb somatosensory cortex, located 1.8–2.2 mm posterior and 2.4–2.8 mm lateral to bregma. One ground screw was implanted 2.0 mm anterior to the coronal and 2.0 mm lateral to the sagittal suture over the right motor cortex. Dental cement was used to secure the screws. One week after screw placement, the tibial, peroneal, and sural nerves were exposed. A stimulation hook electrode was placed around each nerve and electrophysiological recordings were taken from both the contralateral and ipsilateral ECoG screws. Stimulation intensities ranged from 25–1000 μA. Maximum amplitude and latency were recorded for the minimum, median, and maximum stimulation intensities for each nerve.

RESULTS: SSEPs recorded from both the contralateral and ipsilateral screw electrodes were compared in five subjects. Tibial nerve SSEPs recorded from the contralateral side were significantly higher in amplitude when compared to the ipsilateral side (at minimum intensity: $p=.003$, maximum intensity: $p=.048$). For the sural nerve, contralateral SSEPs were also significantly higher in amplitude than the ipsilateral SSEPs (min. intensity: $p=.025$, median intensity: $p=.014$, max. intensity: $p=.011$). No significant differences were found between the responses in the contralateral and ipsilateral SSEPs from the peroneal nerve.

CONCLUSION: Within this study, we have developed and validated an SSEP protocol for analysis of ECoG representation of peripheral nerve stimulation. SSEPs generated from the tibial and sural nerves using this protocol showed significantly greater amplitudes from the contralateral ECoG screw compared to ipsilateral screw. This study demonstrates that

this SSEP procedure can be used in the rat hindlimb to effectively test the viability and health of sensory and mixed nerves. Future studies will use this protocol to test the cortical electrophysiological representation of reinnervated nerves in our sensory RPNI model.

ACKNOWLEDGEMENTS: This work was sponsored by the Defense Advanced Research Projects Agency (DARPA) MTO under the auspices of Dr. Jack Judy through the Space and Naval Warfare Systems Center, Pacific Grant/Contract No. N66001-11-C-4190

P24
Neoadjuvant Chemotherapy is Associated with Decreased Morbidity amongst 77,958 Patients Undergoing Mastectomy-only and Immediate Tissue Expander Reconstruction

Nicholas B Abt, BS[1]; José M Flores, MPH[2]; Pablo A Baltodano, MD[1]; Karim A Sarhane, MD, MSc[1]; Lyonell Kone, MHS[1]; Francis M Abreu, BS[2]; Carisa Cooney, MPH[1]; Martin A Makary, MD, MPH[1]; Gedge D Rosson, MD[1]

[1]Johns Hopkins University School of Medicine, Baltimore, MD, [2]Johns Hopkins School of Public Health, Baltimore, MD

PURPOSE: Neoadjuvant chemotherapy is being increasingly utilized in breast cancer patients and there are limited evidence-based data related to its independent effects on morbidity after mastectomy and immediate reconstruction. Our objective was to determine the impact of neoadjuvant chemotherapy on 30-day postoperative morbidity in women undergoing mastectomy with or without immediate reconstruction.

METHODS: We analyzed data from all females undergoing mastectomy with or without immediate reconstruction from 2005–2011 in the American College of Surgeons National Surgical Quality Improvement Program databases. Patients having underwent neoadjuvant chemotherapy were compared to controls and multivariable regression was used to evaluate 30-day postoperative overall morbidity following mastectomy with or without immediate breast reconstruction. Morbidity included events affecting: cardiac, respiratory, neurological, urinary, venous thromboembolism, wound, and prosthesis/flap failure complications.

RESULTS: 85,851 patients were analyzed; 7,893 patients were excluded due to missing exposure data. The mastectomy-only population included 66,593 (77.57%) patients with 2,876 (4.32%) receiving neoadjuvant chemotherapy. The immediate breast reconstruction population included 19,258 (22.43%) patients with 820 (4.26%) receiving neoadjuvant chemotherapy. We present unadjusted and adjusted odds ratios (OR). Following univariate analysis, neoadjuvant chemotherapy was associated with a lower overall morbidity in the mastectomy-only group (OR_unadjusted=0.80; 95% Confidence Interval [CI]: 0.71–0.91) but had no significant effect in the immediate breast reconstruction group (OR_unadjusted=0.98; CI:0.79–1.23). This observation persisted after extensive adjustment for confounding demonstrating that neoadjuvant chemotherapy independently was associated with lower overall morbidity in the mastectomy-only group (OR_adjusted=0.67; CI:0.53–0.87) and immediate tissue expander reconstruction subgroup (OR_adjusted=0.43; CI:0.36–0.91).

CONCLUSION: Our study supports the safety profile of neoadjuvant chemotherapy in women undergoing mastectomy and immediate breast reconstruction. Additionally, neoadjuvant chemotherapy does not increase postoperative morbidity in implant and flap breast reconstruction while being protective within the mastectomy-only and tissue expander reconstruction setting. We recommend patients receiving neoadjuvant chemotherapy and electing for immediate reconstruction undergo a tissue expander reconstruction due to decreased overall morbidity. The mechanisms behind the protective association of neoadjuvant chemotherapy remain unknown and the mechanisms warrant further investigation.

P25
Readability of Online Patient Resources for Breast Reduction

Danielle J Chuang[1]; Christina R Vargas, MD[2]; Bernard T Lee, MD, MBA[2]

[1]University of Pennsylvania, Philadelphia, PA, [2]Beth Isreal Deaconess Medical Center / Harvard University, Boston, MA

PURPOSE: Access to educational patient health information has been recognized as an important tool in promoting patient and family involvement in medical decision-making, and thereby contributing to higher satisfaction and improved overall outcomes. Internet resources have become more widely available and are increasingly relied upon by patients in evaluating their concerns, deciding to seek care, and understanding procedures. Access to this material, however, is limited by functional health literacy for a significant portion of the adult United States population. The National Institutes of Health and American Medical Association recommend that patient-directed content should be written at a sixth grade reading level. This study aims to evaluate the readability of the most commonly used online patient resources for breast reduction relative to average adult literacy in the United States.

METHODS: The two largest public internet search engines were queried for "breast reduction surgery" and the top fourteen sites common to both searches were identified. Sponsored results were excluded. Relevant patient-targeted content was downloaded from all articles directly accessible from the main sites. Readability of a total of 113 articles was assessed using 10 established analyses: Flesch Reading Ease, Flesch Kincaid Grade Level, SMOG Readability Formula, Coleman-Liau Index, Gunning Fog Index, New Fog Count, New Dale-Chall, FORCAST Formula, Raygor Readability Estimate, and Fry Graph.

RESULTS: Online resources for breast reduction from the fourteen most popular internet sites had an average overall average reading level of 13.2. The Fry readability estimate was 13, with a range from 7th to 17th grade.

CONCLUSION: Available internet resources for patient information about breast reduction uniformly exceed the recommended reading level and are too difficult to be understood by a large portion of American adults.

P26
Characterization of Acute Venous Congestion in a Rat Model Using Indocyanine Green Angiography

Ahmed E Nasser, MD; Mitchell S Fourman, MPhil; Robert P Gersch, PhD; Hsingli Hsi, BS; Brett T Phillips, MD; Alexander B Dagum, MD; Sami U Khan, MD; Mark A Gelfand, MD; Duc T Bui, MD

Stony Brook University Hospital, Stony Brook, NY

PURPOSE: Venous Congestion is the top cause for free flap failure. Postoperative diagnosis of a congested flap still relies on clinical observation as the gold standard. We hypothesized that in a rat lower limb venous congestion model, Indocyanine Green (ICG) Angiography can detect venous congestion and differentiate between a congested and non-congested limb more reliably than clinical observation.

METHODS: A severe venous congestion model was created by bilateral amputation of the lower extremities of male Sprague Dawley rats at the level of the proximal femur leaving only the femoral vessels and femur intact. The femoral vein was occluded at the inguinal ligament while the contralateral limb served as sham control. Complete venous occlusion was achieved by suture ligature (n=11) whereas partial occlusion was achieved by surrounding the vein with a synthetic microtube to achieve 75% (n=6), 85% (n=11) and 92% (n=11) occlusions respectively. Analysis was performed at 10mins post occlusion and consisted of observation (blinded plastic surgeon), temperature, tissue oximetry (VIOPtix Inc.), ICG Angiography and measurement of TNFα and HMGB1 (by qPCR).

RESULTS: Clinical assessment identified all congested limbs in the 100%, 92% and 85% groups as being congested but only 1/7 animals in the 75% occlusion group was diagnosed with congestion. However, the decision to operate on a congested limb, a corollary for the severity of occlusion, was made in 11/11 (100% group) 10/11 (92% group), 9/11 (85% group) and 0/7 (75% group). Temperature and tissue oximetry showed no significant difference between limbs in any group. By comparison, ICG Angiography was able to detect statistically significant differences in limb perfusion within the first 2 minutes of ICG injection (12mins from occlusion) in all animals in the 100%, 92% and 85% groups (paired t-test p=0.001, p=0.040 and p=0.030 respectively). ICG Angiogrpahy did not show a significant difference in limb perfusion in the 75% occlusion group. TNFα and HMGB-1 showed up-regulation as occlusion increased and the latter demonstrated >3-fold increase in the 100% occlusion group compared to the 75% occlusion group (1.49±0.48 vs. 0.44±0.22).

CONCLUSION: We demonstrate that LAICGA is able to detect venous congestion in a rat lower extremity model reliably at occlusion rates greater than 75%. However, clinical judgment is less reliable in determining the severity of congestion. Our model serves as a basis to further study varying venous occlusion levels and their long term effects

P27
The Impact of Conflicts of Interest in Plastic Surgery: An Analysis of Acellular Dermal Matrix, Implant-Based Breast Reconstruction

Joseph Lopez, MD, MBA[1]; Erin Prifogle, BS[2]; Theodore T Nyame, MD[3]; Jacqueline Milton, PhD[4]; James W May, Jr, MD[3]
[1]Johns Hopkins Hospital, Baltimore, MD, [2]TEI Biosciences, Boston, MA, [3]Massachusetts General Hospital, Boston, MA, [4]Boston University School fo Public Health, Boston, MA

PURPOSE: Although "conflicts of interest" (COI) in biomedical research have received significant attention recently, the impact of COI on surgical outcomes has not been fully explored.

METHODS: A systematic electronic search of the literature was performed for studies that evaluated surgical outcomes in "acellular dermal matrix" (ADM) and non-ADM implant-based breast reconstruction. Surgical complications including infection, seroma, hematoma, necrosis, and explantation were used as outcome metrics and extracted from studies. Surgical outcomes were then pooled and compared between studies that disclosed COI and those that did not disclose COI.

RESULTS: A total of 776 abstracts were identified, of which only 35 fulfilled our inclusion criteria. COI were reported in 14 (40%) of these abstracts. The pooled data from studies that reported no COI and studies that reported a COI included a total of 8241 and 5384 breasts and 2852 and 1864 patients, respectively. Taken collectively, surgical complications were less common in studies that reported a COI than in studies that reported no COI. When surgical outcome data was further stratified by ADM use, surgical complications were less common in studies with COI when ADM was used. However, when ADM was not used, surgical complications were similar between authors that reported a COI and those that did not report a COI.

CONCLUSION: Self-reported COI are common in implant-based breast reconstruction research. Studies authored by groups with COI are significantly associated with reporting lower surgical complications and therefore describing positive research findings, especially when industry marketed products are being utilized in the study.

P28
An Interim Analysis of Outcomes Following 5-cm Median Nerve Defect Repair in Non-Human Primates

Jacqueline M Bliley, MSc; Wes Sivak, MD PhD; Donald Crammond, MD; Danielle Minteer, BS; Meghan McLaughlin, BA BS; Rich Liberatore, BS; Ryan Schroth, BS; Han Tsung Liao, MD PhD; Tyler Simpson, MSc; Jim Hokanson, BS; Greg Williamson, BS; Casey Tompkins-Rhoades, BS; Kia Washington, MD; Alex Spiess, MD; Douglas Weber, PhD; Kacey G Marra, PhD
University of Pittsburgh, Pittsburgh, PA

PURPOSE: Nerve injuries may occur due to trauma, tumor removal, and accidental surgical resection. Rodents are the most common pre-clinical nerve defect models; however, accelerated regeneration of the damaged peripheral nerves in rodents and inability to investigate large gaps are major limitations for the rodent model, making large animal models necessary. The purpose of this project is to identify key considerations in developing a non-human primate (NHP) large-gap peripheral nerve model, as well as to provide an interim analysis of our first set of NHPs.

METHODS: 5-cm median nerve defects were created and repaired by either autograft, decellularized nerve allograft, a poly(caprolactone) conduit, or a poly(caprolactone) conduit with embedded glial cell line-derived neurotrophic factor (GDNF)-containing polymeric microspheres. Function: Rhesus macaques were trained to retrieve treats from a modified Klüver board utilizing a pinch between their thumb and forefinger. Functional assessments were performed starting at POD 13 and percentage of successful retrieval attempts (defined as a pinch between the thumb and forefinger) were recorded. Treat retrieval time was also quantified. Electrophysiology: Non-invasive electrophysiology assessments, including somatosensory evoked potentials (SSEPs) and transcranial motor evoked potentials (Tc-MEPs), were used to determine the time course of regeneration. Baseline and post-operative (day 14, 28, 37 and 79) electrophysiological tests were performed. Nerve conduction velocity was obtained prior to and after nerve transection and at the time of explant. Histology: Explants occurred at POD 43, 90, and 180 to establish a time course for regeneration and to correlate histological and electrophysiological results. Histological analysis of nerve architecture, Schwann cells (S-100), and nerve fiber density (PGP 9.5) was performed. Histomorphometry was performed on nerve sections to determine myelination, axon area, and g-ratio.

RESULTS: Function: Pinch percentage steadily increased following nerve repair. Prior to operation, NHPs utilized a thumb and forefinger pinch 70–80% of time. After surgery, thumb usage was diminished with near-baseline functional values

observed at POD 60. A significant increase in retrieval time, after surgery ($p<.05$) was observed with near-baseline retrieval times at POD 86–105.

ELECTROPHYSIOLOGY: SSEP negative peak amplitudes were significantly decreased ($p<.05$) at POD 14, 28, 37, and 79 when compared to baseline with significant recovery at POD 79. SSEP stimulation thresholds were significantly increased ($p<.05$) at POD 37 and 79 with significant recovery occurring at POD 79. Abductor pollicis brevis thresholds obtained from Tc-MEP stimulation were significantly increased at POD 37 and 79. CNAPs were first measured at POD 42 and confirmed with stimulation-response curve. Nerve conduction velocity was 40% baseline at POD 90 with significantly increased CNAP stimulation thresholds ($p<.05$).

HISTOLOGY: Preliminary S-100 and PGP 9.5 data indicate no notable difference between decellularized nerve allograft and autograft. Histomorphometry data indicate larger numbers of smaller fibers present in regenerated nerve through decellularized nerve allograft with normal bimodal frequency being approached.

CONCLUSION: Peripheral nerve regeneration proceeded at a rate of 1.35 mm/day, comparable to the rate commonly observed in humans (1–2 mm/day).

P29
Optimization of Functional, Perfusable Vascular Networks within Tissue Engineered Hydrogels

Rachel C Hooper, MD, FACS; Karina A Hernandez, DO; Tatiana Boyko, MD; Jeremiah Joyce, BA; Adam Jacoby, BA; Ope Asanbe, MD; Kadria N Derrick, MD; Jason A Spector, MD, FACS

Weill Cornell Medical College, New York, NY

PURPOSE: New blood vessels are formed de novo via vasculogenesis or through sprouting from existing blood vessels via angiogenesis. A layer of endothelial cells comprising the tunica intima provides a non-thrombogenic surface and allows continuous blood flow within these new blood vessels. The ability to precisely replicate the intricate design of the vascular system de novo is beyond any current tissue-engineering techniques and remains a major challenge towards creating surgically relevant constructs for clinical application. Here we describe the synthesis of tissue-engineered hydrogels, containing an internal microvessel with "neointima" and "neomedia".

METHODS: Pluronic F127 fibers were sacrificed in type I collagen, creating a central "loop" microchannel, 1.5 mm in diameter. A cell suspension of 5 x106 cells/mL human umbilical vein endothelial cells (HUVEC) was injected into the inlet of a loop microchannel. For co-culture scaffolds, a cell suspension of 5 x106 cells/mL human aortic smooth muscle cells (HASMC) was injected initially and after 24 hours, a HUVEC cell suspension was seeded as above. Following 7 and 14 days of static culture, constructs were injected with 10 μg/mL low-density lipoprotein acetylated-dil complex (Dil-Ac-LDL) to demonstrate HUVEC-receptor mediated endocytosis. Whole constructs were subsequently imaged via multiphoton microscopy and immunohistochemical staining was performed for 4',6-diamidino-2-phenylindole (DAPI), CD31, von Willebrand Factor (vWF), collagen IV, and alpha smooth muscle actin (α-SMA) in order to determine the density and spatial relationship between cell types. Additionally, Lycopersicion esculentum staining was performed to identify the presence of synthesized heparan sulfate, an extracellular matrix protein.

RESULTS: Microchannels were successfully seeded with HUVEC and HUVEC/HASMC. Multiphoton microscopy of microchannels seeded with HUVEC/HASMC after 7 days demonstrated a confluent concentric endothelial lining, which was maintained after 14 days. However, HUVEC-only seeded microchannels demonstrated delamination, which continued through the 14-day time point. HUVEC demonstrated functionality via receptor-mediated uptake of Dil-Ac-LDL along the microchannels seeded with HUVEC alone and in co-culture with HASMC after 7 and 14 days. Histological analysis confirmed co-culture microchannels with HUVEC and HASMC organized in concentric layers with elaboration of additional extracellular matrix (ECM) proteins. HASMC/

HUVEC-seeded constructs exhibited CD31+ and vWF expressing HUVEC along the luminal surface of the microchannel forming a "neointima" with α-SMA expressing HASMC in the subendothelial plane, forming the neomedia. Additionally, after 14 days HUVEC/HASMC-seeded constructs demonstrated elaboration of heparan sulfate, a component of the glycocalyx and ECM as well the deposition of basal lamina protein collagen IV along the abluminal surface of CD31+ HUVEC.

CONCLUSION: We have successfully created tissue-engineered scaffolds with microchannels that support engraftment of smooth muscle and endothelial cells, forming neointimal and neomedia with receptor-mediated endocytosis demonstrating functionality of the seeded endothelial cells. With a preformed vascular network lined by endothelial cells these constructs recreate the architecture found in vivo and provide a surface for thrombosis-free blood flow, thus allowing for surgical implantation via microanastomosis.

P30
The Lateral Intercostal Artery Perforator (LICAP) Flap for Outpatient Total Breast Reconstruction

Lee Squitieri, MD[1]; Cloe Hakakian, BS[2]; Joshua D I Ellenhorn, MD[2]; David Kulber, MD[3]; Joel A Aronowitz, MD[4]

[1]University of Southern California, Los Angeles, CA, [2]Cedars Sinai Medical Center, Los Angeles, CA, [3]University of Southern California, Cedars Sinai Medical Center, Los Angeles, CA, [4]Cedars Sinai Medical Center, University of Southern California, Los Angeles, CA

PURPOSE: The lateral intercostal artery perforator (LICAP) flap is a reliable, axial skin flap described in previous reports for post-bariatric breast augmentation and chest wall reconstruction. The LICAP flap can produce a large skin paddle without dissection of muscle or fascia and, importantly, it can be performed in an outpatient setting. These features make the LICAP flap useful as an adjunct for total breast reconstruction in patients who are not post-bariatric surgery. We report our experience using this procedure for total breast reconstruction following mastectomy in the outpatient setting.

METHODS: A single center retrospective review of 25 LICAP flaps in 19 patients was performed. All patients received LICAP flaps in an outpatient surgery setting for delayed total breast reconstruction after prior mastectomy.

RESULTS: A total of 25 flaps for total breast reconstruction were performed in 19 patients with a mean operative time of 2.24 hours per breast. 23 of the 25 flaps had undergone a prior reconstructive attempt, 3 of which were a failed muscle flap reconstruction. 17 of the 19 patients had an existing prosthesis. Four of the 19 patients had prior radiation therapy and the mean body mass index was (23.7, range 18.3–35.0). Flap dimensions ranged from 6 x 12cm to 16 x 28cm (mean 9.9 x 23.7cm). Concurrent surgery included fat grafting (15 breasts), implant placement (10 breasts), mastopexy (1 breast), capsulectomy (6 breasts), symmetrizing reduction (4 breasts). Patients were followed for a mean follow-up time of 12.5 months, and 4 flaps (16%) experienced post-operative complications including partial flap necrosis (2), painful donor site keloid (1), and implant infection (1).

CONCLUSION: The LICAP flap is a practical alternative for total breast reconstruction. It can reliably provide a significant skin paddle even in patients who are not post-bariatric surgery without the morbidity, hospitalization and cost associated with muscle based flaps. These features may result greater patient acceptance and substantial cost reduction.

P31
Immunomodulatory Effects of Adipose-Derived Stem Cells and Bone Marrow-Derived Stem Cells in Rat Hind-limb Composite Tissue Allotransplantation

Sudheer K Ravuri, PhD; Jonas Schnider, MD; Jan Plock, MD; Wakako Tsuji, MD, PhD; Meghan M McLaughlin, BS; Peter J Rubin, MD; Kacey G Marra, PhD; Mario Solari, MD; Vijay S Gorantla, MD, PhD
University of Pittsburgh, Pittsburgh, PA

BACKGROUND: Mesenchymal stem cells (MSCs) have broad range of applications in nerve repair. In vitro and local administration in vivo studies had well demonstrated enhanced nerve regeneration. However there is unmet need to develop and study systemic application of MSCs for immunomodulation and/or immunosuppression for improving functional outcomes after CTA. Hence this study was intended to investigate whether donor adipose-derived stem cells (ASCs) and bone marrow derived stem cells (BMSCs) have immunomodulatory effects, such as modulation of related cytokines and prolongation of allograft survival in a rodent hind limb model.

PURPOSE: To determine systemic effects on immune modulation and suppression by evaluating the cytokine and growth factor expression profiles of secreted and/or circulatory proteins in sera of hind limb allotransplanted rodent animals that were intravenously administered with rodent ASCs and BMSCs.

MATERIALS AND METHODS: 29 sera were collected from hind-limb transplanted and control animals and subjected to rat model Panomics multiplex Luminex assay, that were separately and systemically injected via intravenous route with PKH26 (red) dye labeled Brown Norway rat ASCs at 1 million and 5 million per injection. Prior to that, rat ASCs and BMSCs were isolated as per laboratory optimized standard protocols. Cytokine and growth factor secretion profiles were demonstrated in sera bled at different time points (4, 6, 18 weeks). Sera was also bled from rejected and control (naïve) animals. 35ul of each neat sera with no preservative was analyzed on Affymetrix Panomics multiplex panel. Core facility optimized standard protocols were applied to analyze the samples in singles (represents 100 analysts).

RESULTS: Graphical representation was made to correlate multiplex cytokine/growth factor targets embedded in panomics multiples luminex panel with error bars plotted +/- one SD. 12 vital cytokines/growth factors were up or down regulated in the analysis. RANKL, ICAM-1, IL-12, IFN-y, IL-13, IL-2, IP-10, Leptin, MIP-2, RANTES, VCAM, VEGF-A were predominantly changed in their expression profile. Groups injected with 1 million ASCs at 4 and 6 weeks showed increased levels in ICAM, but 3-fold reduction in 6 weeks when compared to 4 weeks. Graft rejected and control animals showed low levels of ICAM secretion. BMSCs injected animals showed similar results. IL-2 was increased by 27-fold in 4 weeks when compared to 6 weeks. However, 18 weeks long-term animals showed prolonged secretion upto 30-fold. Conversely BMSCs injected animals showed 42-fold increase in 10 weeks and 18 weeks long-term. Leptin was highly elevated upto 75-fold in 18 weeks long-term and rejected animals. RANKL increased upto 24-fold in 18 weeks long term with ASCs and 10 weeks in BMSCs, but 48-fold increase in BMSCs rejected animals. Poor or no secretion of VEGF-A, TNF-a, MIP-a, MCP-3, IL-4, IL-5, IL-6, IL-10, IL-17, G-CSF, GM-CSF was found in all group analyses.

CONCLUSION: Based on these preliminary results, it was concluded that the cytokine profiles of ASCs and BMSCs were similar to each other in immune modulation and indicative of rejection. Further analysis of molecular targets is in progress to correlate with Luminex data.

P32
Breast Reconstruction Outcomes after Nipple-Sparing Mastectomy and Radiation Therapy

Richard G Reish, MD; Alex Lin, BS; William G Austen, Jr, MD; Jonathan Winograd, MD; Eric C Liao, MD; Curtis L Cetrulo, Jr, MD; Barbara L Smith, MD; Amy S Colwell, MD
Massachusetts General Hospital, Boston, MA

PURPOSE: Nipple-sparing mastectomy (NSM) has significantly increased in prevalence in recent years, and it has the potential for dramatically improved cosmetic results. Concomitantly, chest wall/breast irradiation is a common adjuvant for lumpectomy patients who later need mastectomy, and as adjuvant treatment for mastectomy patients who have opted for breast reconstruction. Few studies in the literature have examined outcomes of immediate breast reconstruction after nipple-sparing mastectomy and radiation therapy.

METHODS: Retrospective analysis of multi-surgeon consecutive implant-based reconstructions after nipple-sparing mastectomy from June 2007 to Dec 2012 was conducted at a single institution. Patient demographics, surgical technique, and patient outcomes including immediate complications, nipple or nipple areolar complex (NAC) removal due to malposition or close oncologic margins, and capsular contracture requiring open capsulotomy or reconstructive failure were analyzed in order to compare outcomes of irradiated patients with nonirradiated patients.

RESULTS: 605 immediate breast reconstructions were performed following nipple-sparing mastectomy. Of the reconstructions, 88 were treated with radiation therapy and 517 had no radiation. Preoperative radiation was administered in 43 while 45 received post-mastectomy radiation to the reconstruction. The mean follow-up period for all patients was 686 days. In comparing the group of patients with radiation to the group without radiation, the radiated patients were older (49.8 years vs. 45.9 years, $p<0.001$) but had similar BMI and smoking status. The group with preoperative XRT had more single stage reconstructions ($p<0.014$) and lower implant volume (300cc vs. 386cc, $p<0.001$) than the patients without radiation. There were more total complications in patients with radiation (19.3% vs. 12.8%, $p<0.01$) and a higher rate of implant loss (5.7% vs. 1.0%). There were no significant differences in nipple removal secondary to malposition or positive oncologic margins in patients who received radiation compared to those who did not receive radiation. Patients with radiation did have a higher incidence of a secondary procedure for capsular contracture (12.5% vs. 2.3%, $p<0.001$) and fat grafting (13.6 vs. 3.9%, $p<0.001$). The total nipple retention rate in patients with radiation and nipple-sparing mastectomy was 90% (79/88), and the reconstruction failure rate was 8%. At 22 months mean follow-up, local recurrence occurred in 4/156 (2.6%) breasts operated on for cancer through 2011. There were no recurrences involving the nipple.

CONCLUSION: Nipple-sparing mastectomy and immediate reconstruction in patients who had or will receive radiation is associated with a 92% success rate and a 90% nipple retention rate at a mean 2 year follow-up with no cancer recurrence in the nipple. Longer follow-up is warranted to assess for recurrent cancer, revisional surgery, and reconstruction failure.

P33
A Distinct Domain of Mcl1 Regulates Senescence Inhibition in Cancer

Abeba Demelash, PhD[1]; Lukas W Pfannenstiel, PhD[2]; Brian T Maybruck, PhD[2]; Simon E Schlanger, BS[2]; Tannenbaum S Charles, PhD[2]; Brian R Gastman, MD[2]

[1]Institutes of Head and Neck, Dermatology and Plastic Surgery, Taussing Cancer Center and Lerner Research Institute, Cleveland Clinic, Cleveland, OH 44195, Cleveland, OH, [2]Institutes of Head and Neck, Dermatology and Plastic Surgery, Taussing Cancer Center and Lerner Research Institute, Cleveland, OH

PURPOSE: Myeloid cell leukemia (Mcl1) protein differs from its anti-apoptotic BCL-2 family members in its large size of 350 residues and extended, non-homologous, regulatory domain-containing N-terminus. We have recently demonstrated that Mcl1 plays an important role in tumor progression through the inhibition of chemotherapy-induced senescence in colon cancer. In the present study, we focused our attention on investigating a distinct domain within Mcl1 responsible for its anti-senescence properties in several colon cancer cell lines.

METHODS: This has been addressed by generating several deletion mutants of Mcl1, and then assessing the sub cellular distribution, extent of senescence inhibition, and occurrence of DNA damage in response to chemotherapy.

RESULTS: We observed that re-expression of a set of Mcl1-N and C-terminal deletion mutants into Mcl1 deficient cells resulted in the accumulation of these mutant proteins in the nucleus. This is in stark contrast to most of its known functions epicentered in the mitochondria. These mutants included those that had deletions of all known functional aspects of the molecule and were nonetheless able to inhibit senescence similar to wild type Mcl1, and resulted in substantial increases in BrdU uptake, reduction in the percentage of senescence-associated beta-galactosidase positive cells, PML and γH2AX foci formation after drug treatment. In addition use of both deletion mutants and substitution mutants of several phosphorylation sites revealed that two of the most important post-translational N-terminal regulation modalities of Mcl-1 were dispensable for its anti-senescence functions.Based on this data, we then developed more specific mutants and identified an internal domain within Mcl-1 key to its senescence function. Specifically residues 198–207 appear to be key in Mcl1's senescence modulation, as cell expressing the Mcl1 Δ198–207 deletion mutant where not protected against drug-induced senescence.

CONCLUSION: Taken together, this study indicates that a newly discovered domain within Mcl-1, through nuclear events is responsible for its anti-senescence properties in cancer cells.

P34
Tumor-Induced Suppressive CD8+ T Cells: Implications for Cancer Immunotherapy

Lukas W Pfannenstiel, PhD; Brian T Maybruck, PhD; Brian R Gastman, MD

Cleveland Clinic, Cleveland, OH

PURPOSE: The immune system has the potential to be a powerful tool to destroy tumors; however despite ample evidence of endogenous anti-tumor immune responses in many patients, as well as years of immunotherapy development, truly effective immune-based therapies remain out of reach. We have previously shown that co-incubation of normal human T cells with various tumor lines can induce dysfunctional changes characterized by the loss of CD27/CD28 expression, hypoproliferation upon activation, and the gain of suppressive function in vitro. We also found that this process could be inhibited by IL-7 signaling, primarily through enhancing expression of the pro-survival molecule Mcl-1. In the current study we sought to determine whether a similar process could not only be found in mice, which would allow the use of in vivo tumor models to study this process in the context of a natural tumor microenvironment, but also in tumor-resident T cells collected from human patient specimens.

METHODS: TC-1 mouse tumor cells were used as a model of HPV+ HNSCC. To model adoptive T cell therapy, T cells from transgenic mice expressing a TCR-beta chain specific for HPV-E7 were used. To induce T cell dysfunction in vitro, TC-1 tumor cells were incubated with purified T cells from C57/BL6 mice in 6 well plates for six hours followed by separation and culture for four days. CD8+ TIL cells were isolated from mouse and human tumors by digestion in collagenase/hyaluronidase followed by magnetic bead purification and sorting by FACS. Suppression was measured by thymidine uptake by responder T cells incubated with suppressor CD8+ T cells at various ratios in anti-CD3/CD28 coated 96-well plates. Surface marker staining was performed using fluorichrome-conjugated antibodies followed by analysis by flow-cytometry. PD-1, Tim-3, and Lag-3 checkpoint inhibitor blockade was performed by the use of purified antibodies both in vivo and in vitro. Exogenous IL-7 was delivered in vivo by i.p. injection.

RESULTS: We show that the process of tumor-induced dysfunction also induces the expression of PD-1 in both human and mouse T cells, and that tumor-exposed mouse T cells are also capable of suppressive function. We further show that the mouse and human tumor microenvironment induces large numbers of PD-1+ CD8+ T cells that are also positive for other negative regulators of T cell function including Tim-3, and that these cells are also suppressive ex vivo. Treatment of mice and T cells with antibody blockade of PD-1 and other negative regulators, as well as treatment with IL-7 cytokine can prevent the induction of suppressive function.

CONCLUSION: These studies demonstrate that a tumor-derived factor can induce the dysfunctional and suppressive ability of CD8+ T cells. These cells then could contribute to the overall immunosuppressive nature of the tumor microenvironment. Blockade of negative regulators of T cell function and use of IL-7 cytokine can help prevent this process, indicating an additional benefit to the clinical use of these immunotherapies. Future work will examine the signaling mechanisms responsible, especially by evaluating the role of Mcl-1 expression in generation of dysfunctional CD8 T cells in vivo.

P35
The Role of Extracellular Matrix Components in Hair Follicle Neogenesis and Cellular Reprogramming

Erin L Weber, MD, PhD; Cheng-Ming Chuong, MD, PhD
Keck School of Medicine of the University of Southern California, Los Angeles, CA

PURPOSE: The main objective of reconstructive plastic surgery is the restoration of form and function after wounding or deformity. Closure of complex wounds is now possible through the use of advanced flaps and skin grafts. However, while most wounds can be repaired with current methods, the reconstructed region often cannot approximate the normal skin in both cosmetics and function. There exists a strong need for successful tissue engineering for optimal wound reconstruction. Advances in stem cell biology suggest that tissue engineering is possible through cellular reprogramming. Dermal fibroblasts have been reprogrammed to become neurons, cardiomyocytes, and hepatocytes through genetic modification. Endogenous reprogramming has been also been observed in adult mice where new hair follicles develop at the center of large wounds. Successes in reprogramming have demonstrated that both the expression of lineage-specific genes and environmental cues play important roles. Hair follicle development requires the early formation of aggregates of dermal and epidermal cells, followed by reciprocal epithelial-mesenchymal signaling, which remains largely uncharacterized. As the epidermal and dermal aggregates are spatially separated within the skin, it stands to reason that the extracellular matrix (ECM) may play a role in the signaling between the two cell groups.

METHODS: One way to investigate the role of the extracellular matrix in hair follicle development and to identify factors for reprogramming is to use decellularized ECM, which retains the extracellular protein components of the dermis, including growth factors, in their native structural configuration. Normally, adult mice are unable to generate new hair follicles to replace those that are lost or non-functional. Newborn mice, however, are able to regenerate hair follicles for a short time after birth. Therefore, a comparison between newborn and adult murine ECM should help to identify important differences responsible for the lack of adult hair follicle neogenesis. Newborn murine dermis was decellularized using Triton X-100 detergent. The decellularization process was optimized to minimize the loss of soluble growth factors and maintain scaffold structure. Newborn or adult murine skin was dissociated into individual dermal and epidermal cell populations and seeded onto newborn acellular ECM. Aggregate formation was evaluated using whole mount immunofluoresence. Complete hair follicle formation was demonstrated by transplantation of the ECM, with aggregates, into the full-thickness wound of a nude mouse.

RESULTS: Newborn acellular dermal matrix is able to support the formation of new hair follicles from dissociated newborn epidermal and dermal cells. In addition, we demonstrated rescue of hair follicle formation from adult murine epidermal and dermal populations. Current efforts are directed towards the identification of the extracellular matrix proteins, configuration, and associated molecules which may support hair follicle neogenesis. Comparative studies between newborn and adult murine matrices are ongoing.

CONCLUSIONS: The dermal extracellular matrix is believed to play an important role in hair follicle neogenesis and the use of crucial ECM components may facilitate tissue engineering. Reprogramming dermal fibroblasts into hair follicle precursor cells has the potential to create a renewable source of hair follicles for the treatment of alopecia and the reconstruction of wounds in hair-bearing areas.

P36
Dynamic Culture Enhances Osteogenic Performance Comparing Donor Matched Human Adipose and Bone Marrow Mesenchymal Stem Cells

Ajul Shah, MD; Miles Pfaff, BS; Wei Wu, MD; Laura Niklason, MD; Derek Steinbacher, DMD, DDS

Yale University School of Medicine, New Haven, CT

PURPOSE: Tissue engineered bone holds translational promise for myriad applications in reconstructive surgery. Both adipose-derived and bone marrow-derived stem cells (ADSCs and BMSCs) have been used for bone regeneration, and can be seeded on a variety of rigid scaffolds. This study aims to compare ADSCs and BMSCs from the same donor in three distinct bioreactor settings to create the most viable osseous engineered construct. We hypothesize that physiologic flow dynamics will optimize osteogenic cell viability and function, which are prerequisites to successful human tissue implantation.

METHODS: Human ADSCs and BMSCs were isolated from the same donor, then cultured and seeded on decellularized porcine bone constructs. The constructs were then subjected to either static or dynamic (stirring or perfusion bioreactor) culture conditions for 7 to 21 days. Afterwards, the constructs were analyzed for cell adhesion and distribution using histology and electron scanning microscopy. Proliferation and osteogenic differentiation were further gauged using DNA quantification, alkaline phosphatase (ALP) assay, immunostaining for osteocalcin and real-time-PCR, and calcium deposition assay.

RESULTS: hADSCs demonstrated higher seeding efficiency and proliferative potential in static culture than hBMSCs. However, dynamic culture, driven by stirring or perfusion flow, significantly increased BMSCs proliferation more than ADSCs proliferation. The highest cellularity was seen in the stirring bioreactor. In all conditions, BMSCs demonstrated stronger osteogenic activity compared to ADSCs, in ALP activity assay and gene expression for various bony markers. Conversely, ADSCs expressed more collagen I. In all constructs (ADSC and BMSC), dynamic conditions (stirring and perfusing bioreactors) enhance overall osteogenic gene expression. BMSCs in the stirring bioreactor exhibited the greatest calcium production, likely secondary to the greater cell proliferation and osteogenic function.

CONCLUSION: Scaffolds seeded with BMSCs in dynamic conditions exhibit the greatest osteogenic proliferation and function. In particular, the stirring bioreactor optimizes the bone engineered construct, and may portend clinical success

P37
Optimizing Cellular Invasion into Hydrogel Scaffolds Using Microspheres to Create Interfaces of Differential Densities

Opeyemi A Asanbe, MD; Rachel C Hooper, MD; John Morgan, PhD Candidate; Jeremiah Joyce, BA; Ross H Weinreb; Adam Jacoby, BA; Kadria N Derrick, MD; Abraham D Stroock, PhD; Jason A Spector, MD, FACS

Weill Cornell Medical College, New York, NY

PURPOSE: Although several acellular engineered tissue templates are available for clinical use, their success is limited to application within well-vascularized wound beds. In poorly vascularized wounds, such as those that have been irradiated or those with exposed hardware, bone or tendon, cellular and vascular invasion into tissue-engineered templates remains largely insufficient, leading to failure of incorporation or infection. Previous work in our lab demonstrated that cells preferentially invade scaffolds at the interface of differential densities, in some cases even more robustly than in scaffolds with well-defined microfeatures such as pores. As such, we fabricated a novel scaffold containing closely packed higher density collagen microspheres encased in a lower density collagen bulk, which created regularly spaced interfaces of differential densities so as to optimize cellular invasion and neovascularization.

METHODS: Using an oil emulsion technique, 1% collagen microspheres, ranging 50 to 150 μm in diameter, were created using neutralized type 1 collagen. 7 mm diameter microsphere scaffolds were fabricated by embedding 1% collagen microspheres in 0.3% type 1 collagen bulk. According to Kepler's conjecture of close-packed spheres, approximately 74% of the density of the scaffold was comprised of higher density microspheres, and the remaining density was taken up by the 0.3% collagen. Microsphere scaffolds underwent thermal gelation at 37° C for 1 hour. Non-microsphere-containing 1% collagen scaffolds and non-microsphere-containing 0.3% collagen scaffolds were also fabricated for comparison. Microsphere and non-microsphere-containing scaffolds were implanted subcutaneously in dorsa of WT C57bl/6 mice. Following 7 or 14 days of implantation, scaffolds were procured and subsequently processed for histological analysis.

RESULTS: Histological analysis following procurement of microsphere scaffolds from mice dorsa after 7 days of implantation revealed substantial and uniform cellular invasion spanning the entire depth of the scaffold. After 14 days of implantation, immunohistochemical analysis identified CD31+ endothelial precursors within microsphere scaffolds, indicative of a progression in cellular invasion with the formation of neovasculature. Comparatively, even after 14 days, cells sporadically and only partially invaded the 0.3% collagen scaffolds and failed to invade the 1% collagen scaffolds, instead proliferating along the periphery of the scaffold.

CONCLUSIONS: We have demonstrated that altering the mechanical and spatial cues within hydrogel scaffolds by creating interfaces of differential collagen densities significantly improves cellular invasion. In addition to optimizing the architectural and structural cues sensed by cells, microspheres may also be impregnated with chemical moieties to further promote cellular invasion. We believe this approach holds tremendous promise for creating the optimal wound scaffold.

P38
Use of Novel BMP-2 Minicircle Plasmid-Releasing Scaffolds for Bone Engineering

Michael T Chung, BS[1]; Kevin J Paik, AB[1]; Adrian McArdle, MD[1]; Michael S Hu, MD[1]; Kshemendra Senarath-Yapa, MD[1]; Shane D Morrison, MS[1]; Graham Walmsley, BS[1]; Ruth Tevlin, MD[1]; Elizabeth Zielins, MD[1]; David Atashroo, MD[1]; Wan Xing Hong, MS[1]; Christopher Duldulao, BS[1]; Taylor Wearda, BS[1]; Rebecca M Garza, MD[1]; Arash Momeni, MD[1]; Michael Keeney, PhD[2]; Fan Yang, PhD[2]; Michael T Longaker, MD, MBA[1]; Derrick C Wan, MD[1]

[1]Hagey Laboratory for Pediatric Regenerative Medicine, Department of Surgery, Plastic and Reconstructive Surgery Division, Stanford, CA, [2]Stem Cell and Biomaterials Engineering Laboratory, Stanford, CA

PURPOSE: Skeletal defects are common problems and are difficult to heal using current therapies. Bone morphogenetic protein (BMP)-2 has very strong osteoconductive activity, however, transient exposure to BMP-2 may not be sufficient to stimulate and sustain adequate bone growth for large defects. A gene-therapy approach to BMP manipulation may offer an alternative strategy, but considering the safety concerns associated with viral vectors, a non-integrating technology would be a safer route to enhance BMP signaling. The present study evaluated the potential of a novel BMP-2 minicircle (mc)-releasing scaffold to promote bone regeneration.

METHODS: A novel mc-releasing scaffold was prepared using supercritical CO2 (scCO2). Luciferase mc was lyophilized with 10% hydroxyapatite (HA) powder and pulverized PLGA. A single-step scCO2 foaming process was utilized to generate porous scaffolds. This scCO2 foaming process was carried out at high pressure (2000 psi) for 1 hour at 35°C. In vitro release assays were performed to determine the release kinetics of Luc-mc from the HA-PLGA scaffolds. The amount of DNA released at each time interval was determined by the PicoGreen® fluorometric assay. To evaluate the time course of mc DNA expression, Luc-mc-releasing scaffolds were implanted into critical-sized (4-mm) calvarial defects in nude mice. To assess minicircle plasmid delivery efficiency, transgene expression was analyzed by in vivo bioluminescence imaging (IVIS). To assess BMP-2 mc's effect on osteogenesis in vitro, parietal osteoblasts from C57BL/6 mice were transfected with BMP-2 mc and cultured in ODM. At Day 14, alizarin red staining was performed and osteogenic gene expression was measured by qRT-PCR. For evaluation of in vivo osteogenesis, critical-sized (4-mm) calvarial defects in nude mice were treated with a BMP-2 mc-releasing scaffold. Healing was followed using micro-CT scans for eight weeks, and sections were stained with Movat's Pentachrome and aniline blue.

RESULTS: The scCO2 gas foaming process had little effect on the release profile or DNA integrity. Scaffolds formed with gas foaming had a sustained release of plasmid for at least six weeks with retention of DNA integrity. For Luc-mc-releasing scaffolds, sustained transgene expression was observed for at least eight weeks. Parietal osteoblasts treated with BMP-2 mc exhibited enhanced osteogenesis and mineralization compared to cells treated with a GFP mc control. Over the course of eight weeks, defects treated with the BMP-2 mc-releasing scaffolds were found to consistently outperform defects treated with scaffolds alone.

CONCLUSION: In summary, porous HA-PLGA scaffolds releasing plasmid DNA induced prolonged in vivo transgene expression up to 8 weeks, which was sufficient to promote physiological response. BMP-2 mc led to increased osteogenic capacity in vitro and scaffold-based delivery of BMP-2 mc facilitated more rapid regeneration of critical-sized calvarial defects.

P39
Vascular Perfusion and the Regenerative Response to Acellular Dermal Matrix

Joani M Christensen, BA; John Pang, BS; Kakali Sarkar, PhD; Saami Khalifian, BS; Evan R Langdale, BS; Karim Sarhane, MD; Damon S Cooney, MD, PhD; Gerald Brandacher, MD; Stephen M Belkoff, PhD; Justin M Sacks, MD

Johns Hopkins University School of Medicine, Baltimore, MD

PURPOSE: Human acellular dermal matrix (ADM) offers mechanical strength while being repopulated by both host cells and connective tissue. ADM is used in breast reconstruction to facilitate submuscular implant placement, allowing improved lower pole expansion and soft-tissue reinforcement. Cellular repopulation and revascularization are central to tissue integration, but the physiologic effect of placement of the ADM relative to muscle is unknown. We hypothesized that optimized placement of ADM relative to muscle in a small animal model would augment regenerative characteristics including revascularization and tensile strength.

METHODS: A 2cm diameter hemispherical silicone implant was placed under the latissimus dorsi muscle of Lewis rats (n=40), creating a gap between the cut muscle edge and the midline muscular insertion. In half of the rats, ADM was placed as an inlay to bridge the gap. In the other half, ADM was placed as an overlay, with 0.5cm overlap between ADM and muscle edge on all sides. Half of the animals in each group were sacrificed on POD7, the remaining on POD28. Before sacrifice, vascular perfusion was assessed using indocyanine green fluorescent laser angiography (ICG-FLA). Fluorescence intensities of a region of interest (ROI) at the ADM interface were divided by intensity of a control ROI over local native musculature. Tissue from the interface zone was then harvested for mechanical strength testing (failure load normalized to specimen width) using a hydraulic materials testing device, angiogenesis gene expression analysis using a PCR array, and hematoxylin and eosin staining of paraffin embedded tissue sections.

RESULTS: ICG-FLA revealed a trend toward increased normalized fluorescence intensity of the interface region of the overlay group compared to the inlay group on POD7 (0.61 vs 0.51, respectively; p=0.17). At the POD7 and POD28 time points, there was a trend toward higher failure load at the overlay interface as compared to the inlay interface (POD7 0.39N vs. 0.28N, respectively; and POD28 0.58N vs. 0.49N, respectively). Gene expression analysis on POD7 showed expression of CXCL1, CXCL2, IFNG, and MMP3 > 2 fold higher than in the unoperated contralateral control in both inlay and overlay groups. Moreover, CXCL1, CXCL2, CCL2, EDN1, IL1b, IL6, TGFBR1 and MMP9 expression levels were significantly increased in the overlay group on POD28 compared to control. Expression was also upregulated in the inlay group at POD 28, but was not statistically significant. Decreased expression of F2 and FGF1 was seen in both inlay and overlay groups on POD7 and POD28. Hematoxylin and eosin staining revealed increased vascular structures in both groups from the POD28 time point compared to POD7 (8.4 vs. 6.7/hpf, respectively).

CONCLUSION: Early revascularization and interface strength may be improved when ADM has closer proximity to vascularized muscle. Vascularity of ADM increased when used as both an inlay and overlay. In addition, a significant upregulation of genes involved in angiogenesis including CXCL1, CXCL2, CCL2, EDN1, IL1b, IL6, TGFBR1 and MMP9 was observed in the overlay group suggesting proximity of vascularized tissue improved tissue integration. Further research is needed to explore revascularization for ADM tissue integration and soft-tissue reinforcement.

P40
Live Fibroblast Harvest Exposes Surface Marker Shift In Vitro

Graham G Walmsley, BA; David D Lo, MD; Michael S Hu, MD; Daniel T Montoro, BS; Adrian McArdle, MB, BCh, BAO, MRCSI; Hermann P Lorenz, MD; Irving L Weissman, MD; Michael T Longaker, MD, MBA
Stanford University School of Medicine, Stanford, CA

PURPOSE: Existing techniques for the harvest of dermal fibroblasts require tissue culture plating of the skin fragments to allow for the migration of fibroblasts out of the tissue and onto the dish. For this reason current knowledge of fibroblast biology is primarily derived from studying their growth and behavior in vitro on plastic substrates as monolayer cultures. Here we describe a detailed protocol for the isolation of fibroblasts from the dorsal dermis of mice that bypasses the need for cell culture, thereby preserving the physiologic transcriptional and proteomic profiles of each cell. Using the described protocol we characterized the transcriptional and surface marker profiles of cultured vs. live harvested fibroblasts. The differential expression patterns we observed highlight the importance of a live harvest.

METHODS: We performed extensive studies testing different combinations of enzymatic and mechanical digestion methods for the harvest of dermal fibroblasts from the dorsal skin of mice. Ultimately, a protocol was selected that resulted in the highest yield of live cells. Cells isolated by mechanical/enzymatic digestion from the dorsal skin of CD1 mice were subjected to ACK buffer treatment to facilitate the lysis of red blood cells. Flow cytometry allowed for the depletion of hematopoietic, endothelial and epithelial lineages. The resulting FACS-isolated fibroblasts were either processed immediately for RNA isolation and microarray analysis, analyzed by flow cytometry using a surface marker screening panel containing purified monoclonal antibodies specific for 176 mouse cell surface markers, or expanded in culture.

RESULTS: The live harvest protocol we developed includes a 2-hour collagenase IV digestion with multiple mechanical digestion steps followed by FACS-based lineage depletion. The protocol allowed for the isolation of approximately 200,000 viable fibroblasts per adult mouse dorsum. Many surface markers that were expressed on a small subset of the live harvested fibroblast population were ubiquitously expressed (>90% positivity) on the cultured population. Prominent among these were integrins and other surface molecules that mediate cell adhesion. In comparison, relatively few surface markers were down-regulated in vitro. Furthermore, transcriptional microarray analysis revealed significant differences in gene expression between uncultured and cultured fibroblasts with over 1,000 differentially regulated genes and a coefficient of determination of R^2 = 0.83, suggesting that serum exposure and the process of adherence to tissue culture polystyrene results in a substantial shift in fibroblast phenotype.

CONCLUSION: The ability of flow cytometry to separate cells based on surface marker expression has become an indispensible tool for furthering our understanding of cellular biology. Critical to this effort is the identification of physiologic surface marker profiles. Given the significant differences between the transcriptional and surface marker profiles of cultured vs. freshly isolated fibroblasts, it is strikingly apparent that the process of culturing of fibroblasts selects for a highly homogenous activated state with distinct transcriptional and surface marker profiles. It is therefore essential that a live harvest approach be employed as researchers seek to identify physiologic surface markers that define specific lineages and discrete subpopulations of fibroblasts in the context of development, wound healing, and cancer stroma.

P41
Will I Need Plastic Surgery after Weight-Loss? Classifying Abdominal Contour Deformities and Severity to Aid in Patient Counseling, a Review of 1006 Patients

Lauren L Zammerilla, BS; Richard H Zou, BS; J Peter Rubin, MD; Jeffrey A Gusenoff, MD

University of Pittsburgh Medical Center, Pittsburgh, PA

PURPOSE: Abdominal contour deformities after massive weight loss are highly variable, ranging from a mild upper protuberance to a true double pannus. Correction of these deformities is often limited with traditional abdominoplasty. A modified approach involving a vertical skin excision, or fleur-de-lis abdominoplasty, may be required. The incidence of patients presenting with various abdominal deformities is not well defined, and factors influencing these deformities remain to be determined. The objectives of this study are to evaluate the patient population presenting with abdominal deformities, modify the Pittsburgh Rating Scale to accommodate complex abdominal wall deformities, and determine factors that may influence deformity and aid in perioperative counseling.

METHODS: All patients who presented for an abdominal contouring procedure between 2002 and 2012 were reviewed. Based on pre-operative photos, deformities were graded using the validated Pittsburgh Rating Scale. A grade of 0 indicated an appearance within a normal range. A grade of 1 indicated redundant skin with rhytids or moderate adiposity without overhang; 2, overhanging pannus; and 3, multiple rolls. The Pittsburgh Rating Scale was modified to address multiple rolls, with 3a representing a double roll with a small upper roll; 3b, a double roll extending to the mid-axillary line; 3c, a double roll extending to the back; and 3d, triple rolls. Data collected for each patient included BMI change (Delta BMI), history of bariatric surgery, operative details, revisions, and complications such as hematoma, seroma, infection, and wound dehiscence.

RESULTS: 1006 patients were evaluated, of which 91.1% were female and 86.3% had prior bariatric surgery. 32 had a Grade 1 deformity, 330 had Grade 2, 386 had Grade 3a, 104 had Grade 3b, 143 had Grade 3c, and 11 had Grade 3d. Delta BMI was positively correlated with deformity grade, with a significant Pearson correlation coefficient of 0.116 ($p<0.001$). 737 of the presenting patients underwent abdominal contouring surgery, of which 210 (28.5%) had a fleur-de-lis. Fleur-de-lis patients had significantly higher deformity grades than traditional abdominoplasty patients ($p<0.001$). Fleur-de-lis patients also had a significantly higher change in BMI than traditional abdominoplasty patients ($p<0.001$) and were more likely to have an additional component to their surgery, such as lower body lift, brachioplasty, or breast reduction ($p<0.001$). No significant difference in complications existed between fleur-de-lis and traditional abdominoplasty ($p=0.328$). Delta BMI was significantly larger in patients who had prior bariatric surgery ($p<0.001$).

CONCLUSIONS: Most patients presenting after massive weight loss have high-grade abdominal deformities with a double roll. Delta BMI is positively correlated with deformity grade and can be used to counsel patients on weight loss prior to body contouring. Patients with larger changes in BMI and higher deformity grades most often choose to add a vertical component to improve vertical and horizontal excess tissue. While minimally invasive approaches to bariatric surgery continue to evolve, our data suggests that most patients would benefit from advanced body contouring procedures that involve lengthy scars. These findings can aid plastic surgeons, bariatric surgeons, and patients in discussions regarding abdominal skin excess after massive weight loss.

P42
The Role of Obesity and Breast Adipose Tissue in Breast Cancer Formation

Naveen Kumar, MD; Irene Pien, BA; Michele Bowie, BA; Catherine Ibarra-Drendall, PhD; Matthew Sweede, BA; Victoria Seewaldt, MD; Scott T Hollenbeck, MD

Duke University Medical Center, Durham, NC

PURPOSE: Obesity is a major risk factor for breast cancer and an adverse prognostic indicator. We hypothesize that adipose tissue may release numerous cytokines that are associated with breast cancer progression. To test this hypothesis, we evaluated the obesity related cytokines; Leptin (Lp), Adiponectin (Adp) and Monocyte Chemoattractant Protein 1 (MCP-1) at the serum, tissue and cellular level.

METHODS:
IRB Approved Clinical Study: Peripheral blood was taken from 74 women followed in our high risk breast cancer clinic. Serum was evaluated using ELISA to quantify Adp, Lp and MCP-1 levels and this was correlated with BMI. In 4 patients with a unilateral breast cancer, Lp and MCP-1 levels were measured from left and right breast adipose tissue effluent following bilateral mastectomies.

In Vitro: Adipose derived stem cell (ASC's), mature adipocyte (MA) and dermal fibroblast (DF) conditioned media was evaluated for production of Lp, Adp and MCP-1 using ELISA or membrane antibody array.

RESULTS:
(1) Serum: In high risk patients, serum Lp levels were 11899 +/- 9668 pg/ml in normal weight individuals (N=25), 22117 +/- 15235 pg/ml in overweight individuals (N=28) and 27800 +/- 10628 pg/ml in obese individuals (N=21) ($p<0.05$, ANOVA). In the same patient cohort, Adp levels were 14096269 +/- 9537649 pg/ml in normal weight individuals, 13295715 +/- 11307016 pg/ml in overweight individuals and 13740182 +/- 16182231 pg/ml in obese individuals (NS). Finally, serum MCP-1 levels were 142 +/- 107 pg/ml in normal weight individuals, 159 +/- 108 pg/ml in overweight individuals and 172 +/- 166 pg/ml in obese individuals ($p=0.7$; ANOVA).

(2) Tissue: Breast adipose tissue cytokines were measured from 4 bilateral mastectomy patients. Three patients had unilateral invasive carcinoma and one patient had unilateral DCIS. Mean age was 41 years (range 35–44). The mean BMI was 29.3 (range 20.8 - 34.4). In breast adipose tissue effluent from bilateral mastectomies, mean MCP-1 levels were higher in the invasive cancer side (6364 +/- 217 pg/ml versus 5606 +/- 442 pg/ml; $p=0.03$, paired T-test). Lp levels did not correlate with cancer laterality.

(3) Cellular: MA's produced significantly more soluble Adp and Lp than ASCs and DFs ($p<0.05$). In 5 primary ASC lines derived from the adipose tissue of mastectomy specimens; MCP-1 was prominently expressed.

CONCLUSION: Serum adipokines are related to BMI in patients at high risk for breast cancer. Within the adipose tissue of matched bilateral mastectomy specimens, MCP-1 levels are elevated in the breast that contains the invasive cancer. Leptin and Adiponectin are released by mature adipocytes while MCP-1 is released from ASC's. The role of adipose tissue in breast cancer formation may be related to the preponderance of cytokines released by both mature adipocytes and ASC's from systemic and local environments.

P43
Neonatal Nerve Injury Past Postnatal Day 5 Results in Significant Neuronal Death and Persistence of Functional Deficits in the Rat

Joseph Catapano, MD; Stephen Kemp, PhD; Tessa Gordon, PhD; Gregory Borschel, MD, FACS, FAPP
University of Toronto, Toronto, ON, Canada

PURPOSE: In obstetrical brachial plexus injuries, the nerves of newborns are stretched and sometimes ruptured. These injuries can be devastating, with more than 25% of infants being left with permanent neurological deficits and potentially chronic pain in the future. Unlike adults, peripheral nerve crush injuries in neonates have demonstrated significant retrograde neuronal death after injury, robbing the nervous system of crucial regenerative components. Loss of viable neurons has been largely overlooked as a cause of morbidity following proximal nerve injuries in newborns. Previous studies have suggested that neonatal susceptibility to motor neuron death after crush injury does not extend past postnatal day 5 (P5) and the time-course of sensory neuron death is poorly understood. We sought to further examine central motor and sensory neuron survival in neonatal crush injuries after P5 and to assess axonal regeneration and functional recovery of behavior and muscle parameters following injury.

METHODS: Groups underwent sciatic nerve crush injury at post-natal day 3, 5, 7 or 30. Following neonatal crush injury, animals were returned to their cages. Weights were monitored for 1 month, at which point all animals underwent retrograde labeling of the sciatic nerve with FluorGold (FG). A 5mm section of sciatic nerve distal to the original injury site was harvested for histomorphometry and analysis of axonal regeneration. Functional and behavioural recovery was tested using SFI (Sciatic Functional Index), muscle twitch and tetanic force analysis, motor unit number estimation (MUNE) and wet muscle weights.

RESULTS: Following sciatic crush injury at P3, the number of retrogradely labeled motoneurons was reduced to approximately 35% in comparison to uninjured animals. Animals injured at P5 and P7 also displayed statistically significant lower neuron numbers than uninjured controls. All animals injured were found to have significantly lower dorsal root ganglion (DRG) counts than controls. Functionally, only animals injured at P30 were able to recover normal walking track SFI values 1 month after injury. Similar results were seen for extensor digitorum longus (EDL) muscle twitch/tetanic force analysis, MUNE and wet muscle weights.

CONCLUSION: Animals in both the P5 and P7 nerve injury groups displayed significant neuron loss and decreased functional recovery following nerve injury, suggesting that neuron loss remains a cause of disability following injury beyond P5 and treatments targeted to rescue neurons after injury may continue to be of benefit past this time.

P44
Improved Wound Healing by Transplantation of Macrophages

Michael Hu, MD, MPH, MS; Graham Walmsley, AB; Kipp Weiskopf, BS; Robert Rennert, BA; Jayakumar Rajadas, PhD; Geoffrey Gurtner, MD; Irving Weissman, MD; H Peter Lorenz, MD; Michael Longaker, MD, MBA
Stanford, Stanford, CA

PURPOSE: Macrophages are essential to normal wound healing. Mice lacking macrophages demonstrate impaired wound healing via reduced neovascularization, granulation tissue formation, and reepithelialization. Although many studies have either depleted macrophages or reduced their activity in the context of wound healing, none have investigated the effects of directly increasing the number of macrophages in the wound site. Here we seek to investigate the effects of increasing the number of macrophages present in the wound site during the initial stages of cutaneous wound healing.

METHODS: Macrophages derived from the bone marrow of *FVB-Tg(CAG-luc,-GFP)L2G85Chco/J* mice, which express firefly luciferase and cytoplasmic eGFP constitutively in all cells, were seeded onto pullulan-collagen composite dermal hydrogels and transplanted (2.5×10^5 cells per wound) into 6-mm full-thickness splinted excisional wounds on the dorsum of *FVB/NJ* mice at the time of wounding. Un-seeded hydrogels were used as controls and wound healing outcomes were assessed. The survival, localization, and behavior of transplanted macrophages in the wound site were characterized using IVIS imaging, histologic analysis of GFP fluorescence, and Maisson's trichrome staining. To investigate how macrophages respond on a transcriptional level to the wound environment, macrophages were FACS-isolated for microfluidic single-cell qPCR analysis on the basis of GFP expression at days 0, 1, 4, and 7 post-transplant from the wound site.

RESULTS: Macrophage-seeded hydrogels demonstrated improved wound healing as compared to un-seeded hydrogel controls on days 4–12 ($^*p<0.05$). The average time for complete wound healing was 11.2 days in the macrophage group versus 13.3 days in the control group ($^*p<0.001$). IVIS imaging showed survival of transplanted macrophages through day 7 of wound healing. Microfluidic single cell analysis revealed remarkable plasticity in the transcriptional response of macrophages to the wound environment through day 7 of healing. Analysis of scar on day 14 showed no significant difference between treatment and control groups.

CONCLUSIONS: Here we demonstrate that by increasing the number of macrophages in the wound site past physiologic

levels, wound healing can be improved. These findings hold promise for translational medicine aimed at improving the outcome of wound healing across a broad range of diseases. In patients with chronic wounds, autologous transplantation of macrophages derived from bone marrow aspirate may represent a viable therapeutic strategy.

P45
The Effect of Fat Harvest Technique on Adipocyte Viability and Adipose-Derived Stem Cell Count

Ava Hosseini, MD[1]; Brian Mailey, MD[1]; Jennifer Baker, MD[1]; Zeni Alfonso, PhD[2]; Paula Strasser, BS[2]; Kevin Hicok, PhD[2]; Steven Cohen, MD[1]; Amanda Gosman, MD[1]; Marek Dobke, MD, PhD[1]; Anne Wallace, MD[1]

[1]University of California, San Diego, San Diego, CA, [2]Cytori Therapeutics, San Diego, CA

PURPOSE: Retrieval of viable adipose-derived stem cells (ADSC) in lipoaspirate may be an important determinant in positive long-term outcomes after autologous fat transfer; however, it is unknown if harvest technique alters lipoaspirate properties. We sought to evaluate the impact of 3 harvesting techniques on adipocyte viability and cell characterization of the isolated stromal vascular fraction (SVF).

METHODS: We compared patients who underwent autologous fat transfer to the breast from a prospectively accrued database using three different techniques. A sample of the lipoaspirate from each patient was collected and analyzed for cell yield and viability utilizing a NucleoCounter. Cell surface marker expression of SVF was characterized via flow cytometry and resolved into four different subpopulations. Outcomes were compared by harvest technique.

RESULTS: Twenty-one patients were accrued to the study. Of those, 7 underwent harvest utilizing hand-operated syringe-aspiration, 7 via water-assisted liposuction technique, and 7 via conventional machine liposuction. There was no difference in cell viability, number of colony forming units (CFU), or cells per gram of lipoaspirate between harvest techniques. The frequency of cell subpopulations identified by cytofluorometric characterization was also similar between groups. Importantly, there was no difference in the proportion of the CD34+/CD31-/CD45- population in SVF (27.3% vs 27.5% vs 27.5%; p=0.99) in the hand-syringe, water-assisted, and conventional machine liposuction respectively.

CONCLUSION: The ADRC cell count, cell viability, CFU, or proportions of SVF subpopulations are not affected by conventional fat harvest technique. Future work can determine if washing and purifying lipoaspirate may affect laboratory and clinical outcomes.

P46
Comparison of Delivery Methods of Adipose-Derived Stem Cells Reveal Differential Survival and Wound Healing Outcomes

Michael S Hu, MD, MPH, MS; Wan Xing Hong, MS; Mika Esquivel; Robert C Rennert, BA; Michael T Chung, BS; Andrew S Zimmermann, BS; Jayakumar Rajadas, PhD; Dominik Duscher, MD; Adrian McArdle, MB, BCh, BAO(NUI), MRCSI; Graham G Walmsley, AB; Geoffrey C Gurtner, MD; Michael T Longaker, MD, MBA; H. Peter Lorenz, MD
Stanford University, Stanford, CA

PURPOSE: Cutaneous defects resulting from burns, trauma, or surgical procedures present a continuing challenge to the field of reconstructive surgery. The onset of stem cell-based therapies, however, promises to promote enhanced wound healing and optimize outcomes. In particular, the application of autologous adult stem cells has emerged as a promising approach, and allows for the utilization of nonimmunogenic cells for the treatment of many soft tissue disorders. In the past decade adipose-derived stem cells (ASCs), adult multipotent stem cells found in the stroma of adipose tissues, have been identified as an attractive donor cell source. Not only can ASCs be harvested through minimally invasive procedures such as liposuction, they are also an abundant stem cell population, and have the potential for stimulating neovascularization after transplantation into ischemic tissues, further enhancing wound healing. However, in the clinical setting, the route of administration of ASCs plays a critical role in determining how efficient the treatment ultimately is. Optimizing administration is a crucial factor in prolonging the survival and functionality of the delivered therapeutic cells. Thus, the goal of our study is to compare several methods for administration of ASCs to excisional wounds in order to determine the delivery method through which the maximal therapeutic efficacy of ASCs, as determined by wound healing rates and resulting scar size, might be attained.

METHODS: Two 6mm full thickness excisional wounds were created on the dorsum of each wild-type (WT) FVB mouse. ASCs harvested from the inguinal fat pads of transgenic FVB-L2G mice were applied to each wound via different cell delivery methods. In all, four different methods for delivering ASCs were studied: cell suspension in PBS injected under the wound, ASCs in matrigel injected under the wound, ASCs in matrigel placed over the wound, and ASCs in bioengineered pullulan-collagen composite dermal hydrogel placed over the wound. Wounds with no therapeutic cells were used as control. As the ASCs from the L2G transgenic mice luminesce when interacting with injected luciferin, this enabled the quantification of ASCs in vivo through bioluminescent imaging (BLI). The effectiveness of the treatments was recorded over a period of two weeks using three parameters: the survival of ASCs in vivo using BLI, quantification of the rate of wound healing and comparison of scar formation.

RESULTS: Cutaneous wounds treated with ASCs delivered with hydrogel displayed the highest therapeutic cell survival on day 5 as well as the fastest wound healing. Wounds treated with ASCs delivered with hydrogel scaffold achieved full closure on day 11.4 versus day 14 for no treatment ($*p<0.001$). This was significantly earlier than excisional wounds treated with all other delivery methods, which fully closed on day 12.9 ($*p<0.004$).

CONCLUSION: We conclude that ASC delivery into wounds via hydrogel scaffolds is the superior method based upon cell survival, wound healing and scar formation. As the precise mechanisms by which hydrogel acts to preserve cell function remains undefined, future studies will be geared towards improving understanding of the characteristics of this technique for stem cell delivery.

ACKNOWLEDGMENT: Support was provided by the Sarnoff Foundation and CIRM.

P47
The Dominant Role of Intrathymic Clone Deletion in the Mixed Chimerism Related VCA Tolerance Induction

Wensheng Zhang, MD, PhD; Yong Wang, MD; Yang Yang, MD, PhD; Yang Li, MD, PhD; Kia M Washington, MD; Vijay S Gorantla, MD; Mario G Solari, MD; Xin Xiao Zheng, MD
University of Pittsburgh, Pittsburgh, PA

PURPOSE: Thymic clonal deletion that ensues after donor hematopoietic cell engraftment is the major mechanism for maintaining donor-specific tolerance. We have reliably achieved stable mixed chimerism (MC) and tolerance in a mouse hind-limb transplant model using a short-term immunosuppressive regimen, and have demonstrated that the deletion of alloreactive T cells occurs in the tolerant recipients. In this study, we provide further evidence of central intrathymic deletion in MC-mediated vascularized composite allograft (VCA) tolerance.

METHODS: B6 mice received hind-limb allografts from B10.A donors and were treated with rapamycin, CTLA4/Fc and anti-CD40L mAb. 120 day after transplantation, thymus lobes from the tolerant mice were isolated and transplanted into the subrenal capsule of B6 nude mice. CD4+CD25- T cells (5 x 10^6) sorted from the splenocytes of same tolerant mice were i.v. injected to the B6.RAG1-/- mice. Naïve B6 thymus or CD4+CD25- T cells were used as controls in thymus transplantation and adoptive transfer. Recipient nude or Rag1-/- mice were further challenged with skin grafts from B10.A (donor specific), BALB/c (third party), and B6 (syngenic control) mice. MC, TCR Vβ expression profiles were analyzed by flow cytometric analysis.

RESULTS: 1) All treated recipients permanently accepted B10.A hind-limb allografts with persist multilineage donor hematopoietic MC (2–4%) for >120 days post transplantation. Tolerance was confirmed in vivo by acceptance of the donor skin grafts and rapid rejection of third party grafts. 2) Nude mice bearing tolerant thymus showed a prolonged engraftment for donor-specific B10.A skin grafts (n=4, MST: 64.5 days) with 50% surviving infinitely (>120 days), as compared with the naïve thymus-bearing recipients (n=4, MST: 11.5 days, p12 weeks).

CONCLUSION: Our findings demonstrate thymus and T cells from tolerant VCA recipients confer donor-specific immunity to nude and RAG1-/- mice with the deletion of donor-specific Vβ clones. It suggests that intrathymic deletional mechanisms play dominant role in the induction of VCA tolerance with stable mixed chimerism.

P48
Are Flaps Really Better than Implants for Breast Reconstruction in Obese Females? An Analysis of 89,514 Women Undergoing Breast Surgery from the ACS-NSQIP Database

Mohamud A Qadi, BS[1]; Pablo A Baltodano, MD[1]; José M Flores, MPH[2]; Sashank Reddy, MD, PhD[1]; Nicholas B Abt, BS[1]; Karim A Sarhane, MD, MScs[1]; Francis M Abreu, BS[3]; Carisa M Cooney, MPH[1]; Gedge D Rosson, MD[1]
[1]Department of Plastic and Reconstructive Surgery, Johns Hopkins University School of Medicine, Baltimore, MD, [2]Department of Epidemiology, Johns Hopkins School of Public Health, Baltimore, MD, [3]Department of Biostatistics, Johns Hopkins School of Public Health, Baltimore, Baltimore, MD

PURPOSE: To determine data-driven recommendations for breast reconstruction in obese women. Obesity is a known risk factor for postoperative morbidity after mastectomy with/without reconstruction. Current evidence support the use of flaps over implants for reconstruction in this population. We searched for the reconstruction strategy associated with the lowest 30-day postoperative overall-morbidity, surgical-site morbidity, and reconstruction-failure rates in the obese population.

METHODS: We analyzed all females undergoing mastectomy with/without reconstruction from 2005–2011 in the American College of Surgeons National Surgical Quality Improvement Program (ACS-NSQIP) databases.[1] Data included demographic, preoperative, and perioperative factors. Patients were stratified by body mass index (BMI), all the overweight (BMI≥25, WHO definition) and obese females (BMI≥30, WHO definition) were identified, and multivariable regression was used to compare 30-day postoperative overall-morbidity, surgical-site morbidity, and reconstruction failure rates between breast-reconstruction procedures. Predefined outcomes included: cardiac, respiratory, neurological, urinary, venous thromboembolism, wound, and prosthesis/flap failure complications. Confidence intervals estimate 95% precision.

RESULTS: 89,514 women underwent mastectomy or breast reconstruction and had NSQIP BMI data, including: 65,827 (73.5%) mastectomy-only, 19,124 (21.4%) immediate breast reconstruction (IBR), and 4563 (5.1%) delayed breast reconstruction (DBR) patients. Overweight was independently associated with higher postoperative overall-morbidity in the mastectomy-only ($OR_{-adjusted}$=1.12; 95%CI:1.04–1.22, p=0.004) and IBR groups ($OR_{-adjusted}$=1.34; 95%CI:1.16–1.55, p<0.001), while trending towards significance in the DBR

group ($OR_{-adjusted}$=1.41; 95%CI:0.95–2.11, p=0.08). Obesity was independently associated with higher overall-morbidity in all groups ($OR_{-adjusted}$=1.91; 95%CI:1.24–2.94, p<0.03). Additionally, multivariable comparison of 30-day postoperative morbidity rates of flaps vs. implants (using tissue expanders as the reference group) in the 6,427 obese patients undergoing reconstruction, showed that flap reconstructions were associated with higher overall-morbidity ($OR_{-adjusted}$=1.49; 95%CI:1.31–1.71, p<0.001), higher surgical-site morbidity ($OR_{-adjusted}$=1.41; 95%CI:1.16–1.72, p=0.001), and higher reconstruction failure rates ($OR_{-adjusted}$=2.74; 95%CI:2.01–3.75, p<0.001) than implant based reconstructions.

CONCLUSION: Our study supports that obesity is associated with higher postoperative morbidity, but more importantly, it brings attention to the overweight population and to a dose response effect of BMI on postoperative morbidity. During the first 30 postoperative days, flap based reconstructions are associated with higher overall-morbidity, surgical-site morbidity, and reconstruction-failure rates compared to implant based reconstructions. The health care cost implications of the higher 30-day postoperative morbidity associated with flap based reconstruction warrant further investigation.

P49
Application of Game-Based 3D Scanning in Craniofacial Analysis

Christian El Amm, MD; Lan Le, MS Eng; John Dwyer, PhD Eng; Kamal Sawan, MD
University of Oklahoma, Oklahoma City, OK

PURPOSE: Motion tracking interfaces commonly available in gaming (Kinect®) can be modified to generate rough 3D surface scans with sufficient resolution for shape analysis methods. We compared the precision of Kinect® generated surfaces to standard CT scanning and applied shape analysis methods on cranial shapes associated with common craniofacial conditions.

METHODS: After IRB approval, 42 patients with craniofacial conditions that underwent CT scans of the craniofacial area were selected for external scanning using commercial kinect® setup. The dense point cloud generated was used to generate a smoothed surface model and compared to the CT scan generated Surface model and compared for accuracy. Two shape analysis algorithms were then applied to the Kinect® generated surfaces to find discriminant descriptors of different craniofacial conditions.

RESULTS: 12 patients with deformational plagiocephaly, 14 with scaphocephaly, 6 with metopic and 10 with unicoronal synostosis were recruited. Kinect® generated surfaces of the cranial vault were within 4mm of the CT scan generated skin surfaces, and most of the errors were related to distortion related to the gantry. The Kinect generated surfaces also related well to the underlying bony anatomy. Ellipsoid Analysis (Kane et al) and Fourrier descriptors applied to the Kinect®-generated surfaces of the cranial vault were found to discriminate reliably between the 4 conditions.

CONCLUSION: Widely available motion tracking game controllers can generate reliable surface models of the cranial vault. Automated, landmark-independent discrimination between deformational plagiocephaly and synostosis conditions may be possible.

Plastic Surgery Research Council Membership Information

PSRC: THE PREMIER FORUM FOR THE BEST CLINICAL RESEARCH PAPERS

You have known the PSRC as a forum for outstanding basic research in plastic surgery. The PSRC meeting format also highlights outstanding clinical papers, and brings the full spectrum of plastic surgery research to a single venue.

University of California Los Angeles - Members Photo at 2013 Annual Meeting

ABOUT THE PSRC BARONIO SHEEP LOGO

The artwork comes from *Baronio, G., Degli Innesti Animali, Stamperia e Fonderia del Genio, Milan, 1804*. In Italy, a charlatan called Gambacurta, showed publicly how she could cut pieces of skin off herself, replace them, and they would live as reported by D. A. Sancassani in 1731. Italian physiologist, Giuseppe Baronio (1759–1811), was inspired by knowledge of this demonstration and carried out a series of successful autografts of sheep skin in 1804 *(Degli innesti animali)*. Baronio removed pieces of sheep skin 12.5 by 7.5 cm, replaced them 80 minutes after excision, and found that the skin survived. Baronio's work predated a reported success in man by thirteen years (1817). At the time of the founding meeting of the Plastic Surgery Research Council, called by Drs. Milton Edgerton and Robin Anderson in 1955 at Johns Hopkins, Dr. Richard Stark submitted the drawing of Baronio's Sheep (1804) with auto and allografts *in situ* as a possible logo for the Council. The design was made into a rectangle with rounded corners, was accepted, and has been the logo of the Council since that time. The PSRC has a fascinating history. The first 35 years were recorded and published by Dr. Peter Randall in a bound volume in 1990, and subsequently updated by Emeritus PSRC Historian, Dr. Tom Davis. Please visit the PSRC website, http://www.ps-rc.org, to learn more about the Council's stellar history and the outstanding past Chairs amongst its members.

PSRC BARONIO SHEEP LOGO

MEMBERSHIP CATEGORIES

Active membership is open to qualified plastic surgeons under the age of 50 who have completed an approved residency in plastic surgery prior to application for membership. Active members have voting privileges and automatically become Senior members when they reach the age of 50.

Associate membership is open to individuals without qualification for Active membership but whose contributions make their inclusion in the Council desirable. Associate members may not vote.

Resident/Fellow membership is open to all Residents and Fellows in the field of plastic surgery. Upon completion of plastic surgery training, Resident/Fellow Members will automatically be elevated to Active Member status and shall comply with requirements of Active Members of The Council. Resident/Fellow Members may not vote.

Senior & Senior Associate Members are Active and Associate members who progress to Senior and Senior Associate membership at the end of the Business Meeting during the year in which they are 50 on January 1. They remain in this category of membership until they become 65 years of age or are retired from practice. They are required to pay reduced dues and have no voting privileges.*

Senior Emeritus Members are Seniors and Senior Associates who progress to Senior Emeritus status when they become 65 years of age or are retired from practice. This conversion takes effect at the end of the Business Meeting during the year they become 65 years of age or are fully retired from practice. They pay no dues and have no voting privileges.*

* Membership is honorary in nature and requires prior Active or Associate membership.

BENEFITS OF MEMBERSHIP

- Reduced registration fees at PSRC meetings
- The ability to participate in the PSRC Mentorship Program
- Opportunity to participate as faculty at PSRC Meetings
- Free listing of your laboratory's openings for fellowship opportunities on the PSRC website
- Publication of abstracts and manuscripts in *PRS Supplements*
- Access to PSRC research grant funds
- Opportunities to interact and network with leaders in the field of plastic surgery, develop valuable connections, and network for employment opportunities
- Access to new Research Council initiatives in the pipeline
- Present your best work to a collegial and engaged audience

ACTIVE AND ASSOCIATE MEMBERSHIP APPLICATION

Applications for Active or Associate membership will be considered when each of the items listed below is received by the PSRC administrative office.

A completed application form
A sponsorship letter from a current Active or Senior member of the PSRC
A copy of your curriculum vitae

Attendance at a PSRC Annual Meeting is also required and may include the meeting in the year an applicant is considered for election. Apply at www.ps-rc.org.

RESIDENT/FELLOW MEMBERSHIP APPLICATION

Application for Resident/Fellow membership will be considered when each of the items listed below is received by the PSRC administrative office.

A completed application form
A letter from your Program Director verifying your resident or fellowship status, including date of anticipated training program completion
A copy of your curriculum vitae

Attendance at a PSRC Annual Meeting is also required and may include the meeting in the year an applicant is considered for election. Apply at www.ps-rc.org.

Disclaimer

Papers are reprinted as they were submitted.

The PRSC takes no responsibility for typographical or other errors.

No Photography or videotaping is allowed during the scientific sessions without prior approval by the Executive Committee.